

Antibacterial Surfaces with Nanoparticle Incorporation for Prevention of Hospital-Acquired Infections

This thesis is presented to UCL in partial fulfilment of the requirements for the
Degree of Doctor of Philosophy

Sandeep K. Sehmi

2016

Supervised by: Professor Alexander J. MacRobert, Professor Ivan
P. Parkin and Dr Elaine Allan



Declaration

I, Sandeep Sehmi, confirm that the work presented in this thesis is my own. Where information has been derived from other sources, I confirm that this has been indicated in the thesis.

Abstract

This thesis describes the incorporation of nanoparticles into polymers as antibacterial surfaces for preventing hospital-acquired infections (HAIs). With a high prevalence of HAIs, the use of antibacterial materials can contribute in reducing bacterial contamination associated with frequently touched surfaces in hospitals (e.g. push plates, bed rails, or keyboards). The combination of nanoparticles and light-activated antibacterial agents demonstrate lethal bactericidal activity when encapsulated into medical grade polymer sheets. Upon white light activation, these polymers exhibit significant photobactericidal activity against a range of Gram-negative and Gram-positive bacteria *via* the production of reactive oxygen species at the polymer surface, through multi-site mechanistic pathways (Type I and/or Type II). These samples are tested under various light intensities to mimic clinical surroundings, but more significantly, some materials show highly efficacious antibacterial activity in dark conditions.

All polymers are prepared using a simple 'swell-encapsulation-shrink' method, which impregnates the nanoparticles into the polymer substrate and on the surface. These include copper and zinc oxide nanoparticles synthesised with different capping agents. The antibacterial activity of a commonly used biocide encapsulated into the polymer is also assessed. The photosensitiser (crystal violet) is then coated onto the polymer surface in the case of ZnO nanoparticles and activated by white light (~500 – 6600 lux).

The combination of crystal violet and zinc oxide nanoparticles is investigated further by adapting the microbiological protocol to more closely replicate a clinical environment and using a lower intensity of light to carry out the antibacterial testing. In addition, the mechanisms operating within the crystal violet and zinc oxide system are examined using specific inhibitors and singlet oxygen quenchers to determine

whether Type I, Type II, or both photochemical pathways are responsible for the reduction of bacteria in the light and dark.

The samples were tested against a range of hospital pathogens, including *Escherichia coli*, *Staphylococcus aureus*, *methicillin-resistant Staphylococcus aureus*, *Pseudomonas aeruginosa* and *Clostridium difficile* endospores. The novel and highly effective antimicrobial materials detailed in this thesis demonstrate a very strong potential to be used in hospitals for reducing the incidence of HAIs.

Acknowledgements

Firstly, I would like to give special thanks to my primary and secondary supervisors, Prof. Alexander MacRobert, Prof. Ivan Parkin and Dr. Elaine Allan for their invaluable expertise, advice and support over the last three years. Thank you for giving me the opportunity to do an inter-disciplinary PhD that I have enjoyed so much and gained countless experience in a range of subject fields. I would especially like to thank Elaine for teaching me microbiology (from scratch!). I have appreciated every discussion and meeting we have had as a group. You have all provided endless guidance and encouragement and I've thoroughly enjoyed being part of this research team.

I would like to thank students and mentors at the Division of Surgery and Interventional Sciences research group and the Eastman Dental Institute who have supported me along the way. Thank you to collaborators from the Chemistry department at Imperial College. UCL Chemistry has been my home for the last 7 years so it will definitely be missed the most! I would like to thank every single person who has helped me and shared the experience with me, in particular, my partner in crime, Sapna Ponja! I look forward to celebrating this moment with you when you become Dr as well ☺. Its going to be so weird not seeing you everyday and I just want to thank you for being a huge part of this crazy amazing experience.

I would like to thank my wonderful best friends and family for their love and support along the way. Last but definitely not least, I would like to thank my parents for being the most supportive and motivational people in my life. All the success throughout my education has been possible because of you and I would not be where I am today if it wasn't for you. You're both extremely hardworking people which has inspired me to strive for excellence and I hope to continue to make you proud in the future. Love you both!

Publications

Publications associated with this thesis:

1. **SK Sehmi**, S Noimark, J Weiner, E Allan, AJ MacRobert, IP Parkin. Potent Antibacterial Activity of Copper Embedded into Silicone and Polyurethane. *ACS Applied Materials & Interfaces*, 7 (41), 22807-22813, 2015.
2. **SK Sehmi**, E Allan, AJ MacRobert and IP Parkin. The Bactericidal Activity of Glutaraldehyde-Impregnated Polyurethane. *MicrobiologyOpen*, 2016. doi: 10.1002/mbo3.378
3. **SK Sehmi**, S Noimark, JC Bear, WJ Peveler, M Bovis, E Allan, AJ MacRobert and IP Parkin. Lethal Photosensitisation of *Staphylococcus aureus* and *Escherichia coli* using Crystal Violet and Zinc Oxide-Encapsulated Polyurethane. *Journal of Materials Chemistry B*, 3 (31), 6490-6500, 2015.
4. **SK Sehmi**, S Noimark, SD Pike, JC Bear, WJ Peveler, CK Williams, E Allan, IP Parkin and AJ MacRobert. Enhancing Antibacterial Activity of Light-Activated Surfaces Containing Crystal Violet and ZnO nanoparticles: Investigation of Nanoparticle Size, Capping Ligand and Dopants. *ACS Omega*, 1 (3), 334-343, 2016.
5. **SK Sehmi**, K Alkhuder, S Noimark, SD Pike, CK Williams, MSP Shaffer, IP Parkin, AJ MacRobert and E Allan. Antibacterial surfaces for Hospitals with Activity against Hospital-Acquired Pathogens and *Clostridium Difficile* Spores. (Manuscript in preparation)

Table of Contents

1. Hospital-Acquired Infections	1
1.1 Introductory remarks	1
1.2 Introduction to the Incidence of Hospital-Acquired Infections . . .	1
1.3 Antimicrobial Resistance	4
1.4 Common Pathogens in Hospitals	5
1.4.1 Methicillin-resistant <i>Staphylococcus aureus</i>	7
1.4.2 <i>Escherichia coli</i>	7
1.4.3 <i>Pseudomonas aeruginosa</i>	8
1.4.4 <i>Clostridium difficile</i>	9
1.5 Prevention Strategies	9
1.6 Alternative methods to basic cleaning	13
1.6.1 Ozone	13
1.6.2 Steam vapour	14
1.6.3 Hydrogen peroxide	14
1.6.4 Gas plasma	15
1.6.5 UV light	15
1.6.6 High-intensity narrow spectrum	16
1.7 Antibacterial Surfaces	16
1.7.1 Biocide leaching	17
1.7.2 Antimicrobial polymers	18
1.7.3 Anti-adhesive coatings	19
1.7.4 Silver-coated surfaces	19
1.7.5 Copper and copper alloy surfaces	20
1.7.6 Light-activated antibacterial surfaces	20
1.7.6.1 Titanium oxide-based antibacterial surfaces	21
1.7.6.2 Dye-based antibacterial surfaces	22
1.7.7 Concerns over antibacterial surfaces	22
2. Photo-Activated Surfaces	38

2.1 Introduction to Photodynamic Therapy	38
2.1.1 Photochemistry	41
2.1.1.1 Non-radiative transitions	42
2.1.1.2 Radiative transitions	42
2.1.2 Mechanism of action	42
2.2 Antibacterial Action of Nanoparticles	47
2.2.1 Use of nanoparticles in a clinical environment	47
2.2.1.1 Antibacterial mechanism of nanoparticles	49
2.2.2 Copper nanoparticles	50
2.2.3 Magnesium oxide nanoparticles	51
2.2.4 Zinc oxide nanoparticles	53
2.3 Dye and nanoparticle-incorporated polymers	54
2.3.1 Polymer types	55
2.3.1.1 Polyvinyl chloride	55
2.3.1.2 Silicone	56
2.3.1.3 Polyurethane	56
2.3.2 Overview of the research at the Materials Research Centre, UCL	56
2.4 Research aims	58

3. Copper-Encapsulated Silicone and Polyurethane; Antimicrobial

Polymers without White Light Activation	75
3.1 Introduction	75
3.2 Experimental	77
3.2.1 Chemicals and Reagents	77
3.2.2 Synthesis of Copper Nanoparticles	78
3.2.3 Material Preparation	78
3.2.3.1 Polymer System Optimisation – Organic Solvent Concentration	78
3.2.3.2 Polymer Samples Prepared for Antibacterial Testing	79
3.2.4 Material Characterisation	79

3.2.4.1	Characterisation of Copper Nanoparticles . . .	79
3.2.4.2	Characterisation of Modified Polymer Samples	80
3.2.5	Antibacterial Activity	80
3.2.5.1	Microbiology Assay	80
3.2.5.2	Statistical Significance	81
3.2.5.3	Further Antimicrobial Testing for Mechanistic Evaluation	82
3.3	Results and Discussion	82
3.3.1	Material Characterisation	82
3.3.1.1	Characterisation of Copper Nanoparticles . . .	82
3.3.1.2	Characterisation of Modified Polymer Samples	84
3.3.2	Antibacterial Activity	88
3.4	Conclusion	95

4. Glutaraldehyde-Encapsulated Polyurethane; Antimicrobial Polymer

without White Light Activation		103
4.1	Introduction	103
4.2	Experimental	107
4.2.1	Chemicals and Reagents	107
4.2.2	Material Preparation	107
4.2.3	Material Characterisation	108
4.2.4	Antibacterial Activity	109
4.2.4.1	Statistical Significance	109
4.3	Results and Discussion	110
4.3.1	Material Preparation	110
4.3.2	Material Characterisation	111
4.3.3	Antibacterial Activity	114
4.4	Conclusion	119

5. Crystal Violet and 18 nm ZnO Nanoparticles Encapsulated into Polyurethane; White Light Activated Antimicrobial Polymers	125
5.1 Introduction	125
5.2 Experimental	129
5.2.1 ZnO Nanoparticles	129
5.2.1.1 Chemicals and Reagents	129
5.2.1.2 Nanoparticle Synthesis	129
5.2.1.3 Nanoparticle Characterisation	130
5.2.2 Polymer Samples	130
5.2.2.1 Chemicals and Reagents	130
5.2.2.2 Material Preparation	131
5.2.2.3 Material Characterisation	132
5.2.3 Antibacterial Activity	134
5.2.3.1 Microbiology Assay	134
5.2.3.2 Statistical Significance	135
5.2.3.3 Hydrogen Peroxide and Singlet Oxygen Detection	135
5.3 Results and Discussion	136
5.3.1 ZnO Nanoparticle Synthesis and Characterisation . . .	136
5.3.2 Preparation and Characterisation of Polymer Samples	137
5.3.3 Antibacterial Activity	144
5.4 Conclusion	156
6. Crystal Violet and 3 nm ZnO Nanoparticles Encapsulated into Polyurethane; Antimicrobial Polymers Activated by Low Intensity White light Source	165
6.1 Introduction	165
6.2 Experimental	169
6.2.1 ZnO Nanoparticles	169
6.2.1.1 Nanoparticle Synthesis	169
6.2.1.2 Nanoparticle Characterisation	170
6.2.2 Polymer Samples	171

6.2.2.1	Polymer Sample Preparation	171
6.2.2.2	Material Characterisation	171
6.2.3	Antibacterial Activity	172
6.2.3.1	Microbiology Assay	172
6.2.3.2	Statistical Significance	174
6.2.3.3	<i>Clostridium difficile</i> Endospore Preparation . .	174
6.2.3.4	Ligand Variation to Determine Oleate Ligand Influence	175
6.2.3.5	Detection of Superoxide and Singlet Oxygen .	175
6.3	Results and Discussion	176
6.3.1	ZnO Nanoparticle Synthesis and Characterisation . . .	176
6.3.2	Preparation and Characterisation of Polymer Samples	180
6.3.3	Antibacterial Activity	186
6.3.3.1	CVZnO_DOPA vs. CVZnO_oleate	186
6.3.3.2	Further Antibacterial Testing of CVZnO_oleate	190
6.3.4	Mechanistic Evaluation of CVZnO_oleate	196
6.4	Conclusion	205
7.	Conclusion	213
7.1	Future Work	218

List of Figures

- Fig. 1.1 Factors affecting the incidence of HAIs.
- Fig. 1.2 Antibiotic resistance cycle.
- Fig. 1.3 Role of antibacterial surfaces in preventing HAIs from the direct transfer of microorganisms.
- Fig. 1.4 Photo-excitation processes of TiO₂.
- Fig. 2.1 Chemical structures of tetrapyrrole based and non-tetrapyrrole based photosensitisers used in PDT.
- Fig. 2.2 Modified Jablonski diagram displaying the electronic states (S_0 , S_1 , S_n , T_0 , T_1 , T_n) of a photosensitiser after the absorption of a photon. Non-radiative transitions are labelled as follows: internal conversion (IC), intersystem crossing (ISC), vibrational relaxation (VR). Diagram also shows the production of singlet oxygen (1O_2) *via* resonant electronic energy transfer.
- Fig. 2.3 (a) Simplified Jablonski diagram displaying the processes involved in photodynamic therapy when a photo-excited photosensitiser undergoes energetic transitions after the absorption of a photon. The photosensitiser in its excited singlet state can undergo radiative decay (fluorescence) or non-radiative decay *via* internal conversion, or convert to the excited triplet state *via* intersystem crossing. The triplet state molecule can decay radiatively by phosphorescence, non-radiatively *via* internal conversion, or interact with molecular oxygen *via* resonant energy transfer (Type II process) or other

substrate molecules *via* electron or proton transfer (Type I process). (b) Common reactions involved in Type I and Type II processes.

- Fig. 2.4 Superoxide dismutation reaction.
- Fig. 2.5 Gram-positive and Gram-negative bacterial cell wall structure.
- Fig. 2.6 Different possible mechanisms of toxicity of nanoparticles against bacteria, including: reactive oxygen species (ROS) production, ion release, protein and DNA damage and disruption of the cell membrane.
- Fig. 3.1 Chemical structures of silicone and polyurethane.
- Fig. 3.2 Schematic diagram illustrating the preparation of copper nanoparticles (Step 1) and encapsulating them into 1 cm² polymer squares for antibacterial testing (Step 2).
- Fig. 3.3. (a) HR-TEM images of Cu NPs. (b) Cu NP size distribution determined by HR-TEM.
- Fig. 3.4 EDX spectrum of Cu NPs.
- Fig. 3.5 Modified polymer samples for antibacterial testing (1 cm²): (a) polyurethane control; (b) Cu-encapsulated polyurethane; (c) silicone control; (d) Cu-encapsulated silicone.

- Fig. 3.6 UV-vis absorbance spectra of polyurethane control, Cu-polyurethane, silicone control and Cu-silicone, measured in the range 350 – 550 nm.
- Fig. 3.7 Cu (2p) region XPS spectra for: (a) Cu-polyurethane surface; (b) Cu-polyurethane sputtered 50 s; (c) Cu-silicone surface; and (d) Cu-silicone sputtered 50 s.
- Fig. 3.8 SEM imaging of polymer squares tested for antimicrobial activity: (a) polyurethane control; (b) Cu-encapsulated polyurethane; (c) silicone control; (d) Cu-encapsulated silicone.
- Fig. 3.9 Viable counts of *S. aureus* NCTC 13143 after incubation on modified polyurethane squares for: (a) 1 h and (b) 2 h, and modified silicone squares for: (c) 4 h and (d) 5 h. All samples were incubated at 20°C in the dark. Control samples are solvent treated. * indicates bacterial numbers reduced below the detection limit of 100 colony forming units/mL (cfu/mL).
- Fig. 3.10 Viable counts of *E. coli* ATCC 25922 after incubation on modified polyurethane squares for: (a) 2 h and (b) 3 h, and modified silicone squares for: (c) 4 h and (d) 6 h. All samples were incubated at 20°C in the dark. Control samples are solvent treated. * indicates bacterial numbers reduced below the detection limit of 100 colony forming units/mL (cfu/mL).
- Fig. 3.11 Viable counts of *S. aureus* NCTC 13143 after incubation on modified polyurethane squares for (a) 2 h and modified silicone squares for (b) 5 h after 90 days from preparation. Viable counts of *E. coli* ATCC 25922 after incubation on modified polyurethane squares for (c) 3 h, and modified silicone squares for

(d) 6 h after 90 days from preparation. All samples were incubated at 20°C in the dark. Control samples are solvent treated. * indicates bacterial numbers reduced below the detection limit of 100 colony forming units/mL (cfu/mL).

- Fig. 4.1 The chemical structure of glutaraldehyde.
- Fig. 4.2 Schematic diagram showing the preparation of glutaraldehyde-encapsulated polyurethane squares (1 cm²) for antibacterial testing.
- Fig. 4.3 ATR-FTIR spectra of (a) solvent treated polyurethane (control), (b) glutaraldehyde-encapsulated polyurethane and (c) glutaraldehyde-coated polyurethane.
- Fig. 4.4 XPS spectra for glutaraldehyde-encapsulated surface: (a) Carbon (1s) region and (b) Oxygen (1s) region and for glutaraldehyde-coated surface: (c) Carbon (1s) region.
- Fig. 4.5 Viable counts of *S. aureus* 8325-4 after incubation at 20°C on modified polyurethane squares for: (a) 30 min and (b) 1 h, and viable counts of *E. coli* ATCC 25922 after incubation on modified polyurethane squares for: (c) 1 h and (d) 2 h. Control samples are solvent treated. * indicates bacterial numbers reduced below the detection limit of 100 colony forming units/mL (cfu/mL).
- Fig. 4.6 Viable counts (colony forming units/mL (cfu/mL)) of (a) *S. aureus* 8325-4 for 1 h and (b) *E. coli* ATCC 25922 for 2 h after incubation at 20°C on modified

polyurethane squares left for 15 days. Control samples are solvent treated.

- Fig. 4.7 Equilibrium reaction scheme of glutaraldehyde in basic conditions (adapted from Margel and Rembaum)
- Fig. 5.1 Molecular structure of crystal violet dye
- Fig. 5.2 Schematic step-by-step method illustrating the preparation of crystal violet and ZnO encapsulated polyurethane samples (CVZnO). Squares indicate 1 cm² polymer squares used.
- Fig. 5.3 (a) TEM images and (b) EDX spectrum of ~18 nm ZnO nanoparticles.
- Fig. 5.4 UV-vis absorbance spectra of crystal violet-coated polyurethane (CV) prepared by dipping in a solution for 72 h at the following concentrations: 0.00001 M, 0.0001 M and 0.001 M. Spectrum for crystal violet and ZnO encapsulated-polyurethane (CVZnO) sample is also shown, prepared by immersion in 0.001 M crystal violet solution (measured in 400 – 700 nm range).
- Fig. 5.5 1 cm² polymer samples prepared by immersion in 0.001 M crystal violet solution for increasing lengths of time (up to 96 h).
- Fig. 5.6 (a) An image of a 15 μm thick crystal violet-coated polyurethane section prepared by immersing the polymer in a 0.001 M crystal violet solution for 72 h. The image was recorded using a 10x objective (scale bar corresponds to 100 μm). The actual thickness of

the polymer sample is 0.8 mm. (b) A CCD false coloured fluorescence microscopy image of the same polymer section shown in (a). The polymer sample is shown on the left hand side of the image, where the black part of the image represents the background (no fluorescence). There is a fluorescence intensity scale, increasing from black (background/no fluorescence) to white (maximum fluorescence). The image resolution is 512 x 512 pixels and corresponds to 557 x 557 μm (100 μm scale bar).

Fig. 5.7 Leaching of dye from crystal violet-coated polyurethane (0.001 M) in PBS solution at 37 °C measured as a function of time.

Fig. 5.8 ATR-FTIR spectra of (a) solvent treated (control), (b) ZnO-encapsulated, (c) crystal violet-coated, and (d) crystal violet and ZnO-encapsulated polyurethane.

Fig. 5.9 Zn 2p region XPS spectra for: (a) ZnO-encapsulated surface; (b) ZnO-encapsulated sputtered 50 s; and (c) ZnO-encapsulated sputtered 100 s.

Fig. 5.10 Viable counts of *S. aureus* 8325-4 after incubation on modified polyurethane samples incubated at 20 °C in the dark and exposed to white light illumination for: (a) 1 h and (b) 2 h. White light source emitted an average light intensity of 6600 ± 990 lux at a distance of 25 cm from the samples. * indicates bacterial numbers reduced to below the detection limit of 100 colony forming units/mL (cfu/mL).

Fig. 5.11 Viable counts of *E. coli* ATCC 25922 after incubation on modified polyurethane samples incubated at 20 °C in the dark and exposed to white light illumination for: (a) 2 h and (b) 4 h. White light source emitted an

average light intensity of 6600 ± 990 lux at a distance of 25 cm from the samples. * indicates bacterial numbers reduced to below the detection limit of 100 colony forming units/mL (cfu/mL).

Fig. 5.12 Radical species and singlet oxygen quenchers/inhibitors of Type I and II photochemical pathways used in this investigation (BSA: bovine serum albumin).

Fig. 5.13 (a) Viable counts of *E. coli* ATCC 25922 following 2 h of white light illumination on modified polyurethane samples for a control, catalase, bovine serum albumin (BSA) and L-histidine experiment. The white light source emitted an average light intensity of 6600 ± 990 lux at a distance of 25 cm from the samples. * indicates that the bacterial numbers were reduced to below the detection limit of 100 colony forming units/mL (cfu/mL). (b) Viable counts of *E. coli* ATCC 25922 following 4 h incubation in the dark on modified polyurethane samples for a control, catalase, BSA and L-histidine experiment.

Fig. 6.1 Diagram illustrating ZnO nanoparticles capped with a (a) di(octyl)-phosphinate ligand (DOPA) and an (b) oleate ligand.

Fig. 6.2 General form of ZnO nanoparticle synthesis: (a) DOPA-capped and (b) oleate-capped.

Fig. 6.3 Powder XRD patterns of ZnO nanoparticles with (a) dioctylphosphinate (DOPA) and (b) oleate, linoleate and stearate ligands (Wurzite ZnO reference pattern indicated, JCPDS card 00-001-1136, patterns stacked with +1000 intensity to each in turn). The size of the particles may be estimated by analysis of the peak

width using the Scherrer equation. The signals at $2\theta = 47.5$ and 56.6 were analysed for each batch of nanoparticles giving sizes of: ZnO_DOPA (5:1), 2.2 nm; ZnO_oleate (5:1), 2.8-4.1 nm; ZnO_oleate (10:1), 4.9-7.4 nm; ZnO_linoleate (5:1), 2.8-3.6 nm, ZnO_stearate (5:1), 2.8-3.3 nm. The broad signals at $2\theta = 18-25^\circ$ are assigned to the organic ligands, in the case of ZnO_stearate a minor trace of impurity Zn(stearate)₂ may also be present.

Fig. 6.4 Tauc plots derived from UV absorption spectra of ZnO nanoparticles. Band gaps determined: (a) ZnO_DOPA (5:1) = 3.76 ± 0.01 eV and (b) ZnO_oleate (5:1) = 3.48 ± 0.01 eV; ZnO_oleate (10:1) = 3.39 ± 0.01 eV; ZnO_linoleate (5:1) = 3.46 ± 0.01 eV, ZnO_stearate (5:1) = 3.47 ± 0.01 eV.

Fig. 6.5 UV spectra of ZnO nanoparticles dissolved in toluene (approx 0.4 mg/mL). An estimate of the particle size can be made by the onset of UV absorption.²⁹ Sizes were calculated from the maximum gradient of the UV absorption onset corresponding to: (a) ZnO_DOPA (5:1), 2.7 nm and (b) ZnO_oleate (5:1), 3.8 nm; ZnO_oleate (10:1), 4.9 nm; ZnO_linoleate (5:1), 4.0 nm, ZnO_stearate (5:1), 3.6 nm. All sizes are a close match for the sizes estimated by XRD (see Fig 6.3).

Fig. 6.6 TEM images of (a) ZnO_DOPA and (b) ZnO_oleate (5:1).

Fig. 6.7 UV-vis absorption spectra measured in the range of 400 – 700 nm of crystal violet-coated polyurethane (CV), CV and ZnO_DOPA-encapsulated polyurethane (CVZnO_DOPA) and CV and ZnO_oleate-encapsulated polyurethane (CVZnO_oleate). Both ZnO NPs with 5:1 metal:ligand ratio.

Fig. 6.8 XPS spectra for Zn (2p) on (a) CVZnO_DOPA surface, (b) CVZnO_DOPA sputtered 50 s, (c) CVZnO_oleate surface and (d) CVZnO_oleate sputtered 50 s (both 5:1).

Fig. 6.9 UV-vis absorbance spectra measured in the range 400 – 700 nm of (a) CV-coated polymer, (b) CV and ZnO_DOPA-incorporated polymer and (c) CV and ZnO_oleate-incorporated polymer. The samples were exposed to a white light source emitting an average light intensity of 3880 ± 200 lux at a distance of 35 cm from the samples. (d) The rate of photodegradation of CV, CVZnO_DOPA and CVZnO_oleate-encapsulated polymers upon exposure to a high lux intensity white light source (60 days; 3880 lux) shown as a change in absorbance at the CV absorbance maxima ($\lambda = \sim 590$ nm) over time. Data shown with control polymer readings subtracted.

Fig. 6.10 Confocal fluorescence imaging of (a) untreated polymer, (b) CV-coated polymer and (c) CV and ZnO_oleate-encapsulated polymer using a Leica TCS SPE confocal system with an upright microscope and a 20x objective. A 532 nm laser was used as the excitation source and CV fluorescence was detected at 630 nm. The polymer sample is on the left hand side of the image, where the black part of the image represents the background (no fluorescence).

Fig. 6.11 Antibacterial activity of CVZnO_DOPA and CVZnO_oleate polymer samples in the dark and under standard laboratory white light (500 ± 300 lux) against: (a) *E. Coli* ATCC 25922 for 2 h, (b) *E. Coli* ATCC 25922 for 3 h, (c) *S. aureus* NCTC 13143 for 2 h and (d) *S. aureus* NCTC 13143 for 3 h. * indicates bacterial numbers reduced to below the detection limit of 100 colony forming units/mL (cfu/mL).

- Fig. 6.12 Viable counts of *P. aeruginosa* NTCC 10662 after incubation on modified polyurethane samples incubated at 20 °C under dark conditions and exposed to standard laboratory white light (500 ± 300 lux) for: (a) 4 h and (b) 6 h. * indicates bacterial numbers reduced to below the detection limit of 100 colony forming units/mL (cfu/mL).
- Fig. 6.13 Viable counts of *E. coli* 1030 after incubation on modified polyurethane samples incubated at 20 °C under dark conditions and exposed to standard laboratory white light (500 ± 300 lux) for: (a) 4 h and (b) 6 h. * indicates bacterial numbers reduced to below the detection limit of 100 colony forming units/mL (cfu/mL).
- Fig. 6.14 Viable counts of *C. Difficile* 630 Δ erm after incubation on modified polyurethane samples incubated at 20 °C under dark conditions and exposed to standard laboratory white light (500 ± 300 lux) for 72 h.
- Fig. 6.15 Structures of (a) stearic acid, (b) oleic acid and (c) linoleic acid.
- Fig. 6.16 Radical species and singlet oxygen quenchers/inhibitors of Type I and II photochemical pathways used in this investigation (SOD: superoxide dismutase; BSA: bovine serum albumin; FFA: furfuryl alcohol).
- Fig. 6.17 Viable counts of *S. aureus* NCTC 13143 after 2 h (a) in the dark and (b) exposure to standard laboratory white light (500 ± 300 lux) on modified polyurethane samples for a control, superoxide dismutase (SOD) and L-histidine experiment. * indicates bacterial

counts were reduced to below the detection limit of 100 colony forming units/mL (cfu/mL).

Fig. 6.18 Viable counts of *E. coli* ATCC 25922 after (a) 2 h in the dark and (b) 2 h of exposure to standard laboratory white light (500 ± 300 lux) on modified polyurethane samples for a control, superoxide dismutase (SOD) and L-histidine experiment. * indicates bacterial counts were reduced to below the detection limit of 100 colony forming units/mL (cfu/mL).

Fig. 6.19 Viable counts in colony forming units/mL (cfu/mL) of *E. coli* ATCC 25922 after 4 h exposure to standard laboratory white light (500 ± 300 lux) on modified polyurethane samples with the addition of L-ascorbic acid (1 mM).

List of Tables

Table 1.1	Examples of pathogens causing nosocomial infections.
Table 1.2	Examples of common disinfectants used in hospitals.
Table 3.1	Extent of polyurethane swelling (%) after different ratios of acetone and water.
Table 3.2	Summary of the antibacterial activity of Cu-polyurethane and Cu-silicone in the dark against <i>S. aureus</i> NCTC 13143 and <i>E. coli</i> ATCC 25922. Bacterial reduction is given in log form.
Table 3.3	Average light intensities in common hospital surroundings in the UK.
Table 4.1	Concentration (%) of aqueous glutaraldehyde solution used in various industries.
Table 4.2	Summary of the antibacterial activity of polyurethane-encapsulated glutaraldehyde and polyurethane-coated glutaraldehyde against <i>S. aureus</i> 8325-4 and <i>E. coli</i> ATCC 25922. Bacterial reduction is given in log form.
Table 5.1	Overview of the antibacterial activity of polymer samples prepared and tested by the Materials Chemistry Research Centre at UCL against <i>E. coli</i> ATCC 25922. (CV: crystal violet-coated polymer, CVAu: crystal violet and 2 nm gold-encapsulated

polymer, CVMBAu: crystal violet, methylene blue and 2 nm gold-encapsulated polymer).

- Table 5.2 Summary of the antibacterial activity of polyurethane coated with CV and encapsulated with CVZnO in the dark and following white light incubation (6600 ± 000 lux) against *S. aureus* 8325-4 and *E. coli* ATCC 25922. The bacterial activity of polyurethane control and coated with ZnO were not included as they did not demonstrate any significant activity. Bacterial reduction is given in log form.
- Table 6.1 Amount of leaching (mg/L) of Zn^{2+} ions from modified polymer samples after 2 hours and 2 days (SD = standard deviation).
- Table 6.2 Antibacterial activity of modified polymer samples following 1 hour exposure to standard laboratory white light (500 ± 300 lux).
- Table 6.3 Summary of the antibacterial activity of ZnO_oleate and CVZnO_oleate-incorporated polymers in the dark and following white light incubation (500 ± 300 lux) against *E. coli* ATCC 25922 (3 h), *P. aeruginosa* NTCC 10622 (6 h), *S. aureus* NCTC 13143 (2 h), *E. coli* 1030 (4 h) and *C. difficile* 630 endospores (72 h). Bacterial reduction is given in log form.
- Table 6.4 Summary of the nanoparticle surface area and ligand coverage of all ZnO nanoparticles. Surface coverage determined for a typical average size nanoparticle as expected from analysis of UV spectra (Fig. 6.4; note that some size dispersity is likely in the particles and this represents an average scenario). Antibacterial activity of the ligands encapsulated into polyurethane (with CV against *E. coli* ATCC 25922) after 2 h exposure to white light (500 ± 300 lux).

Table 6.5 Bacterial reduction (in log form) of *E. coli* ATCC 25922 and *S. aureus* NCTC 13143 after 2 h exposure to ZnO_oleate and CVZnO_oleate-encapsulated polyurethane with and without the addition of bovine serum albumin (BSA; 0.03%) (a) in the dark and (b) following white light incubation (500 ± 300 lux).

Table 6.6 UV-vis absorbance values at 222 nm of furfuryl alcohol after 3 h exposure to standard laboratory white light (500 ± 300 lux) on control, ZnO_oleate CV, and CVZnO_oleate-incorporated polymer samples.

List of Abbreviations

ATR	Attenuated total reflectance
BHI	Brain heart infusion
BSA	Bovine serum albumin
CCD	Charge coupled device
CDI	<i>C. difficile</i> infection
CFU	Colony forming unit
CRE	Carbapenem-resistant Enterobacteriaceae
CV	Crystal violet
DCM	Dichloromethane
DOPA	Di(octyl)phosphinate
EDX	Energy dispersive X-ray
EPR	Electronic paramagnetic resonance
FFA	Furfuryl alcohol
HAI	Hospital-acquired infection
HINS	High-intensity narrow spectrum
HR-TEM	High-resolution transmission electron microscopy
HPV	Hydrogen peroxide vapour
HPV	Human papilloma virus
IC	Internal conversion
ICP-OES	Inductively coupled plasma-optical emission spectroscopy
ICU	Intensive care unit
ISC	Intersystem crossing
LAAA	Light-activated antimicrobial agent
MAC	MacConkey agar
MB	Methylene blue
MRSA	Methicillin-resistant <i>Staphylococcus aureus</i>
MSA	Mannitol salt agar

NP	Nanoparticle
PBS	Phosphate buffer solution
PDT	Photodynamic therapy
PEG	Polyethylene glycol
PHE	Public Health England
PS	Photosensitiser
PVC	Polyvinyl chloride
QAC	Quaternary ammonium compound
RB	Rose Bengal
ROS	Reactive oxygen species
SEM	Scanning electron microscopy
SOD	Superoxide dismutase
TBO	Toluidine blue O
TEM	Transmission electron microscopy
UTI	Urinary tract infection
UV	Ultraviolet
UV-vis	Ultraviolet-visible
VRE	Vancomycin-resistant enterococci
XPS	X-ray photoelectron spectroscopy
XRD	X-ray diffraction

Chapter 1

1. Hospital-Acquired Infections

1.1 Introductory remarks

This thesis describes the development of antibacterial surfaces for reducing the incidence of hospital-acquired infections (HAIs). The main focus is on the antibacterial activity of polymers coated with photosensitisers and encapsulated with nanoparticles following white light activation and in the dark. This literature review chapter details the incidence of HAIs, the problem of antimicrobial resistance and summarises the common bacterial pathogens found in hospital environments. The chapter then focuses on current prevention strategies for combating these infections, as well as the advantages and disadvantages of alternative cleaning/sterilisation methods. There is a detailed comparison of potential antimicrobial surfaces that can be used to combat HAIs, as well as a brief introduction into the use of light-activated antibacterial surfaces.

1.2 Introduction to the Incidence of Hospital-Acquired Infections

HAIs, also known as nosocomial infections, are infections that occur in patients in a hospital or healthcare facility which were not present at the time of admission. These can include infections that are acquired in the hospital but appear after discharge.¹ The incidence of HAIs has been growing exponentially since 1980 due to the emergence of multidrug-resistant bacteria,² affecting both developed and developing countries around the world. Out of every 100 patients who are hospitalised, 7 in developed and 10 in developing countries will obtain at least one HAI,³ significantly affecting low- and middle-income countries more than high-income countries. At any time, more than 1.4 million people suffer from an

infection acquired in a hospital occurring from surgical wounds, urinary tract infections (UTIs) and lower respiratory tract infections.⁴ Various pathogens attach onto medical devices and implants, such as venous and urinary catheters, resulting in increases in hospital cost and discomfort for patients when they have to be replaced.⁵

HAIs are also spread by direct contact between patients, healthcare workers and microorganisms present within hospital environments.⁶ When a person who carries the microorganism is admitted to the hospital, they are a potential source of infection for patients and staff. Subsequently, patients who become infected are a further source of infection. Patient-to-patient transmission of pathogens is encouraged by poor infection controls, such as accommodating multiple patients in one room, overcrowded conditions within the hospital and transferring patients from one unit to another.⁷ In addition to this, patients with compromised or weaker immune systems have an increased susceptibility to infections.⁸ Healthcare workers can also carry the pathogen on their hands from direct contact with an infected patient or a colonised surface. Once surfaces become contaminated, patients and surrounding surfaces in the vicinity are also susceptible to bacterial contamination, which is a major concern as the environment can act as a reservoir for infectious bacteria.⁶ Numerous studies have shown that environmental contamination can persist for many days and months with several pathogens, including methicillin-resistant *Staphylococcus aureus* (MRSA),⁹ vancomycin-resistant *Enterococcus* (VRE),¹⁰ norovirus¹¹ and *Clostridium difficile* (*C. difficile*).¹²

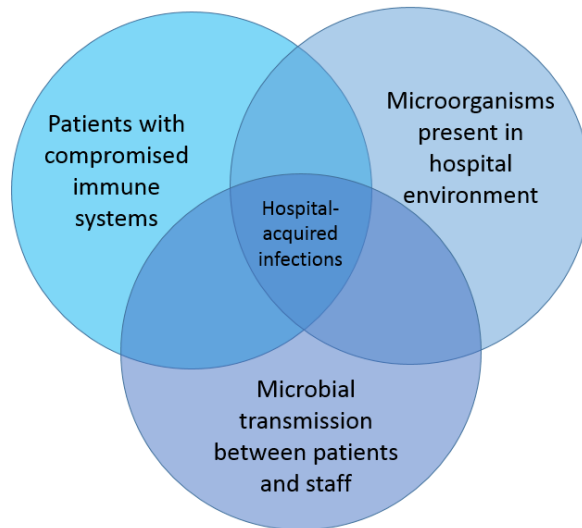


Fig. 1.1 Factors affecting the incidence of HAIs.

The prevalence of HAIs varies across patient groups and hospital wards, partly due to differences in surgical procedures within certain settings. A survey conducted in 2011 found that the prevalence of nosocomial infections was highest amongst patients in intensive care units (ICUs) and surgical wards (23.4% and 8% of patients, respectively).¹³ This may be due to the fact that ICUs care for the most vulnerable patients and procedures common in ICUs and surgical wards (e.g. catheterisation) are associated with increased risk of infection.¹⁴

The endemic burden of HAIs affects hundreds of millions of patients every year, causing emotional stress, disabilities and a reduced quality of life.¹ They are also one of the leading causes of death and result in significant financial and economic costs for the healthcare industry.³ A main contributor to these costs is prolonged hospital stay for infected patients, which also increases the need for drugs, isolation wards, and the use of additional laboratory facilities. Nosocomial infections will become an even greater public health issue as new microorganisms emerge and antibiotic resistance increases.¹⁶

1.3 Antimicrobial Resistance

The discovery of antibiotics in the 1930s transformed medicine and the way we care for patients.¹⁶ Common illnesses became treatable with antibiotics as they served an important role in keeping the public healthy. However, nearly 90 years later, a critical point has been reached in treating infections as new drugs are not being developed rapidly enough in order to keep ahead of the natural ability of bacteria to evolve as they defend themselves against antibiotics.¹⁷ As a result, our most powerful drugs are becoming futile and antibiotic resistance has become one of the greatest global threats to human health. Nearly 2 million Americans develop HAIs per year that are mostly due to multi-drug resistant pathogens, causing around 99,000 deaths.¹⁸ Just one organism, MRSA, kills more Americans every year than Parkinson's disease, HIV/AIDs, emphysema and homicide combined.¹⁹ Multi-drug resistant Gram-negative bacteria cause a high percentage of HAIs, including UTIs, pneumonia and bloodstream infections.²⁰ Patients with infections caused by drug-resistant bacteria are generally more at risk from suffering worse clinical complications and even death, and consume more hospital resources than patients infected with non-resistant forms of the same bacteria.¹⁸

Antibiotic resistance is the resistance of a microorganism to a specific antibiotic drug that was originally effective in treating the infections caused by it.²¹ These resistant microorganisms can survive in the presence of antibacterial drugs so that standard treatment becomes ineffective, allowing the infection to spread and pose a risk to others.²² Antimicrobial resistance, a broader term, is the resistance to drugs for treating infections caused by other microbes as well, such as viruses (e.g. HIV), fungi (e.g. Candida) and parasites (e.g. malaria).²¹ As new resistance mechanisms emerge, our ability to treat common infections weakens, resulting in disability, prolonged illnesses, higher expenditures and a greater risk of death.²³ Antibiotic resistance occurs due to inappropriate use, as antibiotics are not taken at the correct dosage and time and are prescribed

unnecessarily (e.g. for viral infections or for bacteria that are already resistant). People may consume leftover antibiotics from previous prescriptions and pressure doctors for new prescriptions because they want a quick relief from symptoms, regardless of the cause of illness.²⁴ Additionally, patients are frequently prescribed the wrong selection and dosage of antibiotics which are unnecessary for treatment.²³

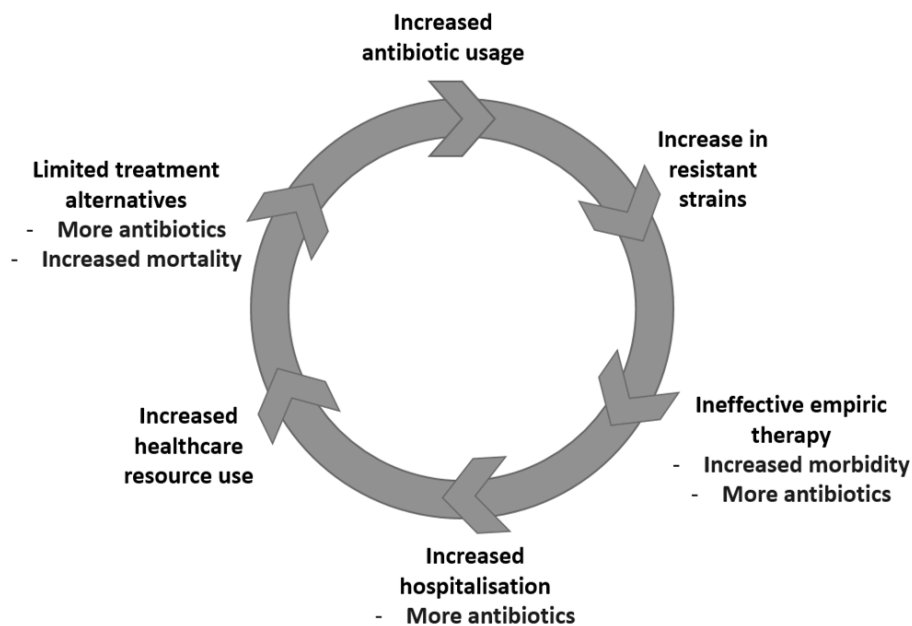


Fig. 1.2 Antibiotic resistance cycle

1.4 Common Pathogens in Hospitals

Most HAIs occur from the patients' own endogenous flora, however, an estimated 20 - 40% are a result of cross-infection *via* healthcare workers in contact with patients or by touching contaminated surfaces.²⁵ Various pathogens can persist for several days and months on surfaces, including MRSA, VRE, *Acinetobacter* species, *C. difficile* and norovirus.²⁶ These pathogens can adhere to surfaces by forming biofilms within 24 hours.²⁷ In fact, most antimicrobial therapies are unable to kill biofilms as the concentration of disinfectants required to kill sessile bacteria may be 1000

times higher than that required to kill planktonic bacteria of the same strain.²⁷ Some studies suggest that Gram-negative bacteria survive longer on surfaces than Gram-positive²⁸ and others suggest that the type of surface can affect adhesion, i.e. a longer persistence of bacteria on plastic or steel compared to glass.²⁹ Environmental factors also affect the survival of bacteria, viruses and fungi on surfaces, as increased humidity (> 70%) and lower temperatures (4 – 6°C) can increase persistence.¹² The characteristics and symptoms of some clinically-relevant infections are summarised in Table 1.1.

Microorganisms	Transmission	Maximum survival length on dry surface	Symptoms
<i>Enterococcus</i> spp., including VRE	Person-to-person contact and food products	16 months	Skin, blood and respiratory tract infection
<i>Staphylococcus aureus</i> , including MRSA	Contact with a purulent lesion or carrier, unsanitary conditions, overcrowding	<i>S. aureus</i> 10 days MRSA 9 weeks	Skin, blood, respiratory tract infection, septicaemia and death
<i>Klebsiella pneumoniae</i>	Contact with contaminated surfaces and medical devices	30 months	Urinary tract infections, pneumonia, septicaemia
<i>Acinetobacter baumannii</i>	Extensive contamination in the environment	5 months	Bloodstream infection and pneumonia
<i>Escherichia coli</i>	Person-to-person transmission and ingestion of contaminated food/water	16 months	Blood and urinary tract infection
<i>Clostridium difficile</i>	Extensive contamination in the environment	5 months (and on hospital floors)	Diarrhoea and colitis

Table 1.1 Examples of pathogens causing nosocomial infections

MRSA and *C. difficile* infections can be a major concern for hospitalised patients and are regularly publicised when looking at the state of HAIs.⁶ In recent years, successful efforts have been made to reduce the rates of these deadly pathogens in hospitals. Based on results obtained from a selection of hospitals in England, there was a large reduction in both MRSA and *C. difficile* rates in 2012 compared to 2006.¹³ Despite this reduction, preventative efforts are still required to keep the incidence of these infections low. However, infections with other organisms, such as *Klebsiella pneumoniae* (*K. pneumoniae*) and *E. coli* have been rapidly emerging, as

infections common in the respiratory tract, urinary tract and on surgical sites are still rife.³⁰ These bacteria belong to a class of organisms called *Enterobacteriaceae*, which are found in the human intestine and are difficult to treat as they are highly resistant to antibiotics.^{31,32}

1.4.1 Methicillin-resistant *Staphylococcus aureus*

MRSA is a type of *Staphylococcus* bacterium that is resistant to antibiotics known as beta-lactams.³³ These antibiotics include methicillin, penicillin, oxacillin and amoxicillin.^{33,34} Methicillin resistance in *S. aureus* was primarily identified in the 1960s amongst hospitalised patients by contamination from healthcare workers. After this outbreak, extensive basic cleaning regimes were put into practice to minimise the spread of this “superbug”. After cleaning shared common areas and changing the blood pressure cuffs of patients, fewer patients were colonised with the bacteria.³⁵ The number of cleaning hours doubled from 60 h to 120 h a week and as a result, there was an immediate reduction in the number of newly-infected patients, saving around £30,000 in hospital costs.³⁶

1.4.2 *Escherichia coli*

E. coli is a Gram-negative bacterium that normally lives in human and animal intestines because it is necessary for bowel function and is an important part of a healthy human intestinal tract.³⁸ However, it becomes problematic when entering our bloodstreams or tissues inside the body, causing up to 40% of septicaemia and 75% of meningitis cases.²⁰ It thrives in moist hospital environments and can also be found in solutions, humidifiers, endotracheal tubes, medical devices and equipment.³⁸ *E. coli* is responsible for 1 in 2000 neonatal meningitis cases, which is caused by invading the bloodstream of infants from the nasopharynx and carried to the meninges.³⁹ It is also the leading cause of bloody diarrhoea as some *E.*

coli strains are responsible for intestinal diseases.⁴⁰ In addition to this, *E. coli* is widely known for causing 90% of UTIs.⁴¹ In some people (children under 5 in particular) the infection causes haemolytic uremic syndrome which is a severely complicated disease that destroys red blood cells and causes kidney failure.⁴²

Recent studies showed that between 2009 and 2014, the incidence of drug-resistant *E. coli* in the US doubled from a rate of 5.28 incidents to a rate of 10.5 incidents per 100,000 patients, with an average age of 72 years old for infected patients.⁴³ A recent report from Public Health England (PHE) showed that more people suffered from significant antibiotic-resistant infections between 2010 and 2014. *E. coli*-related bloodstream infections increased by 15.6% and *K. pneumoniae*-related infections increased by 20.8%.⁴⁴

1.4.3 *Pseudomonas aeruginosa*

Gram-negative bacteria cause around 30% of bloodstream infections in ICUs, in particular, species of *Klebsiella* sp., *E. coli*, *Enterobacter* sp. and *P. aeruginosa*. Studies show that water sources in healthcare environments are a persistent reservoir for *Pseudomonas* spp. and pose a serious risk for vulnerable patients.¹⁴ *P. aeruginosa* can be transmitted from contaminated sinks to hands during hand-washing⁴⁴ and adhere onto surfaces such as pipes, water lines, sink traps and hospital drains.³⁶ It is a versatile pathogen which causes various infection types, particularly in critically ill or immunocompromised patients.¹⁴ Reports from the National Nosocomial Infections Surveillance system (1986 – 2003) described *P. aeruginosa* as the second most common cause of pneumonia (18.1%), the third most common cause of UTIs (16.3%) and the eighth most frequently isolated pathogen from the bloodstream (3.4%).⁴⁶

1.4.4 *Clostridium difficile*

Hospital-acquired *C. difficile* infection (CDI) is a main cause of morbidity and mortality, because *C. difficile* is resistant to several antibiotics. It is an anaerobic Gram-positive bacterium and is able to form dormant spores which are resistant to drying and heating.⁴⁷ The ability of these spores to survive for many months poses a major threat to hospitals. One of the few ways to kill *C. difficile* spores is by using chlorinated products, such as bleach.¹⁴ Highly concentrated products are even more effective disinfectants because they can release higher levels of free chlorine (e.g. 5000 mg/litre).⁴⁸ However, the efficacy of these disinfectants to eliminate environmental spores depends on many factors, such as contact time of disinfectants, training and knowledge of staff, and the time allocated to staff for cleaning.³⁶

CDIs are often caused from surfaces contaminated with faecal species, which then spreads from human contact.⁴⁹ Once *C. difficile* is ingested and reaches the human intestine, it germinates into its vegetative form. It then secretes toxins which cause severe diarrhoea, abdominal pain or colitis.⁵¹ In 2009, around 340,000 patients remained hospitalised due to CDI in the US, causing many fatalities.⁵¹ *C. difficile* has mutated over time and is now resistant to many antibiotics. It is commonly found on hospital surfaces, including bed frames, floors and sinks, with outbreaks occurring where disinfectants are found to be ineffective against spores.⁵²

1.5 Prevention Strategies

When surfaces such as clinical equipment or medical devices are contaminated, they can promote the transfer of microorganisms between patients and healthcare workers. This is also the case for frequently touched surfaces such as bed rails, mattresses, bedside tables, toilets, and any surface within a ward that an infected patient has previously stayed in. In fact, newly admitted patients are at high risk of being contaminated with

the same pathogen that infected the previous patient in that room.³⁶ If any frequently touched surfaces are found to contain more than 250 – 500 CFU/100 cm², improvements in cleaning and disinfecting should be employed.⁵³ In an ICU, it was found that nurses call buttons were harbouring 7118 CFU/100 cm² and bed rails contained 17,336 cfu/100 cm².⁵⁴ Studies have shown that ~50% of toilets, toilet floors and bed rails were contaminated with *C. difficile*, and found some surfaces harbouring around 1300 colonies when sampled with a sponge.⁴⁹

The US-based CDC (Centers for Disease Control and Prevention) has issued guidelines for cleaning and disinfecting the environment as well as personal protective equipment and hand hygiene.⁵⁵ Hand hygiene contributes significantly to the spread of HAIs among patients and staff and is responsible for 20 – 40% of cross-infection *via* the hands of healthcare personnel.⁵⁶ Decontamination of hands prior to patient contact is vital in minimising the spread of bacteria and the use of gloves does not fully protect them either.⁵⁷ Alcohol gel hand sanitisers can be effective if there is no organic material on the persons hands and if it is in direct contact with the bacteria or virus.⁵⁸ However, this should not be substituted for basic hand washing with soap and water.⁵⁹

Hospital surfaces are cleaned hourly, daily or weekly depending on if the surfaces appear dirty, there are spillages, or after patient discharge. In the UK, routine cleaning is performed manually by using basic equipment such as mops, wipes, cloths, buckets and brushes.⁶⁰ Electronic cleaning equipment is also utilised (e.g. vacuum cleaners).⁶¹ The frequency and means of cleaning also depends on the surface itself; whether it is critical or non-critical. Critical surfaces include frequently touched surfaces and thus, must be cleaned and disinfected more thoroughly and regularly.⁶² However, cleaning without a disinfectant merely redeposits the bacteria, rather than killing them, and this results in biofilm formation.⁶³ The CDC recommends the use of bleach and other chemical disinfectants such as

aldehydes, alcohols and quaternary ammonium compounds to eliminate microorganisms.⁶⁴

Disinfection typically involves the use of chemical agents which eliminate most microbes (excluding spores)⁶⁵ and sterilisation destroys all microorganisms by using heat, pressure or chemical methods.⁶⁴ When choosing a sterilant or disinfectant, various factors need to be considered for maximum efficiency. These include user acceptability, types of surfaces and equipment it will clean, infection rates and their mechanism of action.^{2,64} Biocidal agents have many target sites within the bacterial cell; they can penetrate into the cell or interact with the surface, bacterial cell wall and the outer membrane. They can cause reversible or irreversible changes and cause cell death.⁶⁶ However, they must be easy to use, safe against human cells and should not leave any toxic residues.² The chemical structure, pH and temperature of the biocide can also affect its efficiency. Depending on the ability of the biocide to kill bacterial spores, it is categorised as either a sterilant or high-, intermediate- or low disinfectant (as shown in Table 1.2).^{62,66}

Disinfectant	Examples	Result	Use
<i>Sterilants</i>	Steam, dry heat, glutaraldehyde, peracetic acid, hydrogen peroxide	Destroys all microorganisms including bacterial spores	Critical instruments for penetrating tissue, e.g. implants, needles and other surgical equipment
<i>High-level disinfectants</i>	Glutaraldehyde, hydrogen peroxide, peracetic acid, ortho-phthalaldehyde, formaldehyde	Destroys all microorganisms excluding bacterial spores	Semi-critical equipment, e.g. endoscopes and diaphragms
<i>Intermediate-level disinfectants</i>	Alcohols, phenolics, hypochlorites, iodine, iodophors,	Destroys almost all vegetative bacteria, fungi, viruses and inactivates <i>Mycobacterium bovis</i>	Non-critical equipment in contact with skin, e.g. thermometers
<i>Low-level disinfectants</i>	Phenolics, iodophors, quaternary ammonium compounds	Destroys some vegetative bacteria, some fungi and viruses, does not inactivate <i>Mycobacterium bovis</i> or spores	Non-critical equipment and surfaces, e.g. stethoscopes, blood pressure cuffs, bedside tables

Table 1.2 Examples of common disinfectants used in hospitals

Biocides have been used for many years for antiseptic use, including ethanol, phenolics, hypochlorites and quaternary ammonium

compounds.⁶⁷ More recently other compounds have been used, including chlorhexidine, glutaraldehyde and *ortho*-phthalaldehyde.⁶⁸ Disinfectants are not always effective in killing all bacteria because some bacteria are resistant to these compounds and unproductive cleaning methods are frequently employed. Although disinfectants are efficacious against vegetative bacteria, most viruses and fungi, the majority of them are not active against spores or norovirus. However, aldehyde-based disinfectants demonstrate antibacterial activity against several pathogens and spores by denaturing proteins and nucleic acids.^{2,64,66}

Alcohol wipes have been employed on non-critical hospital surfaces and clinical devices to assist in reducing microbial load.³⁹ However, in most cases they have resulted in cross-contamination as they can spread organisms rather than eradicating them on surfaces that are frequently touched by patients or staff. Moreover, a single wipe is used many times to disinfect a surface before it is discarded.^{2,39,64} Mops are repeatedly used to clean hospital floors, but they can also cause contamination if not used appropriately. By using a detergent solution instead of water to rinse mop heads, 80% of microbial burden can be reduced.¹⁵ Water can act as a means for bacteria to spread, thus fresh detergents are more effective and should be replaced every 15 minutes when in use.⁶⁹

Terminal cleaning is performed after a patient contaminated with a pathogen has been discharged. This includes a thorough deep clean of all surfaces and the removal of detachable objects, e.g. bedding and curtains. All medical equipment should be cleaned before and after patient use, regardless of how long or often it is used.³⁹ This is vital as most clinically used equipment will be at a high risk of microbial contamination. Wiping with alcohols is a sufficient way of disinfecting stethoscopes, for example, but this procedure is sometimes overlooked or abandoned when staff are overworked.⁶⁴ Given that many nurses nowadays have taken on duties originally carried out by doctors, it is understandable that basic cleaning has been overlooked compared to other professional responsibilities. It is

also important that the disinfectant is non-toxic towards humans, unaffected by organic contaminants and applied with sufficient exposure time.⁷⁰ Therefore, better disinfection strategies need to be developed that are self-sufficient and can reduce microbial contamination without the constant requirement of manual cleaning.

1.6 Alternative methods to basic cleaning

Over 50% of hospital sites and surfaces remain untouched by conventional manual cleaning methods.⁷¹ Due to the continuing transmission of microbes in hospital environments, innovative solutions have been developed to improve the quality of cleaning as many surfaces remain unclean. New disinfection strategies are imperative as bacterial resistance to certain disinfectants grows, partly due to the formation of biofilms.⁷² Touchless technologies can be used to overcome certain deficiencies of manual cleaning by eliminating human labour.⁷³ These include fumigation methods⁷⁴ and self-sterilising surfaces.^{2,39,75}

1.6.1 Ozone

Ozone is a cheap, highly oxidising agent and is very effective against vegetative bacteria but not against fungi and bacterial spores.⁷⁶ It is potentially toxic and corrosive towards metals and rubber, despite rapid dissociation into oxygen.⁷⁷ Studies have shown that the use of ozone in laundry decontamination has reduced numbers of *E. coli* by 5 log₁₀⁷⁸ and *C. difficile* numbers by >4 log₁₀ on various surfaces.⁷⁶ An earlier study used this gaseous decontaminant in hospital rooms previously occupied by MRSA patients; it did not achieve any significant results and also initiated respiratory symptoms amongst healthcare workers.⁷⁹

1.6.2 Steam Vapour

Steam vapour sterilisation machines can efficaciously reduce a wide range of bacteria to below detection limits within 5 seconds, including *P. aeruginosa* and MRSA.¹⁴ It can be applied to various hard and soft surfaces without prior cleaning, reduces cleaning costs and consumes 90% less water without the use of harsh chemicals.⁸⁰ However, there are impractical problems when the use of steam is applied to frequently touched surfaces such as doorknobs, computers, and other electrical devices.⁸¹ Moreover, residual moisture from the steam could be a health and safety risk for patients and staff, especially on exposed floor surfaces. It may also be difficult to use in overcrowded wards and could potentially aggravate breathing problems for patients or staff with respiratory conditions.⁸² Thus, steam vapour machines should only be used in well-ventilated areas and have been proven effective in non-clinical areas and toilets.³⁶ Ethylene oxide gas is widely used for sterilising healthcare instruments and devices.² It is exposed to the products in a sealed chamber under vacuum and sterilises all accessible surfaces.⁸³ It is highly potent against viruses, bacteria and fungi, but must be used carefully due to high toxicity and flammability.⁸⁴ Hydrogen peroxide vapour (HPV) is also used to disinfectant clinically used materials and surfaces. It has a low toxicity and can be applied to most inanimate materials.^{2,66}

1.6.3 Hydrogen peroxide

Hydrogen peroxide was first isolated in 1818 and has been used in the pharmaceutical industry as a popular substitute for ethylene oxide, chlorine dioxide and ozone.⁶⁴ Several systems containing hydrogen peroxide have been used to disinfect hospital wards and have shown to be effective as HPV systems and dry aerosols.² They are able to eradicate most, if not all, hospital pathogens, but are costly and have to be operated by trained personnel in unoccupied wards.³⁹ Effective hydrogen peroxide

decontamination can take several hours to complete^{39,85} which proves difficult for today's hospitals as most wards are overcrowded and thus, cannot be used in specialist units offering 24 hour care services.

1.6.4 Gas Plasma

Gas plasma is used as an alternative sterilisation method that is mainly targeted towards devices rather than surfaces.⁸⁶ The plasma contains a mixture of atoms, ions, electrons, photons and radicals (including ozone, atomic oxygen, nitrogen oxides, superoxide and hydroxyl).² When the plasma discharges, the gas enters an ionised state (*via* electron transfer) which results in antibacterial activity.⁸⁶ Depending on the conditions used to form the plasma, there are possible types: thermal and non-thermal. Thermal plasmas require a higher pressure and temperature than non-thermal plasmas.^{2,87} Its advantages include ease of use, low cost, does not require chemical products and is non-toxic to the skin.⁶⁴ However, its bactericidal activity is greatly dependant on exposure time and bacteria cell density.^{2,64}

1.6.5 UV Light

UV irradiation has been used at specific wavelengths to disinfect surfaces, medical devices and air.⁸⁸ UV-C light has a specific wavelength of ~254 nm which is within the germicidal range of the electromagnetic spectrum (200 – 320 nm).⁸⁸ The effect of UV irradiation is dependent on many factors; exposure time, light positioning and intensity, barriers between the light and target material and the flow of air movement.³⁹ It has been shown to significantly reduce *C. difficile* spores within 50 minutes⁸⁹ and vegetative bacteria within 15 minutes, but surfaces contaminated with organic soiling can hinder the antimicrobial effect.⁶² Experts have stated that UV light should not be used as a replacement for manual cleaning but as a

supplementary method.⁹⁰ UV-C technology would be expensive, and similarly to hydrogen peroxide, it would only be operated in an empty ward since UV exposure is hazardous to patients. Additionally, it is considerably less effective when shielded from the target surface and could potentially damage materials, such as polymers, if continually exposed.⁹¹

1.6.6 High-intensity narrow spectrum

High-intensity narrow spectrum (HINS) exhibits microbiocidal activity using a narrow bandwidth of high-intensity visible light at 405 nm.⁹² The mechanism of activity is from the photoexcitation of endogenous porphyrin molecules within bacterial cells (i.e. porphyrinogenic bacteria) which produces singlet oxygen and highly reactive species lethal to bacteria. HINS light is harmless to humans and was reported to reduce 90% of surface bacterial levels of a room occupied by an MRSA-infected burns patient.³⁶

1.7 Antibacterial Surfaces

Using regular cleaning regimes to control infections caused by pathogenic microorganisms will not completely eradicate the problem of HAIs, and in recent years, there has been a growing interest in the development of “self-sterilising” or “self-sanitising” antibacterial surfaces. They were first developed in 1964 but were not considered as effective controls for minimising the spread of bacteria until years later.³⁹ Once a surface has been contaminated, a cyclical problem exists as contamination can spread to others in the vicinity and further assist in bacterial transmission.⁹³ Effective antibacterial surfaces have the potential of preventing the spread of infections in a hospital environment between frequently touched surfaces, patients and staff (Fig. 1.3). They can reduce microbial burden without staff having to spend hours manually cleaning surfaces.

There are several types of antibacterial surfaces with coatings that can reduce biofilm formation by killing microbes on the surface or by preventing bacterial adhesion.^{94,95} Bacterial growth can be controlled by three methods of action: (i) surface contact killing of bacteria by disrupting bacterial cell membranes,⁹⁶ (ii) biocide leaching involving the release of cytotoxic species attaching to the bacteria,² and (iii) anti-adhesion surfaces which use super-hydrophobic surfaces to prevent microbial adhesion.⁹⁷

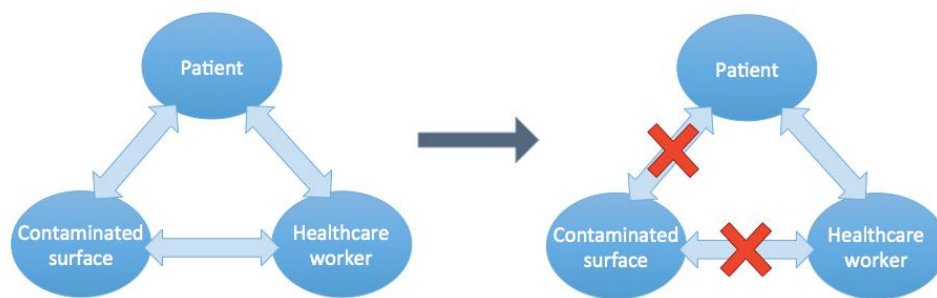


Fig. 1.3 Role of antibacterial surfaces in preventing HAIs from the direct transfer of microorganisms.

1.7.1 Biocide leaching

Some commercially available antibacterial surfaces operate by effective microbicide leaching to suppress microbial growth. Microban® is a well-known product that releases an antimicrobial agent known as triclosan [5-chloro-2-(2,4-dichlorophenoxy)-phenol], making the surface resistant to bacterial growth.⁹³ Triclosan leaches from the surface, resulting in a non-permanent bactericidal activity. This could potentially increase bacterial resistance because the active antibacterial agent is continuously leaching out.⁹⁸ However, many liquid soap products, soap bars and toothpastes⁹⁹ contain triclosan, as well as common kitchen touch surfaces such as cling film and chopping boards.⁹³ Some studies suggest that under UV light activation, triclosan produces dioxins that are very hazardous to humans.¹⁰⁰ Surfacine is another example of biocidal leaching which

incorporates silver iodide as the antimicrobial agent. These surfaces can reduce bacterial levels by 100 CFU/in² for up to two weeks and retains activity after cleaning.² The microorganisms are killed by the biocide penetrating through the cell and causing cell death from an electrostatic interaction between the compound and the bacteria.¹⁰¹

1.7.2 Antimicrobial polymers

Antimicrobial polymers reduce microbial growth by either incorporating biocides or antibiotics on the surface or by inherently killing the microorganisms.¹⁰² Chitosan is widely used in the medical field due to its intrinsic antimicrobial ability. It is a linear polycationic heteropolysaccharide copolymer of β -1,4-linked D-glucosamine and N-acetyl-D-glucosamine, obtained from partial alkaline N-deacetylation of chitin.¹⁰³ Gram-negative bacteria are more susceptible to chitosan than Gram-positive bacteria because Gram-negative bacteria have a more negatively charged surface that allows chelation and electrostatic interaction between the polymer and bacterial cell wall.¹⁰⁴ Gram-positive bacteria have a more stable cell wall structure as they contain a polyanionic lipoteichoic acid.¹⁰⁵

Nitrogen-containing polymers, such as quaternary ammonium compounds (QACs) possess antibacterial activity from an electrostatic interaction between the bacterial cell wall and the positively charged QAC, followed by denaturation of structural proteins and enzymes from the integration of the hydrophobic QAC tail into the bacterial hydrophobic membrane.¹⁰⁶ QACs with 12-14 alkyl chains are highly effective against Gram-positive bacteria.¹⁰⁷ Antimicrobial polymers are suitable materials for frequently touched surfaces in hospitals as they can be applied to a diverse range of objects.

1.7.3 Anti-adhesive coatings

Extremely hydrophobic or hydrophilic materials are an effective way to prevent microbial adhesion because the bacteria cannot colonise a surface to form biofilms. A way to measure hydrophobicity or hydrophilicity is by measuring the water droplet contact angle on a surface.¹⁰⁸ Ideally, self-cleaning surfaces require a contact angle less than 10° (superhydrophilic) or greater than 140° (superhydrophobic).¹⁰⁹ Generally, smoother surfaces are much harder to colonise than rough surfaces.⁹³ One way of preventing microbial adhesion is by coating the surface with a layer of poly(ethylene glycol) (PEG), from hydrophilic interactions with the hydrophobic bacterial cell membrane.¹⁰² PEG and PEG-modified surfaces are well established for reducing microbes and can inhibit bacterial adhesion by up to $3 \log_{10}$.⁹³

Polymers with zwitterionic head groups can also inhibit microbial adhesion and biofilm formation.¹¹⁰ It is proposed that zwitterionic heads can accumulate large amounts of water, making the surface hydrophilic. This causes reversible reactions between the surface and bacterial cells which inhibit bacterial adhesion.¹¹¹ These surfaces can potentially be used to coat catheters and other medical devices as they produce an effective barrier towards biofilm formation that can prevent catheter-related infections.⁹⁵

1.7.4 Silver-coated surfaces

The antibacterial properties of silver have been exploited for centuries; for example, the Greeks and Romans used silver coins to store water.¹¹² In the 1900s, 1% silver nitrate solution was used to prevent blindness from eye infections in newborns.⁹³ Silver ions (Ag^+) can bind to thiol groups ($-\text{SH}$) in the bacteria and affect the cell wall and membrane, causing inhibition of cells.¹¹³ The antibacterial activity of silver is somewhat dependent on surface area of the particles, thus silver nanoparticles are favoured.¹¹⁴ However, Ag^+ ions do not confer long-term antibacterial activity because silver is used up in the process. Silver nanoparticles have been used to

inhibit environmental contamination and colonisation of bacteria on medical devices and catheters.¹¹⁵

1.7.5 Copper and copper alloy surfaces

Metallic copper surfaces have been investigated for antibacterial properties. Some reports have shown copper surfaces to reduce bacterial contamination from hospital pathogens by 7 log₁₀ within 2 hours.³⁹ Another study reported that the risk of HAIs reduced by 58% in ICU rooms fitted with copper alloy surfaces.¹¹⁶ Copper is highly toxic towards bacterial cells; it can bind to proteins, cause oxidation stress *via* the production of hydrogen peroxide and disrupt osmotic balance in the cells.¹¹⁷

1.7.6 Light-activated antibacterial surfaces

Bactericidal polymers can be very effective at killing bacteria by incorporating light-activated antimicrobial agents (LAAAs) into the polymer substrate and onto the surface.⁹³ Unlike most antibacterial agents, they do not target specific areas within a microorganisms and thus, avoid the potential problem of bacteria developing resistance towards this treatment.¹¹⁹ These antibacterial polymers kill microbes by producing reactive oxygen species (ROS) which are produced by the interaction of a photosensitiser with light^{119,120} (described in detail in Chapter 2). Clinical studies have shown that LAAAs are able to kill bacteria, viruses and fungi that are on, or up to a distance of 0.65 mm from the illuminated antibacterial surface, due to the production of free radicals.¹²⁰ There are two main types of antibacterial surface coatings that utilise LAAAs: (1) coatings containing titanium dioxide (TiO₂)-based catalysts⁹³ and (2) coating surfaces with a photosensitiser.^{93,118-120} These LAAA systems can significantly reduce bacterial adhesion and prevent biofilm formation of a wide range of hospital pathogens.¹²⁰

1.7.6.1 Titanium oxide-based antibacterial surfaces

TiO₂ is the most widely used photocatalyst (a substance that generates catalyst activity using energy from light)¹²¹ with the ability to retain maximum antibacterial activity against pathogens during light activation. Unlike antibiotics or the use of silver-containing surfaces, these self-sterilising surfaces are non-specific so organisms are unable to evolve resistance against them. Studies have shown a reduction of MRSA contamination with TiO₂ treatment in a clinical environment.¹²² The mechanism (Fig. 1.4) in which this semiconductor kills the bacteria is by absorbing light, which then promotes an electron from the valence band into the conduction band; creating an electron (-) and a positive hole (+). The electron and hole pair creates reactions at the surface to produce singlet oxygen that can then interfere with the bacterial cell wall causing cell damage.¹²³

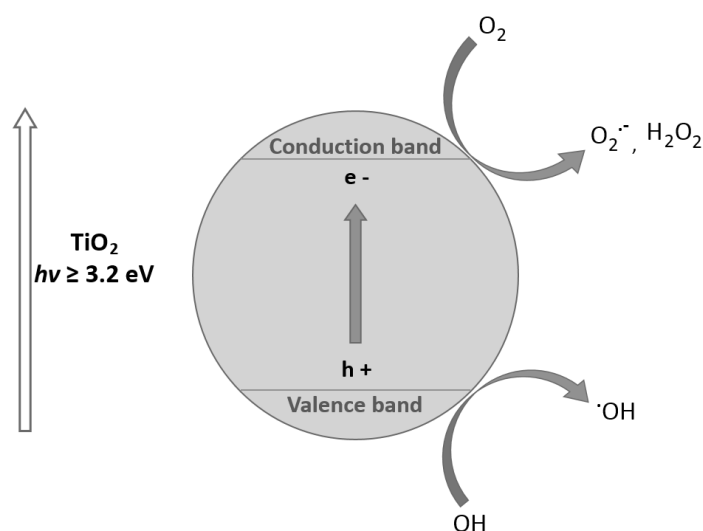


Fig. 1.4 Photo-excitation processes of TiO₂.

The main drawback of TiO₂-based self-sterilising surfaces is that they require UV light activation to kill bacteria, as TiO₂ has a band onset of ~ 3.2 eV.¹²⁴ Therefore, these surfaces would be more effective on the outside of

buildings where UV light is abundant rather than inside buildings where it is less so. For this reason, TiO₂ can be modified to be photocatalytically active under visible light rather than UV light.⁹³ This can be achieved by doping elements such as nitrogen, sulphur or carbon into the TiO₂ structure.¹²³ Additionally, metal nanoparticles (e.g. Ag) can be coated onto the TiO₂ surface to shift the band onset so that the surface can absorb photons of wavelength above 385 nm and operate as a photocatalyst under visible light.^{93,123}

1.7.6.2 *Dye-based antibacterial surfaces*

Light-activated organic dyes, known as photosensitisers, can be incorporated into surface coatings to reduce bacterial contamination by producing highly reactive radical species and/or singlet oxygen *via* two photochemical mechanisms: Type I (electron transfer) and Type II (energy transfer).¹²⁵⁻¹³⁰ Non-toxic photosensitisers have also been incorporated into catheters for preventing catheter-associated infections and have been reviewed extensively by Noimark *et al.*¹³¹ A detailed description of photo-activated surfaces will be given in Chapter 2.

1.7.7 Concerns over antibacterial surfaces

Antibacterial surfaces are highly effective at reducing common microorganisms found in hospitals, but more studies need to investigate the bactericidal effects of these surfaces against more resistant bacteria, as well as *C. difficile* spores. More information needs to be provided on the overall cost-effectiveness of these surfaces, including their long-term durability and whether antibacterial activity is affected by temperature, humidity, organic contamination and the frequency of cleaning.

The increased rate of HAIs and antimicrobial resistance presents a global threat to the healthcare industry as many infections are becoming more difficult to treat. Various hospital pathogens have become resistant to multiple antibiotics, which greatly affects immunocompromised and elderly patients. There is a lack of cleanliness and hygiene that has resulted in contamination between patients, staff and hospital surfaces. Although prevention strategies are in place, alternative cleaning and disinfection methods are required to combat nosocomial infections. This chapter has detailed many alternative methods to basic cleaning and introduces the use of antimicrobial surfaces, in particular, light-activated antimicrobial surfaces. The following chapter highlights the mechanism by which these photo-activated surfaces operate, as well as incorporating nanoparticles into these surfaces for an enhanced bactericidal effect.

References

- 1 Revelas A. Healthcare – associated infections: A public health problem. *Nigerian Medical Journal : Journal of the Nigeria Medical Association*. 2012;53(2):59-64.
- 2 Abreu AC, Tavares RR, Borges A, Mergulhao F, Simeos M. Current and emergent strategies for disinfection of hospital environments. *Journal of Antimicrobial Chemotherapy*. 2013;1-15.
- 3 WHO Guidelines on Hand Hygiene in Health Care: First Global Patient Safety Challenge Clean Care Is Safer Care. Geneva: World Health Organization, 2009. Available from: <https://www.ncbi.nlm.nih.gov/books/NBK144013/>
- 4 Ginawi I, Saleem M, Sigh M, et al. Hospital Acquired Infections Among Patients Admitted in the Medical and Surgical Wards of a Non-Teaching Secondary Care Hospital in Northern India. *Journal of Clinical and Diagnostic Research : JCDR*. 2014;8(2):81-83.
- 5 Ribeiro M, Monteiro FJ, Ferraz MP. Infection of orthopedic implants with emphasis on bacterial adhesion process and techniques used in studying bacterial-material interactions. *Biomatter*. 2012;2(4):176-194.
- 6 Collins AS. Preventing Health Care–Associated Infections. In: Hughes RG, editor. *Patient Safety and Quality: An Evidence-Based Handbook for Nurses*. Rockville (MD): Agency for Healthcare Research and Quality (US); 2008 Apr. Chapter 41.
- 7 Aitken C, Jeffries DJ. Nosocomial Spread of Viral Disease. *Clinical Microbiology Reviews*. 2001;14(3):528-546.
- 8 Ricklin D, Lambris JD. Complement in Immune and Inflammatory Disorders: Pathophysiological Mechanisms. *The Journal of Immunology*. 2013;190(8):3831-3838.
- 9 Gardam MA. Is methicillin-resistant *Staphylococcus aureus* an emerging community pathogen? A review of the literature. *The Canadian Journal of Infectious Diseases*. 2000;11(4):202-211.

- 10 Baden LR, Thiemke W, Skolnik A, Chambers R, Strymish J, Gold HS, Moellering Jr RC, Eliopoulos GM. Prolonged Colonization with Vancomycin-Resistant *Enterococcus faecium* in Long-Term Care Patients and the Significance of "Clearance", *Clinical Infectious Diseases*. 2001;33(10):1654-1660.
- 11 Arias, KM. Contamination and Cross Contamination on Hospital Surfaces and Medical Equipment. *Initiatives in Safe Patient Care*. Available on: <http://www.initiatives-patientsafety.org/assets/initiatives4.pdf>.
- 12 Kramer A, Schwebke I, Kampf G. How long do nosocomial pathogens persist on inanimate surfaces? A systematic review. *BMC Infectious Diseases*. 2006;6:130.
- 13 Byrne JA, Dunlop PSM, Hamilton JWJ, Polo-Lopez P, Sharma PK, Vennard ASM. A Review of Heterogeneous Photocatalysis for Water and Surface Disinfection. *Molecules*. 2015, 20(4), 5574-5615.
- 14 Sydnor ERM, Perl TM. Hospital Epidemiology and Infection Control in Acute-Care Settings. *Clinical Microbiology Reviews*. 2011;24(1):141-173.
- 15 Bourn J. *The Management and Control of Hospital Acquired Infection in Acute NHS Trusts in England*. 2000: National Audit Office.
- 16 Davies J, Davies D. Origins and Evolution of Antibiotic Resistance. *Microbiology and Molecular Biology Reviews*. 2010;74(3):417-433.
- 17 National Institutes of Health (US); Biological Sciences Curriculum Study. NIH Curriculum Supplement Series [Internet]. Bethesda (MD): National Institutes of Health (US); 2007. Understanding Emerging and Re-emerging Infectious Diseases. Available from: <http://www.ncbi.nlm.nih.gov/books/NBK20370/>
- 18 Ventola CL. The Antibiotic Resistance Crisis: Part 1: Causes and Threats. *Pharmacy and Therapeutics*. 2015;40(4):277-283.
- 19 Combating Antimicrobial Resistance: Policy Recommendations to Save Lives: IDSA Public Policy. *Clinical Infectious Diseases (Suppl 5)*. 2011; 52:S397-S428.
- 20 Peleg AY, Hooper DC. Hospital-Acquired Infections Due to Gram-Negative Bacteria. *The New England journal of medicine*. 2010;362(19):1804-1813.

- 21 Hoffman SJ, Caleo GM, Daulaire N, Elbe S, Matsoso P, Mossialos E, Rizvi Z, Rottingen JA. Strategies for Achieving Global Collective Action on Antimicrobial Resistance. *Bull. World. Health. Organ.* 2015;93:867-876.
- 22 World Health Organization: WHO's first global report on antibiotic resistance reveals serious, worldwide threat to public health, 2014.
- 23 Antibiotic resistance threats in the United States, 2013. Centers for Disease Control and Prevention, US Department of Health and Human Services, Atlanta, GA.
- 24 Nomura J. Slowing Antibiotic Resistance by Decreasing Antibiotic Use in Animals, *The Minnesota Journal of Law, Science and Technology.* 2015, 15(1):585-612.
- 25 Quinn MM. Cleaning and Disinfecting Environmental Surfaces in Healthcare: Toward an integrated framework for infection and occupational illness prevention. *American Journal of Infection Control.* 2015;43(5):424-434.
- 26 Otter JA, Yezli S, French GL. The Role Played by Contaminated Surfaces in the Transmission of Nosocomial Pathogens. *Infection Control and Hospital Epidemiology.* 2011;32(7):687-699.
- 27 Olson ME, Ceri H, Morck DW, Buret AG, Read RR. Biofilm bacteria: formation and comparative susceptibility to antibiotics. *Canadian Journal of Veterinary Research.* 2002;66(2):86-92.
- 28 Neely AN, Maley MP. Survival of Enterococci and Staphylococci on Hospital Fabrics and Plastic. *Journal of Clinical Microbiology.* 2000;38(2):724-726.
- 29 Houdt RW, Michiels CW. Biofilm formation and the food industry, a focus on the bacterial outer surface. *Journal of Applied Microbiology.* 2010;109(4):1117-1131.
- 30 Knobler SL, Lemon SM, Najafi M. The Resistance Phenomenon in Microbes and Infectious Disease Vectors: Implications for Human Health and Strategies for Containment: Workshop Summary. Washington (DC): National Academies Press (US); 2003. 5, Factors Contributing to the Emergence of Resistance.

- 31 Carbapenem-resistant Enterobacteriaceae in Healthcare Settings, 2015. Centers for Disease Control and Prevention, US Department of Health and Human Services, Atlanta, GA.
- 32 Guentzel MN. Escherichia, Klebsiella, Enterobacter, Serratia, Citrobacter, and Proteus. In: Baron S, editor. Medical Microbiology. 4th edition. Galveston (TX): University of Texas Medical Branch at Galveston; 1996. Chapter 26.
- 33 Vuong C, Yeh AJ, Cheung GY, Otto M. Investigational Drugs to Treat methicillin-resistant Staphylococcus aureus. *Expert Opinion Investigative Drugs*. 2016;25(1):73-93.
- 34 Holten KB, Onusko EM. Appropriate prescribing of oral beta-lactam antibiotics. *American Family Physician*. 2000;62(3):611-620.
- 35 Methicillin Resistant *Staphylococcus aureus* (MRSA), *Clostridium difficile* and ESBL-producing *Escherichia coli* in the home and community: assessing the problem, controlling the spread; International Scientific Forum on Home Hygiene, 2006.
- 36 Dancer SJ. Controlling Hospital-Acquired Infection: Focus on the Role of the Environment and New Technologies for Decontamination. *Clinical Microbiology Reviews*. 2014;27(4):665-690.
- 37 Bein J, Sokolova O, Bozko P. Role of Uropathogenic *Escherichia coli* Virulence Factors in Development of Urinary Tract Infection and Kidney Damage. *International Journal of Nephrology*. 2011;2012(2012):1-15.
- 38 Gangell C, Gard S, Douglas T, Park J, Klerk D, Keil T, Brennan S, Sly PD. Inflammatory Responses to Individual Microorganisms in the Lungs of Children with Cystic Fibrosis. *Clinical Infectious Diseases*. 2011;53(5):425-432.
- 39 Coureuil M, Join-Lambert O, Lécuyer H, Bourdoulous S, Marullo S, Nassif X. Mechanism of meningeal invasion by *Neisseria meningitidis*. *Virulence*. 2012;3(2):164-172.
- 40 Hodges K, Gill R. Infectious diarrhea: Cellular and molecular mechanisms. *Gut Microbes*. 2010;1(1):4-21.

- 41 Jacobsen SM, Stickler DJ, Mobley HLT, Shirliff ME. Complicated Catheter-Associated Urinary Tract Infections Due to *Escherichia coli* and *Proteus mirabilis*. *Clinical Microbiology Reviews*. 2008;21(1):26-59.
- 42 Wong CS, Mooney JC, Brandt JD, Staples AO, Jelacic S, Boster DR, Watkins SL, Tarr PI. Risk Factors of the Hemolytic Uremic Syndrome in Children Infected with *Escherichia coli* O157:H7: A Multivariable Analysis. *Clinical Infectious Diseases*. 2012;55(1):33-41.
- 43 Abstracts from the 37th Annual Meeting of the Society of General Internal Medicine. *Journal of General Internal Medicine*. 2014;29(Suppl 1):1-545.
- 44 Gilchrist M, Wafe P, Howard P, Sneddon J, Whitney L, Wickens H. Antimicrobial Stewardship from Policy to Practice: Experiences from UK Antimicrobial Pharmacists. *Infectious Diseases and Therapy*. 2015;5:51-64.
- 45 Jumma PA. Hand hygiene: simple and complex. *International Journal of Infectious Diseases*. 2005;9(1):3-14.
- 46 Hirsch EB, Tam VH. Impact of multidrug-resistant *Pseudomonas aeruginosa* infection on patient outcomes. *Expert review of pharmacoeconomics & outcomes research*. 2010;10(4):441-451.
- 47 Rineh A, Kelso MJ, Vatansever F, Tegos GP, Hamblin MR. Clostridium difficile infection: molecular pathogenesis and novel therapeutics. *Expert review of anti-infective therapy*. 2014;12(1):131-150.
- 48 MacLeod-Glover N, Sadowski C. Efficacy of cleaning products for *C difficile*: Environmental strategies to reduce the spread of *Clostridium difficile*-associated diarrhea in geriatric rehabilitation. *Canadian Family Physician*. 2010;56(5):417-423.
- 49 Gerding DN, Muto CA, Owens RC. Measures to Control and Prevent *Clostridium difficile* Infection. *Clinical Infectious Diseases*. 2008;36(Suppl 1):S43-S49.
- 50 Fordtran JS. Colitis due to *Clostridium difficile* toxins: underdiagnosed, highly virulent, and nosocomial. *Proceedings (Baylor University Medical Center)*. 2006;19(1):3-12.
- 51 Nearly half a million Americans suffered from Clostridium difficile infections in a single year, 2013. Centers for Disease Control and Prevention, US Department of

Health and Human Services, Atlanta, GA. [Accessed from:
<http://www.cdc.gov/media/releases/2015/p0225-clostridium-difficile.html>]

- 52 Community Infection Prevention and Control Manual; HSE Dublin North East, 2011. [Accessed from http://www.hse.ie/eng/about/Who/qualityandpatientsafety/Local_Quality_and_Patient_Safety_Offices/QPS_DNE/HCAI/Guidelines%20for%20Infection%20Prevention%20and%20Control.pdf]
- 53 Chirca I, Salgado CD. What strategies are in place to control microbial burden in hospital environments and how could these change in the future. *Future Microbiology*. 2013;8(9):1051-1054.
- 54 Schmidt MG, Attaway Iii HH, Fairey SE, Steed LL, Michels HT, Salgado CD. Copper continuously limits the concentration of bacteria resident on bed rails within the intensive care unit. *Infection Control & Hospital Epidemiology*. 2013;34(5):530-533.
- 55 Siegel JD, Rhinehart E, Jackson M, Chiarello L. Healthcare Infection Control Practices Advisory Committee (HICPAC), 2015. Centers for Disease Control and Prevention, US Department of Health and Human Services, Atlanta, GA.
- 56 Ellingson K, Haas JP, Aiello AE, Kusek L, Maragakis LL, Olmsted RN, Perencevich E, Polgreen PM, Schweizer ML, Trexler P, VanAmringe M, Yokoe DS. Strategies to Prevent Healthcare-Associated Infections through Hand Hygiene. *Infection Control and Hospital Epidemiology*. 2014;35(8):937-960.
- 57 Mathur P. Hand hygiene: Back to the basics of infection control. *The Indian Journal of Medical Research*. 2011;134(5):611-620.
- 58 WHO Guidelines on Hand Hygiene in Health Care: First Global Patient Safety Challenge Clean Care Is Safer Care. Geneva: World Health Organization, 2009. Available from: <https://www.ncbi.nlm.nih.gov/books/NBK144013/>
- 59 Widmer AF. Replace Hand washing with use of a waterless alcohol hand rub? *Clinical Infectious Diseases*. 2000;31(1):136-143.

- 60 Dancer SJ. Controlling Hospital-Acquired Infection: Focus on the Role of the Environment and New Technologies for Decontamination. *Clinical Microbiology Reviews*. 2014;27(4):665-690.
- 61 Iggulden H, Macdonald C, Staniland K. *Clinical Skills: The Essence of Caring*. McGraw-Hill Education. Medical, 2009.
- 62 Mehta Y, Gupta A, Todi S, et al. Guidelines for prevention of hospital acquired infections. *Indian Journal of Critical Care Medicine: Peer-reviewed, Official Publication of Indian Society of Critical Care Medicine*. 2014;18(3):149-163.
- 63 Donlan RM, Costerton JW. Biofilms: Survival Mechanisms of Clinically Relevant Microorganisms. *Clinical Microbiology Reviews*. 2002;15(2):167-193.
- 64 Rutala WA, Weber DJ. Guideline for Disinfection and Sterilization in Healthcare Facilities, Centers for Disease Control and Prevention, 2008. [Accessed on 07/11/16 https://www.cdc.gov/hicpac/pdf/guidelines/Disinfection_Nov_2008.pdf]
- 65 Weinstein RA. Contamination, Disinfection, and Cross-Colonization: Are Hospital Surfaces Reservoirs for Nosocomial Infection? *Clinical Infectious Diseases*. 2004;39 (8):1182-1189.
- 66 McDonnell G, Russell AD. Antiseptics and Disinfectants: Activity, Action, and Resistance. *Clinical Microbiology Reviews*. 1999;12(1):147-179.
- 67 Weber DJ, Rutala WA. Use of Germicides in the Home and the Healthcare Setting: Is There a Relationship Between Germicide Use and Antibiotic Resistance? *Infection Control & Hospital Epidemiology*. 2006;27:1107-1119.
- 68 Maillard J-Y. Antimicrobial biocides in the healthcare environment: efficacy, usage, policies, and perceived problems. *Therapeutics and Clinical Risk Management*. 2005;1(4):307-320.
- 69 Greatorex JS, Page RF, Curren MD, Digard P, Enstone JE, Wreghitt T, Powell PP, Sexton DW, Vivancos R, Nguyen-Van-Tam JS. Effectiveness of Common Household

Cleaning Agents in Reducing the Viability of Human Influenza A/H1N1. *Plos One*, 2012;5(2):e8987.

- 70** Infections and Infectious Diseases, World Health Organization; A manual for nurses and midwives in the WHO European Region. 2001;4-24.
- 71** Carling PC, Von Beheren S, Kim P, Woods C. Intensive care unit environmental cleaning: an evaluation in sixteen hospitals using a novel assessment tool. *Journal of Hospital Infections*. 2008;68(1):39-44.
- 72** Institute of Medicine (US) Forum on Microbial Threats. Antibiotic Resistance: Implications for Global Health and Novel Intervention Strategies: Workshop Summary. Washington (DC): National Academies Press (US); 2010. Appendix A, Contributed Manuscripts.
- 73** Mehta Y, Gupta A, Todi S, Myatra SN, Samaddar DP, Patil V, Bhattacharya PK, Ramasubban S. Guidelines for prevention of hospital acquired infections. *Indian Journal of Critical Care Medicine : Peer-reviewed, Official Publication of Indian Society of Critical Care Medicine*. 2014;18(3):149-163.
- 74** Byrns G, Fuller TP. The risks and benefits of chemical fumigation in the health care environment. *Journal of Occupational and Environmental Hygiene*. 2011;8:104-112.
- 75** Pappas HC, Phan S, Yoon S, Edens LE, Meng X, Schanze KS, Whitten DG, Keller DJ. Self-Sterilizing, Self-Cleaning Mixed Polymeric Multifunctional Antimicrobial Surfaces. *ACS Applied Materials & Interfaces*. 2015;7(50):27632-27638.
- 76** Sharma M, Hudson JB. Ozone gas is an effective and practical antibacterial agent. *Antimicrobial Journal of Infectious Control*. 2008;36(8):559-563.
- 77** Davies A, Pottage T, Bennett A, Walker J. Gaseous and air decontamination technologies for *Clostridium difficile* in the healthcare environment. *Journal of Hospital Infections*. 2011;77(3):199-203.
- 78** Cardoso CC, Fiorini JE, Ferriera LR, Gurjão JW, Amaral LA, Disinfection of hospital laundry using ozone: microbiological evaluation. *Infectious Control of Hospital Epidemiology*. 2000;21(4):248.

- 79** Berrington AW, Pedler SJ, Investigation of gaseous ozone for MRSA decontamination of hospital side-rooms. *Journal of Hospital Infections*. 1998;40(1):61-65.
- 80** Sexton JD, Tanner BD, Maxwell SL, Gerba CP. Reduction in the microbial load on high-touch surfaces in hospital rooms by treatment with a portable saturated steam vapor disinfection system. *Antimicrobial Journal of Infectious Control*. 2011;39(8):655-662.
- 81** Cleaning Hospital Room Surfaces to Prevent Healthcare-Associated infections: A Technical Brief. *Annals of Internal Medicine*. 2015;163(8):598-607.
- 82** Griffith CJ, Dancer SJ. Hospital cleaning: problems with steam cleaning and microfibre. *Journal of Hospital Infections*. 2009;72(4):360-361.
- 83** Lambert BJ, Mendelson TA, Craven MD. Radiation and Ethylene Oxide Terminal Sterilization Experiences with Drug Eluting Stent Products. *AAPS PharmSciTech*. 2011;12(4):1116-1126.
- 84** Gillespie EH, Jackson JM and Owen GR. Ethylene oxide sterilisation – is it safe? *Journal of Clinical Pathology*. 1979;32:1184-1187.
- 85** Falagas ME, Thomaidis PC, Kotsantis IK, Sgouros K, Samonis G, Karageorgopoulos DE. Airborne hydrogen peroxide for disinfection of the hospital environment and infection control: a systematic review. *Journal of Hospital Infections*. 2011;78(3):171-177.
- 86** Shintani H, Sakudo A, Burke P, McDonnell G. Gas plasma sterilization of microorganisms and mechanisms of action. *Experimental and Therapeutic Medicine*. 2010;1(5):731-738.
- 87** Haertel B, von Woedtke T, Weltmann K-D, Lindequist U. Non-Thermal Atmospheric-Pressure Plasma Possible Application in Wound Healing. *Biomolecules & Therapeutics*. 2014;22(6):477-490.
- 88** Reed NG. The history of ultraviolet germicidal irradiation for air disinfection. *Public Health Reports*. 2010;125(1):15-27.

- 89 Rutala WA, Gergen MF, Weber DJ. Room decontamination with UV radiation. *Infectious Control of Hospital Epidemiology*. 2010;31(10):1025-1029.
- 90 Non-Manual Techniques for Room Disinfection in Healthcare Facilities: A Review of Clinical Effectiveness and Guidelines, Canadian Agency for Drugs and Technologies in Health, 2014.
- 91 Nerandzic MM, Cadnum JL, Pultz MJ, Donskey CJ. Evaluation of an automated ultraviolet radiation device for decontamination of *Clostridium difficile* and other healthcare-associated pathogens in hospital rooms. *BMC Infectious Diseases*. 2010;10:197.
- 92 Dai T, Gupta A, Murray CK, Vrahas MS, Tegos GP, Hamblin MR. Blue light for infectious diseases: *Propionibacterium acnes*, *Helicobacter pylori*, and beyond? *Drug Resistance Updates*. 2012;15(4):223-236.
- 93 Page K, Wilson M, Parkin IP. Antimicrobial surfaces and their potential in reducing the role of the inanimate environment in the incidence of hospital-acquired infections. *Journal of Materials Chemistry*. 2009;19:3819-3831.
- 94 Garrett TR, Bhakoo M, Zhang Z. Bacterial adhesion and biofilms on surfaces. *Progress in Natural Science*. 2008;18:1049-1056.
- 95 Chen M, Yu Q, Sun H. Novel strategies for the prevention and treatment of biofilm related infections. *International Journal of Molecular Sciences*. 2013;14(9):18488-18501.
- 96 Mathews S, Hans M, Mucklich F, Solioz M. Contact killing of bacteria on copper is suppressed if bacterial-metal contact is prevented and is induced on iron by copper ions. *Applied and Environmental Microbiology*. 2013;79(8):2605-2611.
- 97 Zhang X, Wang L, Levanen E. Superhydrophobic surfaces for the reduction of bacterial adhesion. *RSC Advances*. 2013;3:12003-12020.

- 98** Braid JJ, Wale MCJ. The antibacterial activity of triclosan-impregnated storage boxes against *Staphylococcus aureus*, *Escherichia coli*, *Pseudomonas aeruginosa*, *Bacillus cereus* and *Shewanella putrefaciens* in conditions simulating domestic use. *Journal of Antimicrobial Chemotherapy*. 2002;49(1):87-94.
- 99** Jones, Rhonda D., et al. "Triclosan: a review of effectiveness and safety in health care settings." *American journal of infection control*. 2000;2(2): 184-196.
- 100** Dhillon GS, Kaur S, Pulicharla R, Brar SK, Cledon M, Verma M, Surampalli RY. Triclosan: Current status, occurrence, environmental risks and bioaccumulation potential. *International Journal of Environmental Research and Public Health*. 2015;12(5):5657-5684.
- 101** Rutala WA, Weber DJ. New disinfection and sterilization methods. *Emerging Infectious Diseases*. 2001;37:20-27.
- 102** Siedenbiedel F, Tiller JC. Antimicrobial Polymers in Solution and on Surfaces: Overview and Functional Principles. *Polymers*. 2012;4:46-71.
- 103** Zhang J, Xia W, Liu P, Cheng q, Tahirou T, Gu W, Li B. Chitosan Modification and Pharmaceutical/Biomedical Applications. *Marine Drugs*. 2010;8(7):1962-1987.
- 104** Raafat D, von Bargen K, Haas A, Sahl H. Insights into the Mode of Action of Chitosan as an Antibacterial Compound. *Applied and Environmental Microbiology*. 2008;74(12):3764-3773.
- 105** Navarre WW, Schneewind O. Surface Proteins of Gram-Positive Bacteria and Mechanisms of Their Targeting to the Cell Wall Envelope. *Microbiology and Molecular Biology Reviews*. 1999;63(1):174-229.
- 106** Alves D, Pereira MO. Mini-review: Antimicrobial peptides and enzymes as promising candidates to functionalize biomaterial surfaces. *Biofouling*. 2014;30(4):483-499.
- 107** Hasan J, Crawford RJ, Ivanova EP. Antibacterial surfaces: the quest for a new generation of biomaterials. *Trends in Biotechnology*. 2013;31(5):295-304.

- 108** Cunliffe D, Smart CA, Alexander C, Vulfson EN. Bacterial Adhesion at Synthetic Surfaces. *Applied and Environmental Microbiology*. 1999;65(11):4995-5002.
- 109** Liu K, Jiang L. Bio-inspired Self-Cleaning Surfaces. *Annual Review of Materials Research*. 2013;42:231-263.
- 110** Schlenoff JB. Zwitteration: Coating Surfaces with Zwitterionic Functionality to Reduce Nonspecific Adsorption. *Langmuir*. 2014;30(32):9625-9636.
- 111** Schreier S, Malheiros SVP, Paula E. Surface active drugs: self-association and interaction with membranes and surfactants. Physicochemical and biological aspects. *Detergents in Biomembrane Studies*. 2000;1508(1):210-234.
- 112** Arvizo RR, Bhattacharyya S, Kudgus R, Giri K, Bhattacharyya R, Mukherjee P. Intrinsic Therapeutic Applications of Noble Metal Nanoparticles: Past, Present and Future. *Chemical Society Reviews*. 2012;41(7):2943-2970.
- 113** Jung WK, Koo HC, Kim KW, Shin S, Kim SH, Park YH. Antibacterial Activity and Mechanism of Action of the Silver Ion in *Staphylococcus aureus* and *Escherichia coli*. *Applied and Environmental Microbiology*. 2008;74(7):2171-2178.
- 114** Pal S, Tak YK, Song JM. Does the Antibacterial Activity of Silver Nanoparticles Depend on the Shape of the Nanoparticle? A Study of the Gram-Negative Bacterium *Escherichia coli*. *Applied and Environmental Microbiology*. 2007;73(6):1712-1720.
- 115** Tran QH, Nguyen VQ, Le A. Silver Nanoparticles: synthesis, properties, toxicology, applications and perspective. *Advances in Natural Sciences: Nanoscience and Nanotechnology*. 2013;4:1-20.
- 116** Michels HT. From Laboratory Research to a Clinical Trial: Copper Alloy Surfaces Kill Bacteria and Reduce Hospital-Acquired Infections, 2015.
- 117** Grass G, Rensing C, Solioz M. Metallic Copper as an Antimicrobial Surface. *Applied and Environmental Microbiology*. 2010;77(5):1541-1547.

- 118** Noimark S, Allan E, Parkin IP. Light-activated antimicrobial surfaces with enhanced efficacy induced by a dark-activated mechanism. *Chemical Science*. 2014;5:2216-2223.
- 119** Sperandio FF, Huang Y, Hamblin MR. Antimicrobial photodynamic therapy to kill Gram-negative bacteria. *Recent Patents on Anti-Infective Drug Discovery*. 2013;8(2):108-120.
- 120** Sehmi SK, Noimark S, Bear JC, Peveler WJ, Bovis M, Allan E, MacRobert AJ, Parkin IP. Lethal photosensitisation of *Staphylococcus aureus* and *Escherichia coli* using crystal violet and zinc oxide-encapsulated polyurethane. *Journal of Materials Chemistry B*. 2015;3:6490-6500.
- 121** Ibhaddon AO, Fitzpatrick P. Heterogeneous Photocatalysis: Recent Advances and Applications, *Catalysts*. 2013;3:189-218.
- 122** Byrne JA, Dunlop PSM, Hamilton JWJ, Fernandez-Ibanez P, Polo-Lopez I, Sharma PK, Vennard ASM. A Review of Heterogeneous Photocatalysis for Water and Surface Disinfection. *Molecules*. 2015;20(4):5574-5615.
- 123** Pelaez M, Nolan N, Pillai S, Seery M, Falaras P. A Review on the Visible Light Active Titanium Dioxide Photocatalysts for Environmental Applications. *Applied Catalysis B: Environmental*. 2012;125:331-349.
- 124** Noimark S, Page K, Bear JC, Sotelo-Vazquez C, Quesada-Cabrera R, Lu Y, Allan E, Darr JE, Parkin IP. Functionalised gold and titania nanoparticles and surfaces for use as antimicrobial coatings. *Faraday Discussions*. 2014;175:273-287.
- 125** Noimark S, Dunnill CW, Kay CWM, Perni S, Prokopovich P, Ismail S, Wilson M, Parkin IP. Incorporation of methylene blue and nanogold into polyvinyl chloride catheters; a new approach for light-activated disinfection of surfaces. *Journal of Material Chemistry*. 2012;22:15388.
- 126** Perni S, Piccirillo C, Kafizas A, Uppal M, Pratten J, Wilson M, Parkin IP, Antibacterial Activity of Light-Activated Silicone Containing Methylene Blue and Gold Nanoparticles of Different Sizes. *Journal of Cluster Science*. 2010;21:427-438.

- 127** Ozkan E, Allan E, Parkin IP, The antibacterial properties of light-activated polydimethylsiloxane containing crystal violet. *RSC Advances*. 2014;4;51711.
- 128** Hwang GB, Allan E, Parkin IP, White Light-Activated Antimicrobial Paint using Crystal Violet. *ACS Applied Materials and Interfaces*. 2015;8(24);15033-15039.
- 129** Noimark S, Bovis M, MacRobert AJ, Correia A, Allan E, Wilson M, Parkin IP, Photobactericidal polymers; the incorporation of crystal violet and nanogold into medical grade silicone. *RSC Advances*. 2013, 3, 18383.
- 130** Noimark S, Weiner J, Noor N, Allan E, Williams CK, Shaffer MSP, Parkin IP, Dual-Mechanism Antimicrobial Polymer-ZnO Nanoparticle and Crystal Violet-Encapsulated Silicone. *Advanced Functional Materials*. 2015;25:1367-1373.
- 131** Noimark S, Dunnill CW, Parkin IP. Shining light on materials – a self-sterilising revolution. *Advanced Drug Delivery Reviews*. 2013;65(4):570-580.

Chapter 2

2. Photo-Activated Surfaces

2.1 Introduction to Photodynamic Therapy

The previous chapter introduced the topic of HAIs and the impact they have on the livelihood and wellbeing of hospitalised patients. Globally, hospitals are faced with many challenges, as HAIs remain a major cause of patient morbidity and mortality. The chapter also assessed the advantages and disadvantages of various cleaning and sterilising strategies that are already employed by hospitals and introduced new techniques to disinfect contaminated surfaces and medical devices. Moreover, the development and use of antimicrobial surfaces in hospitals was discussed as an efficacious approach for reducing the risk of HAIs. This chapter details the use of novel photo-activated surfaces to kill bacteria using a phenomenon known as photodynamic therapy (PDT); a multi-stage process that requires the presence of molecular oxygen and uses non-ionising visible light. It then discusses the development of light-activated polymers and introduces the incorporation of nanoparticles into these surfaces for an enhanced bactericidal response.

Light has been used to treat diseases for many centuries, tracing back over 4000 years to the ancient Egyptians.¹ They used the combination of sunlight and the Amni Majus plant to successfully treat a skin disorder, known as vitiligo. The active ingredient of this plant (psoralen) is now used globally to treat psoriasis.^{2,3} PDT was accidentally discovered by a medical student named Oscar Raab in 1900 whilst studying the interaction of fluorescent dyes with infusoria (microscopic organisms found in fresh water and infusions of organic matter).⁴ He reported rapid destruction of a *Paramecium* species when exposing acridine dye to high intensity light.⁵ Soon after, patients were being treated by this process for cancers,

particularly of the skin.⁶ Despite this breakthrough, PDT remained neglected for nearly 50 years but was reassessed by Lipson and Schwartz in 1960, who revealed that photosensitising agents were capable of ablating tumour tissue from the body following intravenous administration.^{7,8} Then in the 1970s, Thomas Dougherty reinvigorated PDT when studying porphyrin compounds and helped publicise PDT worldwide by creating a commercially available photosensitising drug, known as 'haematoporphyrin derivative'.⁹

PDT is distinct from conventional phototherapy which only uses light, and requires the combination of a photosensitiser, molecular oxygen and light tuned to a wavelength that is efficiently absorbed by the photosensitiser. PDT is commonly used to destroy cancerous tissues by using a photosensitiser that is activated by light at a specific wavelength, most commonly in the red or near-infrared where absorption by haemoglobin and other tissue chromophores is weak.¹⁰ Porphyrins and phthalocyanines were the first photosensitive molecules identified in the mid-nineteenth century. Porphyrins typically contain four pyrrole rings connected by methine bridges in a cyclic formation and phthalocyanines are connected by aza bridges.¹¹ As well as tetrapyrrole-based photosensitisers, non-tetrapyrrole-based photosensitisers are also used, which can be xanthene- or phenothiazine-based.¹² Examples of photosensitisers used in PDT (Fig. 2.1) include PhotofrinTM, a purified form of haematoporphyrin derivative, methylene blue (MB), toluidine blue O (TBO), crystal violet (CV) and Rose Bengal (RB). One major advantage of PDT is that photosensitisers can be administered in a number of ways, such as injected, applied to the skin, or used as a device or surface coating.¹³ Additionally, it avoids the potential development of microbial resistance as PDT operates *via* non-specific mechanistic pathways¹⁴ (as described in section 2.1.2).

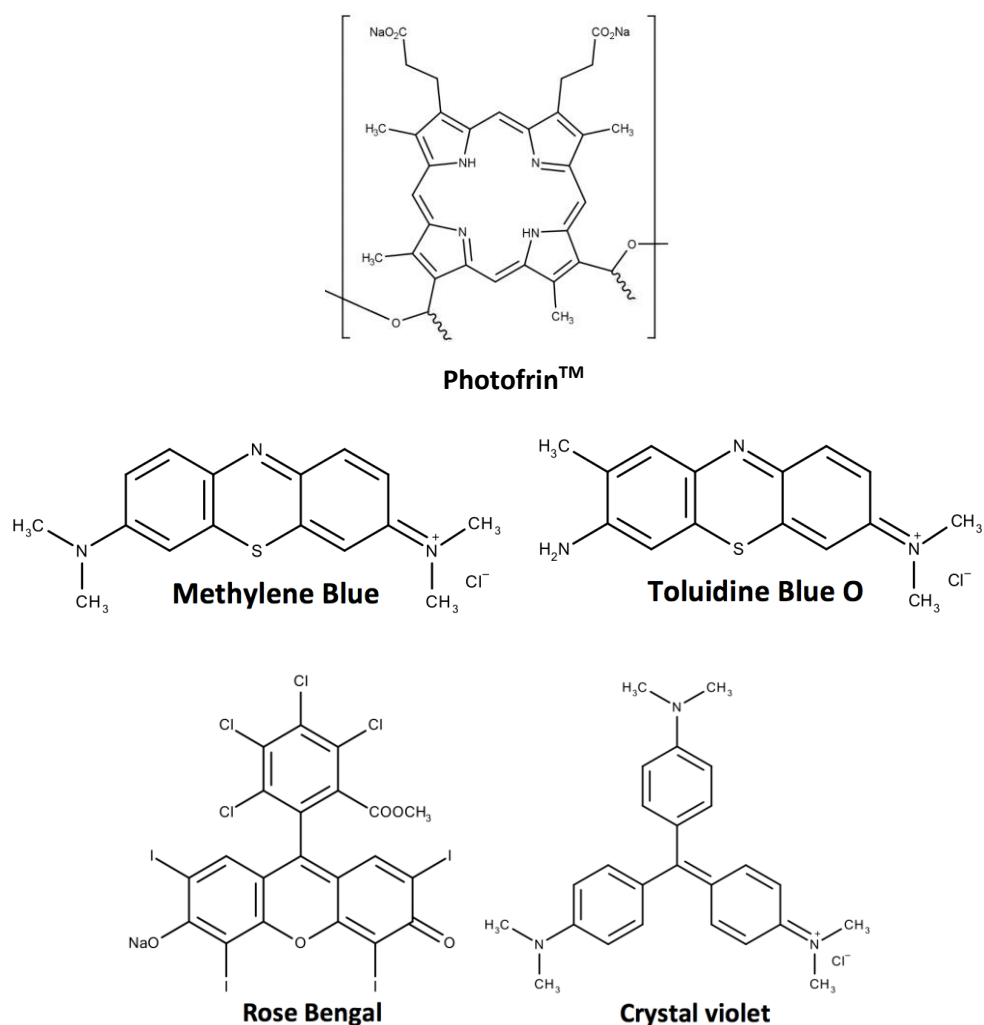


Fig. 2.1 Chemical structures of tetrapyrrole based and non-tetrapyrrole based photosensitisers used in PDT.

Photofrin™ has successfully been used in clinical practice to treat a range of tumours and viral infections, especially human papilloma virus (HPV), when activated by red light at 630 nm.^{15,16} Few clinical trials have been carried out to show the effect of PDT in localised bacterial infections, but one study demonstrated a positive clinical response in patients with brain abscesses after activating hematoporphyrin for 5 minutes.^{14,17} A clinically approved application of antimicrobial PDT is treating oral infections. In dentistry, one of the most common bacterial diseases for humans is periodontal disease, which is a chronic inflammatory condition of the gum and bone support surrounding the teeth.¹⁷ To treat this disease, the

photosensitiser is injected in the target area and light is delivered to the area using a narrow fibre optic tip. PDT with TBO and a 660 nm laser was effective in treating patients with aggressive periodontitis.¹⁶ Furthermore, PDT is used in the sterilisation of root canals in children's primary teeth with necrotic pulps.¹⁸

2.1.1 Photochemistry

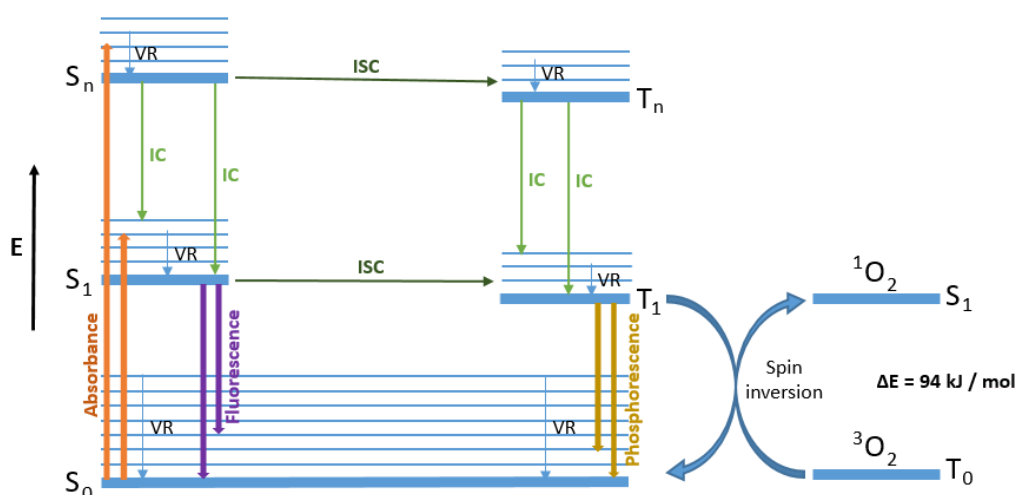


Fig. 2.2 Modified Jablonski diagram displaying the electronic states (S_0 , S_1 , S_n , T_0 , T_1 , T_n) of a photosensitiser after the absorption of a photon. Non-radiative transitions are labelled as follows: internal conversion (IC), intersystem crossing (ISC), vibrational relaxation (VR). Diagram also shows the production of singlet oxygen (1O_2) via resonant electronic energy transfer.

When a chromophore (part of a molecule responsible for colour) absorbs a photon in the form of light energy, an electron is promoted into a higher-energy molecular orbital, and the chromophore is excited from the ground state (S_0) into a short-lived, electronically excited state (S_n), generally a singlet state with no net electronic spin.^{19,20} The chromophore in its excited state can lose energy by decaying rapidly to populate their lowest vibrational levels (S_0 or S_1) by non-radiative and radiative transitions (illustrated in Fig. 2.2).²¹

2.1.1.1 Non-radiative transitions

Vibrational relaxation (VR) is a non-radiative transition that occurs when a molecule in a high vibrational level of an excited state (S_n) rapidly falls to the lowest vibrational level of this state.²² It only occurs between levels of the same vibrational progression.^{22,23} Internal conversion (IC) occurs when a molecule falls from an excited singlet state (S_n or S_1) to a lower or ground state (S_1 or S_0). Intersystem crossing (ISC) is a spin-forbidden process in quantum mechanics due to changes in electron spin; from S_0 or S_1 (antiparallel) to an excited triplet state (T_1 ; parallel).²⁴

2.1.1.2 Radiative transitions

Fluorescence ($S_1 \rightarrow S_0$) is a radiative transition that results from decay of the excited singlet state (S_1) to the ground state (S_0). The lifetime of this transition is very short ($10^{-9} - 10^{-6}$ seconds) since it is considered an “allowed” transition (same spin states: either $S \rightarrow S$ or $T \rightarrow T$).⁸ Alternatively, the singlet state electron (S_1) can undergo ISC and populate the lower-energy first triplet state (T_1); a spin-forbidden process.²⁵⁻²⁷ This excited electron can then undergo another spin-forbidden transition by depopulating the excited triplet state (T_1) and decaying to the ground state (S_0). This process is known as phosphorescence and has a much longer lifetime than fluorescence ($10^{-3} - 1$ second) because it undergoes a spin-forbidden transition ($T_1 \rightarrow S_0$).²⁵⁻²⁷

2.1.2 Mechanism of action

PDT is a photochemical process that uses non-thermal power densities.⁸ After the absorption of light (photons) the photosensitiser (PS) is transformed from its ground singlet state (S_0) to the relatively long-lived electronically excited triplet state (T_1), *via* ISC from the short-lived excited singlet state (S_1).²⁸ The triplet state can undergo two different reactions.

The first is a direct reaction between the excited singlet state or triplet photosensitiser ($^1\text{PS}^*$ [S_1]; $^3\text{PS}^*$ [T_1]) with oxygen or a substrate, resulting in the transfer of electrons to form radicals and other reactive oxygen species (ROS), which is known as the Type I process.²⁹ Alternatively the triplet state photosensitiser ($^3\text{PS}^*$ [T_1]) can transfer its energy directly to ground state triplet oxygen ($^3\text{O}_2$) to form excited state singlet oxygen ($^1\text{O}_2$), which is known as the Type II process.³⁰ These photochemical pathways are summarised in Fig. 2.3(a).

In a Type I process, an electron is transferred from the substrate to the excited state photosensitiser (PS^*), which generates a substrate radical cation ($\text{Subs}^{\cdot+}$) and a photosensitiser radical anion ($\text{PS}^{\cdot-}$).^{8,30} Further reactions with oxygen produce a complex mixture of ROS (shown in Fig. 2.3(b)). Only when the photosensitiser is in its excited state ($^3\text{PS}^*$) can it interact with molecular oxygen ($^3\text{O}_2$; T_1) to produce singlet oxygen ($^1\text{O}_2$; S_1), as it is a spin-allowed transition.^{30,31} This Type II scheme is shown in Fig. 2.3(b).

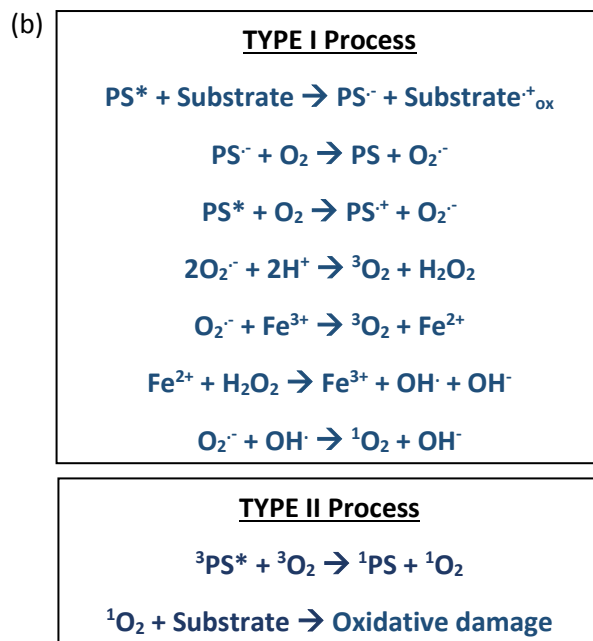
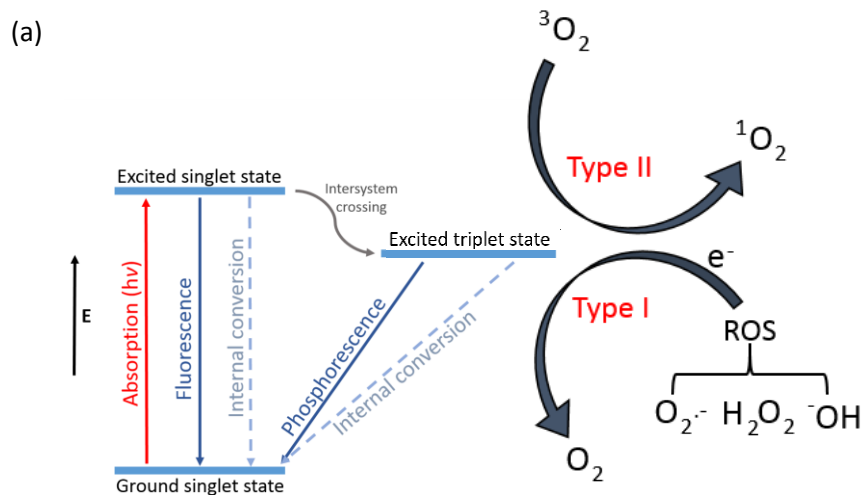


Fig. 2.3 (a) Simplified Jablonski diagram displaying the processes involved in photodynamic therapy when a photo-excited photosensitiser undergoes energetic transitions after the absorption of a photon. The photosensitiser in its excited singlet state can undergo radiative decay (fluorescence) or non-radiative decay *via* internal conversion, or convert to the excited triplet state *via* intersystem crossing. The triplet state molecule can decay radiatively by phosphorescence, non-radiatively *via* internal conversion, or interact with molecular oxygen *via* resonant energy transfer (Type II process) or other substrate molecules *via* electron or proton transfer (Type I process). (b) Common reactions involved in Type I and Type II processes.

Both Type I (electron transfer) and Type II (energy transfer) mechanistic pathways can occur simultaneously but the ratio of these processes are dependent on the type of photosensitiser and the concentration of substrate and oxygen.³² The photosensitiser requires a good triplet state quantum yield and a long triplet state lifetime in order to promote Type I/II processes.¹¹ The quantum yield is defined by the efficiency of a photochemical process,³³ i.e. the number of molecules undergoing a process for each quantum of radiation energy absorbed.³⁰ Superoxide anion ($O_2^{\cdot-}$) is generally produced *via* a Type I pathway involving electron transfer. Superoxide is relatively ineffective at causing oxidative damage on its own compared to singlet oxygen, but it can undergo dismutation to produce oxygen and H_2O_2 , (as shown in Fig. 2.4) which can pass through bacterial cell membranes to cause oxidative damage.²⁹

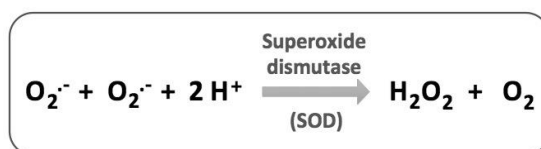


Fig. 2.4 Superoxide dismutation reaction.

$O_2^{\cdot-}$ can also act as a reducing agent to produce ROS by a Fenton reaction process discovered over 100 years ago.³⁴ Superoxide donates an electron to reduce metal ions (e.g. ferric ion or Fe^{3+}) that catalyses the conversion of H_2O_2 into highly reactive hydroxyl radicals ($\cdot OH$).³⁵ The Fenton reaction is important in biological systems because the cells contain small amounts of metal (e.g. iron or copper) which can facilitate this process.³⁶ The reduced metal ions, e.g. ferrous Fe^{2+} ions, induce the decomposition of H_2O_2 to produce $\cdot OH$ and a hydroxide ion (OH^-). Moreover, superoxide anions can react with the hydroxyl radical to produce highly reactive singlet oxygen (a secondary process).^{35,36}

Singlet oxygen and hydroxyl radicals are extremely reactive and have very short half-lives, so only cells that are in close proximity to the photosensitiser are directly affected by PDT.³⁰ Although singlet oxygen has a net spin of zero, the highest energy electrons are in degenerate states (unpaired), therefore, it is highly reactive.³⁷ The half-life of singlet oxygen in biological systems is < 40 ns and the radius of action of singlet oxygen is in the order of < 20 nm.³⁸ It attacks unsaturated bonds in particular which are most vulnerable (i.e. aromatic compounds, amino acids, unsaturated lipids).^{39,40}

Photosensitisers can also undergo degradation upon light exposure, leading to a process known as 'photobleaching' or 'photodegradation'.³⁰ Photobleaching occurs when singlet oxygen or ROS produced by light activation react with the photosensitive molecule resulting in its oxidation thereby decreasing its photosensitisation efficiency, unless there is a photoactive product with comparable absorbance characteristics.⁴¹

For clinical use photosensitisers should exhibit minimal toxicity towards mammalian cells⁴² and absorb light in the red or far-red wavelength range to penetrate tissue.³⁰ They should also be targeted appropriately so that the treatment is pain-free.¹⁶ Absorption bands at wavelengths greater than 800 nm generally entails that the triplet state will have insufficient energy for the photosensitiser to transfer energy to oxygen to form singlet oxygen (energy threshold of 94 kJ/mol).³⁰

PDT is particularly advantageous for antimicrobial application because there is a low risk of developing bacterial resistance.⁴³ When illuminated, ROS generated from the photosensitiser can attack the bacteria at multiple sites at a cellular level.²⁹ Although bacterial cells have many natural defences against ROS, the level of redox imbalance caused by PDT is usually greater than the level of protection given by enzymes and molecular antioxidants within the cell.²⁹ Bacterial cells are capable of defending themselves against H₂O₂ and superoxide anion radicals, but cannot naturally deactivate singlet oxygen or hydroxyl radicals.⁴⁴

A positively charged photosensitiser is more effective at inactivating bacteria and even spores, as they are able to interact with negatively charged bacterial cell walls.¹² Gram-positive bacteria were shown to be more susceptible to PDT compared to Gram-negative bacteria, presumably as a result of differences in their cell wall structures (Fig. 2.5).⁴⁵ The photosensitiser is able to penetrate through a Gram-positive bacteria cell wall as it has a single thick peptidoglycan layer,⁴⁶ whereas Gram-negative bacteria consist of a thinner peptidoglycan layer with an inner and outer membrane.¹² The outer membrane can prevent binding and penetration of the photosensitiser.⁴⁷

2.2 Antibacterial Action of Nanoparticles

2.2.1 Use of nanoparticles in a clinical environment

Conventional antibiotic treatments for reducing HAIs are becoming less effective against multi-drug resistant bacteria. Advances in nanoscience and nanotechnology have resulted in novel nano-sized materials which have the potential of replacing antibiotics within hospitals due to their distinct functional properties.⁴⁸ In particular, the bactericidal effect of metal or metal oxide nanoparticles is of particular interest since they can be immobilised or coated onto surfaces for various applications, such as antibacterial surfaces,⁴⁹ medical devices,⁵⁰ food processing⁵¹ and water treatment.⁵²

Due to their high surface area-to-volume ratio, nanoparticles exhibit different biological properties (e.g. accumulation within the cell tissue),⁵³ chemical properties (e.g. increased reaction rate)⁵⁴ and physical properties (e.g. increased absorption or diffusion rates)⁵⁵ compared to the bulk material. It has been extensively reported in the literature that smaller nanoparticles (< 100 nm) exhibit better antibacterial activity.⁵⁶⁻⁵⁸ The bactericidal mechanism of nanoparticles is specific to a particular bacterial

species, i.e. the antibacterial efficacy is dependent on the bacterial cell structure.⁵⁷

The bacterial cell wall is intended to protect the cell from mechanical damage and osmotic rupture by providing strength, shape and rigidity.⁵⁹ As previously described, the bacterial cell wall can either be categorised as Gram-positive or Gram-negative.⁶⁰ Gram-negative bacterial cell wall structures are more chemically and structurally complex than Gram-positive. The outer membrane of Gram-negative bacteria contain lipopolysaccharides which increase the overall negative charge of cell membranes and maintain structural integrity of the bacteria⁶¹ (Fig. 2.5). Furthermore, Gram-negative bacteria are more resistant to hydrophobic compounds (e.g. detergents).⁶² Similarly to photosensitisers, the bacterial cell wall structure plays a crucial role in determining the ability of nanoparticles to penetrate into the cell.⁶³

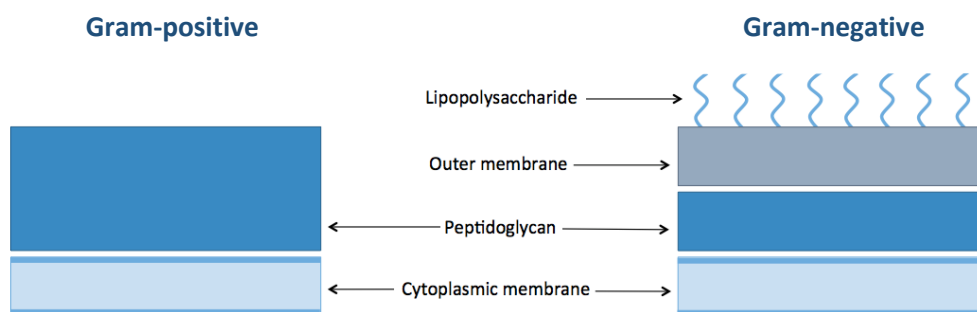


Fig. 2.5 Gram-positive and Gram-negative bacterial cell wall structure.

Additional factors can influence the susceptibility of bacteria to nanoparticles, such as the type of nanoparticle⁶⁴ and the bacterial growth rate.⁶⁵ Some studies have shown that *E. coli* is more susceptible to CuO nanoparticles than *S. aureus*⁴⁸ and it has been reported that the antibacterial activity of Ag nanoparticles is greater than Cu nanoparticles against both Gram-positive and Gram-negative bacteria.⁶⁶ Fast-growing bacteria are more susceptible to nanoparticles than slow-growing bacteria,

possibly because the tolerance of slow-growing bacteria is related to the expression of stress-response genes.⁶⁷

2.2.1.1 Antibacterial mechanism of nanoparticles

The exact antibacterial mechanism of nanoparticles is not completely understood. There are a number of ways in which nanoparticles are reported in the literature to kill bacteria, e.g. disruption/penetration of the cell,⁵⁸ electrostatic interaction,⁵⁷ or generating ROS, causing permanent damage and eventually cell death (summarised in Fig. 2.6).⁶⁸ ROS generation is considered the most effective means of nanoparticle bactericidal activity as it produces severe oxidative stress causing DNA damage.⁶⁹ When ROS production is activated by UV or visible light, the toxicity of nanoparticles is photocatalytic (e.g. TiO₂).⁷⁰

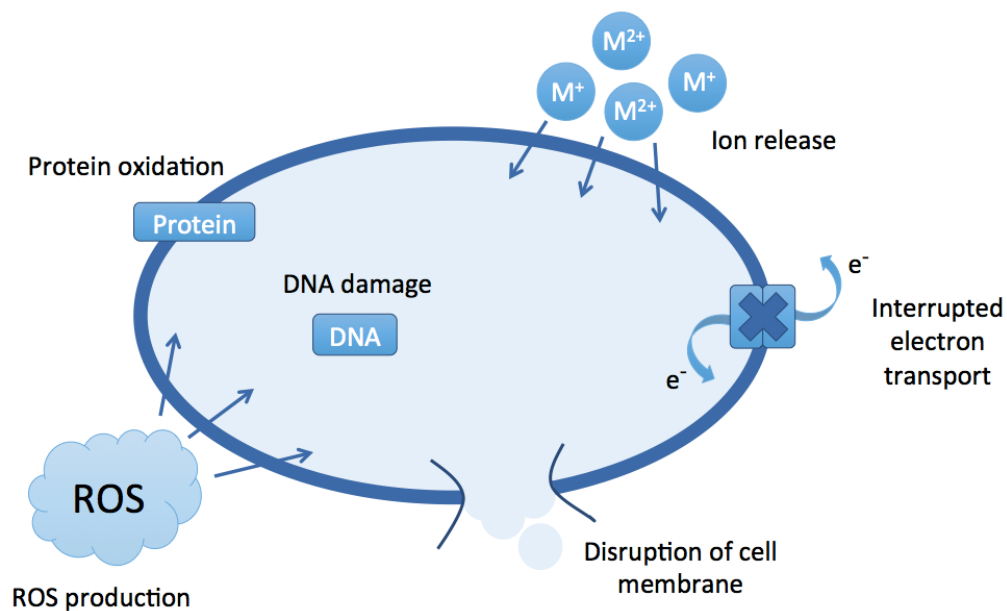


Fig. 2.6 Different possible mechanisms of toxicity of nanoparticles against bacteria, including: reactive oxygen species (ROS) production, ion release, protein and DNA damage and disruption of the cell membrane.

Various metal and metal oxide nanoparticles have been studied for their antibacterial activity which may find applications in the medical field. These include silver, gold, iron, titanium dioxide, copper, zinc oxide and magnesium oxide. Silver has been exploited for its antibacterial properties for many years and is used in a range of applications such as wound dressing,⁷¹ disinfecting water⁷² and for coating medical devices.⁷³ The antibacterial activity of silver nanoparticles (Ag NPs) is size-dependent⁷⁴ and operates *via* ROS production causing structural changes in the cell membrane and ultimately cell death.⁷⁵ However, the main proposed mechanism of action of Ag NPs is considered to be the release of silver ions.⁷⁶ Ag NPs have shown to be very effective in preventing biofilm formation of *E. coli* and *S. aureus*⁷⁷ and exhibit no significant cytotoxicity towards mammalian cells.⁷⁸

Gold nanoparticles (Au NPs) have limited bactericidal effects on their own but when they are bound to antibiotics, such as ampicillin and vancomycin, they demonstrate an enhanced activity of the antibiotic against Gram-positive and Gram-negative bacteria.⁷⁹ Titanium dioxide is the most commonly studied antibacterial metal oxide nanoparticle and was first discovered to reduce levels of *E. coli* in 1985.⁵⁸ The main bactericidal mechanism of TiO₂ nanoparticles is the production of ROS in the presence of UV light (Fig. 1.4, Chapter 1).⁶⁸ Various studies have focused on activating TiO₂ with visible light by metal doping (e.g. Ag, Fe³⁺, Cd or NiO).^{72,80-82}

2.2.2 Copper nanoparticles

Metallic copper has been widely used as an antibacterial surface agent, though only a few studies have reported the antibacterial effects of copper nanoparticles (Cu NPs). Metallic nanoparticles are reported to exhibit 7 – 50 times less toxicity towards mammalian cells than their ionic forms.⁸³ Copper is cost effective to produce and has been used for centuries to

sterilise liquids, textiles and human tissue.⁸⁴ The availability of copper has made it a better alternative to other expensive noble metals, e.g. silver and gold.⁸⁵ Cu NPs have shown a high antibacterial effect against *P. aeruginosa*, *S. aureus*, *E. coli*, viruses and fungi,⁸⁶ but a low toxicity against humans which makes them appropriate for creating wound healing products⁸⁷ and for impregnation into antibacterial surfaces in hospitals.⁸⁸

They have been prepared using a range of methods, such as thermal reduction,⁸⁹ chemical reduction, vacuum vapour deposition and microwave irradiation methods.⁹⁰ These methods use oxygen-free conditions to synthesise the nanoparticles as they rapidly oxidise to Cu²⁺ ions in air or aqueous media.⁷² Thus, it is vital that a method is developed which can stabilise Cu NPs to prevent oxidation and agglomeration. Nanoparticles readily aggregate because they have a high surface energy that prevents effective dispersion into solutions or polymer matrices.⁹¹ Alternative methods have been used to synthesise Cu NPs in the presence of polymers (e.g. chitosan,⁹² polyethylene glycol⁹³) or surfactants (e.g. cetyl trimethyl ammonium bromide) as stabilisers to form coatings around the nanoparticle surface.⁹⁴

The exact bactericidal mechanism of Cu NPs is not fully understood. Their small size and high surface-to-volume ratio allows a close interaction with bacterial cell membranes to alter their permeability and cause irreversible cell damage.⁵⁸ Moreover, they can generate ROS that cause severe oxidative damage to the cell structure.⁹⁵ Cu²⁺ ions can be released from the nanoparticle surface that are adsorbed on the cell membrane from electrostatic interaction, causing DNA damage in the bacteria and ultimately cell death.⁹⁶

2.2.3 Magnesium oxide nanoparticles

Magnesium oxide nanoparticles (MgO NPs) are advantageous compared to other bactericidal agents because they are odourless, non-toxic towards

human cells at low concentrations, and can be synthesised from economically and commercially available precursors and solvents.⁵⁸ They are multi-functional and can be used in catalysis, catalyst supports,⁷⁹ superconductors and lithium ion batteries, and removing pathogenic microorganisms from toxic wastewater.⁹⁷ In medical applications, MgO NPs have been used for bone regeneration,⁹⁸ treating heartburn and sore stomachs, and more recently they have been used in tumour treatment.⁹⁹ MgO NPs have a wide band gap and exhibit antibacterial activity without photo-activation (unlike TiO₂).⁹⁷ It has been reported that the size and shape of MgO NPs gives them a high surface reactivity as they contain a high concentration of edge/corner sites and structural defects on the surface.⁹⁹ Some studies suggest that Mg²⁺ ions can cause cell death when released into solution,^{72,100} whilst others have found no inhibition of *E. coli* or *S. aureus* from ion release.⁷⁹ It has been proposed that active superoxide ions are generated on the surface of metal oxides, such as MgO NPs, which react with peptide linkages in bacteria cell walls and cause disruption. An increase in the production of superoxide ions is caused by an increase in surface area of the nanoparticles.⁹⁷

Many methods have been used to synthesise MgO NPs, including sol-gel, chemical vapour deposition and thermal evaporation.¹⁰¹ The sol-gel method is very common for producing MgO NPs because it prepares controlled homogenous particles at a low cost.⁹¹ Additionally, magnesium fluoride nanoparticles (MgF₂ NPs) can prevent biofilm formation of common bacterial pathogens such as *E. coli* and *S. aureus*.⁷⁹ MgF₂ NPs attach and penetrate into the bacterial cells; causing disruption in the membrane potential, inducing membrane lipid peroxidation and interacting with chromosomal DNA.^{62,79}

2.2.4 Zinc oxide nanoparticles

Zinc oxide nanoparticles (ZnO NPs) are relatively cheap¹⁰² and exhibit effective size-dependent antimicrobial activity against many bacteria, viruses and fungi, including *E. coli*, *S. aureus*, MRSA and *Klebsiella pneumoniae*.⁶⁸ The antibacterial activity of ZnO NPs has attracted much biomedical interest as the nanoparticles show toxicity towards bacteria but exhibit minimal effects on mammalian cells. They are widely used for bioimaging,¹⁰³ drug delivery,^{103,104} and as effective bactericidal agents against food-borne pathogens in food packaging.¹⁰⁵ ZnO NPs have a wide band gap (3.3 eV) in the near-UV region, which affects the electrical conductivity and optical properties.¹⁰⁶ They have a high optical absorption in the UV region and are consequently used as a UV protector in cosmetics.¹⁰⁷

ZnO is highly photocatalytic and is more biocompatible than TiO₂.¹⁰⁸ It can strongly absorb UV light which enhances the conductivity and causes a better interaction between the bacteria and nanoparticles.¹⁰⁷ There are many proposed mechanisms of the antibacterial activity of ZnO NPs, including the disruption of bacterial cell membranes¹⁰⁷ and photo-oxidative stress induced by ROS generation.¹⁰⁹ Some reports suggest that ZnO NPs generate hydroxyl and superoxide anion radicals under UV or visible light activation.⁶⁹ A recent study reported that the antibacterial activity of ZnO NPs is partially due to Zn²⁺ release. These experiments were conducted in the dark so there was minimal photoactivated ROS generation.⁶⁸ Some studies suggest that ZnO NPs are less toxic towards Gram-positive bacteria due to the presence of a thicker peptidoglycan layer,⁵⁷ but many other studies contradict this, demonstrating a lower susceptibility towards Gram-negative bacteria presumably due to the outer cell membrane.^{57,107}

The toxicity of ZnO NPs is dependent on their morphology, which is determined by synthetic conditions.¹¹⁰ Therefore, optimal antibacterial response of these nanoparticles can be obtained by controlling parameters such as solvent type, precursor type, temperature and pH.¹⁰⁷ The surfaces

of ZnO NPs contain many defects that are potential reactive surface sites. It has been suggested that the abrasive surface of ZnO is responsible for its antibacterial properties.¹¹¹ ZnO NPs were coated onto silicone wafers and incorporated into polyvinyl chloride (PVC) to study their effect against biofilm formation.¹⁰⁷ The results indicated 20 - 50% reduction of biofilm growth against *E. coli* and *S. aureus*.^{57,107}

2.3 Dye and nanoparticle-incorporated polymers

Aqueous solutions of photosensitisers are highly effective for killing hospital pathogens following light activation *via* the formation of oxygen-derived, cytotoxic ROS.¹¹² In cellular environments, these ROS can result in cell death and destruction of tissues.³⁰ Photosensitisers are taken up into cells all over the body and are harmless in the absence of light (and usually oxygen), where they have no effect on healthy tissue.¹¹ Preferably, light activation should be controlled so that photoactivation only occurs when a higher concentration of the photosensitiser is present in the diseased tissue and does not cause damage to surrounding, non-cancerous cells.¹¹³ When exposed to bacteria, photosensitisers are very effective at killing the bacteria following light exposure, which has led to the idea of coating photosensitisers onto polymers since ROS can migrate from the polymer to the bugs. By coating the polymer with the photosensitiser, the photosensitiser then becomes less harmful to surrounding tissue/skin compared to aqueous solutions of the dye where the dye is able to enter cells.

The ROS generated are unlikely to cause bacterial resistance, unlike antibiotics, as they attack microorganisms by multiple pathways rather than having a specific mode of attack.^{112,113} At concentrations lethal to bacteria, photosensitisers exhibit minimal toxicity against mammalian cells following light activation.¹¹⁴ Various metal and metal oxide nanoparticles demonstrate significant antibacterial activity against bacteria with or

without light activation.^{79,115} One possible mechanism of action of these nanoparticles is the generation of ROS, but they can also kill bacteria by electrostatically interacting with the cell membrane from the leaching of ions and causing damage by penetrating through the cell membrane.¹¹⁶ It is possible to further enhance the antibacterial properties of photosensitisers and nanoparticles by combining them together in polymers to produce light-activated antibacterial surfaces.¹¹²⁻¹¹⁴

2.3.1 Polymer types

The material of antibacterial surfaces or medical devices in hospitals should be biocompatible and perform its intended function without causing unwanted side effects. It is important to consider physical properties of the material (i.e. surface roughness and rigidity)¹¹⁷ as well as chemical properties (allergenic or toxic).⁸⁸ For invasive medical devices, such as catheters, the material must not cause any side effects to the body that will alter its primary function.¹¹⁸⁻¹¹⁹

2.3.1.1 Polyvinyl chloride

Polyvinyl chloride (PVC) is produced by addition polymerisation of vinyl chloride monomer. The pure plastic is relatively hard and rigid, thus, chemicals (e.g. plasticisers) are added to make PVC more soft and pliable.¹²⁰ As the plasticisers are not chemically bound to the polymer, they can induce acute inflammatory reactions *in vivo* if they leach.¹²¹ PVC polymers have been commercially available for around 50 years and are considered as a 'mature product'. Recently, novel materials have been introduced, including PVC alloys and ultra-high molecular weight PVC polymers that do not require additional plasticisers.¹²²

2.3.1.2 Silicone

Silicone, also known as polydimethylsiloxane (PDMS), is a widely used biomaterial and has been used as a medical device coating for many years. It is durable, hydrophobic, chemically and thermally stable and has a low surface tension.¹²³ Silicone remains unaffected by repeated autoclaving and can also be dry-heat sterilised.¹²⁴ Studies comparing silicone and PVC catheters found that silicone catheters performed much better and maintained their physical properties and flexibility over time.¹²⁵ However, silicone is more expensive than other materials such as latex and PVC.¹²⁴

2.3.1.3 Polyurethane

In Western Europe, thousands of tonnes of polyurethane products are manufactured each year for medical device applications.¹²⁶ They are used for surgical prostheses, catheters, artificial heart, kidney and blood vessels and are replacing silicone in maxillofacial surgery.¹²⁷ Moreover, polyurethane elastomers are used in formulating haemostatic coatings and biomedical adhesive systems.¹²² More flexible polyurethane foams are used in producing bandages, surgical dressings and absorbent materials for general hospital practice.¹²⁸ This polymer is biocompatible and has replaced silicone in some catheters as it can be more comfortable for patients.¹²⁴

2.3.2 Overview of the research at the Materials Research Centre, UCL

Self-sterilising antibacterial surfaces can assist in significantly reducing HAIs, as basic cleaning methods are ineffective against emerging multi-drug resistant bacteria. The Materials Research Centre at University College London (UCL) has developed several photo-activated surfaces and tested them against a range of Gram-positive and Gram-negative bacteria under different lighting conditions (e.g. laser, UV, visible light and in the dark).¹¹³

Some materials have been designed to combat catheter-associated infections, which account for a large proportion of healthcare infections.¹²⁹⁻¹³³ These studies demonstrate that the incorporation of a photosensitiser into a polymer results in highly efficacious kill of pathogens, with a potential to prevent biofilm formation. Metal-based nanomaterials and photosensitisers have been incorporated into polymers using a simple, easily up-scalable 'swell-encapsulation-shrink' method.^{112,129} This preparative route is effective, low maintenance, and does not require any complicated synthetic methods of attachment.¹¹⁴ It is described in more detail in Chapters 3-6.

Earlier studies conducted by Piccirillo *et al*^{127,128} showed lethal photosensitisation of *E. coli* and *Staphylococcus epidermidis* (*S. epidermidis*) with TBO- and MB-incorporated silicone polymers irradiated with 634 nm and 660 nm light, respectively. Further investigations carried out by Perni *et al*¹³⁴ demonstrated a 2 log₁₀ reduction in MRSA and *S. epidermidis* using indocyanine green-containing polyurethane when exposed with a laser light from near-infrared spectrum (808 nm). Following this, Perni *et al*¹³³ examined the antibacterial activity of silicone against *E. coli* and *S. epidermidis* exposed to laser light (660 nm), showing that they were both considerably affected by the presence and size of Au NPs. Noimark *et al*¹³⁰ established that 2 nm sized Au NPs were most effective in reducing bacterial numbers under fluorescent lighting. They demonstrated an enhancement in MB triplet state production with 2 nm Au NPs using time-resolved electron paramagnetic resonance (EPR) spectroscopy, indicating a greater production of ROS in these co-doped materials than with MB alone. Furthermore, they revealed exceptionally effective antibacterial activity of silicone containing CV and Au NPs against Gram-positive and Gram-negative bacteria upon irradiation with a low power laser (635 nm) for short time periods. More significantly, bacterial kill was achieved in the dark.¹²⁹ Bovis *et al*¹³⁵ used 660 nm laser light to confirm

both Type I and Type II mechanisms were occurring within photo-activated silicone containing MB and Au NPs.

Following this, novel multi-dye antibacterial polymers were prepared by Noimark *et al*¹³⁶ using silicone incorporated with CV, MB and 2 nm Au NPs and activated by white light emitting ~3,750 lux. Lethal photosensitisation of *S. epidermidis* and *E. coli* occurred within 3 hours and 6 hours, respectively ($\geq 4 \log_{10}$ reduction). Moreover, potent antimicrobial activity against both bacteria was shown within 18 hours in the dark. Most recently, Noimark *et al*¹³⁷ and Ozkan *et al*¹³⁸ introduced ZnO NPs into silicone-based systems. ZnO NPs combined with CV displayed lethal bactericidal effects against *E. coli* and *S. aureus* when activated by white light emitting ~3,750 – 10,500 lux intensity.

2.4 Research aims

This thesis focuses on photo-activated surfaces incorporated with nanoparticles and/or crystal violet dye. These antibacterial surfaces will be activated by white light and tested in the dark to determine their efficacy against a wide range of hospital-associated bacteria. Polyurethane was used as the main polymer in this thesis since it is replacing silicone for medical applications as detailed above and therefore, represents an advance on the previous studies described in section 2.3.2. The thesis describes the following studies:

- (a) Investigating the antibacterial activity of biocompatible copper nanoparticles impregnated into two widely used polymers: silicone and polyurethane, to understand the differences in bacterial reduction without a photosensitiser (i.e. dark kill). For the first time, two polymers are compared and non-toxic copper nanoparticles will be synthesised *via* a green method.
- (b) Incorporating a well-known biocidal disinfectant used in hospitals into a polymer and studying the efficiency of the 'swell-

encapsulation-shrink' method compared to coating the material with the antibacterial agent. Looking at the activity of a biocide for the first time in our research group to see its efficiency when incorporated into a polymer rather than in solution form.

- (c) An investigation into the effects of ZnO nanoparticle size and capping ligand on the antibacterial activity of crystal violet when incorporated into polymers under varied white light intensity and in the dark.
- (d) A study into the mechanism of the polymeric systems to see how ZnO nanoparticles enhance bactericidal properties of the photosensitiser, an aspect which has not previously been investigated before in our research group. Mechanistic studies will focus on Type I and Type II inhibitors.
- (e) Advancements of a protocol used for antimicrobial testing was developed that provided a closer simulation of real-world conditions and also tested the new materials against wild strains of clinically-relevant bacteria and *C. difficile* endospores rather than laboratory strains, which only have been tested in previous work. By making these changes and studying the best-performing antibacterial polymers against actual clinical strains, evidence is presented which suggests that these surfaces are potentially appropriate to be used in healthcare applications by reducing the spread of bacterial contamination and minimising the risk of HAIs.

References

- 1 Edelson MF. Light-activated drugs. *Scientific American*. 1988;259:68-75.
- 2 Sternberg ED, Dolphin D, Bruckner C. Porphyrin-based photosensitisers for use in photodynamic therapy. *Tetrahedron*. 1998;54(17):4151-4202.
- 3 Bonnett R, Martinez G. Photobleaching of sensitisers used in photodynamic therapy. *Tetrahedron*. 2001;57(47):9513-9547.
- 4 Allison RR, Moghissi K. Photodynamic Therapy (PDT): PDT Mechanisms. *Clinical Endoscopy*. 2013;46(1):24-29.
- 5 Huang Y, Tanaka M, Vecchio D, Garcia-Diaz M, Chang J, Morimoto Y, Hamblin MR. Photodynamic therapy induces an immune response against a bacterial pathogen. *Expert Review of Clinical Immunology*. 2012;8(5):479-494.
- 6 Zhang X, Liu T, Li Z, Zhang X. Progress of photodynamic therapy applications in the treatment of musculoskeletal sarcoma (Review). *Oncology Letters*. 2014;8(4):1403-1408.
- 7 Lipson RL, Baldes EJ. The photodynamic properties of a particular hematoporphyrin derivative. *Archives of Dermatology*. 1960;82(4):508-516.
- 8 Lipson RL, Baldes EJ. Photosensitivity and Heat. *Archives of Dermatology*. 1960;82:517-520.
- 9 Dougherty TJ. Photodynamic therapy (PDT) of malignant tumours. *Critical Reviews in Oncology/Hematology*. 1984;2(2):83-116.
- 10 Huang Z, Xu H, Meyers AD, Musani AI, Wang L, Tagg R, Barqawi AB, Chen YK. Photodynamic therapy for treatment of solid tumors – potential and technical challenges. *Technology in Cancer Research & Treatment*. 2008;7(4):309-320.

- 11 Josefsen LB, Boyle RW. Photodynamic Therapy and the Development of Metal-based Photosensitisers. 2008;2008:276109.
- 12 Sperandio FF, Huang Y, Hamblin MR. Antimicrobial photodynamic therapy to kill Gram-negative bacteria. *Recent Patents on Anti-Infective Drug Discovery*. 2013;8(2):108-120.
- 13 Dolmans D, Fukumura D, Jain K. Photodynamic therapy for cancer. *Nature Reviews*. 2003;3:380-387.
- 14 Hamblin MR, Hasan T. Photodynamic therapy: a new antimicrobial approach to infectious disease? *Photochemical and Photobiological Sciences*. 2004;3(5)436-450.
- 15 Carruth JA. Clinical applications of photodynamic therapy. *International Journal of Clinical Practice*. 1998;52(1):39-42.
- 16 Kharkwal GB, Sharma SK, Huang Y, Dai T, Hamblin MR. Photodynamic Therapy for Infections: Clinical Applications. *Lasers in Surgery and Medicine*. 2011;43(7):755-767.
- 17 Guthmiller JM, Novak KF. Periodontal Diseases. In: Brogden KA, Guthmiller JM, editors. Polymicrobial Diseases. Washington (DC): ASM Press; 2002. Chapter 8.
- 18 Barbosa P, Duarte DA, Leite MF, Anna G R. Photodynamic Therapy in Pediatric Dentistry. *Case Reports in Dentistry*. 2014;2014:1-5.
- 19 DeRosa MC, Crutchley RJ. Photosensitised singlet oxygen and its applications. *Coordination Chemistry Reviews*. 2002;233-234:351-371.
- 20 Berezin MY, Achilefu S. Fluorescence Lifetime Measurements and Biological Imaging. *Chemical reviews*. 2010;110(5):2641-2684.
- 21 Tseng H, Shen J, Kuo T, Tu T, Chen Y, Demchenko AP, Chou P. Excited-state intramolecular proton-transfer reaction demonstrating anti-Kasha behavior. *Chemical Science*. 2016;7:655-665.

- 22** Favaro G, Romani A, Becker RS. Competition between vibrational relaxation and photochemistry: relevance of vibronic quantum effects. *Photochemistry and Photobiology*. 2001;74(3):378-384.
- 23** Dujardin G, Leach S. Intramolecular Relaxation of Excited States of C₆F₆. *Faraday Discussion Chemical Society*. 1983;75:23-43.
- 24** Beljonne D, Shuai Z, Pourtois G, Bredas JL. Spin-orbit coupling and intersystem crossing in conjugated polymers: a configuration interaction description. *Journal of Physical Chemistry*. 2001;105:3899-3907.
- 25** Keating PB, Hinds MF, Davis SJ. A singlet oxygen sensor for photodynamic cancer therapy. *Proceedings of the International Congress on Applications of Lasers and Laser-Optics*, San Diego, California, USA. November 1999.
- 26** Schweitzer C, Schmidt R. Physical mechanisms of generation and deactivation of singlet oxygen. *Chemical Reviews*. 2003;103(5):1685-1757.
- 27** Kochevar IE, Redmond RW. Photosensitized production of singlet oxygen. *Methods in Enzymology*. 2000;319:20-28.
- 28** Henderson BW, Dougherty TJ. How does photodynamic therapy work? *Photochemistry and Photobiology*. 1992;55:145-157.
- 29** Vatansever F, de Melo W.C.M.A., Avci P, Vecchio D, Sadasivam M, Gupta A, Chandran R, Karimi M, Parizotto NA, Yin R, Tegos GP, Hamblin MR. Antimicrobial strategies centered around reactive oxygen species – bactericidal antibiotics, photodynamic therapy and beyond. *FEMS Microbiology Reviews*. 2013;37(6):955-989.
- 30** Castano AP, Demidova TN, Hamblin MR. Mechanisms in photodynamic therapy: part one – photosensitisers, photochemistry and cellular localization. *Photodiagnoses Photodynamic Therapy*. 2004;1(4):279-293.

- 31** Wojcik J, Psezke J, Ratuszna A, Kus P, Wrzalik R. Theoretical investigation of porphyrin-based photosensitisers with enhanced NIR absorption. *2013;15(45):19651-19658.*
- 32** Usacheva M, Swaminathan SK, Kirtane AR, Panyam J. Enhanced Photodynamic Therapy and Effective Elimination of Cancer Stem Cells using Surfactant-Polymer Nanoparticles. *Molecular Pharmaceutics.* 2014;11(9):3186-3195.
- 33** Ormond AB, Freeman HS. Dye sensitizers for photodynamic therapy. *Materials.* 2013;6:817-840.
- 34** Uttara B, Singh AV, Zamboni P, Mahajan RT. Oxidative Stress and Neurodegenerative Diseases: A Review of Upstream and Downstream Antioxidant Therapeutic Options. *Current Neuropharmacology.* 2009;7(1):65-74.
- 35** Flora SJS. Structural, chemical and biological aspects of antioxidants for strategies against metal and metalloid exposure. *Oxidative Medicine and Cellular Longevity.* 2009;2(4):191-206.
- 36** Sharma P, Jha AB, Dubey RS, Pessarakli M. Reactive Oxygen Species, Oxidative Damage and Antioxidative Defense Mechanism in Plants under Stressful Conditions. *Journal of Botany.* 2012;2012:1-26.
- 37** Decker H, van Holde KE. Oxygen, its nature and chemistry: what is so special about this element? Oxygen and the Evolution of life. *Springer Berlin Heidelberg.* 2010;1-19.
- 38** Moan J, Berg K. The photodegradation of porphyrins in cells can be used to estimate the lifetime of singlet oxygen. *Photochemistry and Photobiology.* 1991;53(4):549-553.
- 39** Morales J, Günther G, Zanocco AL, Lemp E. Singlet Oxygen Reactions with Flavonoids. A Theoretical – Experimental Study. Lebedev N, ed. *PLoS ONE.* 2012;7(7):e40548.

- 40 Jefford CW, Rimbault CG. Reaction of singlet oxygen with norbornenyl ethers. Characterisation of dioxetanes and evidence for zwitterionic peroxide precursors. *Journal of the American Chemical Society*. 1978;100(20):6437-6445.
- 41 Firey PA, Rodgers MA, Photo-properties of a silicon naphthalocyanine: a potential photosensitizer for photodynamic therapy. *Photochemistry and Photobiology*. 1987;45(4):535-8.
- 42 Sharma SK, Dai T, Kharkwal GB, Kharkwal GB, Huang Y, Huang L, Bil De Arce VJ, Tegos GP, Hamblin MR. Drug Discovery of Antimicrobial Photosensitizers Using Animal Models. *Current pharmaceutical design*. 2011;17(13):1303-1319.
- 43 Rajesh S, Koshi E, Philip K, Mohan A. Antimicrobial photodynamic therapy: An overview. *Journal of Indian Society of Periodontology*. 2011;15(4):323-327.
- 44 Imlay JA. Cellular defenses against superoxide and hydrogen peroxide. *Annual review of biochemistry*. 2008;77:755-776.
- 45 Fu X, Fang Y, Yao M. Antimicrobial Photodynamic Therapy for Methicillin-Resistant *Staphylococcus aureus* Infection. *BioMed Research International*. 2013;2013:1-9.
- 46 Bourre L, Giuntini F, Eggleston IM, Mosse CA, MacRobert AJ, Wilson M. Effective photoinactivation of Gram-positive and Gram-negative bacterial strains using an HIV-1 Tat peptide-porphyrin conjugate. *Photochemical & Photobiological Sciences*. 2010;9:1613-1620.
- 47 Nikaido H. Molecular Basis of Bacterial Outer Membrane Permeability Revisited. *Microbiology and Molecular Biology Reviews*. 2003;67(4):593-656.
- 48 Azam A, Ahmed AS, Oves M, Khan MS, Memic A. Size-dependent antimicrobial properties of CuO nanoparticles against Gram-positive and -negative bacterial strains. *International Journal of Nanomedicine*. 2012;7:3527-3535.
- 49 Palza H. Antimicrobial Polymers with Metal Nanoparticles. *International Journal of Molecular Sciences*. 2015;16(1):2099-2116.

- 50 Salata OV. Applications of nanoparticles in biology and medicine. *Journal of Nanobiotechnology*. 2004;2(1):3-8.
- 51 Institute of Medicine (US) Food Forum. Nanotechnology in Food Products: Workshop Summary. Washington (DC): National Academies Press (US). 2, Application of Nanotechnology to Food Products, 2009. [Accessed on 08/11/16, available on: Available from: <https://www.ncbi.nlm.nih.gov/books/NBK32730/>]
- 52 Chalew TEA, Ajmani GS, Huang H, Schwab KJ. Evaluating Nanoparticle Breakthrough during Drinking Water Treatment. *Environmental Health Perspectives*. 2013;121(10):1161-1166.
- 53 Mody VV, Siwale R, Singh A, Mody HR. Introduction to metallic nanoparticles. *Journal of Pharmacy and Bioallied Sciences*. 2010;2(4):282-289.
- 54 Chaturvedi S, Dave PN, Shah NK. Applications of nano-catalyst in new era. *Journal of Saudi Chemical Society*. 2012;16(3):307-325.
- 55 Issa B, Obaidat IM, Albiss BA, Haik Y. Magnetic Nanoparticles: Surface Effects and Properties Related to Biomedicine Applications. *International Journal of Molecular Sciences*. 2013;14(11):21266-21305.
- 56 Pal S, Tak YK, Song JM. Does the Antibacterial Activity of Silver Nanoparticles Depend on the Shape of the Nanoparticle? A Study of the Gram-Negative Bacterium *Escherichia coli*. *Applied and Environmental Microbiology*. 2007;73(6):1712-1720.
- 57 Seil JT, Webster TJ. Antimicrobial applications of nanotechnology: methods and literature. *International Journal of Nanomedicine*. 2012;7:2767-2781.
- 58 Beyth N, Hour-Haddad Y, Domb A, Khan W, Hazan R. Alternative Antimicrobial Approach: Nano-Antimicrobial Materials. *Evidence-Based Complementary and Alternative Medicine*. 2015;2015:1-16.

- 59 Sun T, Hao H, Hao W, Yi S, Li X, Li J. Preparation and antibacterial properties of titanium-doped ZnO from different zinc salts. *Nanoscale Research Letters*. 2014;9(1):98.
- 60 Silhavy TJ, Kahne D, Walker S. The Bacterial Cell Envelope. *Cold Spring Harbor Perspectives in Biology*. 2010;2(5):a000414.
- 61 Beveridge TJ. Structures of Gram-Negative Cell Walls and Their Derived Membrane Vesicles. *Journal of Bacteriology*. 1999;181(16):4725-4733.
- 62 Delcour AH. Outer Membrane Permeability and Antibiotic Resistance. *Biochimica et biophysica acta*. 2009;1794(5):808-816.
- 63 De Jong WH, Borm PJ. Drug delivery and nanoparticles: Applications and hazards. *International Journal of Nanomedicine*. 2008;3(2):133-149.
- 64 Israelsen N, Hanson C, Vargis E. Nanoparticle Properties and Synthesis Effects on Surface-Enhanced Raman Scattering Enhancement Factor: An Introduction. *The Scientific World Journal*. 2015;2015:1-12.
- 65 Vardanyan Z, Gevorkyan V, Ananyan M, Vardapetyan H, Trchounian A. Effects of various heavy metal nanoparticles on *Enterococcus hirae* and *Escherichia coli* growth and proton-coupled membrane transport. *Journal of Nanobiotechnology*. 2015;13:69.
- 66 Khan M, Khan ST, Khan M, Adil SF, Musarrat J, Al-Khedhairi AA, Al-Warthan A, Siddiqui MR, Alkhatlan HZ. Antibacterial properties of silver nanoparticles synthesized using *Pulicaria glutinosa* plant extract as a green bioreductant. *International Journal of Nanomedicine*. 2014;9:3551-3565.
- 67 Greulich P, Scott M, Evans MR, Allen RJ. Growth-dependent bacterial susceptibility to ribosome-targeting antibiotics. *Molecular Systems Biology*. 2015;11(3):0796.
- 68 Prasanna VL, Vijayaraghavan R. Insight into the mechanism of antibacterial activity ZnO: surface defects mediated reactive oxygen species even in the dark. *Langmuir*. 2015;31(33):9155-9162.

- 69 Fu PP, Xia Q, Huang H, Ray PC, Yu H. Mechanisms of nanotoxicity: Generation of reactive oxygen species. *Journal of Food and Drug Analysis*. 2014;22(1):64-75.
- 70 Li Z, Mi L, Wang P, Chen J. Study on the visible-light-induced photokilling effect of nitrogen-doped TiO₂ nanoparticles on cancer cells. *Nanoscale Research Letters*. 2011;6(1):356.
- 71 Gunasekaran T, Nigusse T, Dhanaraju MD. Silver Nanoparticles as Real Topical Bullets for Wound Healing. *The Journal of the American College of Clinical Wound Specialists*. 2011;3(4):82-96.
- 72 Tran QH, Nguyen VQ, Le A. Silver nanoparticles: synthesis, properties, toxicology, applications and perspectives. *Advances in Natural Sciences: Nanoscience and Nanotechnology*. 2013;4(3):1-20.
- 73 Ge L, Li Q, Wang M, Ouyang J, Li X, Xing MM. Nanosilver particles in medical applications: synthesis, performance, and toxicity. *International Journal of Nanomedicine*. 2014;9:2399-2407.
- 74 Lu Z, Rong K, Li J, Yang H, Chen R. Size-dependent antibacterial activities of silver nanoparticles against oral anaerobic pathogenic bacteria. *Journal of Materials Science: Materials in Medicine*. 2013;24(6):1465-1471.
- 75 Kim JS, Kuk E, Yu KN, Kim, J, Park SJ, Jeong DH, Cho M. Antimicrobial effects of silver nanoparticles. *Nanomedicine: Nanotechnology, Biology, and Medicine*. 2007;3:95-101.
- 76 Stensberg MC, Wei Q, McLamore ES, Porterfield DM, Wei A, Sepúlveda MS. Toxicological studies on silver nanoparticles: challenges and opportunities in assessment, monitoring and imaging. *Nanomedicine*. 2011;6(5):879-898.
- 77 Gurunathan S, Han JW, Kwon D-N, Kim J-H. Enhanced antibacterial and anti-biofilm activities of silver nanoparticles against Gram-negative and Gram-positive bacteria. *Nanoscale Research Letters*. 2014;9(1):373.

- 78** Jena P, Mohanty S, Mallick R, Jacob B, Sonawane A. Toxicity and antibacterial assessment of chitosan-coated silver nanoparticles on human pathogens and macrophage cells. *International Journal of Nanomedicine*. 2012;7:1805-1818.
- 79** Rana S, Kalaichelvan PT. Antibacterial Activities of Metal Nanoparticles. *Advanced Biotech*. 2011;11(2):21-23.
- 80** Wang M, Loccozia J, Sun L, Lin C, Lin Z. Inorganic-modified semiconductor TiO₂ nanotube arrays for photocatalysis. *Energy & Environmental Science*. 2014;7:2182-2202.
- 81** Boxi SS, Paria S. Visible light induced enhanced photocatalytic degradation of organic pollutants in aqueous media using Ag doped hollow TiO₂ nanosphere. *RSC Advances*. 2015;5:37657-37668.
- 82** Pelaez M, Nolan NT, Pillai SC, Seery MK, Falaras P, Kontos AG, Dunlop PSM, Hamilton JWJ, Byrne JA, O'Shea K, Entezari MH, Dionysiou DD. A review on the visible light active titanium dioxide photocatalyst for environmental applications. *Applied Catalysis B: Environmental*. 2012;125:331-349.
- 83** Tauran Y, Brioude A, Coleman AW, Rhimi M, Kim B. Molecular recognition by gold, silver and copper nanoparticles. *World Journal of Biological Chemistry*. 2013;4(3):35-63.
- 84** Borkow G, Lara HH, Covington CY, Nyamathi A, Gabbay J. Deactivation of Human Immunodeficiency Virus Type 1 in Medium by Copper Oxide-Containing Filters. *Antimicrobial Agents and Chemotherapy*. 2008;52(2):518-525.
- 85** Usman MS, Zowalaty MEE, Shameli K, Zainuddin N, Salama M, Ibrahim NA. Synthesis, characterization, and antimicrobial properties of copper nanoparticles. *International Journal of Nanomedicine*. 2013;8:4467-4479.
- 86** Yah CS, Simate GS. Nanoparticles as potential new generation broad spectrum antimicrobial agents. *DARU Journal of Pharmaceutical Sciences*. 2015;23:43.
- 87** Zakharova OV, Godymchuk AY, Gusev AA, Gulchenko SI, Vasyukova IA, Kuznetsov DV. Considerable Variation of Antibacterial Activity of Cu Nanoparticles Suspensions

Depending on the Storage Time, Dispersive Medium, and Particle Sizes. *BioMed Research International*. 2015;2015:412530.

- 88 Grass G, Rensing C, Solioz M. Metallic Copper as an Antimicrobial Surface. *Applied and Environmental Microbiology*. 2011;77(5):1541-1547.
- 89 Usman MS, Ibrahim NA, Shameli K, Zainuddin N, Yunus WMWY. Copper Nanoparticles Mediated by Chitosan: Synthesis and Characterisation via Chemical Methods. *Molecules*. 2012;17:14928-14936.
- 90 Umer A, Naveed S, Ramzan N. Selection of a suitable method for the synthesis of copper nanoparticles. *NANO: Brief Reports and Reviews*. 2012;7(5):1-18.
- 91 Wu W, He Q, Jiang C. Magnetic Iron Oxide Nanoparticles: Synthesis and Surface Functionalization Strategies. *Nanoscale Research Letters*. 2008;3(11):397-415.
- 92 Worthington KLS, Dodd AA, Wongrakpanich A, Mundunkotuwa IA, Mapuskar KA, Joshi VB, Guymon A, Spitz DR, Grassian VH, Thorne PS, Salem AK. Chitosan coating of copper nanoparticles reduces in vitro toxicity and increases inflammation in the lung. *Nanotechnology*. 2013;24(39):10.1088/0957-4484/24/39/395101.
- 93 Barthe MJ, Angeloni I, Petrelli A, Avellini T, Scarpellini A, Bertoni G, Armirotti A, Moreels I, Pellegrino T. Synthesis of Highly Fluorescent Copper Clusters Using Living Polymer Chains as Combined Reducing Agents and Ligands. *ACS Nano*. 2015;9(12):11886-11897.
- 94 Gawande MB, Goswami A, Felpin F, Asefa T, Huang X, Silva R, Zou X, Zboril R, Varma RS. Cu and Cu-based nanoparticles: synthesis and application in catalysis. 2016;111(6):3722-3811.
- 95 Karlsson HL, Cronholm P, Hedberg Y, Tornberg M, Battice LD, Svedhem S, Wallinder IO. Cell membrane damage and protein interaction induced by copper containing nanoparticles—Importance of the metal release process. 2013;313(1):59-69.
- 96 Oktar FN, Yetmex M, Fikai D, Fikai A, Dumitru F, Pica A. Molecular Mechanism and Targets of the Antimicrobial Activity of Metal Nanoparticles. *Current Topics in Medicinal Chemistry*. 2015;15(16):1583-1588.

- 97 Tang Z, Lv B. MgO nanoparticles as antibacterial agent: preparation and activity. *Brazilian Journal of Chemical Engineering*. 2014;31(3):1-11.
- 98 Sawai J, Kojima H, Igarashi H, Hashimoto A, Shoji S, Sawaki T, Hakoda A, Kawada E, Kokugan T, Shimizu M. Antibacterial characteristics of magnesium oxide powder. *World Journal of Microbiology & Biotechnology*. 2000;16:187-194.
- 99 Sundrarajan M, Suresh J, Gandhi RR. A comparative study on antibacterial properties of MgO nanoparticles prepared under different calcination temperature. 2012;7(3):983-989.
- 100 Sansone V, Pagani D, Melato M. The effects on bone cells of metal ions released from orthopaedic implants. A review. *Clinical Cases in Mineral and Bone Metabolism*. 2013;10(1):34-40.
- 101 Ouraipryvan P, Sreethawong T, Chavadej S. Synthesis of crystalline MgO nanoparticle with mesoporous-assembled structure via a surfactant-modified sol-gel process, *Materials Letters*. 2009;63(21):1862-1865.
- 102 Singh G, Joyce EM, Beddow J, Mason TJ. Evaluation of antibacterial activity of ZnO nanoparticles coated sonochemically onto textile fabrics. *Journal of Microbiology, Biotechnology and Food Sciences*. 2012;2(1):106-120.
- 103 Zhang Y, Nayak TR, Hong H, Cai W. Biomedical Applications of Zinc Oxide Nanomaterials. *Current molecular medicine*. 2013;13(10):1633-1645.
- 104 Xiong HM, ZnO nanoparticles applied to bioimaging and drug delivery. *Advanced Materials*. 2013;25(37):5329-5235.
- 105 Xie Y, He Y, Irwin PL, Jin T, Shi X. Antibacterial Activity and Mechanism of Action of Zinc Oxide Nanoparticles against *Campylobacter jejuni*. *Applied and Environmental Microbiology*. 2011;77(7):2325-2331.

- 106** Jones N, Ray B, Ranjit KT, Manna AC. Antibacterial activity of ZnO nanoparticle suspension on a broad spectrum of microorganisms. *FEMS Microbiology Letters*. 2008;279:71-76.
- 107** Sirelkhatim A, Mahmud S, Seeni A, Kaus NHM, Ann LC, Bakhori SKM, Hasan H, Mohamad D. Review on Zinc Oxide Nanoparticles: Antibacterial Activity and Toxicity Mechanism. *Nano-Micro Letters*. 2015;7(3):219-242.
- 108** Singh S, D'Britto V, Bharde A, Sastry M, Dhawan A, Prasad LV. Bacterial Synthesis of Photocatalytically Active and Biocompatible TiO₂ and ZnO Nanoparticles. *International Journal of Green Nanotechnology: Physics and Chemistry*. 2010;2(2):80-99.
- 109** Wang J, Deng X, Zhang F, Chen D, Ding W. ZnO nanoparticle-induced oxidative stress triggers apoptosis by activating JNK signaling pathway in cultured primary astrocytes. *Nanoscale Research Letters*. 2014;9(1):117.
- 110** Dutta RK, Nenavathu BP, Gangishetty MK, Reddy AVR. Studies on antibacterial activity of ZnO nanoparticles by ROS induced lipid peroxidation. *Colloids and Surfaces B: Biointerfaces*. 2012;94:143-150.
- 111** Prashanth GK, Prashanth PA, Bora U, Gadewar M, Nagabhushana BM, Ananda S, Krishnaiah GM, Sathyananda HM. In vitro antibacterial and cytotoxicity studies of ZnO nanopowders prepared by combustion assisted facile green synthesis. *Science*. 2015;1(2):67-77.
- 112** Sehmi SK, Noimark S, Bear JC, Peveler WJ, Bovis M, Allan E, MacRobert AJ, Parkin IP. Lethal photosensitisation of *Staphylococcus aureus* and *Escherichia coli* using crystal violet and zinc oxide incorporated into polyurethane. *Journal of Materials Chemistry B*. 2015;3:6490-6500.
- 113** Wan MT, Lin JY. Current evidence and applications of photodynamic therapy in dermatology. *Clinical, Cosmetic and Investigational Dermatology*. 2014;7:145-163.
- 114** Noimark S, Dunnill CW, Parkin IP. Shining light on materials- a self-sterilising revolution. *Advanced Drug Delivery Reviews*. 2013;65(4):570-580.

- 115** Komerik N, Nakanishi h, MacRobert AJ, Henderson BM, Speight P, Wilson M. In vivo killing of Porphyromonas gingivalis by toluidine blue-mediated photosensitisation in an animal model. *Antimicrobial Agents of Chemotherapy*. 2003;47(3):932-940.
- 116** Sehmi SK, Noimark S, Weiner J, Allan E, MacRobert AJ, Parkin IP. Potent Antibacterial Activity of Copper Embedded into Silicone and Polyurethane. *ACS Materials & Interfaces*. 2015;7(41):22807-22813.
- 117** Rai AV, Bai JA. Nanoparticles and their potential application as antimicrobials. *Science against microbial pathogens: communicating current research and technological advances*, Mendez-Vilas, A. (Ed.). University of Mysore, India. 2011;197-209.
- 118** Xue Y, Xiao H, Zhang Y. Antimicrobial Polymeric Materials with Quaternary Ammonium and Phosphonium Salts. Piozzi A, ed. *International Journal of Molecular Sciences*. 2015;16(2):3626-3655.
- 119** Sydnor ERM, Perl TM. Hospital Epidemiology and Infection Control in Acute-Care Settings. *Clinical Microbiology Reviews*. 2011;24(1):141-173.
- 120** Collins AS. Preventing Health Care–Associated Infections. In: Hughes RG, editor. *Patient Safety and Quality: An Evidence-Based Handbook for Nurses*. Rockville (MD): Agency for Healthcare Research and Quality (US); 2008 Apr. Chapter 41.
- 121** Hannay F. *Rigid Plastics Packaging: Materials, Processes and Applications*. iSmithers Rapra Publishing, 2002;151.
- 122** Autian J. "Toxicity and health threats of phthalate esters: review of the literature." *Environmental health perspectives*. 1973;4:3.
- 123** Blass CR. *Polymers in Disposable Medical Devices: A European Perspective*. iSmithers Rapra Publishing, 1999.
- 124** Chu PK, Chen JY, Wang LP, Huang N. Plasma-surface modification of biomaterials. *Materials Science and Engineering: R: Reports*. 2002;36(5):143-206.

- 125** Curtis J, Klykken P. A Comparative Assessment of Three Common Catheter Materials. *Dow Corning Corporation*. 1-8.
- 126** Shen L, Haufe J, Patel MK. Product overview and market projection of emerging bio-based plastics PRO-BIP 2009. *Report for European Polysaccharide Network of Excellence (EPNOE) and European Bioplastics*. 2009; 243.
- 127** Zdrahala RJ, Zdrahala IJ. Biomedical applications of polyurethanes: a review of past promises, present realities, and a vibrant future. *Journal of biomaterials applications*, 1999;14(1):67-90.
- 128** Edenbaum MI, Rybalka B. *U.S. Patent No. 4,655,210*. Washington, DC: U.S. Patent and Trademark Office, 1987.
- 129** Noimark S, Bovis M, MacRobert AJ, Correia A, Allan E, Wilson M, Parkin IP. Photobactericidal polymers: the incorporation of crystal violet and nanogold into medical grade silicone. *RSC Advances*. 2013;3:18383–18394.
- 130** Noimark S, Dunnill CW, Kay CWM, Perni S, Prokopovich P, Ismail S, Wilson M, Parkin IP, Incorporation of methylene blue and nanogold into polyvinyl chloride catheters; a new approach for light-activated disinfection of surfaces. *Journal of Materials Chemistry*. 2012;22:15388–15396.
- 131** Piccirillo C, Perni S, Gil-Thomas J, Prokopovich P, Wilson M, Pratten J, Parkin IP, Antimicrobial activity of methylene blue and toluidine blue O covalently bound to a modified silicone polymer surface. *Journal of Materials Chemistry*. 2009;19:6167–6171.
- 132** Perni S, Prokovich P, Piccirillo C, Pratten J, Parkin IP, Wilson M. Toluidine blue-containing polymers exhibit potent bactericidal activity when irradiated with red laser light. *Journal of Materials Chemistry*. 2009;19(18):2715-2723.
- 133** Perni S, Piccirillo C, Kafisas A, Uppal M, Pratten J, Wilson M, Parkin IP. Antibacterial activity of light-activated silicone containing methylene blue and gold nanoparticles of different sizes. *Journal of Cluster Science*. 2010;21(3):427–438.

- 134** Perni S, Piccirillo C, Pratten J, Prokovich P, Chrzanowski W, Parkin IP, Wilson M. The antimicrobial properties of light-activated polymers containing methylene blue and gold nanoparticles. *Biomaterials*. 2009;30(1):89-93.
- 135** Bovis MJ, Noimark S, Woodhams JH, Kay CWM, Weiner J, Peveler WJ, Correia A, Wilson M, Allan E, Parkin IP, MacRobert AJ. Photosensitisation studies of silicone polymer doped with methylene blue and nanogold for antimicrobial applications. *RSC Advances*. 2015;5:54830-54842.
- 136** Noimark S, Allan E, Parkin IP. Light-activated antimicrobial surfaces with enhanced efficacy induced by a dark-activated mechanism. *Chemical Science*. 2014;5(6):2216-2223.
- 137** Noimark S, Weiner J, Noor N, Allan E, Williams CK, Shaffer MSP, Parkin IP. Dual-Mechanism Antimicrobial Polymer-ZnO Nanoparticle and Crystal Violet-Encapsulated Silicone. *Advanced Functional Materials*. 2015;25(9):1367-1373.
- 138** Ozkan E, Ozkan FT, Allan E, Parkin IP. The use of zinc oxide nanoparticles to enhance the antibacterial properties of light-activated polydimethylsiloxane containing crystal violet. *RSC Advances*. 2015;5:8806-8813.

Chapter 3

3. Silicone and Polyurethane-Encapsulated Copper; Antimicrobial Polymers without White Light Activation

3.1 Introduction

Hospital-acquired infections (HAIs) are the most common complication in healthcare and are attained by patients during medical treatments and procedures. They are a result of severely contaminated hospital surfaces and medical devices, and poor adherence towards cleanliness and basic hand washing by patients, staff and visitors. Patients who acquire these infections can be hospitalised 2.5 times longer than those who are uninfected, resulting in additional hospital costs of up to £3,000.¹ Over the last century, new antibiotics have been developed to combat infections that are caused by common microorganisms found in hospitals. Consequently, bacteria have evolved resistance mechanisms that pose a major threat to patients, contributing towards morbidity and mortality.² Carbapenem-resistant Enterobacteriaceae (CRE) are extremely problematic for immunocompromised and catheterised patients as treatment options are limited.³ Methicillin-resistant *Staphylococcus aureus* (MRSA) contaminates around 75% of patient rooms and 42% of those who touch a surface contaminated with MRSA will become contaminated themselves, despite not having direct contact with a patient. It can cause minor skin infections but also more serious problems, such as infected wounds or pneumonia.⁴

Numerous prevention strategies have been developed to reduce the incidence of HAIs. Novel methods, including the use of hydrogen peroxide

mist and ultra violet (UV) light have been shown to reduce microbial burden, but are unsuccessful in significantly reducing the rates of HAIs.⁵ Metallic copper exhibits intrinsic broad-spectrum antimicrobial activity against commonly found bacteria in healthcare.⁶ Studies showed that patients cared for in intensive care units (ICUs) with copper alloy surfaces (e.g. pipes, bed rails and pushplates) had a much lower rate of MRSA and vancomycin-resistant *Enterococcus* (VRE) colonisation than patients treated in standard hospital wards.⁵ However, metallic copper has a limited range of applications within hospital environments as it can only be applied to hard surfaces such as taps, bedrails, overbed tables and visitors chair arms.⁷

Copper nanoparticles (Cu NPs) have gained particular attention due to their availability and cost effectiveness compared to other noble metals, such as silver and gold.⁸ They display bactericidal activity against a wide range of Gram-positive and Gram-negative bacteria, such as *Escherichia coli* (*E. coli*) and *S. aureus*.⁹ There are only a few studies in the literature that report the antibacterial mechanism of Cu NPs. Ruparelia *et al* and Raffi *et al* suggested that an interaction between Cu^{2+} and DNA/protein causes a disruption of bacterial structures and their biochemical processes.¹⁰ Additionally, Wu *et al* found an increased concentration of Cu ions from the antibacterial Cu agent caused 99% killing of bacteria.¹¹ Excess copper causes a reduction in bacterial membrane integrity, leading to desiccation and eventually, cell death.¹² Moreover, an increased concentration of copper inside the bacterial cell can form H_2O_2 *via* oxidative stress (the Fenton reaction).¹³ There are very few reports on synthesising Cu NPs using a “green method” with a low environmental impact. For hospital applications, it is imperative that these nanoparticles are synthesised from nontoxic chemicals, solvents and renewable materials.¹⁴⁻¹⁶

Despite their bactericidal efficacy, Cu NPs suffer from rapid oxidation upon air exposure. Cu oxidises to CuO and Cu_2O and converts to Cu^{2+} during preparation and storage, causing difficulty in synthesising Cu NPs in

ambient conditions.⁸ Therefore, alternative synthetic routes have been developed to form coatings on nanoparticle surfaces, as well as the use of polymers and surfactants as stabilisers.^{8,17} Another method of preventing oxidation of Cu NPs is by incorporating them into polymeric materials for use as antibacterial surfaces in preventing HAIs.¹⁸ Such materials include polyvinyl chloride, silicone and polyurethane.¹⁹⁻²¹

This chapter details the antibacterial activity of environmentally benign Cu NPs (~2.5 nm in size) when incorporated into two widely used polymers, medical grade silicone and polyurethane sheets. These novel bactericidal surfaces were tested against *E. coli* ATCC 25922 as a representative Gram-negative bacterium, and an epidemic strain of MRSA (EMRSA-16; *S. aureus* NCTC 13143), one of two clones known to predominate in the UK (Public Health England),²² as a representative Gram-positive bacterium. Silicone-encapsulated copper and polyurethane-encapsulated copper both demonstrated highly significant antibacterial activity in the dark, i.e. without UV or white light activation, against both bacteria within only a few hours. Moreover, both modified polymer surfaces mostly remain unstained after encapsulation, which should prove commercially appealing.

3.2 Experimental

3.2.1 Chemicals and Reagents

The reagents used to synthesise Cu NPs were commercially supplied by Sigma-Aldrich Chemical Co. Copper (II) chloride dihydrate ($\text{CuCl}_2 \cdot 2\text{H}_2\text{O}$) was used as a precursor for nanoparticle formation and L-ascorbic acid acted as a capping agent and a reducing agent.²³ Medical grade flat silicone sheets with a thickness of 1.0 mm were purchased from NuSil (Polymer Systems Technology Ltd) and medical grade polyurethane sheets with a thickness of 0.8 mm were purchased from American Polyfilm Inc. (Branford, CT, USA). Deionised water (resistivity 15 M Ω cm) was used throughout all synthetic

work carried out and acetone (Sigma-Aldrich, UK) was used to prepare modified polymer substrates *via* the “swell-encapsulation-shrink” method.

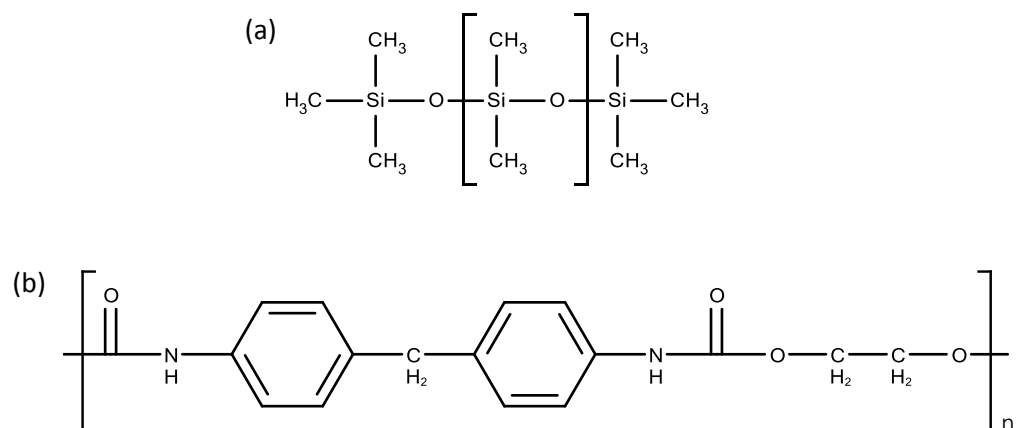


Fig. 3.1 Chemical structures of silicone and polyurethane.

3.2.2 Synthesis of Copper Nanoparticles

Nanosized copper particles were prepared using a method adapted by Xiong *et al.*²⁴ An aqueous solution of $\text{CuCl}_2 \cdot 2\text{H}_2\text{O}$ (0.2 M) in water was heated to 70 °C with constant magnetic stirring, followed by dropwise addition of an aqueous solution of L-ascorbic acid (0.6 M) in water. The reaction mixture was kept at 70 °C and sealed for 3 h until a dark orange/brown solution was obtained.

3.2.3 Material Preparation

3.2.3.1 Polymer System Optimisation – Organic Solvent Concentration

1 cm² polyurethane polymer square sheets were immersed in the following acetone : water ratios – 0:1, 1:1, 9:1 and 1:0. They were allowed to swell for 24 h in the dark, removed, air-dried overnight, and subsequently washed and towel-dried.

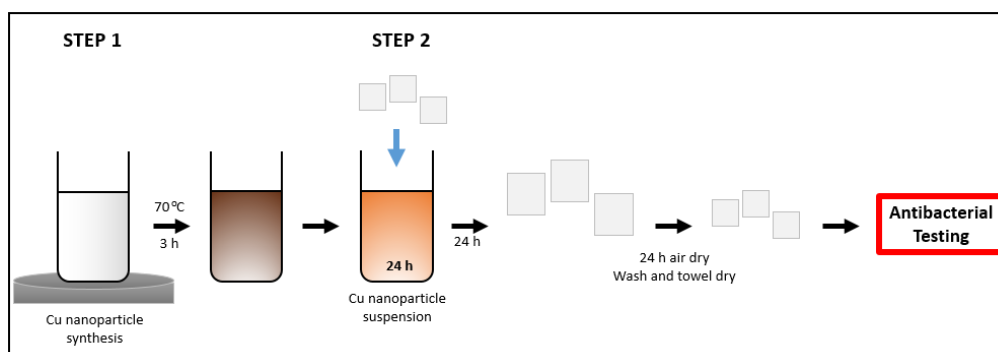


Fig. 3.2 Schematic diagram illustrating the preparation of copper nanoparticles (Step 1) and encapsulating them into 1 cm² polymer squares for antibacterial testing (Step 2).

3.2.3.2 Polymer Samples Prepared for Antibacterial Testing

The following modified silicone and polyurethane samples (1 cm²) were prepared for antimicrobial testing:

- (a) Polyurethane-encapsulated copper (Cu-polyurethane) and silicone-encapsulated copper (Cu-silicone) polymer samples were prepared using a 'swell-encapsulation-shrink' method adapted from Perni *et al.*²⁵ They were immersed in a 9:1 acetone/water swelling solution which contained Cu NPs for 24 h. They were then removed from solution, air-dried overnight and washed with distilled water (as summarised in Fig. 3.2).
- (b) Control silicone and polyurethane samples were prepared by using a 9:1 acetone/water solution for 24 h in the dark. They were removed from the solution, air-dried overnight and washed with distilled water.

3.2.4 Material Characterisation

3.2.4.1 Characterisation of Copper Nanoparticles

An aqueous suspension of Cu NPs was drop-cast onto a 400 Cu mesh lacey carbon film TEM grid (Agar Scientific Ltd) and imaged using a Jeol 2100 high

resolution transmission electron microscope (HR-TEM) with a LaB₆ source, operating at an acceleration voltage of 200 kV with an Oxford Instruments XMax EDS detector running AZTEC software. The TEM images were analysed using ImageJ software and energy-dispersive X-ray (EDX) spectra were obtained.

3.2.4.2 Characterisation of Modified Polymer Samples

A Perkin Elmer Fourier transform Lambda 950 UV-Vis spectrometer (350 – 550 nm range) was used to measure the absorption spectra of all modified polymer samples. X-ray photoelectron spectroscopy (XPS) analysis was performed using a Thermo Scientific *K-Alpha* spectrometer to detect copper as a function of polymer depth, and all binding energies were calibrated to the carbon 1s peak at 284.5 eV. Scanning electron microscopy (SEM) of the modified polymer samples was carried out using secondary electron imaging on a Jeol 6301 field emission instrument with an acceleration voltage of 5 kV. Equilibrium water contact angle measurements (~5.0 µL) were measured to determine the differences in surface hydrophobicity of treated polymer samples. Contact angle measurements were averaged from over 10 measurements using a droplet of deionised water dispensed by gravity from a gauge 30 needle.

3.2.5 Antibacterial Activity

3.2.5.1 Microbiology Assay

The following 1 cm² polyurethane and silicone samples were prepared: (i) control (solvent treated) and (ii) polymer-encapsulated copper. The antibacterial activity of these samples was tested against *E. coli* ATCC 25922 and an epidemic strain of MRSA, (EMRSA-16; *S. aureus* NCTC 13143), which is representative of one of the two types of MRSA that dominate in UK hospitals.²² These organisms were stored at -70 °C in Brain-Heart-

Infusion broth (BHI, Oxoid) containing 20% (v/v) glycerol and propagated onto either MacConkey agar (MAC, Oxoid) in the case of *E. coli* or Mannitol Salt agar (MSA, Oxoid) in the case of *S. aureus* for a maximum of 2 subcultures at intervals of 2 weeks.

BHI broth was inoculated with 1 bacterial colony and cultured in air at 37 °C for 18 h with shaking, at 200 rpm. The bacterial pellet was recovered by centrifugation, (20 °C, 2867.2 g, 5 min), washed in PBS (10 mL), centrifuged again to recover the pellet (20 °C, 2867.2 g, 5 min), after which the bacteria were finally re-suspended in PBS (10 mL). The washed suspension was diluted 1,000-fold to obtain an inoculum of $\sim 10^6$ cfu/mL. In each experiment, the inoculum was confirmed by plating 10-fold serial dilutions on agar for viable counts. Triplicates of each polymer sample type were inoculated with 25 μ L of the inoculum and covered with a sterile cover slip (2.2 cm²). The samples were then incubated in the dark for up to 6 h and 3 h for the modified silicone and polyurethane samples, respectively.

After incubation, the inoculated samples and coverslips were added to PBS (450 μ L) and mixed using a vortex mixer. The neat suspension and 10-fold serial dilutions were plated on agar for viable counts and incubated aerobically at 37 °C for 24 h (*E. coli*) or 48 h (*S. aureus*). To examine the stability of the modified polymer squares, their antibacterial activity was re-tested against both bacteria after 30 days and 90 days storage at room temperature in air.

3.2.5.2 Statistical Significance

The experiment was repeated three times and the statistical significance of the following comparisons was analysed using the Mann-Whitney U test: (i) control polymer vs. inoculum; (ii) Cu NP-incorporated vs. control polymer.

3.2.5.3 Further Antimicrobial Testing for Mechanistic Evaluation

Bovine serum albumin (BSA, 0.03%)²⁶ and superoxide dismutase (SOD, 55 U mL⁻¹),²⁷ purchased from Sigma-Aldrich, UK, were added to the *E. coli* suspension and exposed to both polymers as described in section 3.2.5.1. The BSA and SOD solutions were filter sterilised using a 0.2 µm syringe filter (VWR, UK). BSA was added to simulate contamination in a hospital setting with organic material, as well as acting as a scavenger of reactive oxygen species (particularly singlet oxygen),^{18,26,28} and SOD was added as an inhibitor of superoxide anions in radical formation.^{27,29} The inhibitors were added to the bacterial suspension and exposed to the polymer as described above in section 3.2.5.1.

3.3 Results and Discussion

3.3.1 Material Characterisation

3.3.1.1 Characterisation of Copper Nanoparticles

A facile and environmentally friendly method was used to synthesise Cu NPs by gently heating an aqueous solution of copper (II) chloride dihydrate and adding L-ascorbic acid dropwise to the solution. The dispersion became colourless upon the addition of L-ascorbic acid and gradually turned to yellow, orange and finally dark orange/brown. Narrow size control of the nanoparticles was achieved by using the anti-oxidant, L-ascorbic acid, which acted as both the reducing and capping agent by encapsulating Cu²⁺ ions and reducing them into Cu(0).²⁴ The resulting oxidation products then adsorb onto the surface of Cu NPs, preventing the particles from additional growth.

HR-TEM images showed the Cu NPs to be monodisperse, crystalline and mainly spherical (Fig. 3.3(a)). Size analysis indicated an average size diameter of 2.5 ± 0.7 nm. There was some aggregation of nanoparticles as clusters of ~10 nm in diameter was observed, but generally the images

displayed shape uniformity and a narrow size distribution (Fig. 3.3(b)). EDX elemental composition analysis demonstrated minimal oxidation of the nanoparticles and a strong presence of Cu (Fig. 3.4).

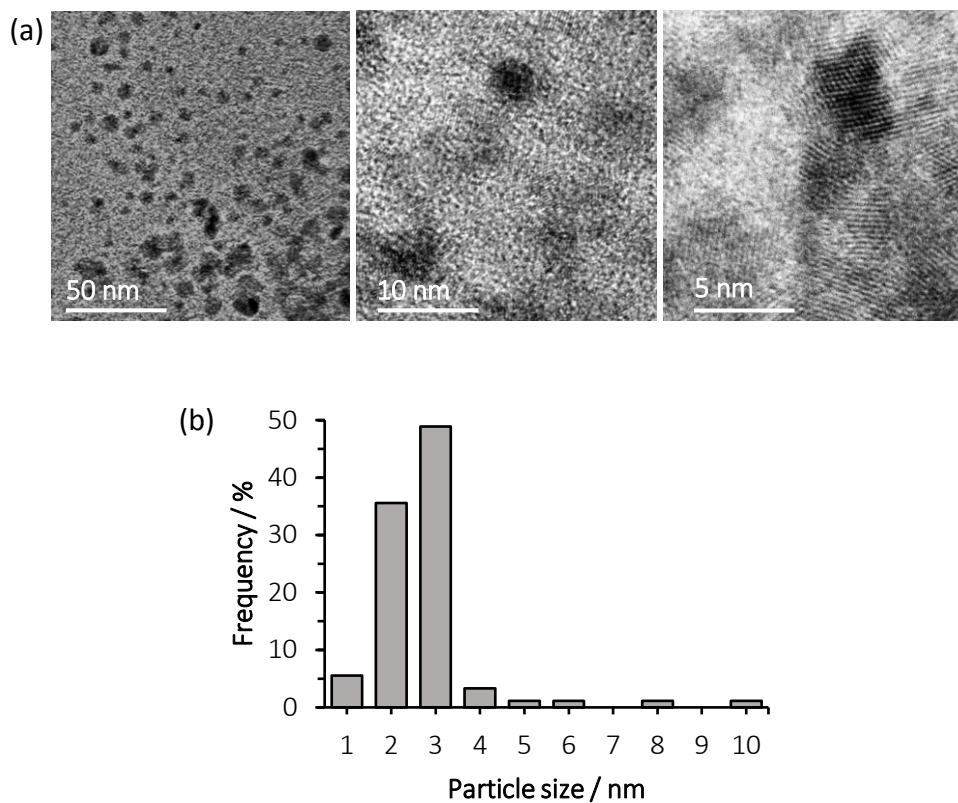


Fig. 3.3 (a) HR-TEM images of Cu NPs. (b) Cu NP size distribution determined by HR-TEM.

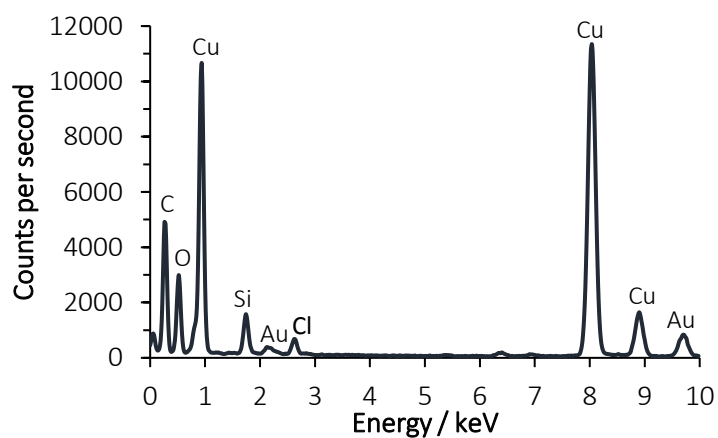


Fig. 3.4 EDX spectrum of Cu NPs.

3.3.1.2 Characterisation of Modified Polymer Samples

The nanoparticles were incorporated into both polyurethane and silicone by using a simple and efficient ‘swell-encapsulation-shrink’ method (Fig. 3.2). This method has proven to be highly efficacious at introducing antibacterial functionality to polymers by impregnating a wide range of small nanoparticles into their matrices.^{25,26,30-33} Previous studies have shown that the extent of polymer swelling is greatly affected by the type of organic solvent used.^{30,34} However, as the Cu NPs were suspended in water, the choice of organic solvents was limited. Perni *et al*²⁵ demonstrated that acetone is very effective at encapsulating gold nanoparticles *via* this preparative route by using a 9:1 ratio of acetone/water suspension containing the nanoparticles. To confirm this, 1 cm² polyurethane squares were immersed into solutions containing the following ratios of acetone/water: 0:1, 1:1, 9:1 and 1:0 for 24 h. Once removed, they were immediately measured to determine the extent of swelling. As shown in Table 3.1, a 1:1 ratio of acetone/water only allowed 22% of swelling, whereas a 9:1 ratio caused 50% swelling (only 5% less than using acetone alone). Moreover, a 9:1 ratio did not cause the polymer to deform or bend. Therefore, a 9:1 acetone/water ratio was used to swell-encapsulate Cu NPs into both polymers for 24 h to maximise the extent of polymer swelling and encapsulation of nanoparticles throughout the polymer bulk.

Table 3.1 Extent of polymer swelling (%) after immersing 1 cm² polyurethane samples in different ratios of acetone and water.

Acetone : water ratio	Extent of polymer swelling (%)
0:1	0
1:1	22
9:1	50
1:0	55

In the interest of aesthetics, Cu NP incorporation into the polymers resulted in a limited change in colouration. This is advantageous as previous studies carried out by our research group have used polymers with distinct colouration upon addition of photosensitisers to achieve their antibacterial functionalities.^{25,26,30-33} As shown in Fig. 3.5, the slight colouration of polyurethane may be attributed to a significantly greater extent of swelling under these conditions. However, this results in an increased uptake of Cu NPs, which subsequently anticipates an enhancement in antibacterial efficacy. UV-vis absorbance spectroscopy displayed a stronger absorbance signal for Cu-polyurethane compared to Cu-silicone and the control polymers (Fig. 3.6), giving evidence of a greater uptake of Cu NPs in polyurethane compared to silicone. Additionally, when immersed in a 9:1 ratio of acetone : water, polyurethane swelled up to 50% of its original size compared to silicone, which only swelled 30% more than its original size. Thus, this also suggests that Cu-polyurethane, which is slightly more coloured than Cu-silicone, contains a higher concentration of Cu NPs.

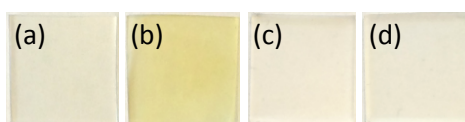


Fig. 3.5 Modified polymer samples for antibacterial testing (1 cm²): (a) polyurethane control; (b) polyurethane-encapsulated copper; (c) silicone control; (d) silicone-encapsulated copper.

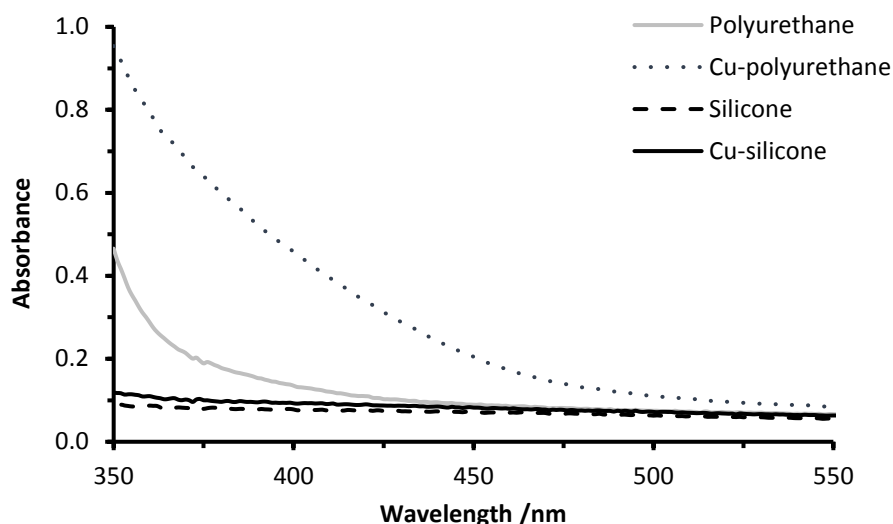


Fig. 3.6 UV-vis absorbance spectra of polyurethane control, Cu-polyurethane, silicone control and Cu-silicone, measured in the range 350 – 550 nm.

XPS analysis was used to examine the diffusion of Cu NPs through the polymer bulk and on the surface (sputtered 50 s). For all polyurethane samples, peaks attributed to the presence of C (1s), O (1s) and N (1s) were found and for all silicone samples, peaks attributed to the presence of C (1s), O (1s) and Si (2p) on the surface were observed (data not shown). The presence of Cu was detected on the polyurethane surface and within the substrate as a peak correlating to Cu (2p) was observed at 952.3 eV (Fig. 3.7(a) and (b)). A peak was also evident at 932.4 eV which confirmed the presence of Cu in CuO, indicating some oxidation of the Cu NPs. Fig. 3.7(c) and (d) showed there was a limited amount of Cu detected on the silicone surface, but a significant amount of Cu NPs incorporated in the silicone bulk. Peaks in the Cu (2p) region indicated this for Cu and CuO (952.3 eV and 933.1 eV, respectively). SEM images shown in Fig. 3.8 indicated there was no physical change in the surface appearances of polyurethane and silicone after encapsulating Cu NPs. XPS data showed a higher content of Cu on the polyurethane surface compared to the silicone surface, but both polymers showed similar Cu content within the polymer matrices (Fig. 3.7).

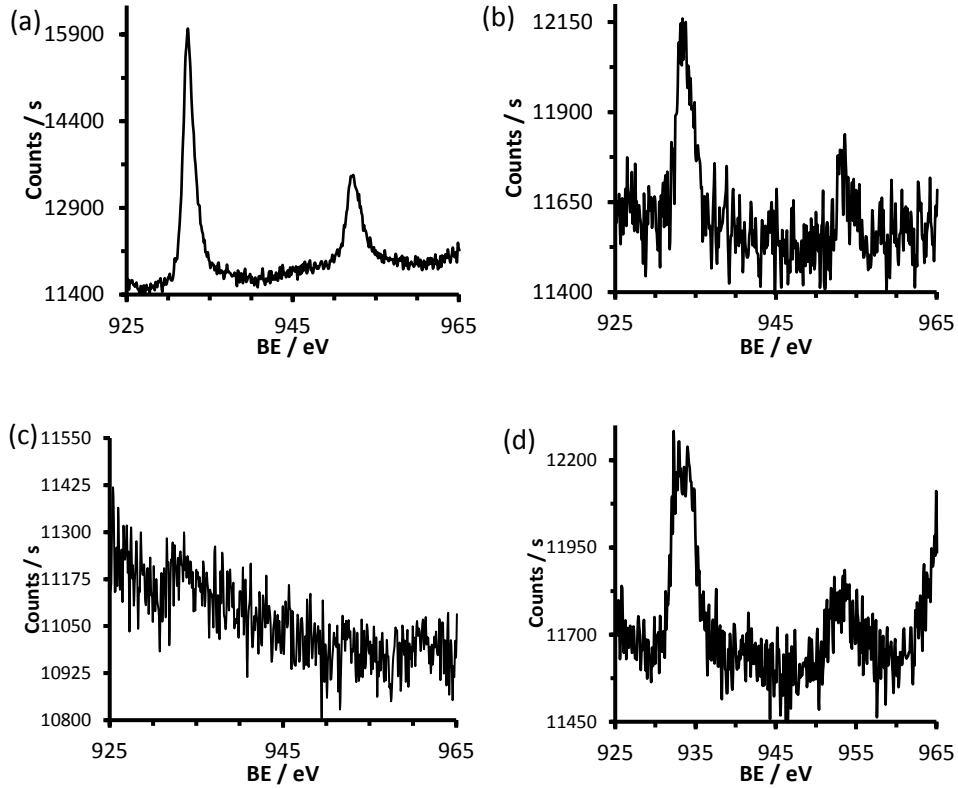


Fig. 3.7 Cu (2p) region XPS spectra for: (a) Cu-polyurethane surface; (b) Cu-polyurethane sputtered 50 s; (c) Cu-silicone surface; and (d) Cu-silicone sputtered 50 s.

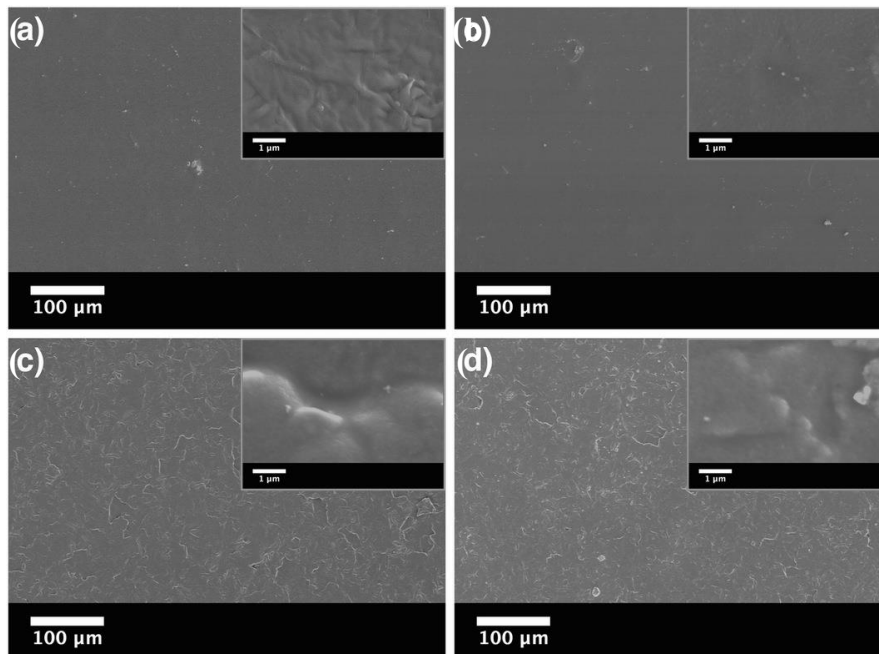


Fig. 3.8 SEM imaging of the following modified polymer squares: (a) polyurethane control; (b) polyurethane-encapsulated copper; (c) silicone control; (d) silicone-encapsulated copper.

Water contact angle measurements were carried out on all modified polymer samples to investigate any changes in wetting properties after encapsulation of Cu NPs. Both control polyurethane and silicone polymers present a hydrophobic surface^{35,36} prior to incorporating the nanoparticles.

3.3.2 Antibacterial Activity

The antibacterial activity of the modified polymer samples was tested against two hospital pathogens as representative Gram-positive and Gram-negative bacteria: an epidemic strain of MRSA (EMRSA-16; *S. aureus* NCTC 13143) and *E. coli* ATCC 25922. Fig. 3.9 illustrates the bactericidal activity of modified polymers against *S. aureus* NCTC 13143. Following 1 h of incubation (Fig. 3.9(a)), the control polyurethane sample did not display any significant kill of *S. aureus*, whereas Cu-polyurethane resulted in a ~ 0.75 log reduction in bacterial numbers ($P < 0.001$). After increasing the exposure time to 2 h (Fig. 3.9(b)), Cu-polyurethane demonstrated highly significant bactericidal activity reducing the bacterial numbers to below the detection limit of 100 cfu/mL (≥ 4 log reduction; $P < 0.001$). The strain of EMRSA-16, *S. aureus* NCTC 13143, was also exposed to silicone and Cu-silicone for longer time periods. After 4 h of incubation (Fig. 3.9(c)), control silicone did not exhibit significant kill of the bacteria, but Cu-silicone caused ~ 1 log reduction. By increasing the incubation time to 5 h, Cu-silicone reduced bacterial numbers to below the detection limit, proving to be highly active against *S. aureus* NCTC 13143 (≥ 4 log; $P < 0.001$).

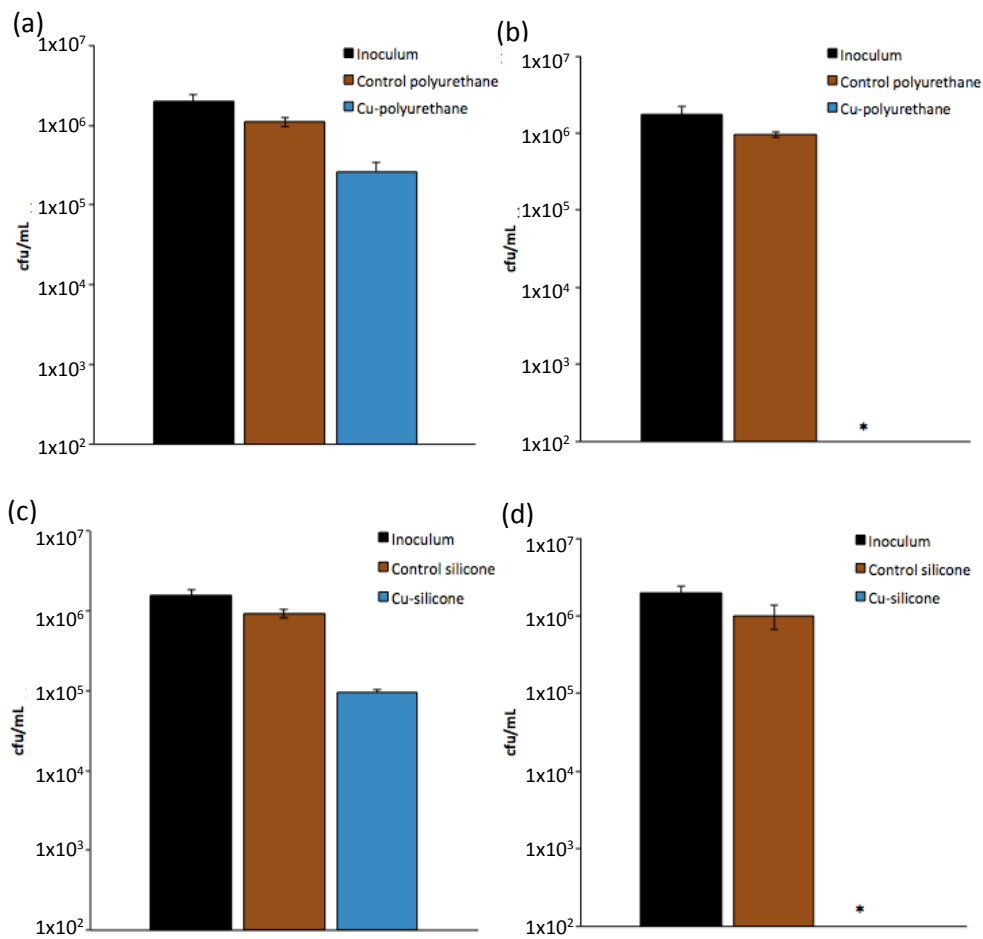


Fig. 3.9 Viable counts of *S. aureus* NCTC 13143 after incubation on modified polyurethane squares for: (a) 1 h and (b) 2 h, and modified silicone squares for: (c) 4 h and (d) 5 h. All samples were incubated at 20°C in the dark. Control samples are solvent treated. * indicates bacterial numbers reduced below the detection limit of 100 colony forming units/mL (cfu/mL).

The bactericidal activity of the modified polymers was then tested against a Gram-negative bacterium, *E. coli*, using the same conditions but for an extended period of time (Fig. 3.10). Following 2 h of bacterial contact, polyurethane displayed no significant antibacterial activity (Fig. 3.10 (a)), whereas Cu-polyurethane caused ~ 0.5 log reduction of *E. coli*. After 3 h (Fig. 3.10(b)), Cu-polyurethane demonstrated efficacious bactericidal activity against *E. coli* (≥ 4 log; $P < 0.001$). Following a 4 h incubation, Cu-silicone resulted in ~ 0.5 log reduction of *E. coli* (Fig. 3.10 (c)). However, by

increasing the incubation time to 5 h, Cu-silicone caused ≥ 4 log reduction in the numbers of *E. coli* ($P < 0.001$).

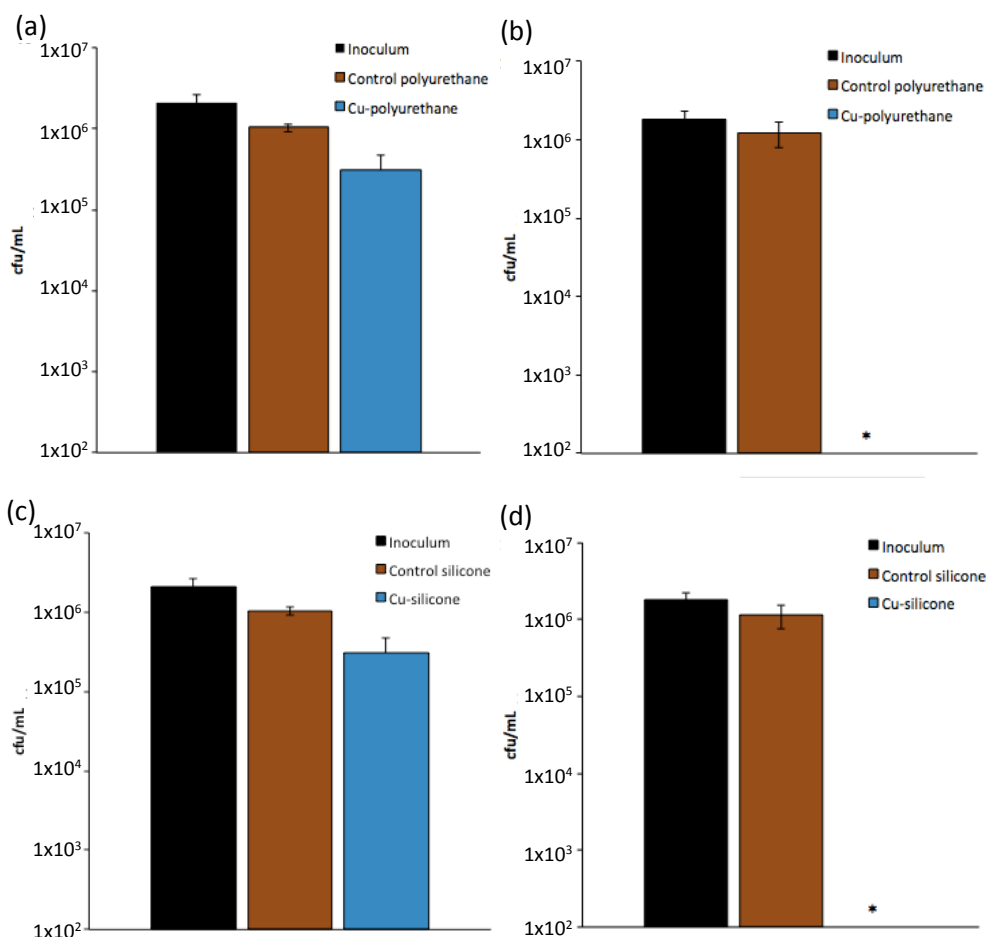


Fig. 3.10 Viable counts of *E. coli* ATCC 25922 after incubation on modified polyurethane squares for: (a) 2 h and (b) 3 h, and modified silicone squares for: (c) 4 h and (d) 6 h. All samples were incubated at 20°C in the dark. Control samples are solvent treated. * indicates bacterial numbers reduced below the detection limit of 100 colony forming units/mL (cfu/mL).

Table 3.2 Summary of the antibacterial activity of Cu-polyurethane and Cu-silicone in the dark against *S. aureus* NCTC 13143 and *E. coli* ATCC 25922. Bacterial reduction is given in log form.

Bacterial strain	Cu-polyurethane	Cu-silicone
<i>S. aureus</i> NCTC 13143	0.75 log (1 h) ≥ 4 log (2 h)	1 log (4 h) ≥ 4 log (5 h)
<i>E. coli</i> ATCC 25922	0.5 log (2 h) ≥ 4 log (3 h)	0.5 log (4 h) ≥ 4 log (6 h)

In the experiments described above, 2.5 nm Cu NPs were synthesised with L-ascorbic acid as a reducing and capping agent and impregnated into flat medical grade 1 cm² polyurethane and silicone squares. To ensure that the capping agent itself was not responsible for the antibacterial properties of the modified polymers, unbound L-ascorbic acid was incorporated into the polymers and tested for bactericidal activity when tested against *S. aureus* NCTC 13143 and *E. coli* ATCC 25922 using the same microbiological conditions described above. It should be noted that L-ascorbic acid is reported in literature as a scavenger of ROS in the light,³⁷⁻³⁹ which would cause a reduction in bacterial kill if ROS production is a mechanism responsible for the bactericidal activity of polyurethane-encapsulated copper.

Xiong *et al* reported that the Cu NP solution was stable even after 2 months of storage.²⁴ To investigate the stability of the nanoparticles incorporated into both polymers, their bactericidal activity was assessed after 30 days and 90 days after their preparation. After 90 days, the samples still remained active (Fig. 3.11), exhibiting similar levels of bacterial kill as shown for the freshly prepared polymers displayed in Fig. 3.9 and 3.10.

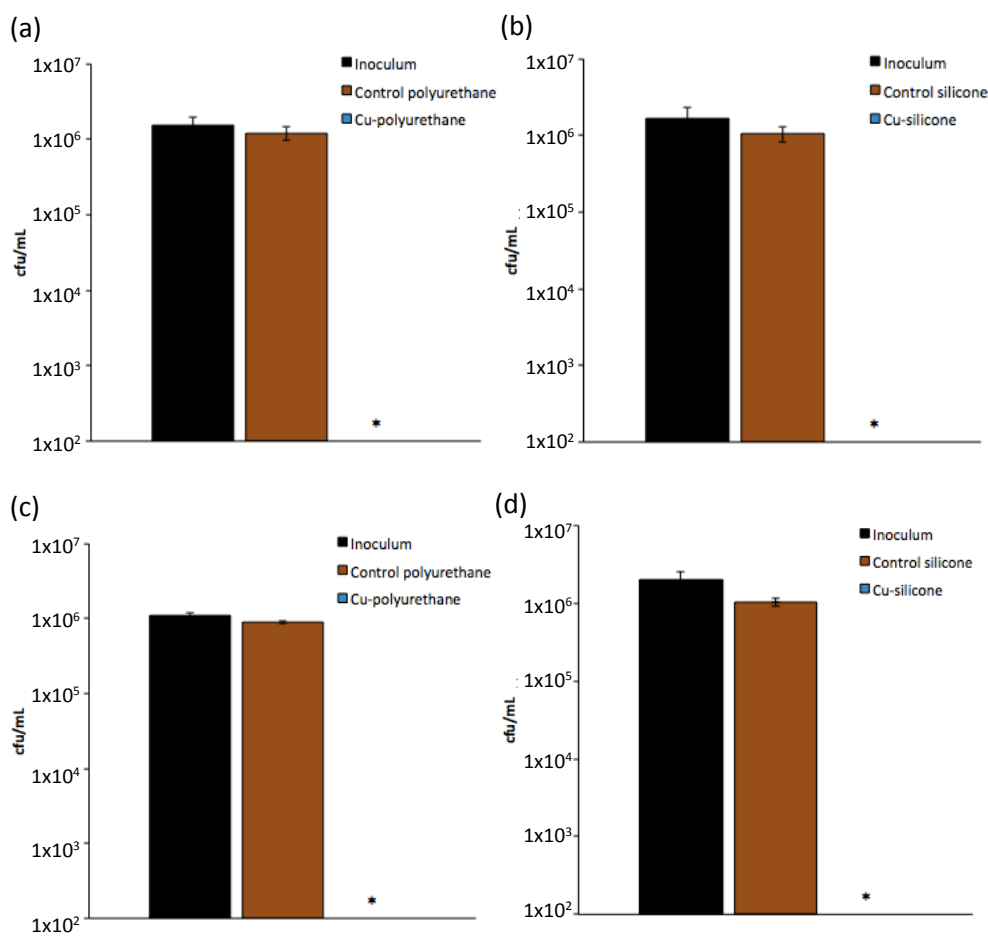


Fig. 3.11 Viable counts of *S. aureus* NCTC 13143 after incubation on modified polyurethane squares for (a) 2 h and modified silicone squares for (b) 5 h after 90 days from preparation. Viable counts of *E. coli* ATCC 25922 after incubation on modified polyurethane squares for (c) 3 h, and modified silicone squares for (d) 6 h after 90 days from preparation. All samples were incubated at 20°C in the dark. Control samples are solvent treated. * indicates bacterial numbers reduced below the detection limit of 100 colony forming units/mL (cfu/mL).

The ‘swell-encapsulation-shrink’ method proves to be highly effective for impregnating small Cu NPs into two widely used polymers. It is an efficient and easily upscalable preparative route that allows the incorporation of nanoparticles within polymeric materials compared to other methods, such as covalent attachment.^{40,41} Furthermore, encapsulating nanoparticles within the polymer matrix minimises particle loss by wiping or washing the

surface. For the first time, Cu NPs are impregnated into polymers for antibacterial surface applications. There are many reports that demonstrate the lethal activity of copper alloys used for pipes, bed rails and other hard surfaces,^{7,41} but these novel polymeric surfaces have the potential of being used for a much wider range of surfaces and medical devices due to their flexibility and biocompatibility.¹⁹⁻²¹

A proposed mechanism for the antibacterial activity of copper incorporated into the polymers is by nanoparticle leaching from the polymer into the surrounding bacterial suspension.¹⁸ A high concentration of copper ions can leach into the suspension and the Cu surface can interact with the bacterial cell wall; causing membrane rupture which weakens the cells through the loss of vital nutrients and water, eventually causing cell death.⁴² Additionally, Cu NPs can produce reactive oxygen species (ROS), causing progressive oxidative damage and cell death.⁴³ Therefore, to gain a better understanding of the bactericidal mechanism involved within this system, superoxide dismutase (SOD, 50 U mL⁻¹) was used to eliminate superoxide anions in radical formation.^{27,29} SOD was added to the antibacterial tests against *E. coli* and neither Cu-polyurethane nor Cu-silicone displayed any reduction in bactericidal activity, indicating that superoxide radicals are not responsible for the lethal activity observed from the Cu NPs (data not shown).

BSA was also added to the antibacterial protocol (without SOD) and no significant change in antibacterial activity of Cu-polyurethane or Cu-silicone was observed against *E. coli* using the same time conditions described above (data not shown). These results signify that the antibacterial activity of these polymeric surfaces is retained even in the presence of organic matter, which suggests that it could be effective in environments where it is contaminated with lipids, for example, that come from hands. It also suggests that singlet oxygen, a major ROS, is also not responsible for the bactericidal activity. This is highly advantageous and differs from experiments involving the incorporation of photosensitisers (described in

Chapter 5) where a substantial reduction in bacterial kill is observed upon addition of BSA to the system. An additional advantage is that compared to previous polymeric antibacterial samples investigated at the Materials Research Centre at University College London (UCL), these copper-containing surfaces do not require light to activate their bactericidal properties. The average light intensity in hospitals is reported to range between 1,000 lux in an accident and emergency (A & E) examination room to 10,000-100,000 lux in an operating theatre (detailed in Table 3.3).⁴⁴ However, actual light intensity measurements in some hospital wards are as low as ~200 lux (Prof. P. Wilson, UCLH, personal communication). Cu-polyurethane and Cu-silicone bactericidal surfaces eliminate the concern associated with variable light intensities of different areas in hospitals by possessing lethal activity in the dark.

Table 3.3 Average light intensities in common hospital surroundings in the UK.⁴⁴

Hospital environment	Light intensity / lux
Ward corridors	≥ 200
A & E examination room	1,000
Pathology laboratory	8,000
Operating theatre	10,000 – 100,000

These bactericidal surfaces have been prepared without altering the appearance of the materials. Aesthetically, a material that is not brightly coloured and rapidly reduces bacterial contamination is appealing for frequently touched surfaces in hospital environments. As shown in Fig. 3.9 and 3.10, the antibacterial activity of surfaces are polymer dependent, demonstrating that Cu-polyurethane was more efficient at reducing both *S. aureus* NCTC 13143 and *E. coli* ATCC 25922 at shorter incubation times. Compared to polyurethane alone, Cu-polyurethane undergoes a slight change in colour and has a greater increase in hydrophobicity than shown by the incorporation of Cu into silicone. As polyurethane swells more than silicone, a greater concentration of nanoparticles is incorporated into

polyurethane which results in a greater antibacterial effect from Cu-polyurethane than Cu-silicone. This is also responsible for the change in appearance and hydrophobicity of the different polymer types. XPS data also suggests that more Cu is present on the surface of polyurethane than silicone, which may explain why Cu-polyurethane reduces bacterial numbers more effectively than Cu-silicone; it contains more free copper on the surface which can potentially leach from the surface and kill bacteria before they can interact with Cu NPs incorporated into the polymer substrate.

Further experiments were carried out to determine whether Cu NPs leached into a solution by immersing the modified polymer samples into PBS for up to 2 weeks. After 2 weeks, the samples were removed from the solution and the solution itself was tested for antibacterial activity. The results indicated no bactericidal activity from the surrounding solution, suggesting a low level of Cu NPs present in the solution (data not shown). This study suggests that the bactericidal activity of Cu-incorporated polymers is not due to Cu ions leaching into the bacterial solution but from the combination of other possible mechanisms.

3.4 Conclusion

An easily reproducible “green strategy” was used to synthesise cost effective and monodisperse Cu NPs (~2.5 nm in size). The synthetic reagents used are non-toxic and environmentally friendly showing that these nanoparticles have biomedical applications²⁴ unlike other Cu NPs reported in the literature.^{45,46} These nanoparticles are uniform in shape and have a narrow size distribution. They have been incorporated into polyurethane and silicone, two commonly used polymers in hospitals used for medical devices which can also be used to coat surfaces such as mousepads, keyboards and other electronic devices such as iPads and tablets.

These antibacterial surfaces have proven to be stable materials after 90 days, demonstrating significant bactericidal activity against *E. coli* and a strain of EMRSA-16, one of two clones known to predominate in the UK.²² Cu-silicone demonstrated efficacious antibacterial activity against both *S. aureus* and *E. coli*, by reducing bacterial numbers to below the detection limit within 5 h and 6 h, respectively. However, Cu-polyurethane reduced numbers of *S. aureus* and *E. coli* to below the detection limit within only 2 h and 3 h, respectively, demonstrating a greater bactericidal effect than Cu-silicone. Upon the addition of organic contaminant to mimic organic material deposition by hand touching, the antibacterial activity of the samples did not change. The exact mechanism for the antibacterial activity of these polymeric systems has not been determined, however, the results from this investigation suggests it is due to a combination of electrostatic interaction between the copper surface and bacterial membrane and the leaching of copper ions, and less likely due to the production of ROS (as L-ascorbic acid is a potential scavenger of ROS).

These novel, highly effective antibacterial materials are easy to synthesise and exhibit lethal antibacterial activity against Gram-positive and Gram-negative bacteria. Polyurethane-encapsulated Cu demonstrates greater bactericidal activity than Cu-silicone, however, Cu-silicone remains completely unchanged visually after the addition of copper, which may prove more commercially attractive for use as protective covers for keyboards and electronic tablets. These materials differ from previous studies that focus on light activation to achieve bacterial kill. Thus, this chapter presents self-sterilising materials with a strong potential to reduce the incidence of HAIs in a clinical environment.

References

- 1 Ramasubramanian V, Iyer V, Sewlikar S, Desai A. Epidemiology of healthcare acquired infection – An Indian perspective on surgical site infection and catheter related blood stream infection. *Indian Journal of Basic and Applied Medical Research*. 2014;3(4):46-63.
- 2 Ventola CL. The Antibiotic Resistance Crisis: Part 1: Causes and Threats. *Pharmacy and Therapeutics*. 2015;40(4):277-283.
- 3 Kanj SS, Kanafani ZA. Current Concepts in Antimicrobial Therapy Against Resistant Gram-Negative Organisms: Extended-Spectrum β -Lactamase-Producing Enterobacteriaceae, Carbapenem-Resistant Enterobacteriaceae, and Multidrug-Resistant *Pseudomonas aeruginosa*. *Mayo Clinic Proceedings*. 2011;86(3):250-259.
- 4 Mathur P. Hand hygiene: Back to the basics of infection control. *The Indian Journal of Medical Research*. 2011;134(5):611-620.
- 5 Salgado CD, Sepkowitz KA, John JF, Cantey JR, Attaway HH, Freeman KD, Sharpe PA, Michels HT, Schmidt MG. Copper Surfaces Reduce the Rate of Healthcare-acquired Infections in the Intensive Care Unit. *Infection Control and Hospital Epidemiology*. 2013;34(5):479–86.
- 6 Beyth N, Houry-Haddad Y, Domb A, Khan W, Hazan R. Alternative Antimicrobial Approach: Nano-Antimicrobial Materials. *Evidence-Based Complementary and Alternative Medicine*. 2015;2015:1-16.
- 7 Warnes SL, Green SM, Michels HT, Keevil CW. Biocidal Efficacy of Copper Alloys against Pathogenic Enterococci Involves Degradation of Genomic and Plasmid DNAs. *Applied and Environmental Microbiology*. 2010;76(16):5390-5401.
- 8 Usman MS, Zowalaty MEE, Shameli K, Zainuddin N, Salama M, Ibrahim NA. Synthesis, characterization, and antimicrobial properties of copper nanoparticles. *International Journal of Nanomedicine*. 2013;8:4467-4479.

- 9 Azam A, Ahmed AS, Oves M, Khan MS, Habib SS, Memic A. Antimicrobial activity of metal oxide nanoparticles against Gram-positive and Gram-negative bacteria: a comparative study. *International Journal of Nanomedicine*. 2012;7:6003-6009.
- 10 Chatterjee AK, Chakraborty R, Basu T. Mechanism of antibacterial activity of copper nanoparticles. *Nanotechnology*. 2014;25(2014):13501.
- 11 Wu X, Ye L, Liu K, Wang W, Wei J, Chen F, Liu C. Antibacterial properties of mesoporous copper-doped silica xerogels. *Biomedical Materials*. 2009;4(4):045008.
- 12 Manzl C, Enrich J, Ebner H, Dallinger R, Krumschnabel G. Copper-Induced Formation of Reactive Oxygen Species Causes Cell Death and Disruption of Calcium Homeostasis in Trout Hepatocytes. *Toxicology*. 2004;196(1):57-64.
- 13 Rdzawski V, Stobrawa J, Gáuchowski W, Konieczny J. Thermomechanical Processing of CuTi₄ Alloy, *Journal of Achievements in Materials and Manufacturing Engineering*. 2010;42(1):9-25.
- 14 Vadlapudi V, Kaladhar DSVGK, Behara M, Sujatha B, Naidu GK. Synthesis of Green Metallic Nanoparticles (NPs) and Applications. *Oriental Journal of Chemistry*. 2013;29(4):1589-1595.
- 15 Yakout SM, Mostafa AA. A novel green synthesis of silver nanoparticles using soluble starch and its antibacterial activity. *International Journal of Clinical and Experimental Medicine*. 2015;8(3):3538-3544.
- 16 Kulkarni N, Muddapur U. Biosynthesis of Metal Nanoparticles: A Review. *Journal of Nanotechnology*. 2014;2014:1-8.
- 17 Sierra-Avila R, Perez-Alvarez M, Cadenas-Pliego G, Avila-Orta CA, Betancourt R, Jimenez E, Jimenez RM, Martinez-Colunga G. Synthesis of Copper Nanoparticles Coated with Nitrogen Ligands. *Journal of Nanomaterials*. 2014;2014:1-8.

- 18 Sehmi SK, Noimark S, Weiner J, Allan E, MacRobert AJ, Parkin IP. Potent Antibacterial Activity of Copper Embedded into Silicone and Polyurethane. *ACS Materials & Interfaces*. 2015;7(41):22807-22813.
- 19 Hannay F. *Rigid Plastics Packaging: Materials, Processes and Applications*. iSmithers Rapra Publishing, 2002;151.
- 20 Chu PK, Chen JY, Wang LP, Huang N. Plasma-surface modification of biomaterials. *Materials Science and Engineering: R: Reports*. 2002;36(5):143-206.
- 21 Zdrahala RJ, Zdrahala IJ. Biomedical applications of polyurethanes: a review of past promises, present realities, and a vibrant future. *Journal of biomaterials applications*, 1999;14(1):67-90.
- 22 Das S, Anderson CJ, Grayes A, Mendoza K, Harazin M, Schora DM, Peterson LR. Nasal Carriage of Epidemic Methicillin-Resistant *Staphylococcus aureus* 15 (EMRSA-15) Clone Observed in Three Chicago-Area Long-Term Care Facilities. *Antimicrobial Agents and Chemotherapy*. 2013;57:4551-4553.
- 23 Yu W, Xie H, Chen L, Li Y, Zhang C. Synthesis and Characterization of Monodispersed Copper Colloids in Polar Solvents. *Nanoscale Research Letters*. 2009;4(5):465-470.
- 24 Xiong J, Wang Y, Xue Q, Wu X. Synthesis of Highly Stable Dispersions of Nanosized Copper Particles using L-Ascorbic Acid. *Green Chemistry*. 2011;13:900-904.
- 25 Perni S, Piccirillo C, Kafisas A, Uppal M, Pratten J, Wilson M, Parkin IP. Antibacterial activity of light-activated silicone containing methylene blue and gold nanoparticles of different sizes. *Journal of Cluster Science*. 2010;21(3):427-438.
- 26 Sehmi SK, Noimark S, Bear JC, Peveler WJ, Bovis M, Allan E, MacRobert AJ, Parkin IP. Lethal photosensitisation of *Staphylococcus aureus* and *Escherichia coli* using crystal violet and zinc oxide-encapsulated polyurethane. *Journal of Materials Chemistry B*. 2015;3:6490-6500.

- 27** Ergaieg K, Chevanne M, Cillard J, Seux R. Involvement of both type I and type II mechanisms in Gram-positive and Gram-negative bacteria photosensitization by a meso-substituted cationic porphyrin. *Solar Energy*. 2008;82(12):1107–1117.
- 28** Kawamura-Sato K, Wachino J, Kondo T, Ito H, Arakawa Y. Reduction of disinfectant bactericidal activities in clinically isolated *Acinetobacter* species in the presence of organic material. *Journal of Antimicrobial Chemotherapy*. 2008;61:568-576.
- 29** Luo Z, Chen Y, Chen S, Welch W, Andresen B, Jose P, Wilcox C. Comparison of inhibitors of superoxide generation in vascular smooth muscle cells. *British Journal of Pharmacology*. 2009;157(6):935-943.
- 30** Noimark S, Bovis M, MacRobert AJ, Correia A, Allan E, Wilson M, Parkin IP. Photobactericidal polymers: the incorporation of crystal violet and nanogold into medical grade silicone. *RSC Advances*. 2013;3:18383–18394.
- 31** Noimark S, Dunnill CW, Kay CWM, Perni S, Prokopovich P, Ismail S, Wilson M, Parkin IP, Incorporation of methylene blue and nanogold into polyvinyl chloride catheters; a new approach for light-activated disinfection of surfaces. *Journal of Materials Chemistry*. 2012;22:15388–15396.
- 32** Noimark S, Weiner J, Noor N, Allan E, Williams CK, Shaffer MSP, Parkin IP. Dual-Mechanism Antimicrobial Polymer-ZnO Nanoparticle and Crystal Violet-Encapsulated Silicone. *Advanced Functional Materials*. 2015;25(9):1367-1373.
- 33** Ozkan E, Ozkan FT, Allan E, Parkin IP. The use of zinc oxide nanoparticles to enhance the antibacterial properties of light-activated polydimethylsiloxane containing crystal violet. *RSC Advances*. 2015;5:8806-8813.
- 34** Crick CR, Noimark S, Peveler W, Bear JC, Ivanov AP, Edel J, Parkin IP. Advanced analysis of nanoparticle composites-A means towards increasing the efficiency of functional materials. *RSC Advances*. 2015;5:53789-53795.

- 35 Garrett TR, Bhakoo M, Zhang Z. Bacterial adhesion and biofilms on surfaces. *Progress in Natural Science*. 2008;18(9):1049-1056.
- 36 Donlan RM, Costerton JW. Biofilms: Survival Mechanisms of Clinically Relevant Microorganisms. *Clinical Microbiology Reviews*. 2002;15(2):167-193.
- 37 Sauer M, Branduardi P, Valli M, Porro D. Production of L-Ascorbic Acid by Metabolically Engineered *Saccharomyces cerevisiae* and *Zygosaccharomyces bailii*. *Applied and Environmental Microbiology*. 2004;70(10):6086-6091.
- 38 Wu CY, Lee HJ, Liu CF, Korivi M, Chen HH, Chan MH. Protective role of L-ascorbic acid, N-acetylcysteine and apocynin on neomycin-induced hair cell loss in zebrafish. *Journal of Applied Toxicology*. 2015;35(3):273-279.
- 39 Branduardi P, Fossati T, Sauer M, Pagani R, Mattanovich D, Porro D. Biosynthesis of vitamin C by yeast leads to increased stress resistance. *PLoS One*. 2007;2(10):e1092.
- 40 Piccirillo C, Perni S, Gil-Thomas J, Prokopovich P, Wilson M, Pratten J, Parkin IP. Antimicrobial activity of methylene blue and toluidine blue O covalently bound to a modified silicone polymer surface. *Journal of Materials Chemistry*. 2009;19(34):6167-6171.
- 41 Borkow G, Monk A. Fighting nosocomial infections with biocidal non-intrusive hard and soft surfaces. *World Journal of Clinical Infectious Diseases*. 2012;2(4):77-90.
- 42 Grass G, Rensing C, Solioz M. Metallic Copper as an Antimicrobial Surface. *Applied and Environmental Microbiology*. 2011;77:1541-1547.
- 43 Shi M, Kwon HS, Peng Z, Elder A, Yang H. Effects of Surface Chemistry on the Generation of Reactive Oxygen Species by Copper Nanoparticles. *ACS Nano*, 2012;6(3):2157-2164.
- 44 Ozkan E, Allan E, Parkin IP. The antibacterial properties of light-activated polydimethylsiloxane containing crystal violet. *RSC Advances*. 2014;4:51711-51715.

- 45** Prabhu BM, Ali SF, Murdock RC, Hussain SM, Srivatsan M. Copper nanoparticles exert size and concentration dependent toxicity on somatosensory neurons of rat. *Nanotoxicology*. 2010;4(2):150-160.
- 46** Kim JS, Adamcakova-Dodd, O'Shaughnessy PT, Grassian VH, Thorne PS. Effects of copper nanoparticle exposure on host defence in a murine pulmonary infection model. *Particle and Fibre Toxicology*. 2011;8(29):1-14.

Chapter 4

4. Polyurethane-Encapsulated Glutaraldehyde; Antimicrobial Polymer without White Light Activation

4.1 Introduction

Much progress has been made in recent years in minimising the risk of hospital-acquired infections (HAIs), but as many bacterial pathogens become resistant to multiple antibiotics, we need to evaluate existing methods and find new and better ways of preventing these sometimes life-threatening infections. In particular, genera of Enterobacteriaceae (a family of Gram-negative bacteria), which are normally found in the human intestine,¹ exhibit multiple antibiotic resistances and present a major threat to healthcare worldwide.² Various control measures can be implemented to reduce the spread of HAIs, including improvements in hand washing, the use of disposable equipment and medical devices, and isolating patients with appropriate ventilation.³ Regular and effective cleaning regimes for hospitals is mandatory as unproductive cleaning can assist in transferring bacteria between healthcare personnel, patients and surfaces.⁴

Chapter 3 introduced novel antibacterial surfaces made by encapsulating nanosized copper particles into medical grade polyurethane and silicone sheets. The results showed that polyurethane was able to swell more effectively, suggesting that a greater concentration of antibacterial agent was likely to be incorporated into polyurethane compared to silicone. Thus, for the remaining chapters, all antibacterial surfaces investigated are prepared from polyurethane, which has shown to exhibit effective

bactericidal activity within short exposure times. In this chapter, glutaraldehyde, a well-known disinfectant in hospitals, is impregnated into polyurethane at a low concentration to minimise toxicity. These surfaces are tested against Gram-positive and Gram-negative bacteria and their antibacterial activity over time is examined.

Biocides are extensively used in healthcare for sterilising medical devices and heat sensitive equipment, preserving pharmaceutical products, and disinfecting contaminated surfaces and water.⁵ They are extremely effective in controlling HAIs because they can inhibit or kill some of the most clinically relevant bacteria.⁶ They can target different locations on the bacteria by interacting with the cell wall and outer membrane, or penetrating the cell and causing cell death.⁷ However, due to insufficient cleaning protocols, most disinfectants almost never clean 100% of the targeted surface sufficiently.⁸ When choosing a disinfectant, there are many factors to be considered, such as compatibility with instruments and medical devices, types of surfaces, and compliance with health and safety regulations.⁹ It must be easy to use and not leave any toxic residues.¹⁰

Glutaraldehyde is a saturated dialdehyde (Fig. 4.1) that is commonly used in hospitals as a chemical sterilant and disinfectant.¹¹ It can inactivate a wide range of pathogens, including *Staphylococcus aureus* (*S. aureus*), methicillin-resistant *S. aureus* (MRSA), *Klebsiella pneumoniae*, *Pseudomonas aeruginosa* (*P. aeruginosa*) and *Escherichia coli* (*E. coli*).^{8,11,12} The antibacterial activity of glutaraldehyde is due to the alkylation of hydroxyl, carbonyl and amino groups which affects DNA, RNA and protein synthesis.¹³ In addition to this, Maillard *et al* reported a strong binding of glutaraldehyde to the outer membrane of *E. coli* and inhibition of membrane transport in other Gram-negative bacteria.¹⁴

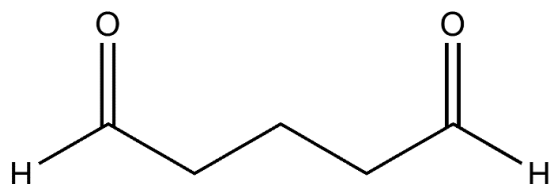


Fig. 4.1 The chemical structure of glutaraldehyde.

Glutaraldehyde is active in mildly alkaline conditions (pH 7.5 – 8.5) and is not biocidal against bacteria when in acidic aqueous conditions.¹⁵ At a higher pH there are more reactive sites formed at the surface (e.g. more free hydroxyl, carbonyl groups) which lead to a faster bactericidal effect.¹¹ Studies have shown that >2% glutaraldehyde solution (buffered to pH 7.5 – 8.5) effectively killed vegetative bacteria, such as *S. aureus*, *E. coli* and *P. aeruginosa* within 2 minutes, *Mycobacterium tuberculosis*, viruses and fungi within 10 minutes and *Bacillus* and *Clostridium* spores within 3 hours.¹¹ However, some studies have found no significant difference between the bactericidal effects of alkaline and acidic solutions of glutaraldehyde.^{12,15} It is widely used in hospitals because it is non-corrosive towards rubber, plastic, thermometers and endoscopic equipment^{9,16} and it still has significant microbicidal activity in the presence of organic matter (20% bovine serum).^{9,11,15}

There is no evidence for carcinogenic activity, but at high concentrations, glutaraldehyde is considered toxic and a strong irritant.¹⁷ Glutaraldehyde has many uses besides from being a commonly used disinfectant in healthcare environments, thus the recommended concentration for each application differs (Table 4.1).^{9,11} In hospitals, 1 – 2% aqueous glutaraldehyde solution is used, which is then activated by an alkaline buffer (e.g. sodium bicarbonate).¹⁸ On the other hand, 10 – 50% glutaraldehyde is used for water treatment and up to 0.1% as a preservative for cosmetics in Europe (not allowed in aerosols or sprays).¹⁹

However, one major drawback of glutaraldehyde in aqueous solution is that it loses bactericidal activity after approximately 14 days because the molecule begins to polymerise by Aldol condensation.²⁰ When polymerisation occurs, the active sites (aldehyde groups) are blocked and biocidal activity is reduced.²¹

Table 4.1 Concentration (%) of aqueous glutaraldehyde solution used in various industries.^{18,19}

Glutaraldehyde Use	Concentration
Healthcare industry	1 – 2%
Water treatment	10 – 50%
Biocide in pulp & paper industry	10 – 50%
Retail cleaning agent	0.05 – 0.1%
Animal health	0.1 – 0.3%
Microscopy/histology	1.5 – 6%
Cosmetics	0.1%

The biocidal activity of glutaraldehyde in solution is well recognised, but the incorporation of the biocide into polymers as antibacterial surfaces for hospitals has not yet been examined. In this chapter, novel materials are prepared by encapsulating glutaraldehyde into polyurethane and compared with materials prepared from simply coating the biocide on to the polymer surface. The antibacterial activity of these materials is assessed against *S. aureus* 8325-4²² and *E. coli* ATCC 25922 to test the efficiency of the ‘swell-encapsulation-shrink’ method against two hospital pathogens. The stability of glutaraldehyde in the polymer is examined after 15 and 30 days of preparation.

4.2 Experimental

4.2.1 Chemicals and Reagents

Glutaraldehyde solution grade II (containing ~3% w/v glutaraldehyde in water) was purchased from Sigma-Aldrich Chemical Co. Medical grade flat polyurethane sheets (thickness 0.8 mm) were purchased from American Polyfilm Inc. (Branford, CT, USA). Acetone (Sigma-Aldrich, UK) was used to prepare polyurethane-encapsulated glutaraldehyde and deionised water (resistivity 15 M Ω cm) was used throughout all synthetic work.

4.2.2 Material Preparation

Glutaraldehyde solution grade II (~3% w/v glutaraldehyde in water) was diluted by a factor of 100 (~0.03% w/v glutaraldehyde in water).

The following polymer samples (1 cm²) were prepared for antibacterial testing:

- (a) Polyurethane-encapsulated glutaraldehyde samples were prepared using the 'swell-encapsulation-shrink' method. They were immersed into a 1:1 acetone/glutaraldehyde solution in water for 24 h (containing ~0.015% w/v glutaraldehyde). They were removed from solution, air-dried overnight and washed with distilled water (as shown in Fig. 4.2).
- (b) Glutaraldehyde-coated polyurethane samples were prepared by using a 1:1 ratio of water/glutaraldehyde solution in water for 24 h (no swelling solution, containing ~0.015% w/v glutaraldehyde). They were removed from solution, air-dried overnight and then washed with distilled water.
- (c) Control polyurethane samples (for polymer-encapsulated glutaraldehyde) were prepared by using 1:1 acetone/water solution

for 24 h. They were washed, air-dried overnight and washed with distilled water.

(d) Control polymer samples (for glutaraldehyde-coated samples) were prepared by immersing them in water for 24 h, removed and air-dried overnight.

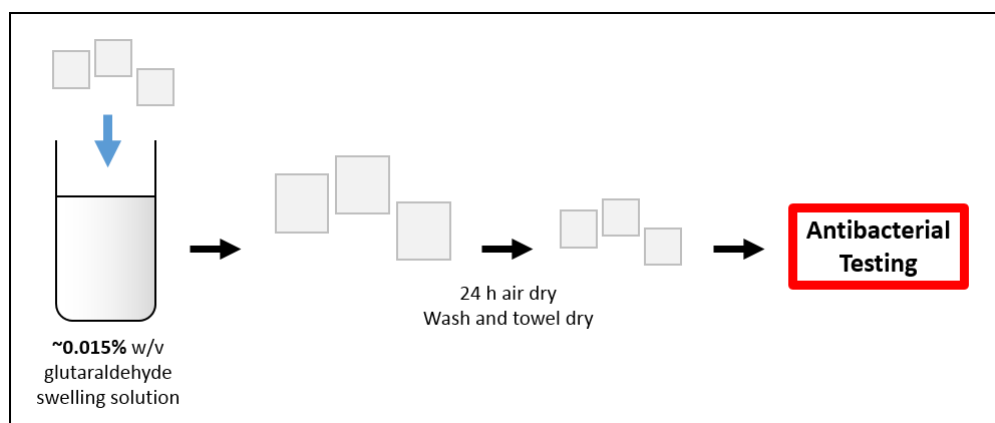


Fig. 4.2 Schematic diagram showing the preparation of polyurethane-encapsulated glutaraldehyde squares (1 cm^2) for antibacterial testing.

4.2.3 Material Characterisation

Infrared absorbance spectra of modified polyurethane samples were measured using a Brüker Platinum ATR with an accumulation of 16 scans per sample (range $4000 - 400 \text{ cm}^{-1}$). X-ray photoelectron spectroscopy (XPS) was carried out using a Thermo Scientific *K-Alpha* spectrometer to classify the different elements present as a function of polymer depth on all polymer samples. All binding energies were calibrated to C (1s) at 284.5 eV. Equilibrium water contact angle measurements were obtained for all samples using a FTA 1000 Drop Shape Instrument. The average contact angle was measured over ≥ 10 measurements using a droplet of deionised water ($\sim 5.0 \mu\text{L}$) dispensed by gravity from a gauge 30 needle. A camera was

attached to the side in order to photograph the samples and the data were analysed using FTA32 software.

4.2.4 Antibacterial Activity

The following polymer samples (1 cm²) were prepared: (i) control samples (solvent treated and water treated), (ii) polyurethane-encapsulated glutaraldehyde and (iii) polyurethane coated with glutaraldehyde. The antibacterial activity of these samples was tested against *S. aureus* 8325-4²² and *E. coli* ATCC 25922. BHI broth (10 mL) was inoculated with 1 bacterial colony and cultured in air (37 °C, 200 rpm, 18 h). The bacterial pellet was recovered by centrifugation, (20 °C, 2867.2 g, 5 min), washed in PBS (10 mL), centrifuged again to recover the bacteria (20 °C, 2867.2 g, 5 min) and finally the bacteria were re-suspended in PBS (10 mL). The washed bacterial suspension was diluted 1000-fold to achieve an inoculum of ~10⁶ cfu/mL. In each experiment, the inoculum was confirmed by plating 10-fold serial dilutions on agar for viable counts. Triplicates of each polymer sample type were inoculated with 25 µL of the inoculum and covered with a sterile cover slip (2.2 cm²). The samples were incubated for up to 2 h (dark conditions). After incubation, the inoculated samples and cover slips were added to PBS (450 µL) and mixed thoroughly using a vortex mixer. The neat suspension and 10-fold serial dilutions were plated on agar for viable counts and incubated aerobically at 37 °C for 48 (*S. aureus*) or 24 hours (*E. coli*).

4.2.4.1 Statistical Significance

The antibacterial experiments were repeated three times and the statistical significance of the following comparisons was analysed using the Mann-Whitney U test: (i) control polymer vs. inoculum; (ii) polyurethane-encapsulated glutaraldehyde vs. control polymer; (iii) polyurethane coated with glutaraldehyde vs. control polymer.

4.3 Results and Discussion

4.3.1 Material Preparation

Glutaraldehyde solution grade II was purchased from Sigma-Aldrich Chemical Co., containing 3% w/v glutaraldehyde in water. This solution was diluted by a factor of 100 to contain only ~0.03% w/v glutaraldehyde. By diluting the solution, the pH naturally increased from ~pH 3 to ~pH 8 and contained a low concentration of the biocide to minimise potential toxicity towards patients, visitors and staff in a clinical setting. Even though a concentration of up to 2% glutaraldehyde is acceptable within hospitals,¹⁵ the application of these antibacterial surfaces differs from using the biocide solution to sterilise medical equipment and devices.^{9,15} The application for these polymer-encapsulated glutaraldehyde surfaces would be for frequently touched surfaces in a hospital (e.g. keyboard and electronic device covers), whereas glutaraldehyde solution used as a disinfectant is only handled by trained staff at specific times throughout their daily cleaning regime.⁸ The diluted biocidal solution (~0.03%) was further diluted by half (~0.015%) to prepare the modified polyurethane samples.

To prepare the glutaraldehyde incorporated polymer samples, the biocidal solution was prepared in a 1:1 mix of acetone and glutaraldehyde solution in water for up to 24 hours at room temperature and pressure. This method of swell-encapsulation (as shown in Fig. 4.2) ensures uniform coating and incorporation of the biocide into the polymer substrate and across the surface. To prepare the glutaraldehyde-coated samples, the dilution was simply performed in pure water to obtain the same concentration of the biocide as the polyurethane-encapsulated glutaraldehyde samples. These polymer squares were immersed into a 1:1 mix of water and aqueous glutaraldehyde solution for up to 24 hours and then removed, washed and towel-dried.

4.3.2 Material Characterisation

Infrared absorbance spectroscopy was obtained for all modified polymer samples (Fig. 4.3). The spectra demonstrated that neither encapsulating the biocide into the polymer nor coating the polymer with the biocide caused any chemical change of the polymer substrate. It also showed that there were no significant changes between the treated and untreated polyurethane samples. This can be attributed to the low concentration of glutaraldehyde used in the experiments and also due to strong absorbance bands of the polymer. XPS was used to determine the efficacy of swell-encapsulating glutaraldehyde into the polymer (Fig. 4.4). XPS depth profile data (after samples were sputtered for 50 seconds) indicated that the carbon content did not decrease with polymer depth, but nitrogen and oxygen content did decrease with polymer depth across all polymer types tested, and therefore cannot be attributed to the presence of glutaraldehyde. All modified polymer surfaces showed characteristic peaks corresponding to the presence of carbon (284.5 eV), nitrogen (399.3 eV) and oxygen (531.7 eV), showing no significant differences in percentage element composition between solvent treated (control) and samples treated with glutaraldehyde (data not shown). However, XPS data did show the presence of a new carbon environment on the surface of both polyurethane-encapsulated glutaraldehyde polyurethane coated with glutaraldehyde (287.6 eV; Fig. 4.4(a) and (c)). This indicates the presence of a new ketone-type C (1s) environment, corresponding to glutaraldehyde (Fig. 4.1). Additionally, another oxygen peak was shown exclusively on the surface of polyurethane-encapsulated glutaraldehyde, indicating the presence of an aldehyde group representing the biocide at the surface (Fig. 4.4(b)). This data suggests that even after encapsulating the biocide, it mainly resides on the polymer surface.

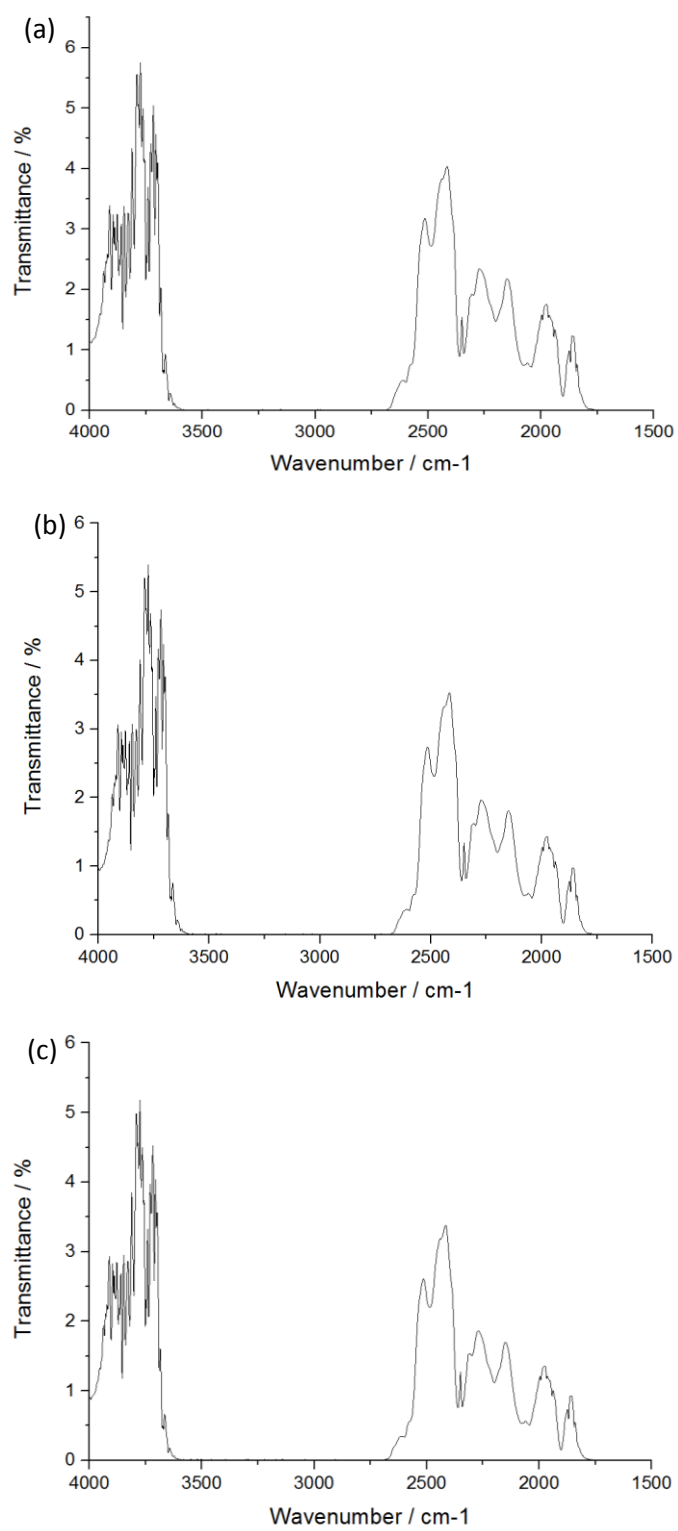


Fig. 4.3 ATR-FTIR spectra of (a) solvent treated polyurethane (control), (b) polyurethane-encapsulated glutaraldehyde and (c) polyurethane coated with glutaraldehyde.

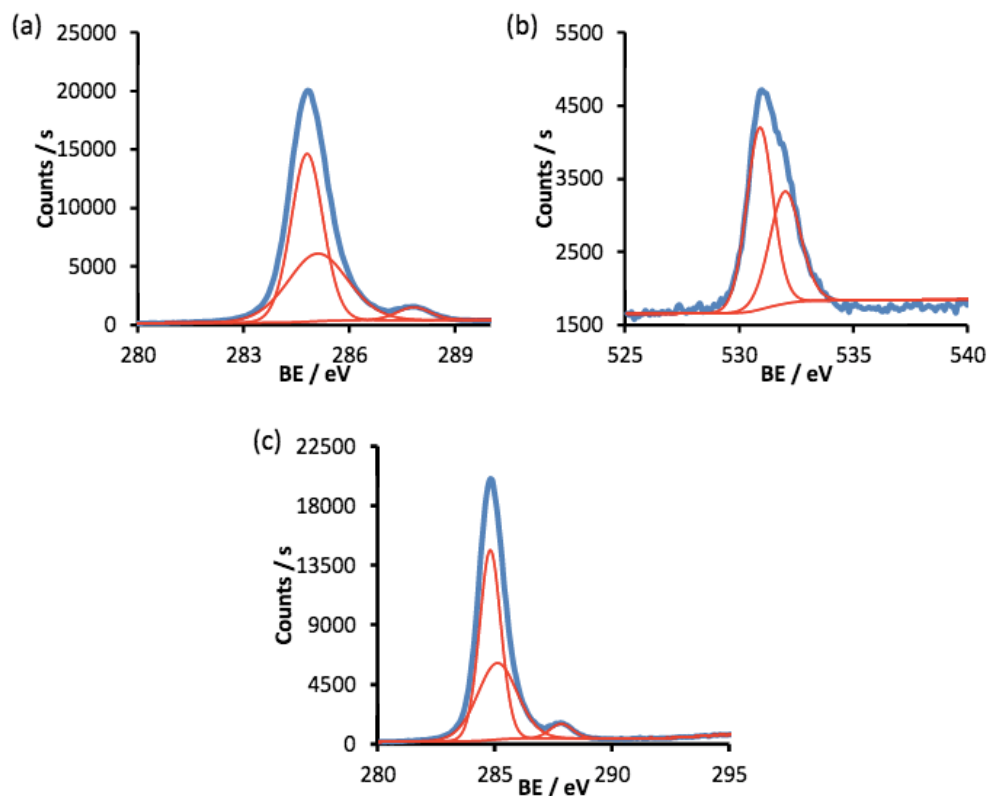


Fig. 4.4 XPS spectra for polyurethane-encapsulated glutaraldehyde surface: (a) carbon (1s) region and (b) oxygen (1s) region and for polyurethane surface coated with glutaraldehyde: (c) carbon (1s) region.

The wetting properties of all modified samples were tested to see any changes in hydrophobicity of the samples when the biocide was incorporated either by encapsulating or coating. The water contact angles of untreated and treated samples indicate that polyurethane has a hydrophobic surface. After adding glutaraldehyde to the polymer (either by coating or encapsulating), there was a negligible change in hydrophobicity of the material, with contact angles varying by a maximum of ± 1 degree.

4.3.3 Antibacterial Activity

The antibacterial activity of the following modified polyurethane samples was tested against *S. aureus* 8325-4²² and *E. coli* ATCC 25922 in the dark: (a) control (solvent treated), (b) polyurethane-encapsulated glutaraldehyde and (c) glutaraldehyde-coated polyurethane. There are two control samples for this investigation: one is treated with a 1:1 ratio of acetone/water and the other is treated with water only. Both were tested for antibacterial activity and there was no significant difference between them, therefore the results shown in Fig. 4.5 and 4.6 only show the antibacterial activity of one control polymer (treated with 1:1 ratio of acetone/water).

Following 30 minutes of incubation (Fig. 4.5(a)), the control and glutaraldehyde-coated samples did not show significant kill of *S. aureus* 8325-4, whereas polyurethane-encapsulated glutaraldehyde displayed ~0.5 log reduction of *S. aureus* 8325-4 ($P < 0.001$). After 1 hour (Fig. 4.5(b)), control polyurethane did not show any significant kill, but glutaraldehyde-coated polymer demonstrated an ~1.5 log reduction in bacterial numbers. Polyurethane-encapsulated glutaraldehyde exhibited the greatest kill, reducing numbers of *S. aureus* 8325-4 to below the detection limit of 100 cfu/mL (≥ 4 log; $P < 0.001$). After 1 hour of incubation (Fig. 4.5(c)), control polymer and glutaraldehyde-coated polyurethane did not show any reduction of *E. coli* ATCC 25922. However, polyurethane-encapsulated glutaraldehyde demonstrated a statistically significant reduction of the bacteria (~1.3 log; $P < 0.001$). Following 2 hours of exposure to *E. coli* ATCC 25922 (Fig. 4.5(d)), solvent treated polyurethane did not demonstrate any significant bacterial kill, however, glutaraldehyde-coated polyurethane resulted in ~0.7 log reduction of the bacteria ($P < 0.001$). Furthermore, polyurethane-encapsulated glutaraldehyde showed considerable antibacterial activity by reducing bacterial numbers to below the detection limit (≥ 4 log; $P < 0.001$).

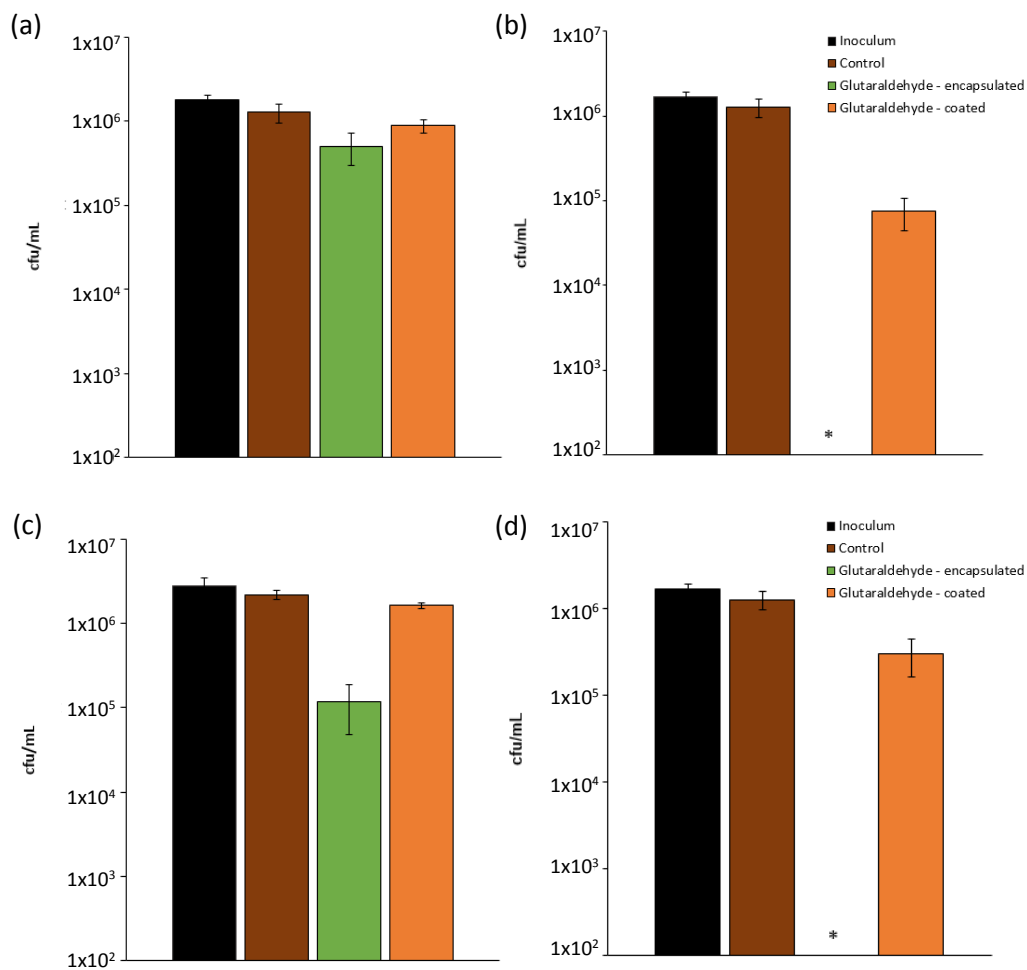


Fig. 4.5 Viable counts of *S. aureus* 8325-4 after incubation at 20°C on modified polyurethane squares for: (a) 30 min and (b) 1 h, and viable counts of *E. coli* ATCC 25922 after incubation on modified polyurethane squares for: (c) 1 h and (d) 2 h. Control samples are solvent treated. * indicates bacterial numbers reduced below the detection limit of 100 colony forming units/mL (cfu/mL).

Table 4.2 Summary of the antibacterial activity of polyurethane-encapsulated glutaraldehyde and polyurethane-coated glutaraldehyde against *S. aureus* 8325-4 and *E. coli* ATCC 25922. Bacterial reduction is given in log form.

Bacterial strain	Polyurethane-encapsulated glutaraldehyde	Polyurethane-coated glutaraldehyde
<i>S. aureus</i> 8325-4	0.5 log (0.5 h) ≥4 log (1 h)	No kill (0.5 h) 1.5 log (1 h)
<i>E. coli</i> ATCC 25922	1.3 log (1 h) ≥4 log (2 h)	No kill (1 h) 0.7 log (2 h)

Following 15 days of storage at room temperature, the antibacterial longevity of polyurethane encapsulated and coated with glutaraldehyde was tested against *S. aureus* 8325-4 and *E. coli* ATCC 25922 (Fig. 4.6). Polyurethane-encapsulated glutaraldehyde showed a reduced bactericidal effect against *S. aureus* 8325-4 and *E. coli* ATCC 25922, as both bacteria were only reduced by ~ 0.5 log in comparison to previous results which demonstrated ≥ 4 log reduction after 1 hour and 2 hours, respectively. Glutaraldehyde-coated polyurethane exhibited no significant antibacterial activity following 15 days and after 30 days, the bactericidal activity of both samples was undetectable (data not shown).

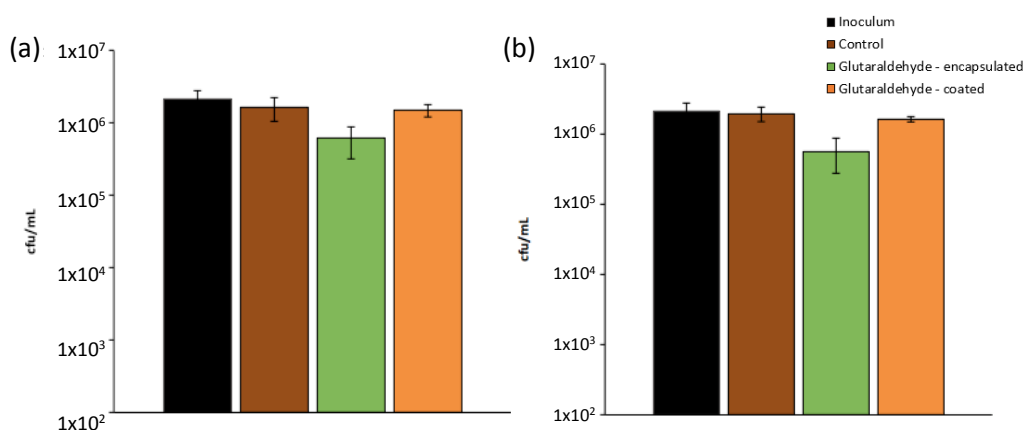


Fig. 4.6 Viable counts (colony forming units/mL (cfu/mL)) of (a) *S. aureus* 8325-4 for 1 h and (b) *E. coli* ATCC 25922 for 2 h after incubation at 20°C on modified polyurethane squares left for 15 days. Control samples are solvent treated.

A commonly used disinfectant in hospitals was incorporated into polyurethane at a very low concentration to test its bactericidal activity against *S. aureus* 8325-4 and *E. coli* ATCC 25922 as representative Gram-positive and Gram-negative bacteria. The results clearly show that the antibacterial activity of polyurethane-encapsulated glutaraldehyde is much greater than glutaraldehyde coated onto polyurethane. Polymer-encapsulated glutaraldehyde samples reduced both bacteria to below the detection limit within 2 hours, whereas glutaraldehyde-coated

polyurethane only caused ~0.7 – 1.5 log reduction against the bacteria within the same duration (Fig. 4.5). However, according to XPS data and water contact angle measurements, they contain similar amounts of biocide on the surface. The only known difference is the indication of an aldehyde group on the surface of the polyurethane-encapsulated glutaraldehyde (oxygen (1s) region; Fig. 4.4(b)) that is not shown on the XPS data for glutaraldehyde-coated polyurethane. This difference could be due to a greater concentration of the biocide at the surface that remains on polyurethane-encapsulated glutaraldehyde compared to glutaraldehyde coated onto the polymer after it has been washed and towel-dried.

As described previously, monomeric glutaraldehyde undergoes polymerisation at alkaline pH, which blocks the active sites on the molecule and reduces its biocidal activity.²³ This mechanism involves an Aldol condensation reaction; causing dehydration and yielding ethylene linkages conjugated with aldehyde functionalities.²⁰ In basic conditions, this polymerisation reaction shifts the equilibrium of the reaction scheme shown in Fig. 4.7 to the left, resulting in more free aldehyde groups.²⁴ Therefore, by increasing the pH of the biocidal solution used in this investigation from ~pH 3 to ~pH 8, we encourage more free aldehyde groups to be formed which can undergo the condensation reaction to form poly-glutaraldehyde and limit the antibacterial activity of the solution. However, this pH change is inevitable when diluting the solution to reduce its toxicity, which is a main concern for its potential application as an antibacterial surface coating in hospitals.

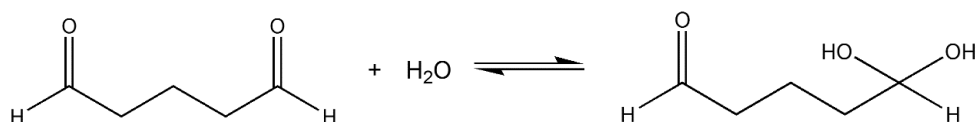


Fig. 4.7 Equilibrium reaction scheme of glutaraldehyde in basic conditions (adapted from Margel and Rembaum)²⁴

The difference between the antibacterial activity of polyurethane coated and encapsulated with glutaraldehyde is possibly due to the rate of polymerisation that occurs on the biocide film once the samples have been prepared. It is likely that encapsulating the biocide prevents or delays polymerisation of the biocide, whereas coating the polymer with glutaraldehyde allows this process to occur at a faster rate. Even though XPS detected a similar low level of glutaraldehyde at the surface of both modified samples, it is still an effective amount to completely reduce both bacteria within only 2 hours. It is possible that encapsulating glutaraldehyde into the polymer substrate protects it from polymerisation and then it slowly leaches out causing an increased concentration of the biocide at the surface. Polymerisation may occur more slowly when the biocide is impregnated into the polymer matrix where there is a lower oxygen concentration and the molecule has less opportunity for monomer-monomer interaction as a result of reduced diffusion.²⁰

Glutaraldehyde solution has many benefits as a hospital sterilant, including cost effectiveness²⁵ and exceptional material compatibility.²⁶ It is used as a cold sterilant to disinfect and clean heat-sensitive medical, surgical and dental equipment. Its biocidal activity is very similar to formaldehyde and works by either denaturing proteins or modifying nucleic acids by alkylation.²⁷ This is favoured by more basic conditions (\geq pH 8), but in such conditions the molecule undergoes polymerisation and loses its bactericidal response.²⁸ Following 15 days of storage, the antibacterial activity of polyurethane-encapsulated glutaraldehyde significantly reduced. Thus, these polymeric materials would be more suited for temporary uses, for example, disposable plastic covers to cover light handles in operating theatres and equipment.^{29,30}

4.4 Conclusion

For the first time, a well-known biocide used in hospitals was incorporated into polyurethane to show the effectiveness of the 'swell-encapsulation-shrink' method compared to simply coating the polymer surface with the antibacterial agent. Polyurethane samples encapsulated and coated with glutaraldehyde were tested against representative Gram-positive and Gram-negative bacteria for potential use in hospitals in lowering the risk of spreading nosocomial infections. To minimise toxicity, a very low concentration of glutaraldehyde was used compared to reports in the literature.^{9,12,15,18} Functional tests showed that the hydrophobicity of the samples did not change as a result of adding glutaraldehyde, which is important in preventing biofilm formation at the surface.

These antibacterial polymers have shown significant bactericidal activity in the dark compared to previous work on light-activated materials.³¹⁻³⁶ Chapter 3 revealed a greater swelling capability of polyurethane in comparison to silicone; thus, polyurethane was used in this investigation to ensure a larger amount of glutaraldehyde was impregnated into the polymer. For polyurethane-encapsulated glutaraldehyde, numbers of *S. aureus* 8325-4 and *E. coli* ATCC 25922 were reduced to below the detection limit after only 1 or 2 hours, respectively. However, glutaraldehyde-coated polyurethane did not exhibit such efficacious bactericidal activity. The outstanding results obtained from these polymers show that they could be suitable for surfaces that are not exposed to light, where light-activated surfaces would be less effective.

This investigation has shown the potential for glutaraldehyde to be used as an antibacterial surface for reducing HAIs if the longevity of its antibacterial activity can be improved. The results have shown that encapsulating the biocide into the polymer retains bactericidal activity for longer than when the biocide is coated onto the polymer, but further work is needed to identify new methods that will increase its antibacterial activity over time.

Traditionally this biocide is widely used in solution form to disinfect medical and surgical equipment. However, this investigation has demonstrated that glutaraldehyde can be incorporated into a polymer matrix as a potential short-term antibacterial surface or coating.

References

- 1 Sydnor ERM, Perl TM. Hospital Epidemiology and Infection Control in Acute-Care Settings. *Clinical Microbiology Reviews*. 2011;24(1):141-173.
- 2 Ventola CL. The Antibiotic Resistance Crisis: Part 1: Causes and Threats. *Pharmacy and Therapeutics*. 2015;40(4):277-283.
- 3 Mehta Y, Gupta A, Todi S, Myatra SN, Samaddar DP, Patil V, Bhattacharya PK, Ramasubban S. Guidelines for prevention of hospital acquired infections. *Indian Journal of Critical Care Medicine : Peer-reviewed, Official Publication of Indian Society of Critical Care Medicine*. 2014;18(3):149-163.
- 4 Collins AS. Preventing Health Care–Associated Infections. In: Hughes RG, editor. *Patient Safety and Quality: An Evidence-Based Handbook for Nurses*. Rockville (MD): Agency for Healthcare Research and Quality (US); 2008 Apr. Chapter 41.
- 5 Russell AD, Furr JR, Maillard JY. Bacterial target sites for biocide action. *ASM News*. 1997;63,481-487.
- 6 Maillard JY. Antimicrobial biocides in the healthcare environment: efficacy, usage, policies, and perceived problems. *Therapeutics and Clinical Risk Management*. 2005;4:307–320.
- 7 Russell AD. Bacterial resistance to disinfectants: present knowledge and future problems. *Journal of Hospital Infection*. 1999;43:S57-68.
- 8 Abreu AC, Tavares RR, Borges A, Mergulhao F, Simeos M. Current and emergent strategies for disinfection of hospital environments. *Journal of Antimicrobial Chemotherapy*. 2013;1-15.
- 9 Fraise AP. Choosing disinfectants. *Journal of Hospital Infection*. 1999;43:255-64.

- 10 Simões M, Simões LC, Vieira MJ. A review of current and emergent biofilm control strategies. *Food Science and Technology*. 2010;43:573-83.
- 11 Rutala WA, Weber DJ. Disinfection and Sterilization in Health Care Facilities: What Clinicians Need to Know. *Healthcare Epidemiology*. 2004;39:702-709.
- 12 McDonnell G, Russell AD. Antiseptics and Disinfectants: Activity, Action, and Resistance. *Clinical Microbiology Reviews*. 1999;12(1):147-179.
- 13 McGucken PV, Woodside W. Studies on the Mode of Action of Glutaraldehyde on *Escherichia coli*. *Journal of Applied Bacteriology*. 1973;36(3):419-426.
- 14 Maillard JY. Bacterial target sites for biocide action. *Journal of Applied Microbiology*. 2002;92(Suppl:16S):16S-27S.
- 15 Guideline for Disinfection and Sterilization in Healthcare Facilities, Centers for Disease Control and Prevention, 2008.
- 16 Juwarkar CS. Cleaning and Sterilisation of Anaesthetic Equipment. *Indian Journal of Anaesthesia*. 2013;57(5):541-550.
- 17 Takigawa T, Endo Y. Effects of glutaraldehyde exposure on human health. *Journal of Occupational Health*. 2006;48:75-87.
- 18 Bennett JE, Dolin R, Blaser MJ. Principles and Practice of Infectious Diseases, 8th, Volume 1. *Elsevier Health Sciences*. 2014.
- 19 Glutaraldehyde, CAS No: 111-30-8, *OECD SIDS*. [cited 2016 21/04/2016]; Available from: <http://www.inchem.org/documents/sids/sids/111308.pdf>
- 20 Migneault I, Dartiguenave C, Bertrand MJ, Waldron K. Glutaraldehyde: behavior in aqueous solution, reaction with proteins, and application to enzyme crosslinking. *Biotechniques*. 2004;37(5):790-802.

- 21 Kiernan JA. Formaldehyde, formalin, paraformaldehyde and glutaraldehyde: What they are and what they do. *Microscopy Today* 2001;1:8-12.
- 22 Herbert S, Ziebandt AK, Ohlsen K, Schafer T, Hecker M, Albrecht D, Novick R, Gotz F. Repair of global regulators in *Staphylococcus aureus* 8325 and comparative analysis with other clinical isolates. *Infection and Immunity*. 2010;78(6):2877-2889.
- 23 Aiello AE, Larson EL, Levy SB. Consumer antibacterial soaps: effective or just risky? *Clinical Infectious Diseases*. 2007;45(5):S137-S147.
- 24 Margel S, Rembaum A. Synthesis and Characterization of Poly(glutaraldehyde). *Macromolecules*. 1980;13:19-24.
- 25 D'Ercole S, Catamo G, De Fazio P, Piccolomini R. In vitro antimicrobial activity of glutaraldehyde plus O-phenylphenol association. *Minerva Stomatologica*. 2002;51(1-2):29-33.
- 26 Glutaraldehyde: Safe Handling and Storage Guide, *DOW Chemical Company*, 2003. [cited 2016 21/04/2016]; Available from: http://msdssearch.dow.com/PublishedLiteratureDOWCOM/dh_0049/0901b803800490ae.pdf?filepath=biocides/pdfs/noreg/253-01338.pdf&fromPage=GetDoc
- 27 Maris P. *Revue Scientifique Et Technique De L Office International Des Epizooties*. 1995;14:47-55.
- 28 Sehmi SK, Allan E, MacRobert AJ, Parkin IP. The bactericidal activity of glutaraldehyde-impregnated polyurethane. *MicrobiologyOpen*. 2016.
- 29 Loveday HP, Wilson JA, Pratt RJ, Golsorkhi M, Tingle A, Bak A, Browne J, Prieto J, Wilcox M. National Evidence-Based Guidelines for Preventing Healthcare-Associated Infections in NHS Hospitals in England. *Journal of Hospital Infection*. 2014;86S1:S1-S70.

- 30** Dancer SJ. Controlling Hospital-Acquired Infection: Focus on the Role of the Environment and New Technologies for Decontamination. *Clinical Microbiology Reviews*. 2014;27(4):665-690.
- 31** Noimark S, Bovis M, MacRobert AJ, Correia A, Allan E, Wilson M, Parkin IP. Photobactericidal polymers: the incorporation of crystal violet and nanogold into medical grade silicone. *RSC Advances*. 2013;3:18383–18394.
- 32** Noimark S, Dunnill CW, Kay CWM, Perni S, Prokopovich P, Ismail S, Wilson M, Parkin IP, Incorporation of methylene blue and nanogold into polyvinyl chloride catheters; a new approach for light-activated disinfection of surfaces. *Journal of Materials Chemistry*. 2012;22:15388–15396.
- 33** Noimark S, Weiner J, Noor N, Allan E, Williams CK, Shaffer MSP, Parkin IP. Dual-Mechanism Antimicrobial Polymer-ZnO Nanoparticle and Crystal Violet-Encapsulated Silicone. *Advanced Functional Materials*. 2015;25(9):1367-1373.
- 34** Ozkan E, Ozkan FT, Allan E, Parkin IP. The use of zinc oxide nanoparticles to enhance the antibacterial properties of light-activated polydimethylsiloxane containing crystal violet. *RSC Advances*. 2015;5:8806-8813.
- 35** Piccirillo C, Perni S, Gil-Thomas J, Prokopovich P, Wilson M, Pratten J, Parkin IP. Antimicrobial activity of methylene blue and toluidine blue O covalently bound to a modified silicone polymer surface. *Journal of Materials Chemistry*. 2009;19(34):6167–6171.
- 36** Perni S, Piccirillo C, Kafisas A, Uppal M, Pratten J, Wilson M, Parkin IP. Antibacterial activity of light-activated silicone containing methylene blue and gold nanoparticles of different sizes. *Journal of Cluster Science*. 2010;21(3):427–438.

Chapter 5

5. Polyurethane Encapsulated with Crystal Violet and 18 nm ZnO Nanoparticles; White Light Activated Antimicrobial Polymers

5.1 Introduction

HAIs have become a severe burden to the NHS, costing them around £1 billion each year.¹ Patients who acquire these infections can experience discomfort, disability, and even death. Almost 80% of HAIs are transmitted by touch, due to the fact that a significant amount of patients, visitors and staff infrequently practice the high standard of personal hygiene that is required in healthcare environments.² Frequently touched surfaces, such as push plates, door handles, electronic devices and food trays, act as bacterial reservoirs for transmission.³ Therefore, staff and visitors can become contaminated by either direct contact with a patient or from touching a contaminated surface, facilitating the spread of these infections.

Chapters 3 and 4 focused on the encapsulation of antibacterial agents into polymers that do not require UV or white light to activate their bactericidal properties. These polymers have proven to reduce hospital pathogens in the dark within exposure times of only a few hours. However, as shown in Chapter 4 with polyurethane-encapsulated glutaraldehyde, the antibacterial activity of these polymers dramatically declines after 2 weeks following preparation. It is possible that glutaraldehyde is killing the bacteria by leaching from the polymer surface which diminishes its antibacterial activity over time. Chapter 3 demonstrated the highly effective bactericidal effect of copper-incorporated polymers. Mechanistic studies suggested that these polymers might reduce bacteria by leaching

copper ions and/or by electrostatic interaction between the nanoparticle surface and the bacterial membrane. The results indicated that ROS were not being produced and thus, were not responsible for the antibacterial activity observed from these polymers.

This chapter introduces the development of self-sterilising surfaces which incorporate photosensitiser dyes into the polymer. These photo-activated surfaces reduce bacteria by producing ROS when illuminated at specific wavelengths of light, using a process known as photodynamic therapy (PDT).⁴ The main advantage of PDT is that these antibacterial agents can destroy bacteria *via* multiple pathways, thus, the development of resistance is unlikely.⁵ These photosensitisers (molecular dyes) are non-toxic, but when irradiated by light, the molecule is promoted from an excited singlet state to an excited triplet state, producing ROS species *via* a Type I (electron transfer) and/or Type II (energy transfer) photochemical processes.⁶ Type I involves the production of cytotoxic ROS such as superoxide anion and hydroxyl radicals, and Type II produces highly reactive singlet oxygen.⁷ It is difficult to determine whether a Type I or Type II mechanism is causing the photodamage because it is unclear if the effects are exclusively due to the production of ROS. Photosensitisers do not display the same toxicity towards mammalian cells as bacterial cells. It requires a much greater density of photosensitiser molecules to cause irreversible cell damage to mammalian cells as they are more resistant and larger than bacterial cells.^{8,9}

As demonstrated in Chapter 3, some nanoparticles are highly effective at killing bacteria without light activation. However, other nanoparticles, such as TiO₂, require UV illumination to induce antibacterial activity.^{10,11} Metal oxide nanoparticles (such as MgO, CuO, Fe₂O₃ and ZnO) have been studied previously for their antibacterial properties against a wide range of bacteria, including *E. coli* and *S. aureus*.¹²⁻¹⁵ ZnO nanoparticles (ZnO NPs) have been extensively reviewed for their bactericidal activity because they are non-toxic, cheap and used in many applications such as food

packaging¹³ and as a UV protector in cosmetics.¹⁶ The exact mechanism of the antibacterial activity of ZnO NPs is not yet understood, although some studies suggest that their antibacterial activity is a result of releasing Zn²⁺ that cause bacterial cell membrane disruption and from producing ROS (and consequently H₂O₂), which are harmful towards the cells.^{13,17} ZnO has a wide band gap of 3.3 eV and exhibits high absorption in the UV region.¹⁸ However, ZnO NPs have shown to produce ROS without UV illumination, i.e. in the dark, due to surface defects that can enable electron transfer to oxygen.¹³ They demonstrate selective antibacterial activity but exhibit a minimal effect on mammalian cells.¹⁹

The Materials Research Centre at UCL has studied the antibacterial activity of photosensitisers, such as crystal violet (CV), methylene blue (MB) and toluidine blue O (TBO), when incorporated into polymers.²⁰⁻²² Moreover, the incorporation of nanoparticles with the photosensitiser can significantly enhance the bacterial kill of the photosensitiser.²³⁻³⁰ This has either been achieved by activating the polymer samples using short-term illumination from a laser source, or over a longer period using hospital lighting of different intensities. These samples have been prepared by using a simple, two step 'swell-encapsulation-shrink' method which incorporates the nanoparticles into the polymer (step 1) and then incorporates the dye in the polymer (step 2). In particular, CV dye has demonstrated efficacious antibacterial activity when coated onto two different types of silicone material.^{22,23,28-30} Table 5.1 summarises the antibacterial activity of polymers containing CV against *E. coli* ATCC 25922 within various irradiation times and intensities.

CV, also known as Gentian Violet, is a cationic triarylmethane dye which is FDA approved and known to exhibit antimicrobial properties.^{31,32} Fluorophores such as CV are a type of molecular rotor, which contain an electron donor group in π -conjugation with an electron acceptor group (Fig. 5.1).³³ Unlike other typical photosensitisers such as MB and TBO, the emission properties of CV are highly dependent on solvent viscosity.³¹

Solvents with high viscosity can limit any intramolecular twisting from the planar, non-twisted conformation, resulting in a change in the photophysical properties of CV.³⁴ In solvents such as water with a relatively low viscosity, CV is unable to produce singlet oxygen since the triplet state quantum yield is negligible. However, under an increased viscosity the molecular rotor is restricted, which stabilises the excited singlet state to allow intersystem crossing to populate the triplet state.³¹ Therefore, by incorporating CV into a polymer matrix (i.e. an environment with high viscosity), singlet oxygen can be produced *via* the Type II mechanism.

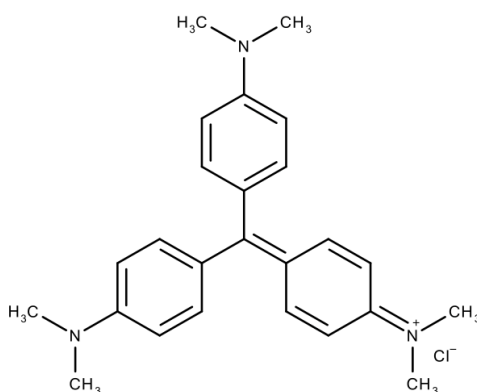


Fig. 5.1 Molecular structure of crystal violet dye

In this study, CV dye is coated onto medical grade polyurethane sheets and tested for antibacterial activity against *S. aureus* 8325-4³⁵ and *E. coli* ATCC 25922. Monodisperse ZnO NPs (~18 nm) were synthesised from the thermal decomposition of a metal-oleate precursor and incorporated into the polymer. Lethal photosensitisation was observed from CV-coated polyurethane against both bacteria and a further enhancement in antibacterial activity of the dye was observed when the semi-conducting ZnO NPs are incorporated into the polymer. Lastly, the mechanism of antibacterial activity of these CV and ZnO-incorporated polyurethane samples (CVZnO) was investigated to determine whether Type I and/or

Type II processes are responsible for killing the bacteria when exposed to a white light source and in the dark.

Table 5.1 Overview of the antibacterial activity of silicone polymer samples prepared and tested by the Materials Chemistry Research Centre at UCL against *E. coli* ATCC 25922. (CV: crystal violet-coated polymer, CVAu: crystal violet and 2 nm gold-incorporated polymer, CVMBAu: crystal violet, methylene blue and 2 nm gold-incorporated polymer)

Polymer	Dye combination	Irradiation	Time	Log kill
<i>Medical grade silicone sheets</i> ^{23,28,29}	CV	635 nm laser	13.5 min	No kill
	CVAu	635 nm laser	13.5 min	~ 2.5
	CVMBAu	White light (4,000 lux)	3 h	~ 2
	CVMBAu	Dark	18 h	~ 1.5
<i>Silicone elastomers from viscous liquid polydimethylsiloxane</i> ^{22,30}	CV	White light (11,500 lux)	6 h	≥ 4
	CVZnO	White light (11,500 lux)	4 h	≥ 4
	CVZnO	Dark	4 h	~ 0.5

5.2 Experimental

5.2.1 ZnO Nanoparticles

5.2.1.1 Chemicals and Reagents

All chemicals used to synthesise the ZnO NPs were purchased from Sigma-Aldrich Chemical Co; including zinc chloride (98%), oleylamine (technical grade, ≤70%), sodium oleate (≤82% fatty acid content), 1-octadecene (technical grade, 90%), and oleic acid (technical grade, 90%).

5.2.1.2 Nanoparticle Synthesis

ZnO NPs were synthesised by a thermal decomposition of zinc oleate, adapted from a method developed by Park *et al.*³⁶ Firstly, zinc oleate was prepared by heating a zinc (II) chloride suspension (10 mmol, 1.36 g) and

sodium oleate (20 mmol, 6.08 g) in a solvent mixture of hexane (140 ml), ethanol (80 ml) and deionised water (60 ml) at 60 °C for 4 h. To remove sodium oleate, the organic layer was separated and washed, and then dried *in vacuo* to remove hexane, forming a white solid (zinc oleate). Zinc oleate (1 g, 1.6 mmol) and oleic acid (0.1784 ml) were dissolved in 1-octadecene (20 ml) and stirred at room temperature. The reaction mixture was heated at a rate of 3.3 °C min⁻¹ to 320 °C under nitrogen and then held at a constant temperature of 320 °C for 1 h, yielding a brown solution. Once the solution cooled to room temperature, ethanol (80 ml) was added to precipitate the nanoparticles. This solution was centrifuged (20 °C, 504 g, 6 min) to form a solid precipitate. The supernatant was discarded and the solid precipitate was dispersed in hexane (30 ml).

5.2.1.3 Nanoparticle Characterisation

The nanoparticles were characterised (in hexane) using transmission electron microscopy (TEM) and energy dispersive X-ray spectroscopy (EDX). TEM micrographs and EDX spectra were performed using a Jeol 2100 HRTEM with a LaB₆ source operating at an acceleration voltage of 200 kV with an Oxford Instruments XMax EDS detector running AZTEC software. The images were recorded on a Gatan Orius Charge-coupled device (CCD). The ZnO NP suspension was drop-casted onto a 400 Cu mesh lacy carbon film TEM grid (Agar Scientific Ltd). The images were analysed using ImageJ software.

5.2.2 Polymer Samples

5.2.2.1 Chemicals and Reagents

Medical grade flat polyurethane sheets (thickness 0.8 mm) were purchased from American Polyfilm Inc. (Branford, CT, USA). To prepare the polymer samples, the following reagents were used: CV (Sigma, UK), ZnO NPs

suspended in hexane (method adapted from Park *et al*³⁶), hexane (Sigma-Aldrich, UK) and dichloromethane (VWR, UK). Deionised water was used (resistivity 15 MΩ cm) during synthesis and preparation.

5.2.2.2 Material Preparation

Polymer System Optimisation

(a) **Organic Solvent** - 1 cm² polyurethane sheets were immersed in the following organic solvent solutions made up at a 1:1 ratio: hexane/dichloromethane (DCM), hexane/acetone, and hexane/tetrahydrofuran (THF). They were left to swell for 24 h in the dark, then removed, air-dried overnight, washed and towel-dried.

(b) **Hexane/DCM Ratio** - 1 cm² polyurethane squares were immersed in the following hexane/DCM ratios: 1:0, 7.5:2.5, 1:1, 2.5:7.5 and 0:1. They were allowed to swell for 24 h in the dark, removed and air-dried overnight, and then washed and towel-dried.

(c) **CV Dye Concentration** - Polyurethane squares were immersed in the following CV solutions in distilled water for up to 72 h: 0.00001 M, 0.0001 M and 0.001 M. The squares were then removed from solution, washed and towel-dried.

(d) **CV Dye Immersion Time** - The samples were immersed in 0.001 M CV solution for various dipping times: 0, 0.5, 1, 4, 8, 16, 24, 48, 72 and 96 h. They were removed from solution, washed and towel-dried.

Polymer Samples Prepared for Antibacterial Testing

The following modified polyurethane samples (1 cm²) were prepared for antibacterial testing (Fig. 5.2):

- (a) Control samples were immersed in a 1:1 hexane/DCM swelling solution (24 h, dark conditions).

- (b) Crystal violet-coated samples (CV) were (i) immersed in a 1:1 hexane/DCM swelling solution (24 h, dark conditions), removed, washed and dried, and then (ii) dipped into a 0.001 M CV solution for 72 h, removed, washed and towel-dried.
- (c) Polyurethane-encapsulated ZnO nanoparticles (ZnO) immersed in a 1:1 ratio of hexane/DCM swelling solution containing ZnO nanoparticles (24 h, dark conditions), washed and towel-dried.
- (d) Polyurethane coated with CV and encapsulated with ZnO (CVZnO) were prepared by: (i) immersion in a 1:1 hexane/DCM swelling solution containing ZnO NPs (24 h, dark conditions), followed by (ii) immersion in 0.001 M crystal violet solution for 72 h in the dark, washed and towel-dried.

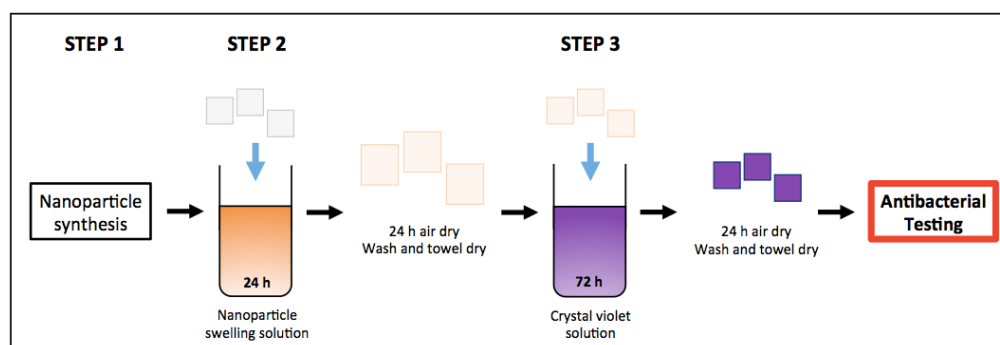


Fig. 5.2 Schematic step-by-step method illustrating the preparation of crystal violet and ZnO incorporated into polyurethane (CVZnO). Squares indicate 1 cm² polymer squares used.

5.2.2.3 Material Characterisation

A Perkin Elmer Fourier transform Lambda 950 UV-vis spectrometer was used to measure the absorption spectra of the modified polyurethane polymers over a wavelength range of 400 – 700 nm. 1 cm² flat polyurethane sheets were immersed in a 0.001 M CV solution for 72 h. They were removed from solution, washed, towel-dried and then

embedded vertically in paraffin blocks. 15 μm thick cross-sections of the polymer were cut using a microtome and mounted on Vectabond (Vecta Laboratories, UK) treated slides for fluorescence imaging. The cross-sections were imaged using a 10x objective light microscope (Olympus UK Ltd., model BH2) with a colour CCD digital camera (Lumenera Inc., model Infinity 1) using Infinity capture software for analysis. The same 15 μm thick cross-sections were used in fluorescence microscopy; they were imaged (10x objective) using a cooled scientific-grade 16-bit digital CCD camera (Princeton Instruments Inc., Model PIXIS 512) operated by Win-Spec software, coupled to an inverted fluorescence microscope (Olympus UK Ltd., Model IMT-2). The fluorescence signal from CV present in the polymer was detected using a bandpass filter centred at 640 nm (Omega Optical Inc., 640DF35) using excitation by a 532 nm laser diode (Thorlabs Inc.).

Inductively coupled plasma-optical emission spectroscopy (ICP-OES) was used to determine the extent of ZnO NPs leaching from the polymer samples. ICP-OES was measured on a Perkin Elmer Optima 2000 DV. ZnO-incorporated samples were immersed in 2 mL deionised water for up to 48 h. The solution was diluted to 5 mL and the concentration of zinc was calculated using a calibration curve determined from solutions containing $[\text{Zn}] = 0, 0.1, 1$ and 10 mg/L .

The infrared absorbance spectra of the modified polymer samples were measured using a Brüker Platinum ATR, within the range $4000 - 400 \text{ cm}^{-1}$ with an accumulation of 16 scans per sample. X-ray photoelectron spectroscopy (XPS) analysis was carried out on the modified polymers using a Thermo Scientific *K-Alpha* spectrometer to classify the different elements present as a function of polymer depth. All binding energies were calibrated to C 1s peak at 284.5 eV. Equilibrium water contact angle measurements were obtained for each type of sample prepared for microbiological investigation, using a FTA 1000 Drop Shape Instrument. The average contact angle measurement over ≥ 10 measurements was

calculated using a droplet of deionised water (~5.0 μL) dispensed by gravity from a gauge 30 needle, with a camera to photograph the samples side on. The data was analysed using FTA32 software.

The stability of crystal violet coated-polyurethane was investigated in phosphate buffered saline (PBS, Dulbecco A) to determine the extent of leaching of the dye (2.5 mL PBS, 37 $^{\circ}\text{C}$) over an extended period of time. The UV-vis absorbance (596 nm, Pharmacia Biotech Ultrospec 2000) of PBS was measured periodically to monitor any leaching of the dye from the modified polymer into the surrounding solution. The concentration of CV released into PBS was determined by comparing the absorbance of the solution at 596 nm with a CV dye calibration curve. The extent of leaching of ZnO NPs from the modified polymer was tested in a similar fashion, where the UV-vis absorbance of the ZnO NP suspension was compared to the PBS solution containing polymer-encapsulated ZnO sample up to 48 h at room temperature.

5.2.3 Antibacterial Activity

5.2.3.1 Microbiology Assay

The antibacterial activity of the following polymer samples were tested against *S. aureus* 8325-4 and *E. coli* ATCC 25922 as representative Gram-positive and Gram-negative bacteria, respectively: (a) solvent treated (control), (b) CV-coated polyurethane (CV), (c) polyurethane-encapsulated ZnO (ZnO) and (d) polyurethane-encapsulated CV and ZnO (CVZnO). *S. aureus* 8325-4 and *E. coli* ATCC 25922 were stored at -70 $^{\circ}\text{C}$ in Brain-Heart-Infusion broth (BHI, Oxoid) containing 20% (v/v) glycerol and propagated onto Mannitol Salt agar (MSA, Oxoid) in the case of *S. aureus* or MacConkey agar (MAC, Oxoid) in the case of *E. coli* for a maximum of 2 subcultures at 2 week intervals.

BHI broth was inoculated with 1 bacterial colony and cultured in air with shaking (37 °C; 18 h; 200 rpm). The bacterial pellet was recovered by centrifugation, (20 °C, 2867.2 g, 5 min), washed in PBS (10 mL), centrifuged again to recover the pellet (20 °C, 2867.2 g, 5 min), and then the bacteria were re-suspended in PBS (10 mL). The washed suspension was diluted 1000-fold to obtain an inoculum of $\sim 10^6$ cfu/mL. In each experiment, the inoculum was confirmed by plating 10-fold serial dilutions on agar for viable counts. A minimum of duplicates of each polymer sample type were inoculated with 25 μ L of the inoculum and covered with a sterile cover slip (2.2 cm²). The samples were irradiated for up to 4 h using a white light source (General Electric 28 W Watt Miser™ T5 2D compact fluorescent lamp) emitting an average light of 6600 \pm 990 lux at a distance of 25 cm from the samples. A further set of samples (minimum of duplicates) was incubated in the dark for the same duration as the irradiated samples.

Following incubation, the inoculated samples and cover slips were added to PBS (450 μ L) and vortexed (20 s). The neat suspension and 10-fold serial dilutions were plated on agar for viable counts and incubated aerobically at 37 °C for 48 h (*S. aureus*) or 24 h (*E. coli*).

5.2.3.2 Statistical Significance

Each experiment contained a minimum of 2 technical replicates and the experiment was repeated three times. The statistical significance of the following comparisons in both the light and dark was analysed using the Mann-Whitney U test: (i) control polymer vs. inoculum; (ii) CV or ZnO alone vs. control polymer; (iii) CVZnO vs. CV alone.

5.2.3.3 Hydrogen Peroxide and Singlet Oxygen Detection

Specific hydrogen peroxide and singlet oxygen inhibitors were used against *E. coli* ATCC 25922 to understand the mechanism operating in the

photobactericidal activity of the CVZnO polymers and in the dark. Bovine catalase, bovine serum albumin (BSA) and L-histidine (Sigma-Aldrich, UK) were filter sterilised using a 0.2 μm syringe filter (VWR, UK). Catalase (220 U mL^{-1} in PBS) was used to eliminate hydrogen peroxide in radical formation, and BSA (0.03% in water) and L-histidine (1 mM in PBS) were used as singlet oxygen quenchers. The enzyme/ROS inhibitors were added to the *E. coli* suspension and exposed to the polymer using the protocol described above.

5.3 Results and Discussion

5.3.1 ZnO Nanoparticle Synthesis and Characterisation

ZnO NPs were synthesised *via* a two-step method adapted from Park *et al.*³⁶ A reaction between zinc chloride and sodium oleate produced zinc-oleate precursors, followed by the formation of nanoparticles using a thermal decomposition method in a mixture of solvents at 320°C. The nanoparticles were finally centrifuged, re-suspended in hexane and characterised using TEM and EDX (Fig. 5.3). They were prepared for TEM by drop-casting the nanoparticle suspension (in hexane) onto a gold TEM grid with a holey carbon film (Agar Scientific, UK) and left to dry before analysis. The TEM images displayed monodisperse ZnO NPs (18.3 ± 4.9 nm in average diameter size) forming anisotropic hexagonal and triangular shaped particles. EDX analysis showed the elemental composition of ZnO NPs, demonstrating ratios well within error limits.

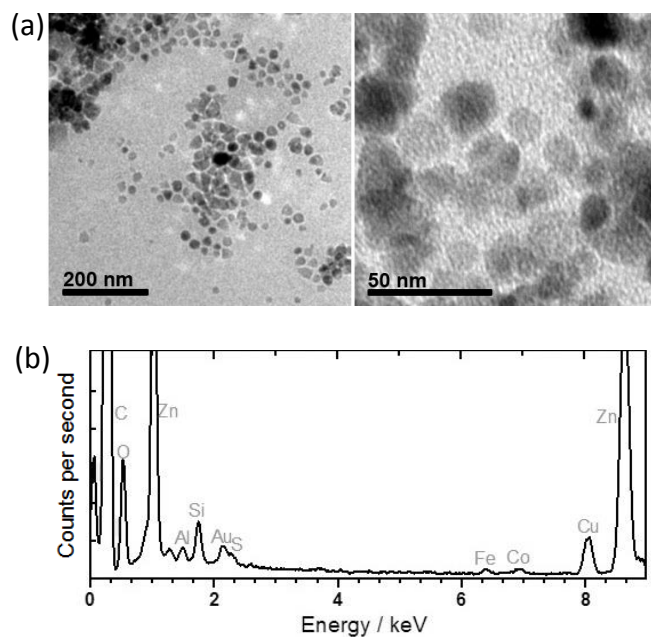


Fig. 5.3 (a) TEM images and (b) EDX spectrum of ~18 nm ZnO nanoparticles.

5.3.2 Preparation and Characterisation of Polymer Samples

Hexane alone is unable to swell polyurethane samples, therefore another organic solvent was required to swell-encapsulate the nanoparticles into the polymer matrix. 1 cm² polyurethane samples were immersed into different organic solvent solutions made up at a 1:1 ratio with hexane. Hexane/acetone swelled the polymer 30% more than its original size, however, hexane/DCM swelled the polymer up to 42% more than its original size. Hexane/THF swelled the polymer the most (72%) but after the polymer was left to shrink and dry overnight it became distorted and curled around the edges. As hexane/DCM swelled polyurethane effectively without deforming its size and shape, various ratios of this solvent mixture were tested to optimise the 'swell-encapsulation-shrink' method. The following hexane/DCM ratios were used: 1:0, 7.5:2.5, 1:1, 2.5:7.5 and 0:1. 100% hexane did not swell the polymer at all and 100% DCM resulted in a very distorted polymer. 7.5:2.5 ratio of hexane/DCM did not swell the polymer as much as 1:1, and a 2.5:7.5 hexane/DCM solution resulted in distorted polymer squares which were curled at the edges. To carry out

reproducible antibacterial testing on the samples, it is essential that all 1 cm² polymer squares return back to their original size and shape after the swelling process. Therefore a 1:1 hexane/DCM ratio was used to swell-encapsulate the NPs into the polymer.

The polymer squares were also immersed in different concentrations of CV dye: 0.00001 M, 0.0001 M and 0.001 M. UV-vis absorption spectroscopy was used to determine the best concentration of CV to use. As shown in Fig. 5.4, all CV-coated polymer samples exhibited an absorption peak for CV at $\lambda = \sim 590$ nm and a smaller shoulder peak at $\lambda = \sim 548$ nm. As the concentration of the dye increased to 0.001 M, there was a greater uptake of the dye. Additionally, the absorbance values did not directly scale linearly with dye concentration, implying that some dimerisation has occurred. To further optimise the polymer system, the samples were immersed in 0.001 M CV solutions for various immersion times for up to 96 h (Fig. 5.5). An immersion time of 72 h was optimal as it allowed an even colouration of the polymer without absorbing too much of the dye.

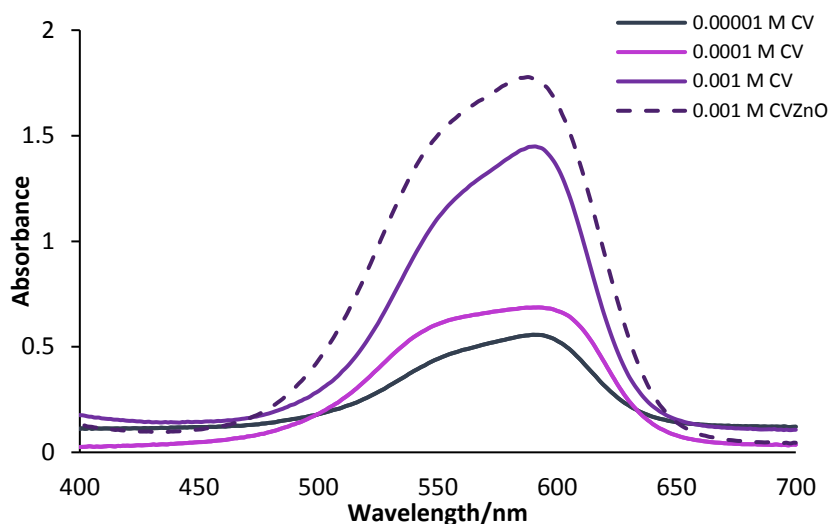


Fig. 5.4 UV-vis absorbance spectra of crystal violet-coated polyurethane (CV) prepared by dipping in a CV solution for 72 h at the following concentrations: 0.00001 M, 0.0001 M and 0.001 M. Spectrum for crystal violet and ZnO incorporated into polyurethane (CVZnO) sample is also shown, prepared by immersing in a 0.001 M CV solution (measured in 400 – 700 nm range).

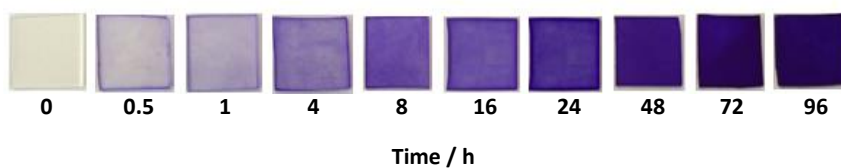


Fig. 5.5 1 cm² polymer samples prepared by immersion in 0.001 M crystal violet solution for increasing lengths of time (up to 96 h).

A polymer sample immersed in 0.001 M CV solution for 72 h was analysed using a light microscope attached to a CCD camera to determine the efficiency of dye uptake and distribution within the polymer (Fig. 5.6). Fig. 5.6(a) shows that the dye diffuses throughout the polymer bulk with a greater uptake towards the edges of the sample. It also shows that the polymer matrix contains many straight ridges and scattered ‘spots’. The same polymer section was analysed using fluorescence microscopy, shown in false colour (Fig. 5.6(b)). The false colour scale corresponds to a low fluorescence (shown in black) to a high fluorescence (shown in white). The fluorescence measurements also confirmed that the dye diffuses throughout the polymer bulk but is more concentrated at the surface.

There is a stronger fluorescence at the surface and inside the ‘spots’ located within the polymer substrate, where the dye has possibly aggregated within the pores.

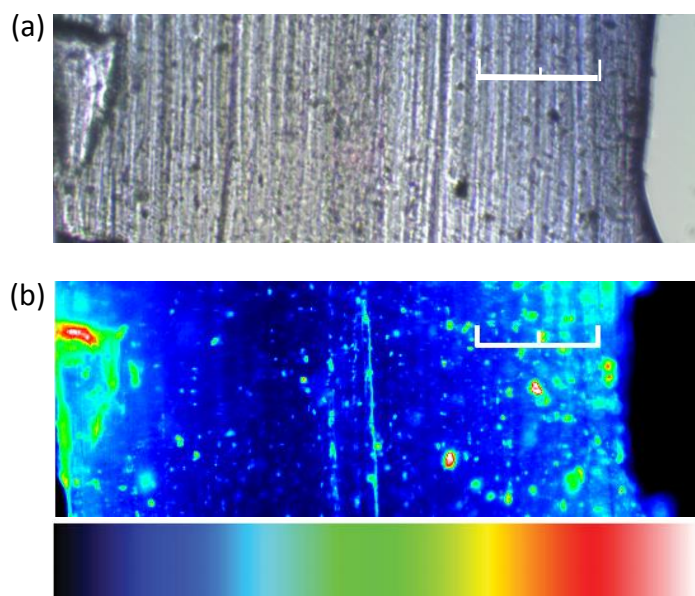


Fig. 5.6 (a) An image of a 15 μm thick crystal violet-coated polyurethane section prepared by immersing the polymer in a 0.001 M crystal violet solution for 72 h. The image was recorded using a 10x objective (scale bar corresponds to 100 μm). The actual thickness of the polymer sample is 0.8 mm. (b) A CCD false coloured fluorescence microscopy image of the same polymer section shown in (a). The polymer sample is shown on the left hand side of the image, where the black part of the image represents the background (no fluorescence). There is a fluorescence intensity scale, increasing from black (background/no fluorescence) to white (maximum fluorescence). The image resolution is 512 x 512 pixels and corresponds to 557 x 557 μm (100 μm scale bar).

The amount of CV released from CV-coated polyurethane was measured using UV-vis absorption spectroscopy. The samples were immersed in a pre-heated solution of PBS (37 $^{\circ}\text{C}$) for up to 360 h. The concentration of CV dye leached from the sample was compared to the optical density of the surrounding PBS solution with a CV calibration curve. Fig. 5.7 shows that a small amount of dye leaches into the solution initially, which then plateaus rapidly over time. Overall, the leaching concentrations were at the

detection limit of the spectrometer and remained below 1.5×10^{-6} M after 360 h. Temperatures of 37 °C were used as these novel materials are potentially for use in medical devices. The amount of dye that leached from the polymer was minimal at 37 °C, thus it is expected that at room temperature (appropriate if these materials were used for hospital surfaces), it would be even less significant. A major disadvantage of PDT is the ability of the photosensitiser to localise at high concentrations within the body or onto the skin.³⁷ For example, swelling, sunburn and blistering can result from the unwanted accumulation of a photosensitiser to the skin and eyes if the patient is exposed to bright light for several days after treatment.³⁸ Thus, this would not be an issue for CV-coated polyurethane as a potential material for invasive devices as it demonstrates minimal amounts of leaching.

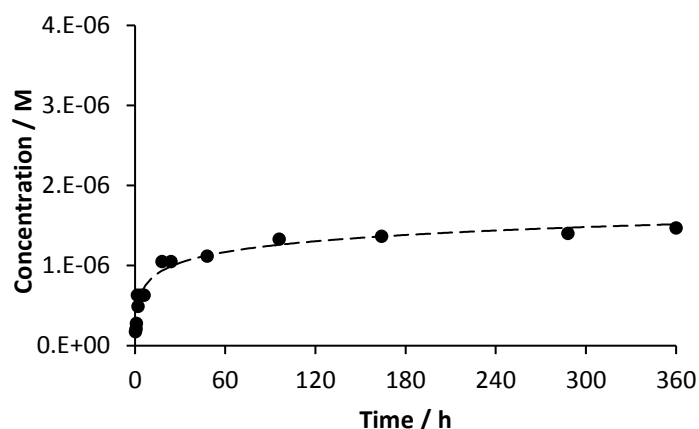


Fig. 5.7 Leaching of dye from crystal violet-coated polyurethane (0.001 M) in PBS solution at 37 °C measured as a function of time.

The two-step 'swell-encapsulation-shrink' method was used to incorporate ZnO NPs into the polymer substrate and then coat the polymer with CV dye (Fig. 5.2). It is a simple method that enables the nanoparticles to diffuse throughout the polymer bulk without the need for covalent attachment. ICP-OES analysis was used to determine whether any zinc species leached

from the modified polymer samples when the films were immersed in water for up to 48 h. The results showed that only 0.132 ± 0.0002 mg/L of zinc leached from the polymer after 2 h and 1.696 ± 0.017 mg/L after 48 h. Although the nanoparticles are non-toxic, they are well incorporated into the polymer with minimal amounts of leaching into surrounding solutions or possibly transferred by human contact.

CVZnO was analysed using UV-vis spectroscopy (Fig. 5.4). When ZnO NPs were added with CV to the polymer, there was an increase in the absorption maxima of the main absorption peak at ~ 590 nm and shoulder peak at 548 nm. There was also a minor blue (hypsochromic) shift as the main absorption peak for CV shifted to ~ 586 nm and the peaks became broader. Thus, the presence of the ZnO NPs affects dye uptake, since spectral features such as peak shape, position and intensity differ from CV-coated polyurethane. The addition of ZnO NPs alone affects the colour of the polymer prior to adding CV. This is because the nanoparticle suspension is slightly yellow in colour due to the surfactants present in the solution. Therefore, CVZnO samples are slightly darker than CV-coated polyurethane.

ATR-FTIR spectra (Fig. 5.8) did not show any significant changes between the modified and untreated polyurethane samples. This can be attributed to the strong absorbance bands of the polymer and due to the low concentrations of dye and nanoparticles present in the samples. Nevertheless, this confirms that the “swell-encapsulation-shrink” method does not affect the polyurethane substrate in terms of a recognisable chemical change when incorporating the dye or ZnO NPs. Water contact angle measurements exhibited a negligible difference between material hydrophobicity of untreated and modified polyurethane samples, varying in contact angle $\pm 10^\circ$.

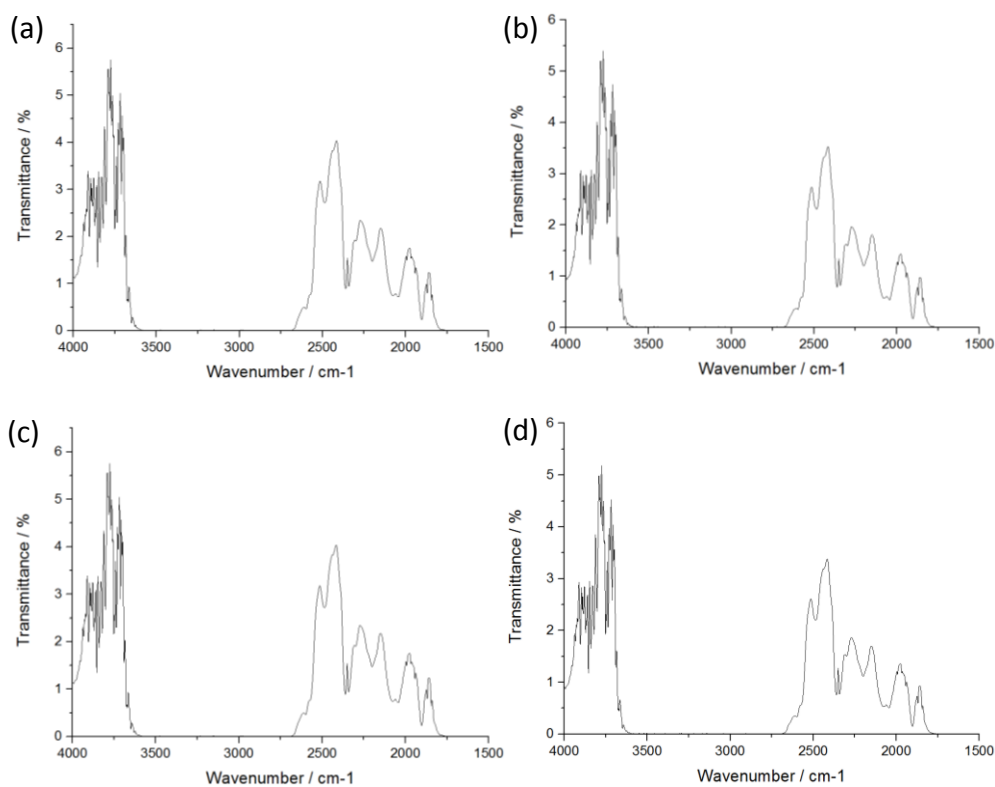


Fig. 5.8 ATR spectrum of (a) solvent treated (control), polyurethane encapsulated with (b) ZnO, (c) crystal violet, and (d) crystal violet and ZnO.

XPS was used to determine the efficacy of the ‘swell-encapsulation-shrink’ method for incorporating ZnO NPs into the polymer (Fig. 5.9). From both the control and ZnO-incorporated polymer, peaks attributed to the presence of carbon 1s (284.5 eV), nitrogen 1s (399.5 eV) and oxygen 1s (531.9 eV) on the surface were observed, with no significant difference in percentage element composition between the samples (data not shown). XPS depth profile analysis for all samples demonstrated no change in carbon and nitrogen composition, but a decrease in oxygen content with polymer depth. Zn (2p) was detected on the surface of ZnO-incorporated polyurethane (Fig. 5.9(a)) and an even higher zinc content (1021.5 eV) was demonstrated within the bulk in comparison to the surface (Fig. 5.9(b) and (c)).

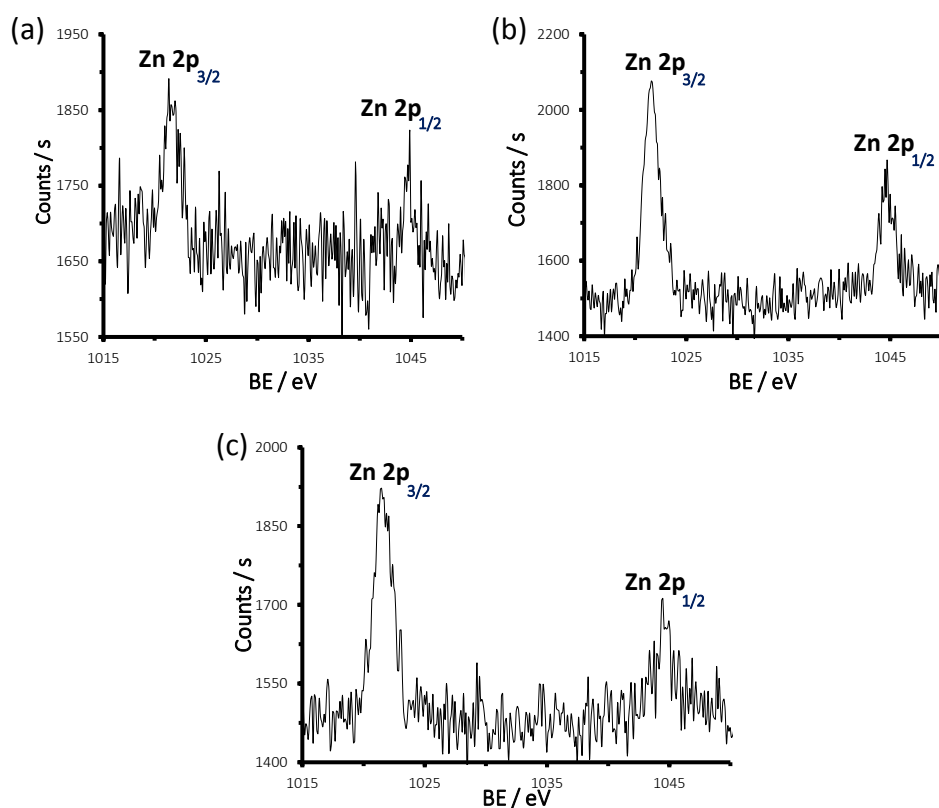


Fig. 5.9 Zn 2p region XPS spectra for: (a) ZnO-incorporated surface; (b) ZnO-incorporated polymer sputtered 50 s; and (c) ZnO-incorporated polymer sputtered 100 s.

5.3.3 Antibacterial Activity

The photobactericidal activity of the following modified polyurethane samples was tested against *S. aureus* 8325-4 and *E. coli* ATCC 25922 as representative Gram-positive and Gram-negative nosocomial pathogens, respectively: (i) solvent treated (control), (ii) crystal violet-coated (CV), (iii) encapsulated with ZnO NPs (ZnO), and (iv) encapsulated with CV and ZnO (CVZnO). The samples were exposed to a white light source for up to 4 h, mimicking the lighting in a typical UK hospital ward (~6600 lux) and a further set of samples were incubated in the dark for the same incubation time.

Fig. 5.10 displays the lethal photosensitisation of *S. aureus* 8325-4 following 1 or 2 h of white light exposure emitting an average light

intensity of 6600 ± 990 lux at a distance of 25 cm from the modified samples. After 1 h of incubation in the dark (Fig. 5.10(a)), none of the control, CV or ZnO-coated polymers caused any significant kill of *S. aureus* 8325-4, whereas CVZnO demonstrated a statistically significant reduction in bacterial numbers (~ 1.5 log; $P = 0.002$). Following 1 h of white light exposure, there was no bactericidal activity observed from the control or ZnO sample. However, CV-coated polyurethane resulted in ~ 2 log reduction in bacterial numbers ($P = 0.002$). In addition to this, CVZnO resulted in the greatest kill, reducing *S. aureus* 8325-4 numbers to below the detection limit (≥ 4 log; $P = 0.002$).

Following 2 h of exposure in the dark (Fig. 5.10(b)), control and ZnO-coated polyurethane did not cause any significant kill of *S. aureus* 8325-4, whereas CV alone caused ~ 1.4 log reduction in bacterial numbers. Furthermore, CVZnO demonstrated statistically significant bactericidal activity (≥ 4 log; $P = 0.002$). By exposing the samples to white light for 2 h, both CV and CVZnO resulted in highly significant bactericidal activity (≥ 4 log; $P = 0.002$).

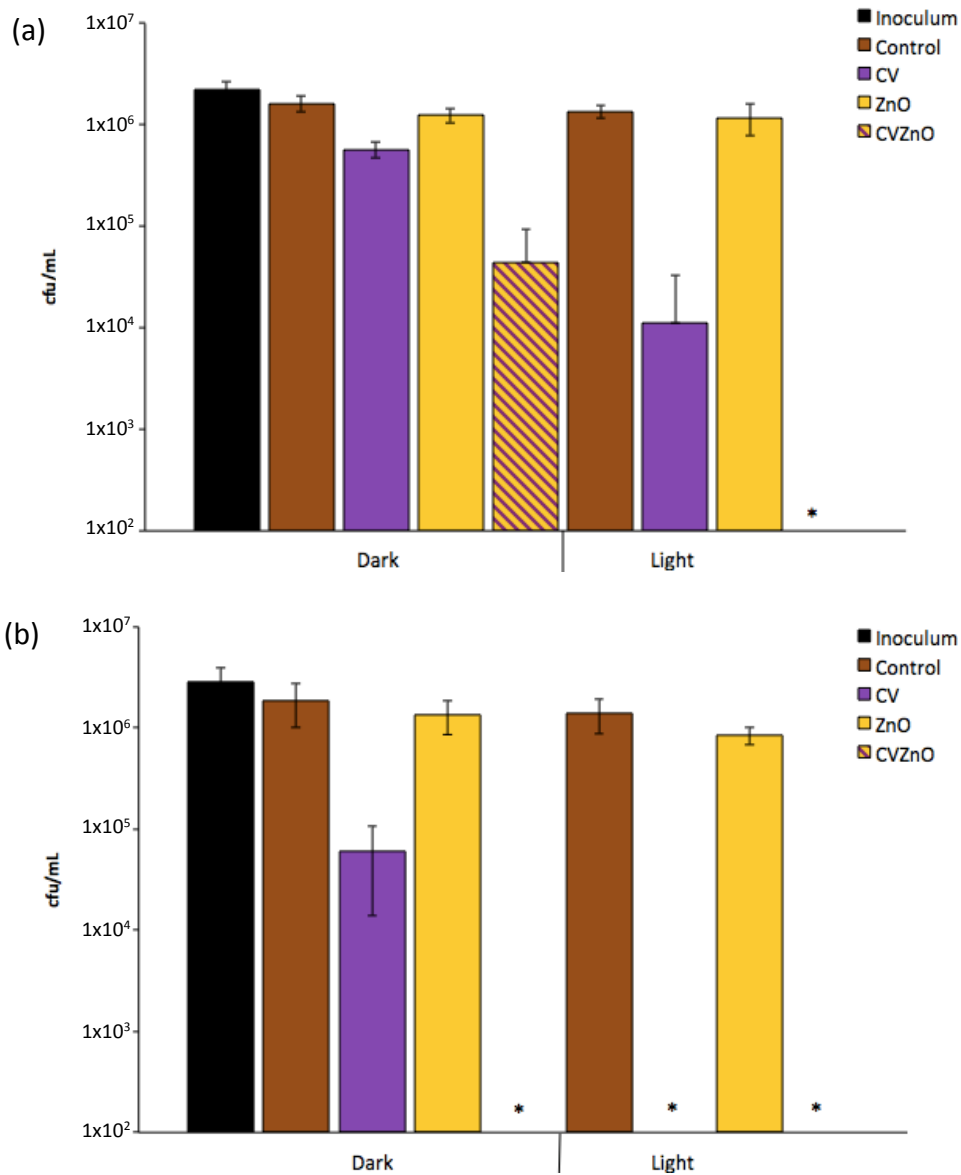


Fig. 5.10 Viable counts of *S. aureus* 8325-4 after incubation on modified polyurethane samples incubated at 20 °C in the dark and exposed to white light illumination for: (a) 1 h and (b) 2 h. White light source emitted an average light intensity of 6600 ± 990 lux at a distance of 25 cm from the samples. * indicates bacterial numbers reduced to below the detection limit of 100 colony forming units/mL (cfu/mL).

The photobactericidal activity of the modified polyurethane samples was also tested against *E. coli* ATCC 25922 under the same conditions but for an extended period of time. As shown in Fig. 5.11(a) none of the samples demonstrated any significant kill of *E. coli* ATCC 25922 after 2 h of incubation in the dark. However, a 2 h exposure to white light induced ~1

log reduction in bacterial numbers with CV alone, whereas the control and ZnO samples did not cause any significant kill. The combination of CV and ZnO in the polymer enhanced the bactericidal activity demonstrated by CV alone, resulting in ~2.5 log reduction of *E. coli* ATCC 25922 (P = 0.004).

By increasing the incubation time to 4 h in the dark (Fig. 5.11(a)), the control and ZnO samples still did not display significant kill of *E. coli* ATCC 25922, whereas CV alone caused ~1.3 log reduction. Most significantly, CVZnO exhibited lethal photobactericidal activity against *E. coli* ATCC 25922 by reducing bacterial numbers to below the detection limit (≥ 4 log; P = 0.002). Following 4 h of white light exposure, both CV and CVZnO caused ≥ 4 log reduction in the numbers of *E. coli* ATCC 25922 (P = 0.002).

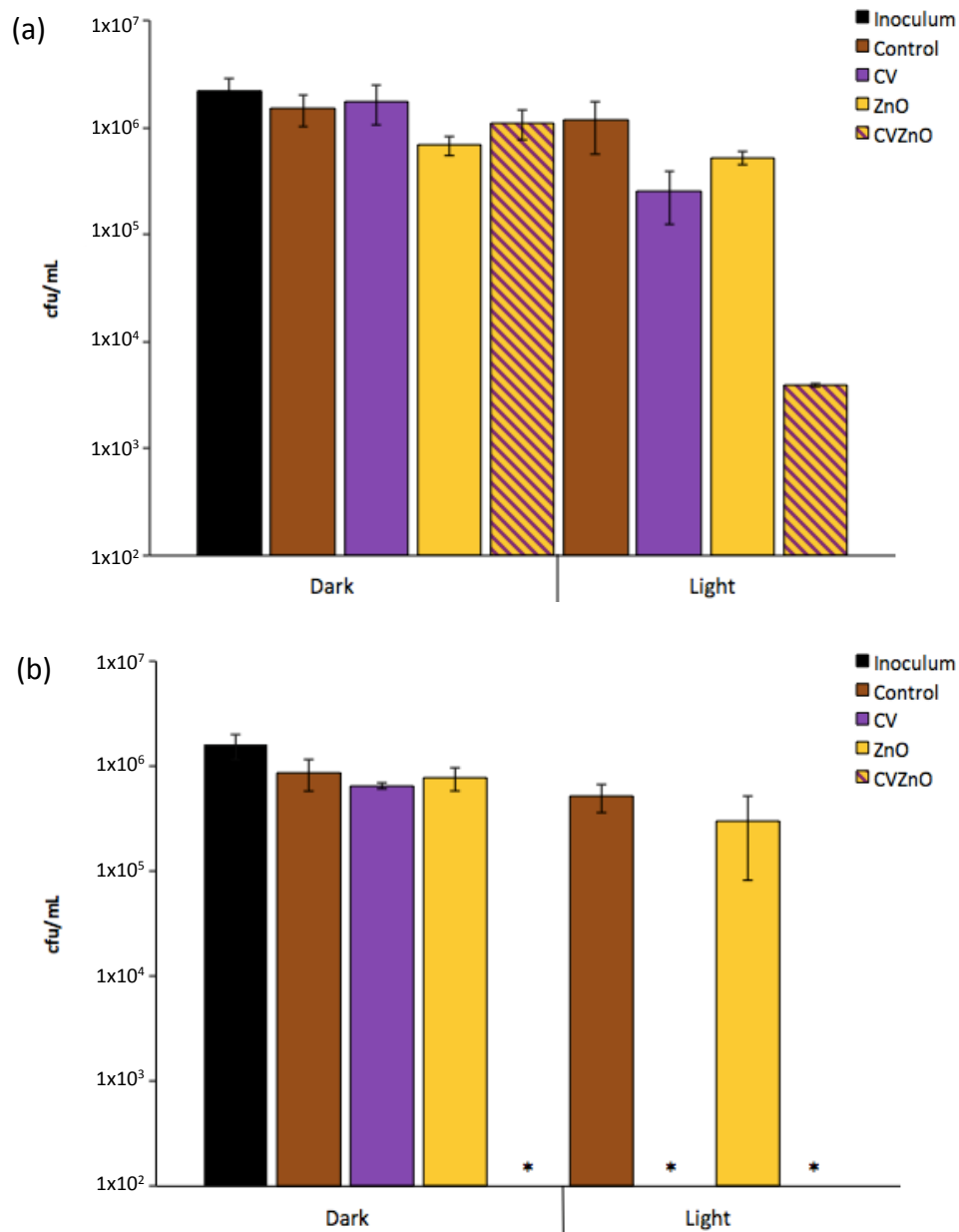


Fig. 5.11 Viable counts of *E. coli* ATCC 25922 after incubation on modified polyurethane samples incubated at 20 °C in the dark and exposed to white light illumination for: (a) 2 h and (b) 4 h. White light source emitted an average light intensity of 6600 ± 990 lux at a distance of 25 cm from the samples. * indicates bacterial numbers reduced to below the detection limit of 100 colony forming units/mL (cfu/mL).

Table 5.2 Summary of the antibacterial activity of polyurethane coated with CV and encapsulated with CVZnO in the dark and following white light incubation (6600 ± 900 lux) against *S. aureus* 8325-4 and *E. coli* ATCC 25922. The bactericidal activity of control polyurethane and coated with ZnO were not included as they did not demonstrate any significant activity. Bacterial reduction is given in log form.

Bacterial strain	CV dark	CV white light	CVZnO dark	CVZnO white light
<i>S. aureus</i> 8325-4	No kill (1 h) 1.4 log (2 h)	2 log (1 h) ≥ 4 log (2 h)	1.5 log (1 h) ≥ 4 log (2 h)	≥ 4 log (1 h) ≥ 4 log (2 h)
<i>E. coli</i> ATCC 25922	No kill (2 h) 1.3 log (4 h)	1 log (2 h) ≥ 4 log (4 h)	No kill (2 h) ≥ 4 log (4 h)	2.5 log (2 h) ≥ 4 log (4 h)

Oleic acid-capped ZnO NPs (~18 nm) have been synthesised and incorporated into medical grade polyurethane sheets. These modified polymers have been coated with CV dye and their antibacterial activity has been examined against two hospital pathogens; *S. aureus* 8325-4 and *E. coli* ATCC 25922. CVZnO has shown exceptional bactericidal effects against both bacteria in the light, but more significantly, considerable dark kill has been observed within only 4 h. Thus, these polymeric surfaces have the potential of reducing bacteria in a clinical environment where lighting conditions are not optimal. Previous studies using CV and ZnO nanoparticles (as shown in Table 5.1) have demonstrated a lesser bactericidal effect against *E. coli* ATCC 25922.^{22,23,28-30} For example, CV and ZnO coated onto silicone has demonstrated lethal activity using a higher white light intensity of ~11,500 lux after 6 h and only exhibits ~0.5 log reduction of *E. coli* ATCC 25922 after 4 h in the dark.³⁰ Moreover, silicone samples containing CV combined with MB and/or 2 nm Au NPs also do not display the same bactericidal activity as this CVZnO combination.^{23,28} This could be due to the fact that these ZnO NPs are more effective at enhancing the bactericidal effect of the dye. On the other hand, it could be due to the polymer itself; as shown in Chapter 3 with Cu NPs, NP-incorporated polyurethane is more effective at reducing bacteria than NP-incorporated silicone.

The exact mechanism of the CVZnO polymer materials is not yet fully understood. XPS depth profile data show that the ZnO NPs are well-incorporated into the polyurethane matrix as well as adsorbed onto the surface. Leaching experiments show that the dye and the NPs exhibit minimal leaching over an extended period of time. It is possible that the nanoparticles are leaching at a concentration that causes an enhanced bactericidal effect of the dye, as it should be noted that the NPs have no activity alone. However, this does imply that the NPs are not leaching at a concentration significant enough to induce any bactericidal activity on their own. The ZnO NPs increase the antibacterial activity of CV in the light and in the dark compared to CV alone; enhancing any light-activated and intrinsic (dark) bactericidal effects of the dye itself. Therefore, this suggests that the mechanism of CVZnO operates *via* a Type I and/or Type II photochemical pathway.

The two possible mechanisms for the photosensitised generation of ROS include electron transfer (Type I) and energy transfer from the photosensitiser triplet state to molecular oxygen to form singlet oxygen (Type II). To investigate this further, quenchers of Type I and Type II mechanisms were added to the antibacterial testing protocol to see their effects on the bactericidal results obtained above in Fig. 5.10 and 5.11. A H₂O₂ scavenger (catalase, 220 U mL⁻¹) and quenchers of ¹O₂ (BSA, 0.03% and L-histidine, 1 mM) were used in the microbiological investigation against *E. coli* ATCC 25922. The concentration of these inhibitors is based on other studies reported in the literature.^{31,39,40} As described in Chapter 3, BSA acts as an organic contaminant to mimic a 'real-world' clinical environment (e.g. from hand sebum) as well as a quencher of singlet oxygen. It also contains tryptophan which reacts readily with singlet oxygen, similar to other aromatic amino acids such as L-histidine.^{41,42,43} Fig. 5.12 shows the bactericidal activity of control polymer, CV, and CVZnO-incorporated samples against *E. coli* ATCC 25922 using the same conditions described above with the addition of catalase, BSA and L-histidine. An

experiment labelled 'control' (as shown in Fig. 5.13) has also been carried out to show the effects of adding each variable separately to the experiment. ZnO-incorporated polyurethane was not tested in these experiments as it did not demonstrate any significant kill in the previous results (Fig. 5.10 and 5.11).

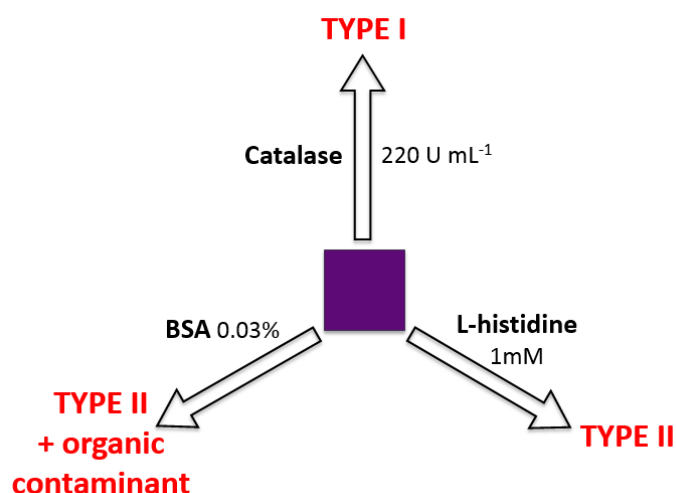


Fig. 5.12 Radical species and singlet oxygen quenchers/inhibitors of Type I and II photochemical pathways used in this investigation (BSA: bovine serum albumin).

Fig. 5.13(a) illustrates the lethal photosensitisation of the polymer samples against *E. coli* ATCC 25922 when exposed to white light for 2 h. The addition of catalase, BSA and L-histidine to the bacterial suspension did not affect the bacterial count for the control polymer sample. Conversely, CV-coated polymer only demonstrated ~0.8 log reduction in the presence of catalase and ~1 log reduction when BSA was added, compared to ~1.5 log reduction of *E. coli* ATCC 25922 when no quencher or scavenger was present ($P = 0.002$). Additionally, the addition of L-histidine to the bacteria resulted no significant bactericidal activity of CV ($P = 0.002$).

For CVZnO samples, the bacterial count was reduced by ~3 log when no quencher/scavenger was added to the system following 2 h white light

activation. However, the reduction in bacterial numbers decreased to ~0.5 log, ~1 log and ~2 log with the addition of L-histidine, BSA and catalase, respectively. These results show that the singlet oxygen scavengers have affected the lethal activity of CVZnO more than catalase, however, all additives have negatively impacted the antibacterial activity observed in the control experiment. These samples were also tested with and without the quenchers in the dark for 2 h and did not exhibit any significant kill (data not shown).

The samples were then tested against *E. coli* ATCC 25922 for 4 h in the dark with the addition of catalase, BSA or L-histidine (Fig. 5.13(b)). Within this time, neither the control nor CV samples showed any significant bactericidal activity. In the control experiment (without any additives), CVZnO demonstrated ≥ 4 log reduction ($P = 0.002$) in the numbers of *E. coli* ATCC 25922. However, with the addition of catalase or BSA, the antibacterial activity of CVZnO decreased by ~2.5 log, and no bacterial kill was observed when L-histidine was added to the bacterial suspension. Following 4 h of white light activation, the antibacterial activity of the samples did not change between the control, catalase, BSA and L-histidine experiments (data not shown).

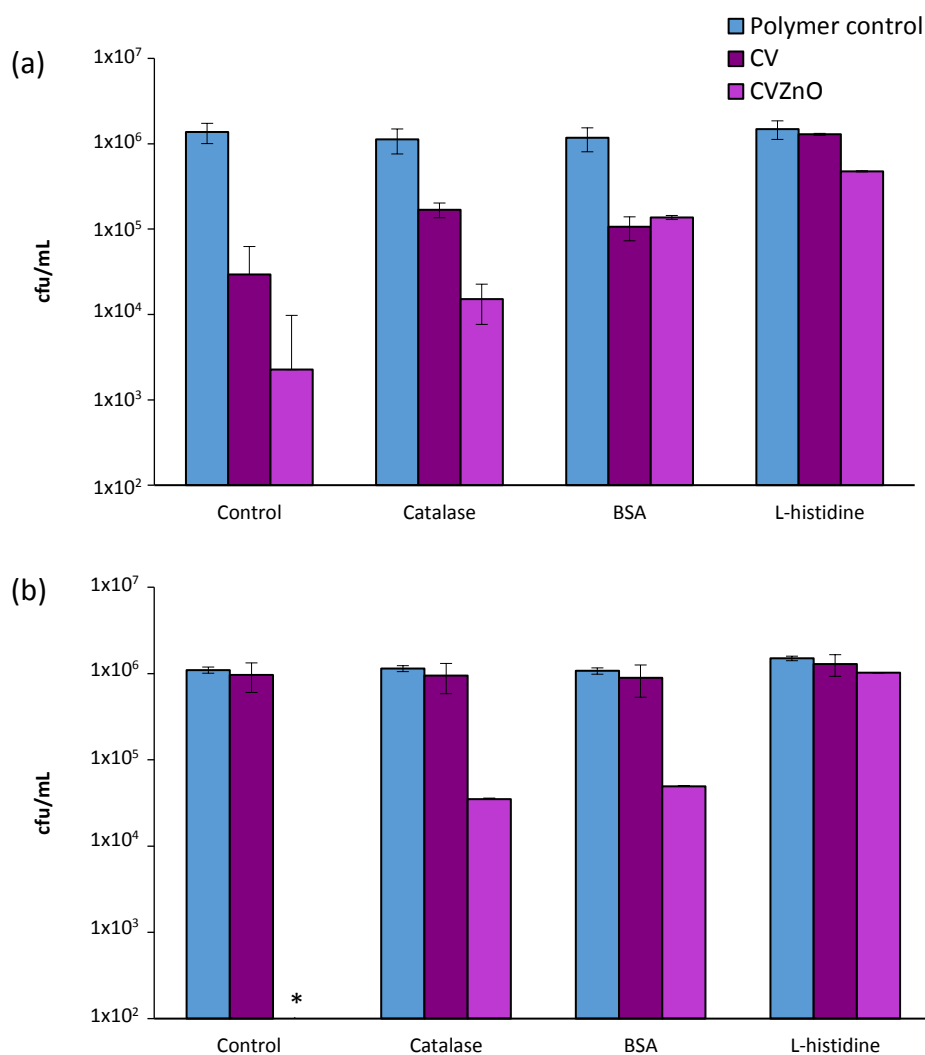


Fig. 5.13 (a) Viable counts of *E. coli* ATCC 25922 following 2 h of white light illumination on modified polyurethane samples for a control, catalase, bovine serum albumin (BSA) and L-histidine experiment. The white light source emitted an average light intensity of 6600 ± 990 lux at a distance of 25 cm from the samples. * indicates that the bacterial numbers were reduced to below the detection limit of 100 colony forming units/mL (cfu/mL). (b) Viable counts of *E. coli* ATCC 25922 following 4 h incubation in the dark on modified polyurethane samples for a control, catalase, BSA and L-histidine experiment.

The results clearly show that all scavengers effectively reduce the antibacterial activity of CV-coated polyurethane in the light and CVZnO in the light and dark. This suggests that both Type I and Type II mechanisms are occurring in the CV and CVZnO polymeric system. The addition of catalase reduces the antibacterial effectiveness of the CVZnO system,

which suggests that any production of H_2O_2 that would normally damage the bacteria has been 'deactivated' by conversion to H_2O and O_2 using catalase. This process also prevents the formation of hydroxyl species formed from the Fenton reaction. Catalase is able to react with singlet oxygen; however, at the low concentrations used in this investigation it is not possible. Therefore, the Type I mechanism is operating in the bactericidal activity of CVZnO in the light and dark. It is possible that CV is adsorbed or is in close proximity to the surface of the ZnO NPs, which allows electron transfer to or from its excited singlet state through interaction with the conduction band of the semiconductor (ZnO). This has been suggested for the interaction between ethyl ester of fluorescein (FLEt) and colloidal TiO_2 particles under visible light excitation.⁴⁴ A Type I electron transfer mechanism will produce more ROS (superoxide anion radicals in particular), which can dismutate to form H_2O_2 that can diffuse to the bacterial cell. H_2O_2 can also decompose *via* the Fenton reaction to produce cytotoxic hydroxyl radicals.⁴⁵

The addition of BSA and L-histidine to the bacterial suspension has also provided evidence to suggest that a Type II mechanism is occurring within this dye and nanoparticle combination. When the bacterium is in contact with CVZnO, BSA significantly reduces the kill (more so in the dark). Additionally, BSA acts as an organic contaminant during the experiment. The results indicate that in a real clinical setting, the bacterial kill could be suppressed in the presence of organic impurities, such as skin oils from patient or staff contact. Moreover, the addition of L-histidine to the experiment shows an even greater reduction in bactericidal activity in both the light and dark. These quenchers have inhibited singlet oxygen production, indicating that singlet oxygen contributes to the bactericidal activity of CVZnO (i.e. a Type II mechanism). By adding L-histidine to the bacterium, singlet oxygen is able to chemically react with the imidazole ring of the quencher to produce oxidised products instead.⁴⁶ Therefore, the data strongly suggests that there is a synergistic enhancement in

bactericidal activity of CV combined with ZnO NPs and both Type I and Type II mechanisms are occurring together.

Surprisingly, the inhibitors have a greater effect on the antibacterial activity of CVZnO in the dark compared to the photoactivated experiment. This suggests that both mechanisms also occur in the dark, where the NPs are able to significantly increase the antibacterial activity of CV without white light activation. This could be due to surface defects on the ZnO NPs which allow CV to further produce ROS. Additionally, the encapsulation of the NPs could be responsible for a greater uptake of the dye (as shown by UV-vis absorption spectra; Fig. 5.4), which in turn allows a greater production of radical species and singlet oxygen. However, it should be noted that CV-coated polymers have been pre-treated with 1:1 hexane/DCM prior to coating with the dye so the organic solvents are not responsible for this change. Although the results show that both mechanisms play a pivotal role in killing the bacterium, there is evidence to suggest that the Type II process dominates in inducing bacterial cell damage (as shown by adding BSA and L-histidine). There are many studies that have supported that a Type II process is more responsible for photo-initiated cell death,^{37,47-49} as some cells *in vivo* are partially protected against the effects of PDT by scavengers such as L-histidine, and some skin cells are rather resistant to PDT in the absence of molecular oxygen.⁵⁰⁻⁵²

For conventional applications of a photosensitiser *in vivo*, it is vital that the photosensitiser exhibits minimal dark toxicity and negligible cytotoxicity in the absence of light.⁴⁷ This is so that when the photosensitiser is introduced into the body and accumulates in diseased tissue it does not cause any adverse side effects to the body when the treatment is not undergoing. However, this is not a concern for the purpose of antibacterial surface coatings. In fact, any dark kill observed from these polymer samples is especially beneficial in hospital environments with dim or no lighting. As described above, the polymeric materials allow CV to produce

singlet oxygen as its molecular rotor is restricted. In an aqueous solution of CV (a low viscosity environment) singlet oxygen is not produced.

5.4 Conclusion

In this chapter, oleate-capped ZnO NPs have been synthesised *via* a thermal decomposition method developed from Park *et al*, forming monodisperse nanoparticles with an average diameter size of 18 nm. They were suspended in a 1:1 ratio of hexane/DCM and incorporated into 1 cm² flat polyurethane sheets. They were then dip-coated into an aqueous solution of CV (0.001 M) to produce CVZnO polymer samples. Fluorescence microscopy showed that the dye was incorporated throughout the polymer matrix but resided mostly at the polymer surface and XPS data confirmed that the NPs were also incorporated throughout the polymer bulk and incorporated onto the surface. CV-coated polyurethane exhibited insignificant leaching of the dye into the surrounding PBS solution. At certain concentrations CV is non-toxic to mammalian cells and is widely used medically and in dentistry. It has antibacterial and antifungal properties and was previously used as a topical antiseptic.^{32,33} It is still listed by the World Health Organisation despite being replaced by newer drugs in medical treatment.³¹

For the first time, CV and ZnO NPs have been incorporated into polyurethane and tested for antibacterial activity against *E. coli* and *S. aureus* as representative Gram-negative and Gram-positive bacteria. The results showed a clear photobactericidal response; with CVZnO reducing numbers of *S. aureus* 8325-4 and *E. coli* ATCC 25922 to below the detection limit (≥ 4 log reduction) within only 1 h and 4 h, respectively. More significantly, CVZnO was able to reduce both bacteria without any white light activation within only 2 h (in the case of *S. aureus* 8325-4) and 4 h (in the case of *E. coli* ATCC 25922). This is, to our knowledge, the best dark kill

achieved by any photosensitiser and/or nanoparticle combination incorporated into a polymer.

In order to gain a better understanding of the mechanism operating within the CVZnO polymer, ROS and singlet oxygen scavengers (catalase, BSA and L-histidine) were added to the bacterium to examine their effect on the bacterial kill observed in Fig. 5.11 against *E. coli* ATCC 25922. A clear reduction in bacterial kill was observed in the light and in the dark when all three scavengers were added to the microbiological protocol. This indicated that both Type I and Type II mechanistic pathways are responsible for the lethal antibacterial activity observed from CV and CVZnO. Moreover, by adding BSA to the bacterium, there is a possibility that organic contaminants found in hospital environments may affect the efficiency of these polymers. However, this enzyme also scavenges singlet oxygen so the result is most likely a combination of both factors. Fig. 5.13 also suggests that Type I and Type II photochemical pathways are operating without any light activation, which could be a result of ZnO NP surface defects that allow the photosensitiser to produce additional ROS. This could be due to any stored energy within the ZnO lattice structure that allows electrons and holes at the surface to react with the photosensitiser, possibly causing an enhanced bactericidal effect. It is unlikely that the NPs leach to cause any cell damage, especially due to the fact that they do not cause any bacterial reduction themselves. It is only when the ZnO NPs and CV are combined that they exhibit considerable bactericidal activity.

These antibacterial surfaces have the potential to maintain low bacterial levels and minimise the risk of HAIs spreading around hospitals. They can be applied to a wide range of medical devices and frequently touched surfaces such as telephones, keyboards and iPad covers. There is a synergistic enhancement in bactericidal activity when the NPs are combined with CV, compared to CV or ZnO alone. For the first time, mechanistic studies have provided evidence to support both Type I and Type II photochemical pathways are responsible for the antibacterial

activity of CVZnO in the light and the dark, although there is more evidence to suggest a greater contribution of singlet oxygen production (Type II). The exceptional dark kill observed from CVZnO against a Gram-negative bacterium within only a few hours is promising for these materials to be useful for reducing the impact of HAIs in a clinical environment. Further studies using electron paramagnetic resonance (EPR) detection would be valuable to confirm Type I vs. Type II mechanisms.

References

- 1 Wilson APR, Kiernan M. Recommendations for surveillance priorities for healthcare-associated infections and criteria for their conduct. *Journal of Antimicrobial Chemotherapy*. 2012, 67(suppl 1):i23-i28.
- 2 Tierno PM, *The Secret Life of Germs: What They Are, Why We Need Them, and How We Can Protect Ourselves Against them*. Atria Books. New York, 1st edition, 2001;2:89-92.
- 3 Page K, Wilson M, Parkin IP. Antimicrobial surfaces and their potential in reducing the role of the inanimate environment in the incidence of hospital-acquired infections. *Journal of Materials Chemistry*. 2009;19:3819-3831.
- 4 Sperandio FF, Huang Y, Hamblin MR. Antimicrobial photodynamic therapy to kill Gram-negative bacteria. *Recent Patents on Anti-Infective Drug Discovery*. 2013;8(2):108-120.
- 5 Noimark S, Dunnill CW, Kay CWM, Perni S, Prokopovich P, Ismail S, Wilson M, Parkin IP. Incorporation of methylene blue and nanogold into polyvinyl chloride catheters; a new approach for light-activated disinfection of surfaces. *Journal of Materials Chemistry*. 2012;22:15388-15396.
- 6 Noimark S, Dunnill CW, Parkin IP. Shining light on materials – A self-sterilising revolution. *Advanced drug delivery reviews*. 2013;65(4):570-580.
- 7 Piccirillo C, Perni S, Gil-Thomas J, Prokopovich P, Wilson M, Pratten J, Parkin IP. *Journal of Materials Chemistry*. 2009;19:6167-6171.
- 8 Noimark S, Dunnill CW, Parkin IP. The role of surfaces in catheter-associated infections. *Chemical Society Reviews*. 2009;38(12):3435-3448.
- 9 Noimark S, Allan E, Parkin IP. Light-activated antimicrobial surfaces with enhanced efficacy induced by a dark-activated mechanism. *Chemical Science*. 2014;5(6):2216-2223.

- 10 Li Y, Zhang W, Niu J, Chen Y. Mechanism of photogenerated reactive oxygen species and correlation with the antibacterial properties of engineered metal-oxide nanoparticles. *ACS Nano*. 2012;6(6):5164-5173.
- 11 Kubacka A, Diez MS, Rojo D, Bargiela R, Ciordia S, Zapico I, Albar JP, Barbas C, Matrins dos Santos VAP, Fernandez-Garcia M. Understanding the antimicrobial mechanism of TiO₂-based nanocomposite films in a pathogenic bacterium. *Scientific Reports*. 2014;4(4134):1-9.
- 12 Azam A, Ahmed AS, Oves M, Khan MS, Memic A. Size-dependent antimicrobial properties of CuO nanoparticles against Gram-positive and –negative bacterial strains. *International Journal of Nanomedicine*. 2012;7:3527-3535
- 13 Sirelkhatim A, Mahmud S, Seeni A, Kaus NHM, Ann LC, Bakhori SKM, Hasan H, Mohamad D. Review on Zinc Oxide Nanoparticles: Antibacterial Activity and Toxicity Mechanism. *Nano-Micro Letters*. 2015;7(3):219-242.
- 14 Shi L, Xing L, Hou B, Ge H, Guo X, Tang Z. Inorganic nano metal oxides used as anti-microorganism agent for pathogen control. *Current research, technology and education topics in applied microbiology and microbial biotechnology*. A. Mendez-Vilas (Ed.), Formatex, 2010;361-368.
- 15 Leung YH, Ng AM, Xu X, Shen Z, Gethings LA, Wong MT, Chan CM, Guo MY, Ng YH, Djurisic AB, Lee PK, Chan WK, Yu LH, Philips DL, Ma AP, Leung FC. Mechanisms of antibacterial activity of MgO: non-ROS mediated toxicity of MgO nanoparticles towards Escherichia coli. *Small*. 2014;10(6):1171-1183.
- 16 Smijs TG, Pavel S. Titanium dioxide and zinc oxide nanoparticles in sunscreens: focus on their safety and effectiveness. *Nanotechnology, Science and Applications*. 2011;4:95-112.
- 17 Seil JT, Webster TJ. Antimicrobial applications of nanotechnology: methods and literature. *International Journal of Nanomedicine*. 2012;7:2767-2781.
- 18 Soosen SM, Bose L, KC G. Optical properties of ZnO nanoparticles. *1 & 2 SB Academic Review*. 2009;16:57-65.

- 19 Reddy KM, Feris K, Bell J, Wingett DG, Hanley C, Punnoose A. Selective toxicity of zinc oxide nanoparticles to prokaryotic and eukaryotic systems. *Applied physics letters*. 2007;90(213902):213902-1-213902-213903.
- 20 Piccirillo C, Perni S, Gil-Thomas J, Prokopovich P, Wilson M, Pratten J, Parkin IP, Antimicrobial activity of methylene blue and toluidine blue O covalently bound to a modified silicone polymer surface. *Journal of Materials Chemistry*. 2009;19:6167–6171.
- 21 Perni S, Prokovich P, Piccirillo C, Pratten J, Parkin IP, Wilson M. Toluidine blue-containing polymers exhibit potent bactericidal activity when irradiated with red laser light. *Journal of Materials Chemistry*. 2009;19(18):2715-2723.
- 22 Ozkan E, Allan E, Parkin IP. The antibacterial properties of light-activated polydimethylsiloxane containing crystal violet. *RSC Advances*. 2014;4:51711-51715.
- 23 Noimark S, Bovis M, MacRobert AJ, Correia A, Allan E, Wilson M, Parkin IP. Photobactericidal polymers: the incorporation of crystal violet and nanogold into medical grade silicone. *RSC Advances*. 2013;3:18383–18394.
- 24 Noimark S, Dunnill CW, Kay CWM, Perni S, Prokopovich P, Ismail S, Wilson M, Parkin IP, Incorporation of methylene blue and nanogold into polyvinyl chloride catheters; a new approach for light-activated disinfection of surfaces. *Journal of Materials Chemistry*. 2012;22:15388–15396.
- 25 Perni S, Piccirillo C, Kafisas A, Uppal M, Pratten J, Wilson M, Parkin IP. Antibacterial activity of light-activated silicone containing methylene blue and gold nanoparticles of different sizes. *Journal of Cluster Science*. 2010;21(3):427–438.
- 26 Perni S, Piccirillo C, Pratten J, Prokovich P, Chrzanowski W, Parkin IP, Wilson M. The antimicrobial properties of light-activated polymers containing methylene blue and gold nanoparticles. *Biomaterials*. 2009;30(1):89-93.

- 27** Bovis MJ, Noimark S, Woodhams JH, Kay CWM, Weiner J, Peveler WJ, Correia A, Wilson M, Allan E, Parkin IP, MacRobert AJ. Photosensitisation studies of silicone polymer doped with methylene blue and nanogold for antimicrobial applications. *RSC Advances*. 2015;5:54830-54842.
- 28** Noimark S, Allan E, Parkin IP. Light-activated antimicrobial surfaces with enhanced efficacy induced by a dark-activated mechanism. *Chemical Science*. 2014;5(6):2216-2223.
- 29** Noimark S, Weiner J, Noor N, Allan E, Williams CK, Shaffer MSP, Parkin IP. Dual-Mechanism Antimicrobial Polymer-ZnO Nanoparticle and Crystal Violet-Encapsulated Silicone. *Advanced Functional Materials*. 2015;25(9):1367-1373.
- 30** Ozkan E, Ozkan FT, Allan E, Parkin IP. The use of zinc oxide nanoparticles to enhance the antibacterial properties of light-activated polydimethylsiloxane containing crystal violet. *RSC Advances*. 2015;5:8806-8813.
- 31** Sehmi SK, Noimark S, Bear JC, Peveler WJ, Bovis M, Allan E, MacRobert AJ, Parkin IP. Lethal photosensitisation of *Staphylococcus aureus* and *Escherichia coli* using crystal violet and zinc oxide-encapsulated polyurethane. *Journal of Materials Chemistry B*. 2015;3:6490-6500.
- 32** Edwards K. New twist on an old favourite: gentian violet and methylene blue antibacterial foams. *Advanced Wound Care*. 2016;5(1):11-18.
- 33** Maley AM, Arbiser JL. Gentian violet: a 19th century drug re-emerges in the 21st century. *Experimental Dermatology*. 2013;22(12):775-780.
- 34** Haidekker MA, Theodorakis EA. Environment-sensitive behaviour of fluorescent molecular rotors. *Journal of Biological Engineering*. 2010;4(11):1-14.
- 35** Herbert S, Ziebandt AK, Ohlsen K, Schafer T, Hecker M, Albrecht D, Novick R, Gotz F. Repair of global regulators in *Staphylococcus aureus* 8325 and comparative analysis with other clinical isolates. *Infectious Immunology*. 2010;78:2877-2889

- 36 Park J, An K, Hwang Y, Park J, Noh H, Kim J, Park J, Hwang N, Hyeon t. Ultra-large-scale syntheses of Monodisperse nanocrystals. *Nature Materials*. 2014;3:891-895.
- 37 Castano AP, Demidova TN, Hamblin MR. Mechanisms in photodynamic therapy: part one – photosensitisers, photochemistry and cellular localization. *Photodiagnoses Photodynamic Therapy*. 2004;1(4):279-293.
- 38 Chatterjee DK, Fong LS, Zhang Y. Nanoparticles in photodynamic therapy: an emerging paradigm. *Advanced Drug Delivery Review*. 2008;60(15):1627-1637.
- 39 Berezin MY, Achilefu S. Fluorescence Lifetime Measurements and Biological Imaging. *Chemical Reviews*. 2010;110(5):2641-2684.
- 40 Sehmi SK, Noimark S, Weiner J, Allan E, MacRobert AJ, Parkin IP. Potent Antibacterial Activity of Copper Embedded into Silicone and Polyurethane. *ACS Materials & Interfaces*. 2015;7(41):22807-22813.
- 41 Michaeli A, Feitelson J. Reactivity of singlet oxygen toward amino acid and peptides. *Photochemistry and Photobiology*. 1994;59(3):284-289.
- 42 Michalski R, Zielonka J, Gapys E, Marcinek A, Joseph J, Kalyanaraman B. Real-time Measurements of Amino Acid and Protein Hydroperoxides Using Coumarin Boronic Acid. *The Journal of Biological Chemistry*. 2014;289(32):22536-22553.
- 43 Jensen RL, Arnbjerg J, Ogilby PR. Reaction of Singlet Oxygen with Tryptophan in Proteins: A Pronounced Effect of the Local Environment on the Reaction Rate. *Journal of the American Chemical Society*. 2012;134(23):9820-9826.
- 44 He J, Zhao J, Hidaka H, Serpone N. EPR Characteristics of a dye/colloidal TiO₂ system under visible light irradiation. *Journal of the Chemical Society, Faraday Transactions*. 1998;98:2375-2378.
- 45 Buettner GR, Doherty TP, Bannister TD. Hydrogen peroxide and hydroxyl radical formation by methylene blue in the presence of ascorbic acid. *Radiation and Environmental Biophysics*. 1984;23(4):235-243.

- 46** Wei C, Song B, Yuan J, Feng Z, Jia G, Li C, Luminescence and Raman spectroscopic studies on the damage of tryptophan, histidine and carnosine by singlet oxygen, *Journal of Photochemistry and Photobiology A: Chemistry*, 2007;189(1):39
- 47** Josefsen LB, Boyle RW. Photodynamic Therapy and the Development of Metal-based Photosensitisers. 2008;2008:276109.
- 48** Oschner M. Photophysical and photobiological processes in the photodynamic therapy of tumours. *Journal of Photochemistry and Photobiology B*. 1997;39(1):1-18.
- 49** Ma LW, Moan J, Berg K. Evaluation of a new photosensitiser, meso-tetrahydroxyphenyl-chlorin, for use in photodynamic therapy. A comparison of its photobiological properties with those of two other photosensitisers. *International Journal of Cancer*. 1994;57(6):883-888.
- 50** Sternberg ED, Dolphin D, Bruckner C. Porphyrin-based photosensitisers for use in photodynamic therapy. *Tetrahedron*. 1998;54(17):4151-4202.
- 51** Allison RR, Moghissi K. Photodynamic Therapy (PDT): PDT Mechanisms. *Clinical Endoscopy*. 2013;46(1):24-29.
- 52** Bonnet R. Photosensitisers of the porphyrin and phthalocyanine series for photodynamic therapy. *Journal of National Cancer Institute*. 1998;90(12):889-905.

Chapter 6

6. Polyurethane Encapsulated with Crystal Violet and 3 nm ZnO Nanoparticles; Antimicrobial Polymers Activated by Low Intensity White light Source

6.1 Introduction

Photodynamic therapy (PDT) is widely used in medicine to treat patients without the need for surgery. It can be used to treat parts of the body where a light source can reach easily, including the skin, eyes, mouth, oesophagus and lungs.¹ PDT can also be used to treat certain types of cancer, such as lung, skin, mouth and oesophageal cancer.¹⁻³ Chapter 5 has shown the efficacy of coating polymers with a photosensitiser for use as self-sterilising surfaces. By coating the polymer with the photosensitiser, there is a minimal risk to the patient that would otherwise occur from prolonged exposure to the dye *in vivo*.^{4,5} These light-activated antibacterial surfaces have the potential of reducing the risk of hospital-acquired infections (HAIs) under standard laboratory white light and more significantly, in the dark.

As shown previously, 18 nm-sized zinc oxide nanoparticles (ZnO NPs) were incorporated into medical grade polyurethane sheets and demonstrated strong bactericidal activity against Gram-negative and Gram-positive bacteria when combined with crystal violet (CV) dye. The ZnO NPs were synthesised *via* a metal-oleate precursor and were incorporated into the polymer substrate as well as adsorbed onto the surface. It was the combination of CV with ZnO NPs (CVZnO) in the polymer that induced lethal activity, as the ZnO NPs themselves displayed no significant

antibacterial effect alone. Not only did the CVZnO polymer samples demonstrate highly significant bactericidal activity, they also caused significant kill in the dark within only a few hours. For the first time, the mechanism of the dye-nanoparticle combination was examined by using radical species and singlet oxygen quenchers to inhibit either a Type I or Type II photochemical pathway. The results indicated that both pathways were responsible for the bactericidal activity of CVZnO, with a greater contribution from the Type II mechanism, i.e. by producing singlet oxygen. The antibacterial activity exhibited by CVZnO is very promising, however, there are some improvements that can be made on the experimental set-up to more closely mimic a clinical environment.

HAIs cause an estimated 5000 deaths per year in the UK and lead to increased financial costs for the NHS.⁶ As the incidence of HAIs rises due to bacteria expressing multidrug resistance, the development of novel antibacterial procedures becomes increasingly urgent.⁷ Carbapenem-resistant Enterobacteriaceae (CRE) and methicillin-resistant *Staphylococcus aureus* (MRSA) infections are resistant to most antibiotics that are currently available and are a major problem in healthcare environments.⁸ The use of broad-spectrum antibiotics also is a problem because it increases the risk of hospital-associated diarrhoea due to infection from *C. difficile*.⁹ Patients who acquire this infection shed endospores (a dormant form of *C. Difficile* that have evolved for prolonged survival in the environment) in their faeces that subsequently transmits to patients and frequently touched surfaces. These spores can survive in the environment for many months and orally infect patients whose protective microbiota has been damaged by broad-spectrum antibiotics.^{9,10} Furthermore, *Pseudomonas* infections can easily occur in hospitals from healthcare workers spreading the bacteria on their hands or from contaminated equipment which is not properly cleaned.¹¹ Patients with compromised immune systems are mostly at risk, however, mild illnesses caused by

Pseudomonas aeruginosa (*P. aeruginosa*) can also affect healthy people after exposure to contaminated water.^{11,12}

As previously described, the antibacterial activity of ZnO NPs has attracted much attention in recent years due to their biocompatibility and multifunctionality.¹³ They demonstrate selective toxicity towards bacteria showing a minimal effect on mammalian cells.¹⁴ The suggested mechanisms of the bactericidal activity of ZnO NPs includes disruption to the bacterial cell membrane from Zn^{2+} ions and the production of cytotoxic reactive oxygen species (ROS).¹³ Particle properties such as size, surface defects, morphology and concentration can affect the antibacterial action of NPs. For example, smaller sized NPs (i.e. a larger surface area) and a higher concentration of NPs results in greater bactericidal activity; they can easily penetrate into bacterial cell membranes due to their large interfacial area.^{13,15} When considering shape, truncated-triangular NPs are reported to be more effective at killing bacteria. However, spherical-shaped NPs are still considered to be optimal for practical applications.^{16,17} In this chapter, smaller ZnO NPs (3-4 nm) are synthesised using the same method but with two different capping agents, di(octyl)-phosphonic acid and oleic acid, to form ZnO NPs capped with di(octyl)phosphinate (DOPA) and oleate ligands (as shown in Fig. 6.1).

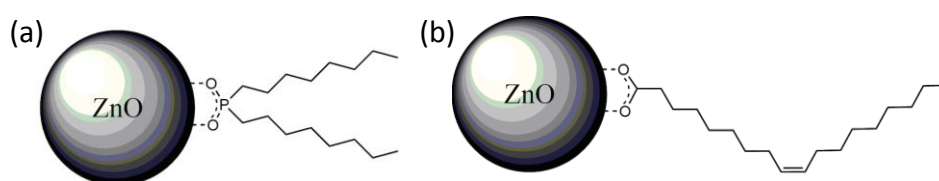


Fig. 6.1 Diagram illustrating ZnO nanoparticles capped with a (a) di(octyl)-phosphinate ligand (DOPA) and an (b) oleate ligand.

This study used various modifications from the previous protocol in an effort to more closely simulate a 'real world' clinical environment: (i) using

natural 'wild' isolates of bacteria rather than adapted laboratory strains; (ii) using a lower light intensity than previously used to replicate the lighting commonly experienced in UK hospitals¹⁸ (~500 lux compared to ~6600 lux). Thus, the polymer samples are exposed to ambient lighting on a laboratory bench; (iii) the bacterial suspension was not covered with a coverslip when in contact with the polymer and the samples are not placed into a humidity chamber. Previously, a coverslip has been used (Chapter 3-5) to ensure a close, uniform contact between the bacteria and the hydrophobic polymer surface, and the humidity chamber was used to prevent evaporation of the bacterial suspension. Instead, the bacterial suspension was simply dropped onto the polymer surface and allowed to dry naturally rather than being 'forced' to interact with the entire surface area of the polymer.

ZnO NPs capped with a DOPA ligand (ZnO_DOPA) and ZnO NPs capped with an oleate ligand (ZnO_oleate) were incorporated separately into medical grade polyurethane squares and coated with CV to obtain CVZnO_DOPA and CVZnO_oleate polymer samples. Their antibacterial activity was assessed against *Escherichia coli* (*E. coli*) ATCC 25922 and an epidemic strain of MRSA (EMRSA-16), one of two clones known to predominate in the UK (PHE).¹⁹ The best performing polymer was then tested against highly resistant hospital pathogens such as *P. aeruginosa* NTCC 10662, *E. coli* 1030 and *C. difficile* spores. Both ZnO NPs enhance the photobactericidal activity of CV under low intensity lighting within relatively short incubation times. More surprisingly, for the first time, significant bactericidal activity of both ZnO NPs alone was demonstrated against *E. coli* ATCC 25922 under low intensity lighting and in the dark within only 2/3 h. These antibacterial polymer surfaces exhibited higher activity than previously reported for the CVZnO combination, showing outstanding potential in combating the incidence of HAIs. Finally, an in depth analysis into the antibacterial mechanism of these NPs was carried out using a variety of quenchers to inhibit both Type I and Type II photochemical pathways.

6.2 Experimental

6.2.1 ZnO Nanoparticles

6.2.1.1 Nanoparticle Synthesis

All chemicals and reagents were purchased from Sigma-Aldrich Chemical Co. except for toluene (Fischer Scientific, UK). The Schlenk line and glovebox techniques were used to manipulate air sensitive chemicals (i.e. diethyl zinc is pyrophoric). Liquid chemicals (e.g. diethyl zinc, oleic acid) were measured by negative weight of the donor flask. Toluene was pre-dried over potassium hydroxide and then further dried by refluxing over sodium. It was then degassed by freeze pump thaw techniques and stored under nitrogen to halt any ripening of the NPs which may occur in the solid state.²⁰ ZnO NPs were kindly provided by Dr. Sebastian Pike (Imperial College London, UK) and prepared with DOPA and oleate ligands following an established route (summarised in Fig. 6.2)²¹:

- (i) **DOPA-capped ZnO NPs:** ZnEt_2 and 0.2 equivalents of dioctylphosphinic acid were dissolved in toluene and to this a 0.4 M solution of water (in excess, two equivalents used) in acetone was added dropwise to hydrolyse the organometallic reagent. Acetone was then added to precipitate the formed NPs, which were centrifuged, washed with acetone and left to air dry overnight.
- (ii) **Oleate-capped ZnO NPs:** Oleic acid was placed into a Schlenk flask with a stirrer and dried under vacuum. Dry toluene was added to the ligand in a glovebox and then either 5 equivalents of diethyl zinc (ZnEt_2) was added dropwise to the solution whilst stirring. A 0.4 M solution of water in acetone was added to the mixture to hydrolyse the organometallic precursors to form ZnO NPs. The NP suspension was precipitated by adding acetone, centrifuged and washed by toluene and acetone with

subsequent centrifugation steps. The particles were air dried overnight.

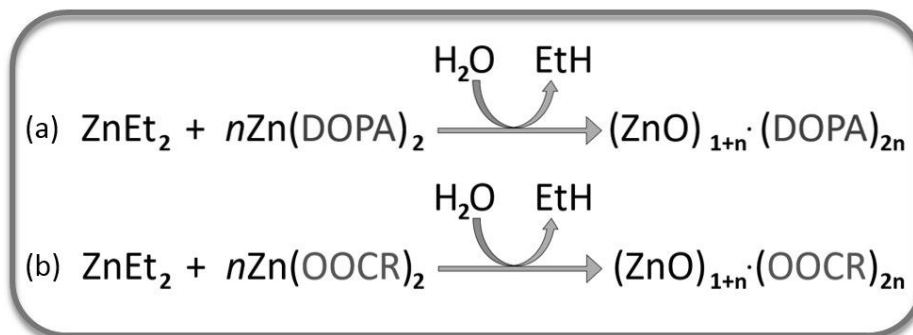


Fig. 6.2 General form of ZnO nanoparticle synthesis: (a) DOPA-capped and (b) oleate-capped.

6.2.1.2 Nanoparticle Characterisation

X-ray diffraction (XRD) was performed using an X'Pert Pro diffractometer (PANalytical B. V., The Netherlands) and X'Pert Data Collector software, version 2.2b. It was used in the theta/theta reflection mode and fitted with a nickel filter, 0.04 rad Soller slit, 10 mm mask, 1/4° fixed divergence slit, and 1/2° fixed antiscatter slit. The XRD diffraction patterns were analysed using Fityk (version 0.9.0; Marcin Wojdyr, 2010) and the peaks were fitted to a SplitPearson7 function. The particle size was calculated using the fitted full-width half-maximum using the Scherrer Equation. UV-vis spectroscopy was recorded using a PerkinElmer Lambda 950 spectrophotometer from NPs suspended in toluene. Elemental micro-analysis was determined by Stephen Boyer at London Metropolitan University. Thermogravimetric analysis was undertaken under an air atmosphere using a Mettler/Toledo TGA/DSC 1LF/UMX instrument at a heating rate of 10K/min. TEM micrographs were taken using a Jeol 2100 HR-TEM with a LaB₆ source operating at an acceleration voltage of 200 kV with an Oxford Instruments XMax EDS detector running AZTEC software. TEM samples were prepared by drop-casting the NP suspension (in toluene) onto a 400 Cu mesh lacy

carbon film TEM grid (Agar Scientific Ltd). Micrographs were recorded onto a Gatan Orius charge-coupled device and analysed using ImageJ software.

6.2.2 Polymer Samples

6.2.2.1 Polymer Sample Preparation

Polymer squares (1 cm²) were prepared from medical grade polyurethane sheets (0.8 mm thickness), purchased from American Polyfilm Inc. (Branford, CT, USA). They were then prepared by using the 'swell-encapsulation-shrink' method as described in Chapter 5 (Fig. 5.2). The polymer squares were immersed into swelling solutions containing DOPA-capped and oleate-capped ZnO NPs separately in toluene (1 mg/mL). They were kept in the swelling solutions for 24 h to incorporate the NPs, removed and left in the dark for 24 h to shrink back to their original shape and size. They were then washed, air-dried and dipped into an aqueous solution of CV (0.001 M) for 72 h (dark conditions, RT). For antibacterial testing, control samples were also prepared (solvent treated only) as well as polymer samples containing only ZnO NPs or CV alone.

6.2.2.2 Material Characterisation

UV-vis absorption spectra of modified polymer samples were measured in the range 300 – 750 nm using a PerkinElmer Lambda 25 UV-vis spectrometer. A Thermo K-Alpha spectrometer using monochromated Al K α radiation was used to perform X-ray photoelectron spectroscopy (XPS) of modified polymer samples. High-resolution scans (0.1 eV) were collected at a pass energy of 50 eV, including principal peaks of Zn (2p), O (1s), N (1s) and C (1s). A depth profile was measured at the polymer surface and sputtered 50 seconds. All binding energies were calibrated to the C (1s) peak (284.5 eV).

Water contact angle measurements of all modified polymer squares were obtained using a FTA 1000 Drop Shape Instrument. The average contact angle measurement was calculated using a droplet of deionised water (~5 μL) dispensed by gravity from a gauge 30 needle with a camera to photograph the samples side on, and the data was analysed using FTA32 software. ZnO_DOPA and ZnO_oleate samples were placed in 2 mL of deionised water for up to 48 h to determine the extent of NP leaching into the surrounding solution. After removing the polymer squares from the aqueous solutions, they were diluted to 5 mL and analysed by inductively coupled plasma optical emission spectrometry (ICP-OES) using a Perkin Elmer Optima 2000 DV. The zinc concentration in each solution was calculated using a calibration curve determined from solutions containing $[\text{Zn}] = 0, 0.1, 1$ and 10 mg/L .

All polymers containing CV dye were stored in a light box for up to 60 days to measure the photo-degradation of the dye when exposed to a white light source emitting an average light intensity of $2800 \pm 510 \text{ lux}$ at a distance of 33 cm from the samples. The UV-vis absorption spectra of the samples were measured (range 400 – 750 nm) to determine the extent of photodegradation over time. Confocal fluorescence imaging of CV-coated and CVZnO_oleate polymers were performed using a Leica TCS SPE confocal system with an upright microscope and a 20x objective (UCL confocal microscopy facility, Rockefeller building). A 532 nm laser was used as the excitation source and CV fluorescence was detected at 630 nm.

6.2.3 Antibacterial Activity

6.2.3.1 Microbiology Assay

The antibacterial activity of the following modified polymer samples was tested against *E. coli* ATCC 25922 and *S. aureus* NCTC 13142 (one of two types of MRSA that dominates in UK hospitals; EMRSA-16¹⁹): control (solvent treated), polyurethane-coated CV (CV), polyurethane-

encapsulated ZnO (ZnO_DOPA and ZnO_oleate), and polyurethane-encapsulated CV and ZnO (CVZnO_DOPA and CVZnO_oleate). Further antibacterial testing was carried out on ZnO_oleate-containing polymer samples only (i.e. ZnO_oleate and CVZnO_oleate) against the following bacteria: *P. aeruginosa* NCTC 10662, a multidrug resistant strain of *E. coli* positive for both NDM and OXA-48-like carbapenemase genes, (J. Wade, King's College Hospital, London) and endospores of *C. difficile* 630 Δ erm using a protocol designed to mimic a 'real world' clinical situation.

E. coli ATCC 25922, *S. aureus* NCTC 13143, *P. aeruginosa* NCTC 10662 and *E. coli* 1030 were stored at -70 °C in Brain-Heart-Infusion broth (BHI, Oxoid) containing 20% (v/v) glycerol and propagated on MacConkey agar (MAC, Oxoid) in the case of Gram-negative bacteria (*P. aeruginosa* and *E. coli*) or Mannitol Salt agar (MSA, Oxoid) in the case of Gram-positive bacterium (*S. aureus* NCTC 13143), for a maximum of 2 subcultures at intervals of 2 weeks.

BHI broth was inoculated with 1 bacterial colony and cultured in air with shaking (37 °C, 200 rpm, 18 h). The bacterial suspension was centrifuged to recover the bacterial pellet, (20 °C, 2867.2 g, 5 min), washed in PBS (10 mL), centrifuged again to recover the pellet (20 °C, 2867.2 g, 5 min), and finally re-suspended in PBS (10 mL). The washed suspension was diluted 1000-fold to achieve an inoculum ($\sim 10^6$ cfu/mL). The inoculum was confirmed by plating 10-fold serial dilutions on agar for viable counts. Triplicates of each polymer sample type were inoculated with 25 μ L of the inoculum and incubated in the dark or irradiated for up to 6 h using standard laboratory white light emitting an average light intensity of ~ 500 lux. Following exposure to light, the inoculated samples were added to PBS (450 μ L) and mixed using a vortex mixer (15 s). The neat suspension and 10-fold serial dilutions were plated on agar for viable counts and incubated aerobically at 37 °C for 24 h (*E. coli*/*P. aeruginosa*) or 48 hours (*S. aureus*).

6.2.3.2 Statistical Significance

The experiment was repeated three times and the statistical significance of the following comparisons was analysed using the Mann-Whitney U test: (i) control polymer vs. inoculum; (ii) CV or ZnO_DOPA/ZnO_oleate vs. control; (iii) CVZnO_DOPA/CVZnO_oleate vs. CV alone.

6.2.3.3 *Clostridium difficile* Endospore Preparation

C. difficile endospores were prepared as described by Burns *et al*²² with the following modifications. *C. difficile* 630Δerm was grown on BHI blood agar for 48 h, and then one bacterial colony was inoculated into 10 ml of BHIS (brain heart infusion supplemented with L-cysteine [0.1%; Sigma] and yeast extract [5 mg/ml; Oxoid]) broth. The culture was incubated anaerobically with shaking (37° C, 50 rpm, 16 h). 1 ml of the overnight culture was used to inoculate 60 mL of BHIS broth. The culture was then incubated in the anaerobic cabinet with shaking (37° C; 50 rpm; 6 days to ensure the highest level of sporulation). The spores were harvested by centrifugation (5000 rpm; 10 min) and resuspended in sterile water (5 mL). The suspension was heated in a water bath to kill any remaining vegetative cells (80°C; 30 min). The spores were then washed 3 times with sterile, ice-cold water and the pellet was resuspended in PBS (2 mL). The suspension was then divided into 200 µL aliquots and stored at -80° C. Prior to use, one aliquot of the bacterial suspension was thawed and diluted with PBS (20 mL), ready for antibacterial testing. Sodium taurocholate (0.1%; Sigma, UK) was added to BHI agar (Oxoid) to stimulate spore germination. The spores were added to the polymer samples for up to 72 h using the same method described above.

6.2.3.4 Ligand Variation to Determine Oleate Ligand Influence

To investigate the influence of the oleate ligand on bactericidal activity, ZnO NPs were synthesised with different capping ligands (with a 5:1 metal to ligand ratio). In addition to this, oleate-capped ZnO NPs were also prepared with a 10:1 metal to ligand ratio. The following NPs were synthesised and incorporated into the polymer with CV using a similar method as described in section 6.2.1: 3.6 nm stearate-capped ZnO (5:1), 4.0 nm linoleate-capped ZnO (5:1), and 4.9 nm oleate-capped ZnO (10:1).

6.2.3.5 Detection of Superoxide and Singlet Oxygen

Superoxide dismutase (SOD), L-histidine and bovine serum albumin (BSA)²³⁻²⁵ were purchased from Sigma-Aldrich, UK, filter-sterilised and added to bacterial suspensions of *S. aureus* NCTC 13143 and *E. coli* ATCC 25922 in the microbiology protocol to determine the mechanism of CVZnO_oleate. SOD (50 U mL⁻¹) was used to eliminate superoxide (a precursor of hydrogen peroxide in radical formation), L-histidine (1 mM) was added as a quencher of singlet oxygen and BSA (0.03% in water) was added as an organic contaminant as well as a singlet oxygen quencher. Furfuryl alcohol (FFA) was also used as a singlet oxygen trap²⁶ using the decrease in its UV absorbance upon photo-oxidation. Since FFA does not absorb in the visible region it is unaffected by the visible illumination source used for bacterial treatment. FFA was added to the solution covering the CVZnO_oleate samples (no bacteria present) and were illuminated with the same visible light source and time conditions used in the antibacterial testing. 200 µL of deionised water containing 5.75 x 10⁻⁸ M of FFA was used to measure the concentration of singlet oxygen after contact with the sample.²⁷ The absorbance of this compound was measured at 222 nm from the control polymer and compared with CV and CVZnO_oleate to see any reductions in absorption intensity. Finally, L-ascorbic acid (1 mM)²⁸ was also added to the

bacterial suspension to quench singlet oxygen production from CV and CVZnO_oleate samples.

6.3 Results and Discussion

6.3.1 ZnO Nanoparticle Synthesis and Characterisation

~3 nm ZnO NPs were synthesised and surface stabilized by either DOPA or oleate ligands. They were synthesised by the controlled hydrolysis of ZnEt₂ in the presence of 0.2 equivalents of di-octylphosphinic acid (in the case of DOPA-capped ZnO NPs) or oleic acid (in the case of oleate-capped ZnO NPs) to give a 5:1 metal to ligand ratio.²¹ The NPs were kept under N₂ to be contained in an inert environment, as there is evidence to suggest that they may slowly ripen over several months if exposed to atmospheric moisture.²⁰ Elemental micro-analysis and thermal gravimetric analysis determined the ligand content of these samples and calculated the metal:ligand ratio as 6:1 and 5.4:1 for DOPA-capped and oleate-capped ZnO NPs, respectively, suggesting a very slight loss of ligand during the NP synthesis. ZnO surface coverage (%) was determined by UV spectra analysis, indicating a partial coverage of the DOPA-capped NPs (~60%) and less ligand coverage of the oleate-capped NPs (~95%).

The NPs were characterised by powder XRD (Fig. 6.3) and UV spectroscopy (Fig. 6.4-6.5) to determine the size of the particles.²⁹ The size of the NPs was determined from XRD spectra (Fig. 6.3) by use of the Scherrer equation and gave estimated diameters of 2.2 ± 0.3 nm for the DOPA-capped ZnO NPs and 3.4 ± 0.6 nm for the oleate-capped ZnO NPs. Due to the small size of these ZnO NPs, quantum confinement increases their absorption energy relative to bulk ZnO.³⁰ A Tauc plot measured from UV spectroscopy measured the band onset of the particles suspended in toluene, estimating the band gap to be 3.76 ± 0.1 eV for DOPA-capped ZnO NPs (Fig. 6.4(a)) and 3.48 ± 0.01 eV for oleate-capped ZnO NPs (Fig. 6.4(b)). Both sets of

ZnO NPs were relatively spherical and monodisperse, as shown by TEM (Fig. 6.6).

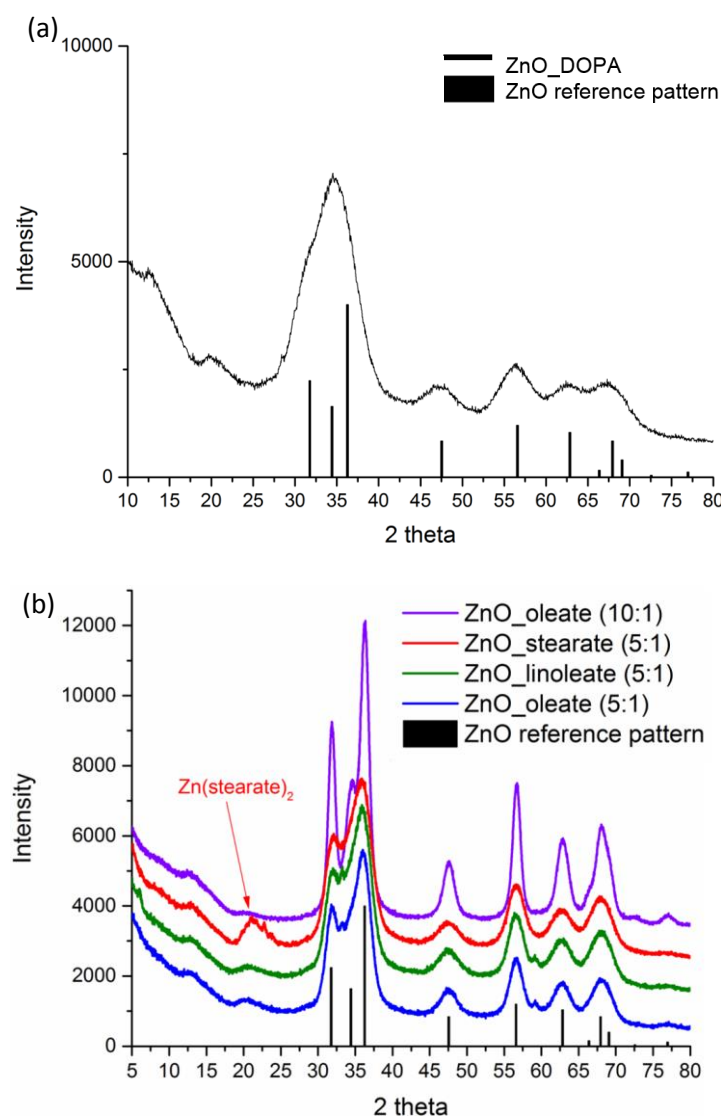


Fig. 6.3 Powder XRD patterns of ZnO nanoparticles with (a) dioctylphosphinate (DOPA) and (b) oleate, linoleate and stearate ligands (Wurzite ZnO reference pattern indicated, JCPDS card 00-001-1136, patterns stacked with +1000 intensity to each in turn). The size of the particles may be estimated by analysis of the peak width using the Scherrer equation. The signals at $2\theta = 47.5$ and 56.6 were analysed for each batch of nanoparticles giving sizes of: ZnO_DOPA (5:1), 2.2 nm; ZnO_oleate (5:1), 2.8-4.1 nm; ZnO_oleate (10:1), 4.9-7.4 nm; ZnO_linoleate (5:1), 2.8-3.6 nm, ZnO_stearate (5:1), 2.8-3.3 nm. The broad signals at $2\theta = 18-25^\circ$ are assigned to the organic ligands, in the case of ZnO_stearate a minor trace of impurity $\text{Zn}(\text{stearate})_2$ may also be present.²¹

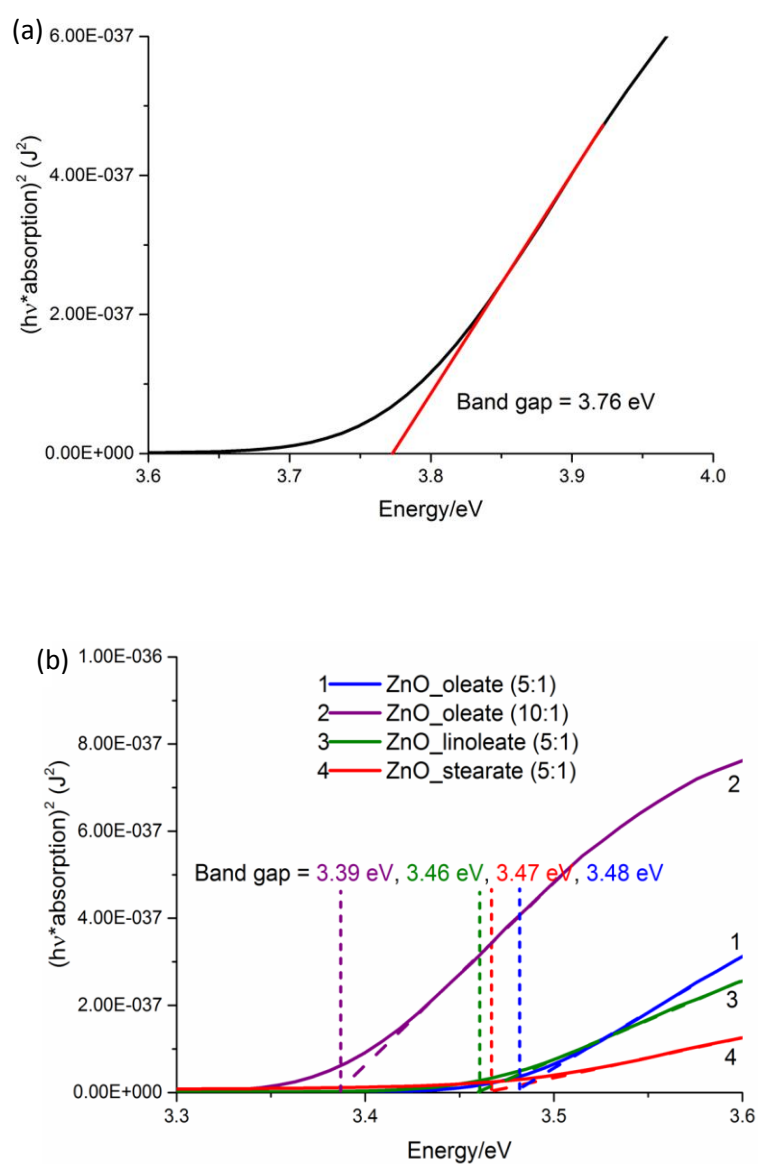


Fig. 6.4 Tauc plots derived from UV absorption spectra of ZnO nanoparticles. Band gaps determined: (a) ZnO_DOPA (5:1) = 3.76 ± 0.01 eV and (b) ZnO_oleate (5:1) = 3.48 ± 0.01 eV; ZnO_oleate (10:1) = 3.39 ± 0.01 eV; ZnO_linoleate (5:1) = 3.46 ± 0.01 eV, ZnO_stearate (5:1) = 3.47 ± 0.01 eV.

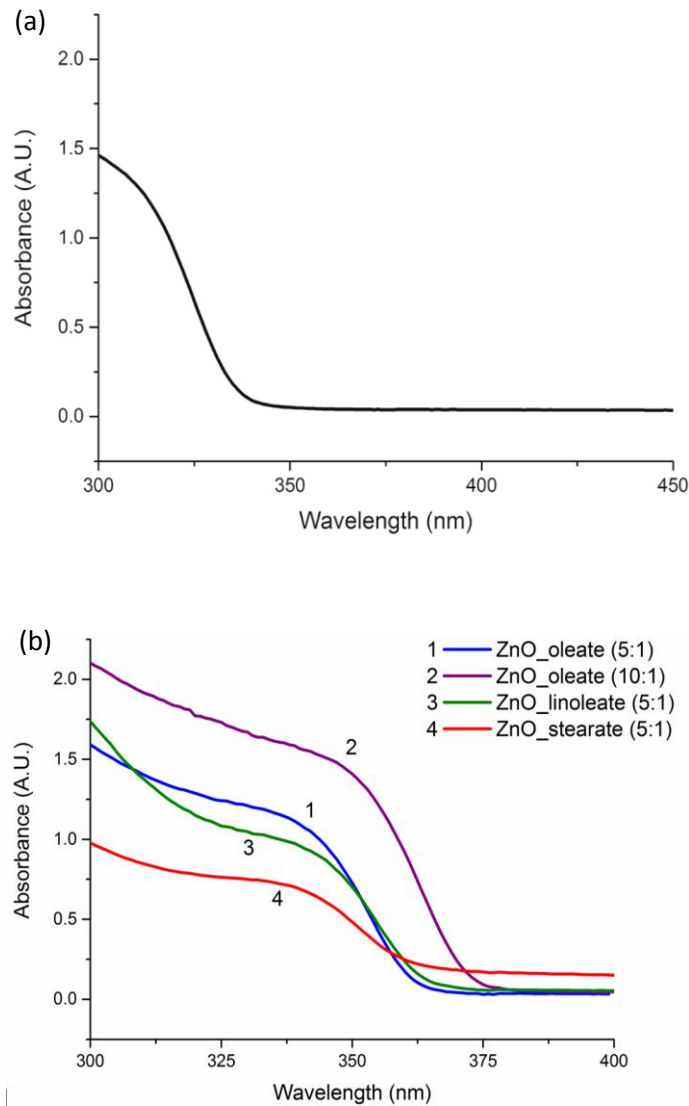


Fig. 6.5 UV spectra of ZnO nanoparticles dissolved in toluene (approx 0.4 mg/mL). An estimate of the particle size can be made by the onset of UV absorption.²⁹ Sizes were calculated from the maximum gradient of the UV absorption onset corresponding to: (a) ZnO_DOPA (5:1), 2.7 nm and (b) ZnO_oleate (5:1), 3.8 nm; ZnO_oleate (10:1), 4.9 nm; ZnO_linoleate (5:1), 4.0 nm, ZnO_stearate (5:1), 3.6 nm. All sizes are a close match for the sizes estimated by XRD (see Fig 6.3).

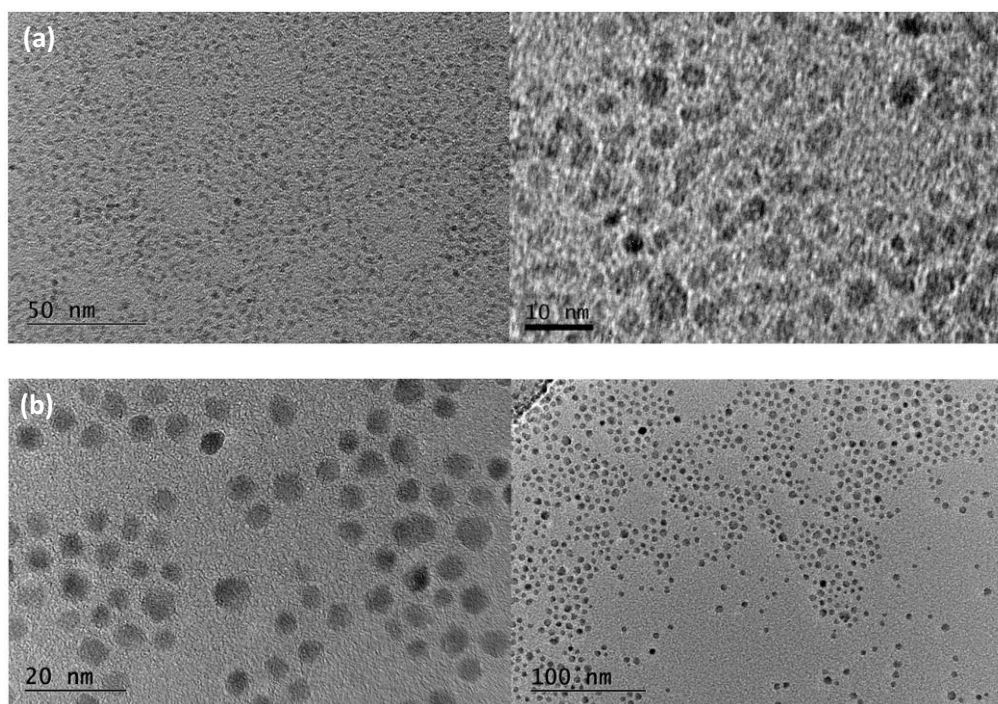


Fig. 6.6 TEM images of (a) ZnO_DOPA and (b) ZnO_oleate (5:1).

6.3.2 Preparation and Characterisation of Polymer Samples

DOPA-capped and oleate-capped ZnO NPs were synthesised and incorporated within polyurethane squares to test their antibacterial efficacy against Gram-positive and Gram-negative bacteria with and without crystal violet dye (ZnO_DOPA / ZnO_oleate / CVZnO_DOPA / CVZnO_oleate). The NPs were added to the toluene swelling solution (1 mg/mL) and 1 cm² polymer samples were immersed into the NP suspension for 24 h in the dark. They were removed and left to dry for 24 h to allow enough time for the polymer squares to shrink back to their original shape and size. They were then washed, towel-dried and immersed into a solution of CV (0.001 M) for 72 h.

The modified polymer samples were characterised by UV-vis spectroscopy and XPS, and the wetting properties, extent of NP leaching and photostability of the samples were examined. As shown in the UV-vis spectrum (Fig. 6.7), CV-coated polyurethane, CVZnO_DOPA and CVZnO_oleate showed an absorbance maxima at $\lambda = 590$ nm. However,

there was no characteristic absorption peak observed for the ZnO NPs in either sample, presumably due to the low concentration of NPs incorporated. The absorption intensity of CV increased with the addition of the NPs, implying a greater concentration of CV added to the polymer samples. However, CV-coated polyurethane was pre-treated with toluene, so the solvent is not responsible for the differences in absorption intensity.

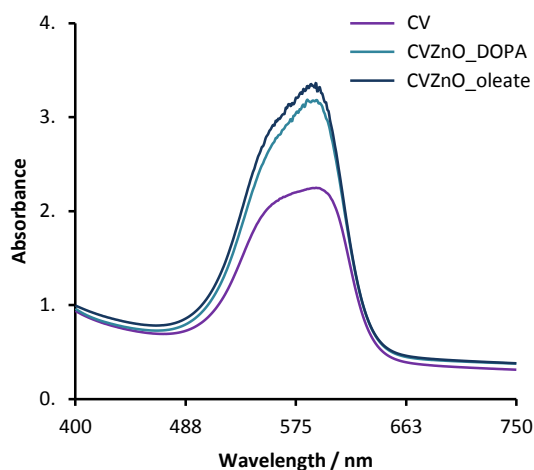


Fig. 6.7 UV-vis absorption spectra measured in the range of 400 – 700 nm of crystal violet-coated polyurethane (CV), CV and ZnO_DOPA-incorporated polyurethane (CVZnO_DOPA) and CV and ZnO_oleate-incorporated polyurethane (CVZnO_oleate). Both ZnO NPs with 5:1 metal:ligand ratio.

XPS was used to determine intensity of the NPs at the polymer surface and throughout the bulk (Fig. 6.8). Peaks in the C (1s) region, N (1s) region and O (1s) region were observed on all modified polyurethane samples (data not shown). A doublet in the Zn (2p) region indicating Zn in ZnO was shown on the surface and within the polymer substrate for CVZnO_DOPA (Fig. 6.8(a) and (b)). XPS depth profile data demonstrated a decrease in zinc content within the polymer bulk. For CVZnO_oleate the data also confirmed that the NPs were incorporated throughout the polymer bulk and on the polymer surface (Fig. 6.8(c) and (d)), illustrating a doublet in the Zn (2p) region. XPS depth profile data for CVZnO_oleate demonstrated an increase in zinc content within the polymer substrate rather than on the

polymer surface. Equilibrium water contact measurements ($\sim 5.0 \mu\text{l}$) of all modified polymer samples were measured under standard laboratory conditions. The results showed a slight increase in hydrophobicity of the samples with the addition of the ZnO NPs and the photosensitiser (varying $\pm 8^\circ$ in contact angle).

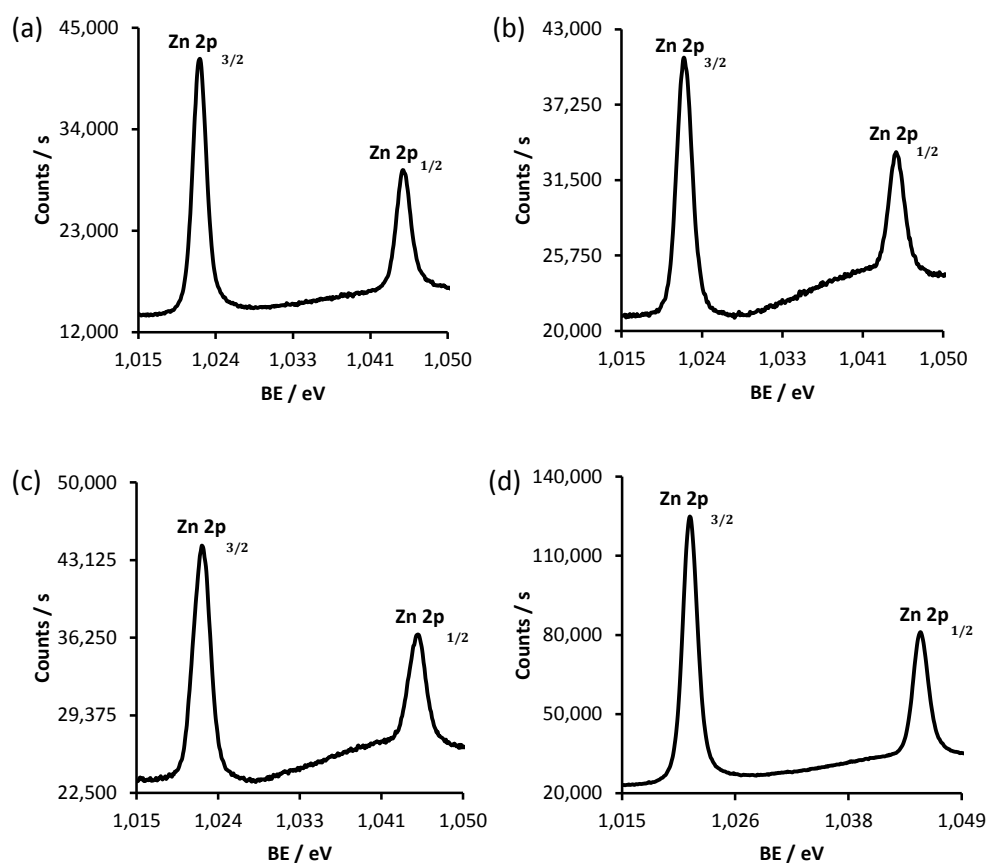


Fig. 6.8 XPS spectra for Zn (2p) on (a) CVZnO_DOPA surface, (b) CVZnO_DOPA sputtered 50 s, (c) CVZnO_oleate surface and (d) CVZnO_oleate sputtered 50 s (both 5:1).

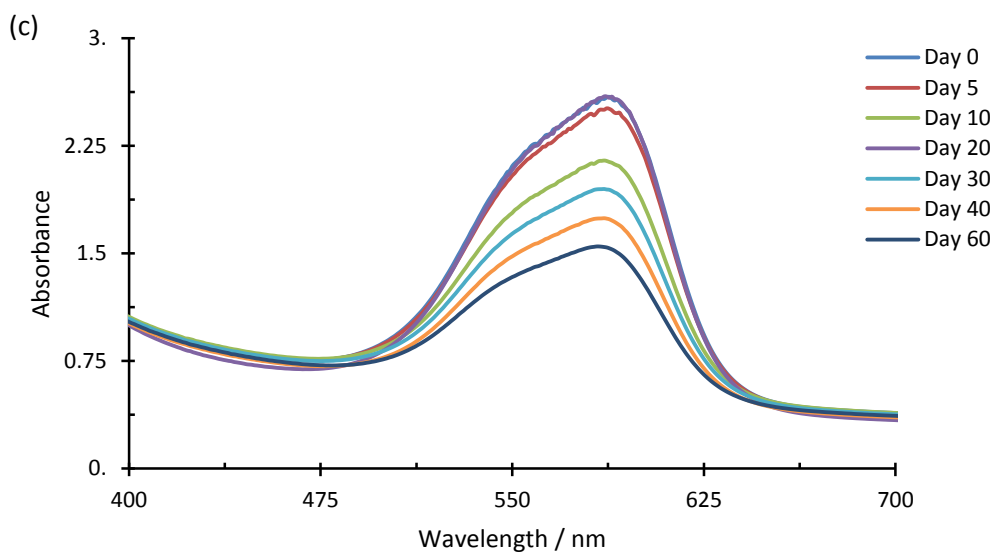
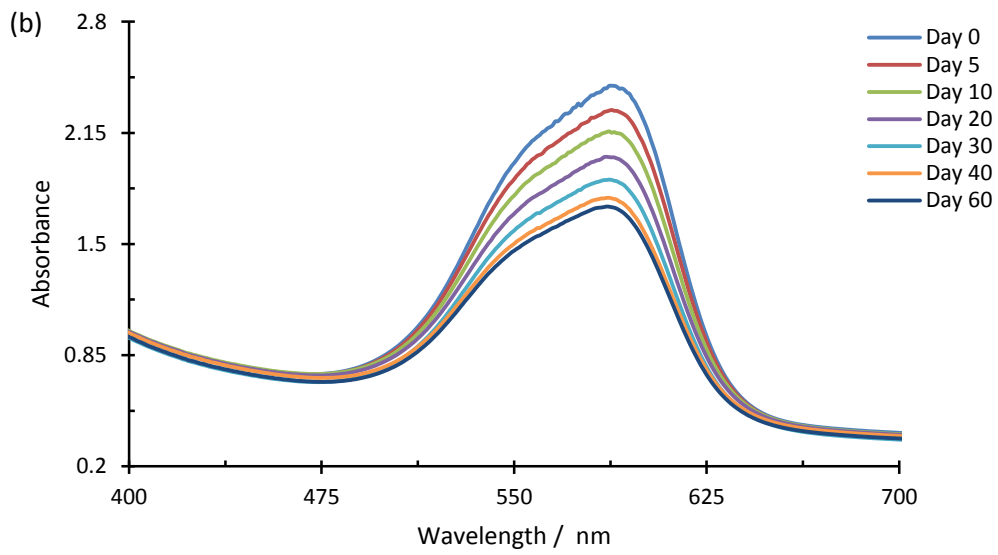
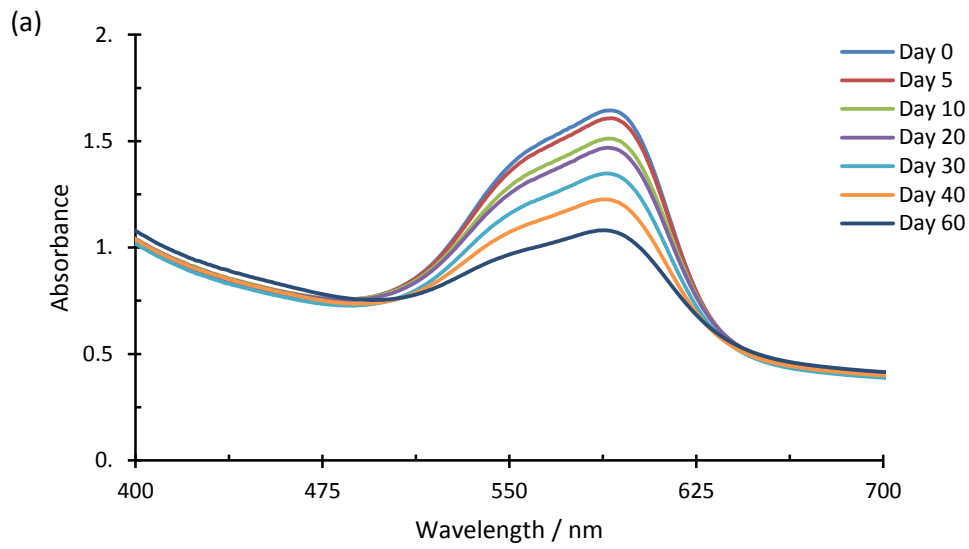
ICP–OES was used to determine if any zinc species leached from ZnO_DOPA or ZnO_oleate polymer samples when they were immersed in 2 mL distilled water for a period of 2 h and 48 h. After removing the polymer sample from the solution, it was diluted to 5 mL and analysed by ICP-OES for [Zn]. The results (summarised in Table 6.1) showed that a higher concentration of Zn^{2+} leached from ZnO_oleate compared to ZnO_DOPA,

especially after 2 days. However, the amount of leaching (mg/L) was negligible compared to the amount of ZnO incorporated into the sample (from using a NP swelling solution of 1 mg/mL).

Table 6.1 Amount of leaching (mg/L) of Zn²⁺ ions from modified polymer samples after 2 hours and 2 days (SD = standard deviation).

Polymer sample	2 hours		2 days	
	[Zn]	SD	[Zn]	SD
ZnO_DOPA (5:1)	0.083	0.001	0.169	0.005
ZnO_oleate (5:1)	0.096	0.002	1.008	0.006

The photostability of CV, CVZnO_DOPA and CVZnO_oleate polyurethane samples was examined under a ~3880 lux white light source for up to 60 days (Fig. 6.9). The UV-vis spectra showed that all samples were strongly photostable (Fig. 6.9(a) and (b)), even under a light source ~19-fold more intense than that of many hospital corridors and wards (~200 lux).¹⁸ Over 60 days, CV-coated polyurethane demonstrated 34% photodegradation compared to 30% for CVZnO_DOPA and 39% for CVZnO_oleate, showing that these materials are likely to exhibit long term photostability within hospitals.



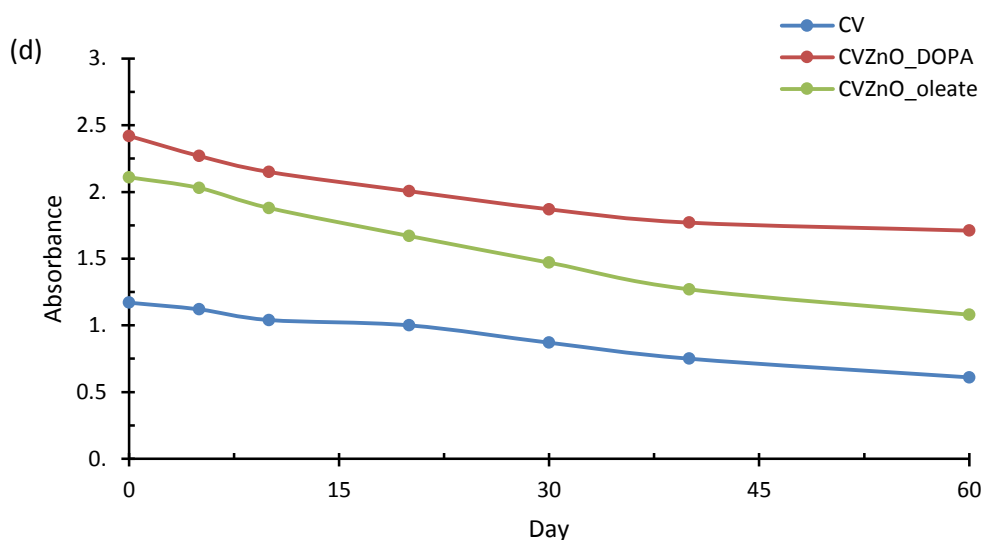


Fig. 6.9 UV-vis absorbance spectra measured in the range 400 – 700 nm of (a) CV-coated polymer, (b) CV and ZnO_DOPA-incorporated polymer and (c) CV and ZnO_oleate-incorporated polymer. The samples were exposed to a white light source emitting an average light intensity of 3880 ± 200 lux at a distance of 35 cm from the samples. (d) The rate of photodegradation of CV, CVZnO_DOPA and CVZnO_oleate polymers upon exposure to a high lux intensity white light source (60 days; 3880 lux) shown as a change in absorbance at the CV absorbance maxima ($\lambda = \sim 590$ nm) over time. Data shown with control polymer readings subtracted.

Confocal images of CV-coated and CVZnO_oleate showed that the photosensitiser penetrated uniformly throughout the polymer bulk (Fig. 6.10), as demonstrated in Chapter 5 using fluorescence microscopy.

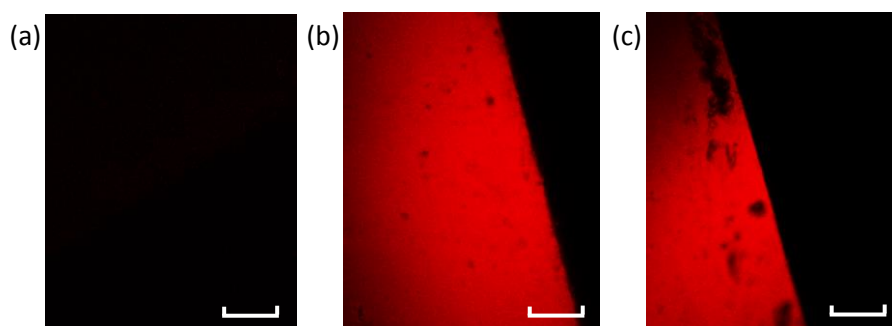


Fig. 6.10 Confocal fluorescence imaging of (a) untreated polymer, (b) CV-coated polymer and (c) CV and ZnO_oleate-incorporated polymer using a Leica TCS SPE confocal system with an upright microscope and a 20x objective. A 532 nm laser was used as the excitation

source and CV fluorescence was detected at 630 nm. There is a 100 μm scale bar on the image. The polymer sample is on the left hand side of the image, where the black part of the image represents the background (no fluorescence). The image resolution is 512 x 512 pixels and corresponds to 367 x 367 microns.

6.3.3 Antibacterial Activity

6.3.3.1 CVZnO_DOPA vs. CVZnO_oleate

The antibacterial activity of CVZnO_DOPA and CVZnO_oleate was compared by testing them against two species of bacteria commonly found in hospitals: *E. coli* ATCC 25922 and *S. aureus* NCTC 13143 (a clinical strain of EMRSA-16), in the dark and under low intensity white light (~ 500 lux). This lower light intensity has been used to mimic the ambient light levels found in most hospital wards and corridors. The protocol used to test the antibacterial activity of the samples against the Gram-negative bacterium, *E. coli* ATCC 25922, was similar to the previous set-up described in Chapter 5, which included the use of a coverslip (2.2 cm^2) to spread the bacteria evenly on the polymer surface and a humidity chamber to provide a moist environment for the samples. This was to ensure that a direct comparison could be made between the bactericidal activity of 18 nm ZnO NPs (Chapter 5) and these 3 nm ZnO NPs when incorporated into polyurethane in the dark. However, when testing the samples against *S. aureus* NCTC 13143 (and all bacteria hereafter), the protocol does not include a coverslip or humidity chamber in order to investigate the behaviour of the antibacterial polymers using conditions that more closely simulate a real world exposure.

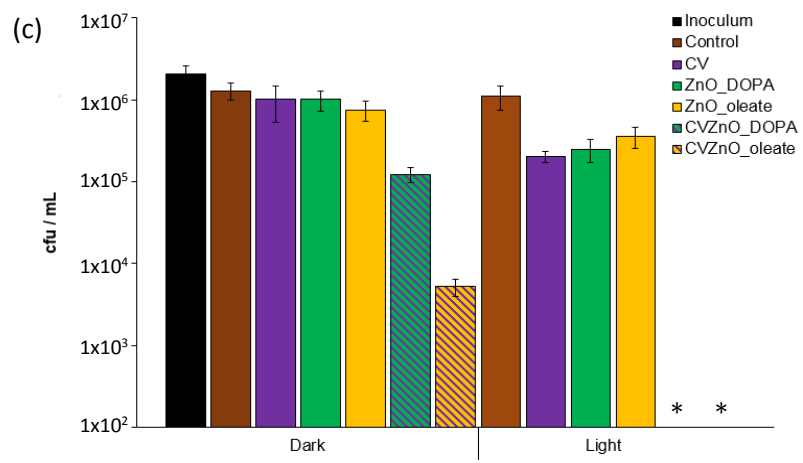
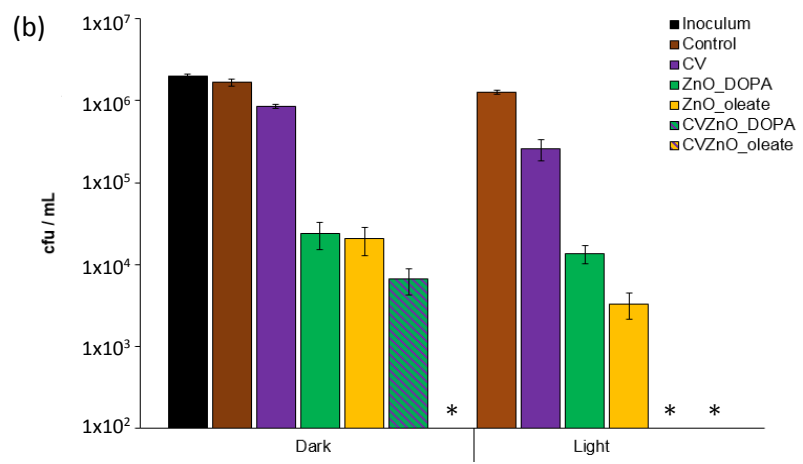
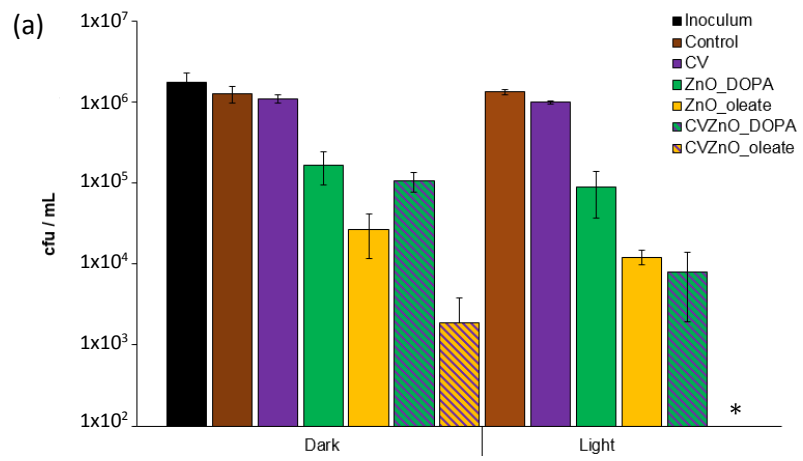
Within 2 h of incubation in the dark, the control and CV-coated polyurethane displayed no bactericidal activity (Fig. 6.11(a)). However, for the first time in this type of study, both ZnO NPs demonstrated significant antibacterial activity, with ZnO_DOPA and ZnO_oleate reducing bacterial numbers by ~ 0.8 and ~ 1.7 log, respectively ($P = 0.001$). With the addition of a photosensitiser, CVZnO_DOPA reduced *E. coli* ATCC 25922 by ~ 1 log,

whereas CVZnO_oleate caused a ~2.8 log reduction ($P = 0.001$). Following 2 h of white light exposure, ZnO_DOPA and ZnO_oleate reduced bacterial numbers by ~1.1 log and 2 log, respectively. CVZnO_DOPA reduced *E. coli* ATCC 25922 by ~2.2 log, but the most effective antibacterial activity was shown by CVZnO_oleate, which reduced bacterial numbers to below the detection limit (≥ 4 log; $P = 0.001$).

By increasing the incubation time to 3 h (Fig. 6.11(b)) in the dark, both ZnO_DOPA and ZnO_oleate reduced *E. coli* ATCC 25922 by ~1.6 log and CVZnO_DOPA was able to reduce the bacteria by ~2.2 log. Most significantly, CVZnO_oleate reduced the bacteria to below the detection limit within only 3 h without photoactivation (≥ 4 log; $P = 0.001$). ZnO_DOPA exhibited similar antibacterial activity after 3 h of white light illumination as it did in the dark (~2 log), whereas ZnO_oleate reduced the bacteria by ~2.5 log after 3 h. Both CVZnO_DOPA and CVZnO_oleate produced highly significant photobactericidal effects against *E. coli* ATCC 25922 (≥ 4 log; $P = 0.001$).

ZnO_DOPA and ZnO_oleate-incorporated samples were also tested for antibacterial activity against *S. aureus* NCTC 13143 without the use of a coverslip or humidity chamber in the experimental set-up. As shown in Fig. 6.11(c), only the combination of CV and ZnO was capable of reducing *S. aureus* NCTC 13143 within 2 h in the dark; with CVZnO_DOPA and CVZnO_oleate reducing bacterial numbers by ~0.8 and ~2.3 log, respectively. However, by illuminating the samples for 2 h, CV reduced the bacteria by ~0.75 log and both CVZnO_DOPA and CVZnO_oleate exhibited ≥ 4 log reduction of the EMRSA-16 strain ($P = 0.001$).

After 3 h in the dark (Fig. 6.11(d)), ZnO_DOPA and ZnO_oleate caused ~0.35 log reduction of *S. aureus* NCTC 13143, whereas CVZnO_DOPA and CV_ZnO_oleate reduced the bacteria by ~0.9 and ~2.3 log, respectively. Following 3 h of white light exposure, CV-coated polyurethane reduced *S. aureus* NCTC 13143 by ~1.4 log. Moreover, ZnO_DOPA and ZnO_oleate reduced the bacteria by ~0.6 log ($P = 0.001$).



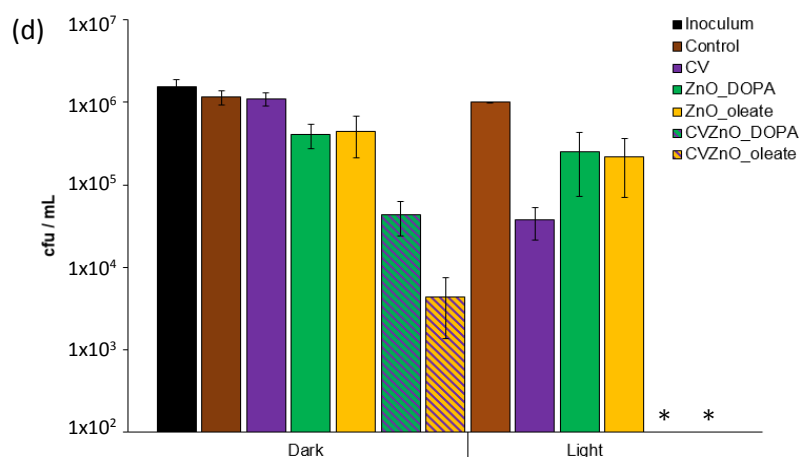


Fig. 6.11 Antibacterial activity of CVZnO_DOPA and CVZnO_oleate polymer samples in the dark and under standard laboratory white light (500 ± 300 lux) against: (a) *E. coli* ATCC 25922 for 2 h, (b) *E. Coli* ATCC 25922 for 3 h, (c) *S. aureus* NCTC 13143 for 2 h and (d) *S. aureus* NCTC 13143 for 3 h. * indicates bacterial numbers reduced to below the detection limit of 100 colony forming units/mL (cfu/mL).

The antibacterial activity of CVZnO_DOPA and CVZnO_oleate was then tested against both *E. coli* ATCC 25922 and *S. aureus* NCTC 13143 for 1 h in the dark and under white light activation (Table 6.2). The results clearly show that CVZnO_oleate is more effective at reducing both bacteria than CVZnO_DOPA. This is also apparent at longer incubation times (as shown in Fig. 6.11), where CVZnO_oleate proves to be more effective in the light and dark. DOPA-capped ZnO and oleate-capped ZnO NPs were synthesised using similar experimental procedures, producing NPs with an average diameter size of 3 nm. Thus, both of these factors are not responsible for the differences in antibacterial activity. However, these results do suggest that the oleate ligand is responsible for the better antibacterial activity exhibited from ZnO_oleate compared to ZnO_DOPA, even though previous studies have shown that the ligands on their own do not demonstrate any significant antibacterial activity when incorporated into a polymer.^{23,31}

Table 6.2 Antibacterial activity of modified polymer samples following 1 hour exposure to standard laboratory white light (500 ± 300 lux).

Polymer sample	Bacteria	Bacterial reduction
CVZnO_DOPA	<i>E. coli</i> ATCC 25922	No kill
CVZnO_oleate	<i>E. coli</i> ATCC 25922	~1 log
CVZnO_DOPA	<i>S. aureus</i> NCTC 13143	~0.5 log
CVZnO_oleate	<i>S. aureus</i> NCTC 13143	~1.75 log

Most strikingly, for the first time, ZnO NPs have been incorporated into polyurethane and demonstrated bactericidal activity against a Gram-negative and a Gram-positive bacterium without a photosensitiser. Both ZnO_DOPA and ZnO_oleate are able to reduce *E. coli* ATCC 25922 within only 2 h (in the light and dark). Moreover, they have demonstrated some activity against a clinical strain of EMRSA-16. The reduction of both bacteria in the dark suggests that these NPs could be killing the bacteria *via* different mechanisms to the photosensitiser, for example, Zn²⁺ leaching into the bacterial cell membrane or electrostatic interaction between the metal ions and the negatively charged bacterial cell wall.¹³⁻¹⁵

6.3.3.2 Further Antibacterial Testing of CVZnO_oleate

Following the results shown above in 6.3.3.1, the best performing ZnO NP, ZnO_oleate, was incorporated into polyurethane with CV and tested against more resistant bacterial strains. The antibacterial efficacy of CVZnO_oleate was tested against *P. aeruginosa* NTCC 10662, *E. coli* 1030 and *C. difficile* 630Δerm endospores.²² In these experiments, no coverslip was used, and the bacterial suspension was simply dropped onto the polymer and allowed to dry rather than being ‘forced’ to interact with the

entire polymer surface. Against all bacteria tested in Fig. 6.12-6.14, none of the control nor ZnO_oleate polymers produced any significant kill of in the dark or after white light illumination.

Fig. 6.12(a) illustrates the bactericidal activity of modified polymer samples tested against *P. aeruginosa* NCTC 10662 following 4 h of incubation in the light and dark. After 4 h in the dark, none of the modified polymers demonstrated any bactericidal activity. However, following 4 h exposure to white light, CV reduced *P. aeruginosa* NCTC 10662 by ~ 0.8 log and CVZnO_oleate caused ~ 2.5 log reduction in bacterial numbers ($P = 0.001$). By increasing the incubation time in the dark to 6 h (Fig. 6.12(b)), CV and CVZnO_oleate caused a ~ 0.6 and ~ 1 log reduction of *P. aeruginosa* NCTC 10662, respectively. Within 6 h of white light activation, CV alone caused a ~ 1.3 log reduction of bacteria, whereas CVZnO_oleate reduced bacterial numbers to below the detection limit (≥ 4 log reduction; $P = 0.001$).

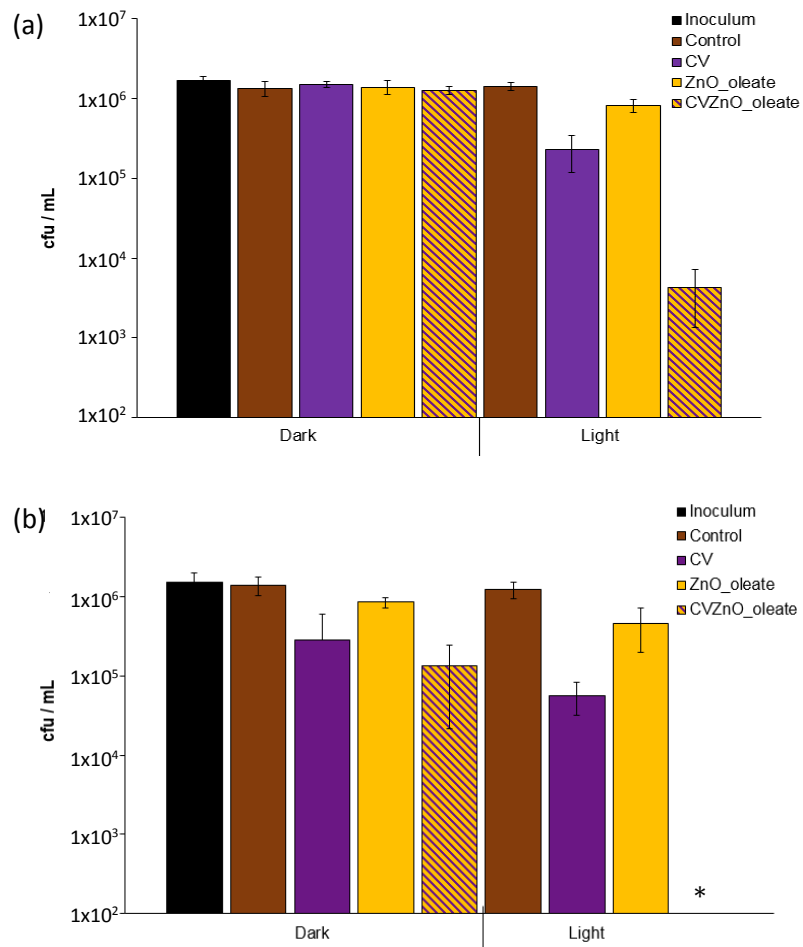


Fig. 6.12 Viable counts of *P. aeruginosa* NTCC 10662 after incubation on modified polyurethane samples incubated at 20 °C under dark conditions and exposed to standard laboratory white light (500 ± 300 lux) for: (a) 4 h and (b) 6 h. * indicates bacterial numbers reduced to below the detection limit of 100 colony forming units/mL (cfu/mL).

The ZnO_oleate samples were then tested against *E. coli* 1030, a multidrug-resistant clinical isolate positive for both NDM and OXA-48-like carbapenemase genes. None of the samples caused any bacterial kill within 4 h in the dark except CVZnO_oleate, which demonstrated statistically significant bactericidal activity (~1.9 log reduction, $P = 0.001$). Following 4 h in the light (Fig. 6.13(a)), CV alone reduced the numbers of *E. coli* 1030 by ~1.5 log, whereas exposure to the CVZnO_oleate polymer reduced the numbers by ~4 log ($P = 0.001$). After 6 h exposure to the bacteria in the dark (Fig. 6.13(b)), only the CVZnO_oleate sample reduced bacterial numbers (~1.7 log; $P = 0.001$). However, after 6 h of white light activation,

CV caused ~2 log reduction of *E. coli* 1030 and CVZnO_oleate reduced bacterial numbers to below the detection limit (≥ 4 log reduction; $P = 0.001$).

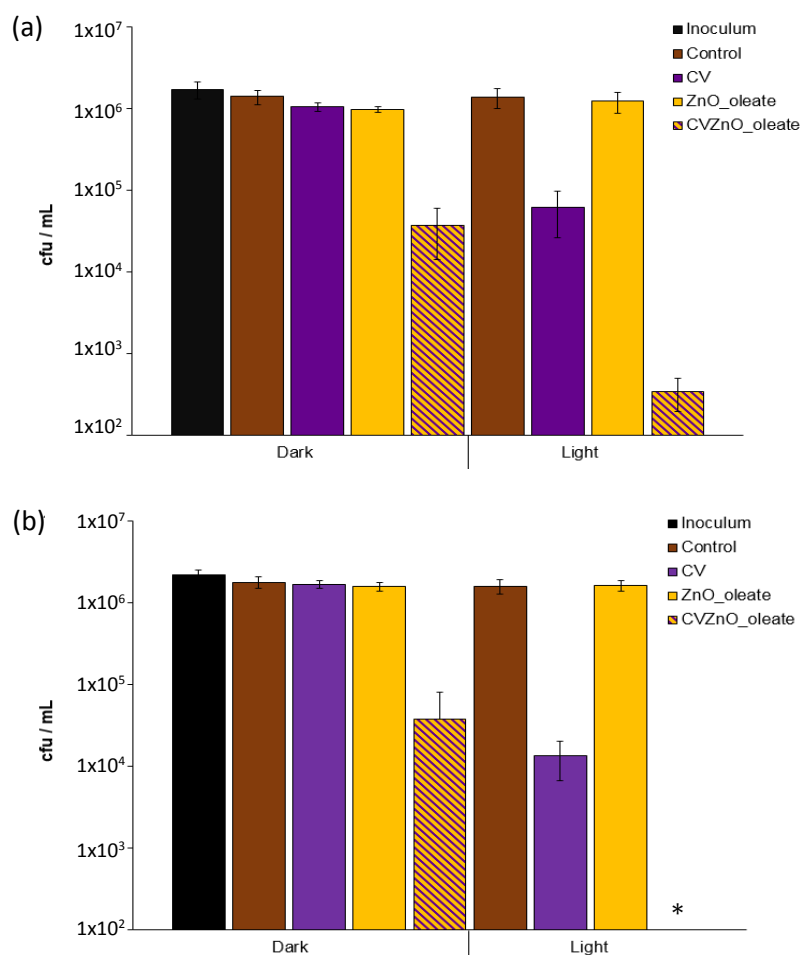


Fig. 6.13 Viable counts of *E. coli* 1030 after incubation on modified polyurethane samples incubated at 20 °C under dark conditions and exposed to standard laboratory white light (500 ± 300 lux) for: (a) 4 h and (b) 6 h. * indicates bacterial numbers reduced to below the detection limit of 100 colony forming units/mL (cfu/mL).

Lastly, the photobactericidal efficacy of these polymers containing CV and ZnO_oleate were tested against highly resistant *C. difficile* endospores. A reduction in the number of spores would be greatly beneficial as it is currently a major threat to patients in hospitals.³² No significant sporicidal activity was evident in the dark. However, following 72 h of white light

exposure (Fig. 6.14), the polymer containing CVZnO_oleate achieved a further ~1.2 log reduction in the number of spores compared to the control (P = 0.001).

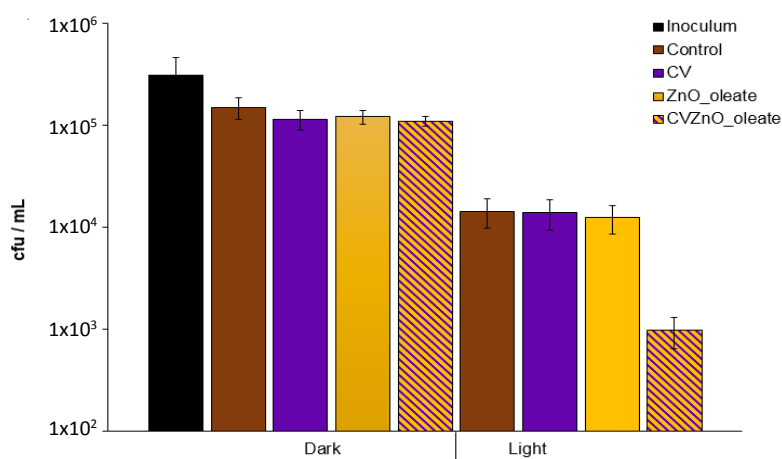


Fig. 6.14 Viable counts of *C. Difficile* 630Δerm after incubation on modified polyurethane samples incubated at 20 °C under dark conditions and exposed to standard laboratory white light (500 ± 300 lux) for 72 h.

Table 6.3 Summary of the antibacterial activity of ZnO_oleate and CVZnO_oleate-incorporated polymers in the dark and following white light incubation (500 ± 300 lux) against *E. coli* ATCC 25922 (3 h), *P. aeruginosa* NTCC 10622 (6 h), *S. aureus* NCTC 13143 (2 h), *E. coli* 1030 (4 h) and *C. difficile* 630 endospores (72 h). Bacterial reduction is given in log form.

Bacterial strain / incubation time	ZnO_oleate dark	ZnO_oleate white light	CVZnO_oleate dark	CVZnO_oleate white light
<i>E. coli</i> ATCC 25922 (3 h)	2 log	2.5 log	≥4 log	≥4 log
<i>P. aeruginosa</i> NTCC 10662 (6 h)	No kill	No kill	1 log	≥4 log
<i>S. aureus</i> NCTC 13143 (2 h)	No kill	No kill	2.4 log	≥4 log
<i>E. coli</i> 1030 (4 h)	No kill	No kill	1.9 log	4 log
<i>C. difficile</i> 630 (72 h)	No kill	No kill	No kill	1.2 log

For the first time, ZnO NPs were synthesised with two different capping agents and exhibited significant bactericidal activity against *E. coli* ATCC 25922 and *S. aureus* NCTC 13143 within only 3 h when incorporated into medical grade polyurethane squares. Both ZnO_DOPA and ZnO_oleate were able to significantly reduce the bacteria without the addition of CV or illumination. The results also showed that ZnO_oleate exhibited a greater bactericidal effect than ZnO_DOPA, with and without a photosensitiser. Further antibacterial testing of ZnO_oleate and CVZnO_oleate was then carried out for longer time periods against wild bacterial strains more recently isolated from hospitals and *C. difficile* spores.

ZnO_oleate was unable to reduce the more resistant bacteria (*P. aeruginosa* NTCC 10662, *E. coli* 1030 or *C. difficile* spores) without CV. Figs. 6.11 – 6.14 show that under a lower white light intensity of ~500 lux, CV alone is much less effective than previously demonstrated in Chapter 5, where a greater white light intensity was used (~6600 lux). However, the antibacterial activity of these smaller ZnO NPs supercedes the activity exhibited by 18 nm ZnO NPs shown in the previous chapter. The 18 nm ZnO NPs were also capped with oleic acid, thus, the smaller sized NPs have proven to be better at killing bacteria based on size alone. The antibacterial efficacy of the 18 nm and 3 nm ZnO NPs on their own differ, as 18 nm ZnO NPs were unable to reduce *E. coli* ATCC 25922, whereas the smaller ZnO NPs (both DOPA- and oleate-capped) prove to be very effective at killing the same bacteria. Additionally, the combination of CV and 18 nm ZnO NPs is not effective at reducing *E. coli* ATCC 25922 within 2 h in the dark (Chapter 5; Fig. 5.10), whereas 3 nm ZnO_oleate combined with CV reduces the bacteria by ~2.8 log (Fig. 6.11(a)). It should be noted that different swelling solutions were used to incorporate 18 nm and 3 nm ZnO NPs into polyurethane (1:1 ratio of dichloromethane and hexane in the case of 18 nm ZnO NPs and toluene in the case of 3 nm ZnO NP). However, both solutions caused the polymer to swell up to 142% of its original size and therefore, their antibacterial activities can be compared. It is possible

that the smaller nanoparticles are able to penetrate through the bacterial cell wall at a higher concentration than the larger ZnO NPs.

CVZnO_oleate polyurethane samples have demonstrated highly significant light-activated bactericidal activity against all pathogens tested in this investigation (Figs. 6.11 - 6.14) and even showed good activity against *P. aeruginosa* and a highly resistant strain of *E. coli* in the dark (Table 6.3). As shown for all bacteria tested, there was an increase in the antibacterial activity of CV when ZnO_oleate NPs were combined, implying that the NPs are responsible for enhancing the intrinsic (dark) bactericidal activity of CV itself and also enhancing the light-activated bactericidal activity of the dye. CVZnO_oleate demonstrated some photobactericidal activity against *C. difficile* spores. This is encouraging and may have a positive impact on infection control, as faecal shedding of spores by *C. difficile*-infected patients and contamination of environmental surfaces is a major infection source driving hospital outbreaks.^{33,34} It is not understood why ≥ 1 log reduction in the numbers of *C. difficile* spores occurred on the control polymer. Since no reduction in the spore counts was apparent on the control polymer in the dark, this could be due to reduced recovery of the spores from the surface of the light-exposed material as a result of drying.

6.3.4 Mechanistic Evaluation of CVZnO_oleate

To understand the effect of the oleate ligand on the antibacterial activity of CVZnO_oleate, ZnO NPs were synthesised with either oleate, stearate or linoleate ligands (structures shown in Fig. 6.15). Moreover, ZnO was synthesised again with an oleate capping, but with a greater NP metal:ligand ratio (10:1 compared to 5:1 used previously). Furthermore, ZnO NPs were synthesised with stearate and linoleate ligands (5:1) to see if changes in the ligand chain structure would alter the antibacterial activity of the ZnO NPs. Studies in the literature have shown these ligands to possess bactericidal properties.³⁵⁻³⁷ As shown in Table 6.4, the total surface

area of 1 mg of the ZnO NPs remained consistent across all NPs, as the ZnO NPs with lesser ligand (more ZnO/g) are coincidentally larger in diameter with a lower surface area per particle. This is significant as the swelling solutions were prepared with 1 mg of ZnO per mL. It should also be noted that the solubility in organic solvents (e.g. toluene) of these ZnO NPs given in Table 6.4 was reduced compared to the original oleate-capped ZnO NPs (5:1) system.

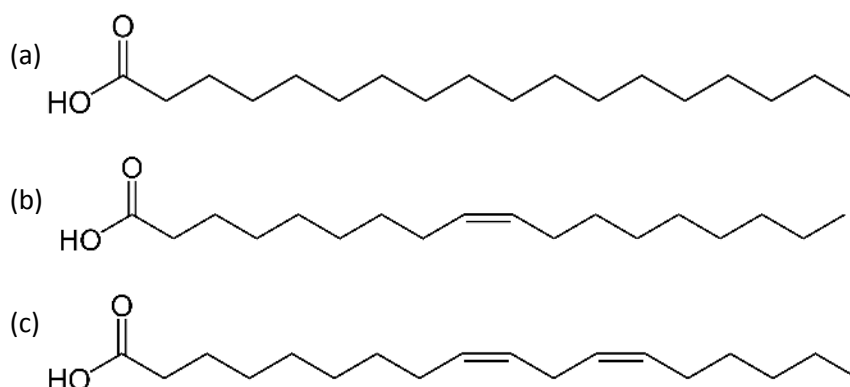


Fig. 6.15 Structures of (a) stearic acid, (b) oleic acid and (c) linoleic acid.

To assess the antibacterial activity of polyurethane containing these different ligand:metal combinations with CV dye, they were tested against against *E. coli* ATCC 25922 after 2 h of standard laboratory white light exposure (~500 lux). The results showed (Table 6.4) that the bactericidal activity of both linoleate- and stearate-capped ZnO with CV was significantly less than CVZnO_oleate (5:1) in the light. CV and linoleate-capped ZnO and CV and stearate-capped ZnO only achieved ~1 log reduction in the numbers of *E. coli* ATCC 25922 ($P = 0.001$) compared to ≥ 4 log reduction observed from CV and oleate-capped ZnO (5:1). Linoleate-capped ZnO was the least soluble and did not demonstrate any significant kill in the dark when combined with the photosensitiser. CV combined with stearate-capped ZnO reduced bacterial numbers by ~1 log in the dark

whereas polyurethane containing CV and oleate-capped ZnO (5:1) produced a ~2.8 log reduction (P = 0.001).

Moreover, the antibacterial activity of the different ratios of oleate-capped ZnO was compared. The 10:1 ratio was not as effective as the 5:1 ratio, presumably because the 10:1 oleate-capped ZnO NPs were larger in size (4.9 nm compared to 3.8 nm). Within 2 h of white light activation, polyurethane containing CV and oleate-capped ZnO (10:1) reduced numbers of *E. coli* ATCC 25922 by ~2 log (P = 0.001) and exhibited no significant kill in the dark. This suggests that a reduction in the ligand coverage of the ZnO NP surface (from 95% in the 5:1 ratio to 65% in the 10:1 oleate-capped ZnO) is not beneficial in enhancing the bactericidal properties of the NPs. As reported in the literature and shown by the difference in antibacterial activity observed from 3 nm and 18 nm ZnO NPs (Chapter 5), this study also shows that the antibacterial activity of ZnO NPs is size dependent.^{13,15,38,39}

Table 6.4 Summary of the nanoparticle surface area and ligand coverage of all ZnO nanoparticles. Surface coverage determined for a typical average size nanoparticle as expected from analysis of UV spectra (Fig. 6.4; note that some size dispersity is likely in the particles and this represents an average scenario). Antibacterial activity of the ligands incorporated into polyurethane (with CV against *E. coli* ATCC 25922) after 2 h exposure to white light (500 ± 300 lux).

Ligand	Ratio	wt % ligand by elemental analysis (carbon %)	Approximate diameter (nm)	ZnO surface area of 1 mg of NP (m ²)	Metal : ligand ratio	Estimated ligand coverage (% ZnO surface)	Antibacterial activity after 2 h white light (500 ± 300 lux) with CV
Oleate	5:1	39	3.8	0.17	5.3:1	95	≥4 log
Oleate	10:1	25.6	4.9	0.16	10.1:1	65	~2 log
Stearate	5:1	40	3.6	0.18	5.2:1	93	~1 log
Linoleate	5:1	35.2	4.0	0.17	6.3:1	86	~1 log

In addition to investigating the properties of the capping ligand on the NPs, different Type I and II inhibitors were used to help understand the mechanism operating within the ZnO_oleate and CVZnO_oleate (5:1) polymer systems (Fig. 6.16). Previous studies have suggested that a Type I

process is dominant within antibacterial polymers,⁴⁰ whereas others show a greater contribution from the Type II process, depending on the photosensitiser.⁴¹ Bovis *et al* demonstrated that both Type I and Type II mechanisms can operate in the photosensitisation of silicone doped with methylene blue and nanogold,⁴² and results from Chapter 5 show that both photochemical pathways are involved in the bactericidal activity of 18 nm CVZnO_oleate, but there is a greater involvement from the Type II mechanism.²³

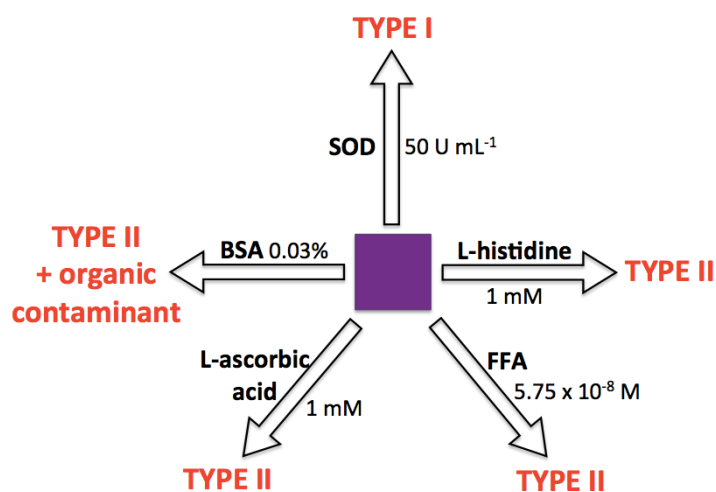


Fig. 6.16 Radical species and singlet oxygen quenchers/inhibitors of Type I and II photochemical pathways used in this investigation (SOD: superoxide dismutase; BSA: bovine serum albumin; FFA: furfuryl alcohol).

To investigate the mechanism responsible for the bactericidal activity of polyurethane containing CVZnO_oleate, superoxide dismutase (SOD) and L-histidine were added separately to the antibacterial protocol as Type I and Type II inhibitors, respectively.²³⁻²⁵ SOD (50 U mL^{-1}) was added to the bacterial suspension to eliminate superoxide anions and determine the contribution of a Type I photochemical pathway. Moreover, L-histidine (1 mM) was used as a singlet oxygen quencher to study the involvement of the Type II mechanism. SOD or L-histidine was added to the bacterial

suspension prior to exposure to CVZnO_oleate and tested against *S. aureus* NCTC 13143 and *E. coli* ATCC 25922 for 2 h in the light and dark to assess any changes in antibacterial activity compared to a control experiment without inhibitors (Figs. 6.17 - 6.18). It should be noted that these standard concentrations of SOD and L-histidine are taken from literature and SOD at this concentration does not affect singlet oxygen production.

Fig. 6.17 shows the antibacterial activity of control polyurethane and CVZnO_oleate against *S. aureus* NCTC 13143 following 2 h in the dark and after exposure to standard laboratory white light (~500 lux). The antibacterial activity of ZnO_oleate on its own was not tested as it displayed no significant kill within 2 h. After 2 h in the dark (Fig. 6.17(a)), both SOD and L-histidine reduced the antibacterial activity of CVZnO_oleate by ~0.8 - 1 log. Following 2 h of white light exposure, both inhibitors caused ~3.3 log reduction in the antibacterial activity of CVZnO_oleate, whereas in the control experiment the polymer was able to reduce *S. aureus* NCTC 13143 to below the detection limit without the inhibitors. In addition, the antibacterial efficacy of control polyurethane, ZnO_oleate and CVZnO_oleate was tested against *E. coli* ATCC 25922 using the same experimental conditions. This time, the antibacterial activity of ZnO_oleate was tested as it significantly reduced numbers of *E. coli* ATCC 25922 in the control experiment within 2 h. Fig. 6.18 displays a similar effect of the inhibitors on CVZnO_oleate, as both SOD and L-histidine reduced its antibacterial response by a similar extent (in the light and dark). Therefore, these tests confirm that both Type I and II photochemical pathways contribute to the antibacterial activity of CVZnO_oleate at a similar rate in the dark and after white light exposure.

However, the results of this experiment implied that the Type I and II mechanisms were not involved in the bactericidal mechanism observed from ZnO_oleate on its own, as they did not affect its antibacterial activity. ICP-OES data showed that some leaching of Zn²⁺ occurred from ZnO_oleate after 48 h of immersion in water (1.008 mg/L). To see whether the amount

of leaching was significant enough to reduce the bactericidal activity of ZnO_oleate, it was removed from water after 48 h and tested against *E. coli* ATCC 25922. The results demonstrated no change between the antibacterial activity of ZnO_oleate immersed in water and ZnO_oleate control (data not shown). Therefore, this shows that the ZnO NPs do not leach at a significant concentration in the surrounding solution to cause bacterial reduction.

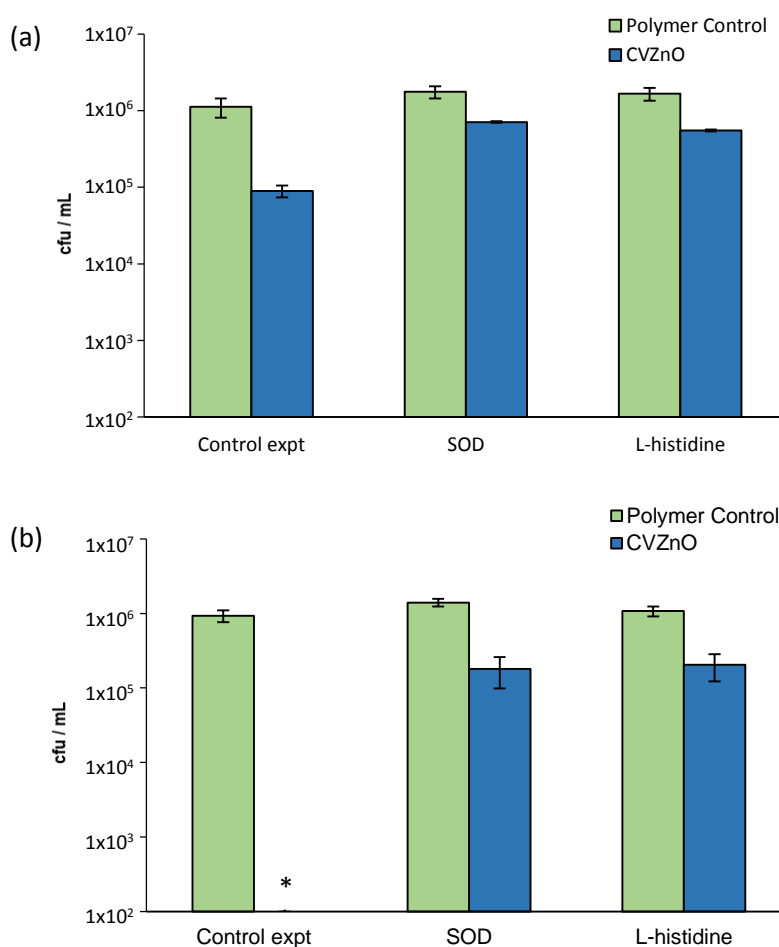


Fig. 6.17 Viable counts of *S. aureus* NCTC 13143 after 2 h (a) in the dark and (b) exposure to standard laboratory white light (500 ± 300 lux) on modified polyurethane samples for a control, superoxide dismutase (SOD) and L-histidine experiment. * indicates bacterial counts were reduced to below the detection limit of 100 colony forming units/mL (cfu/mL).

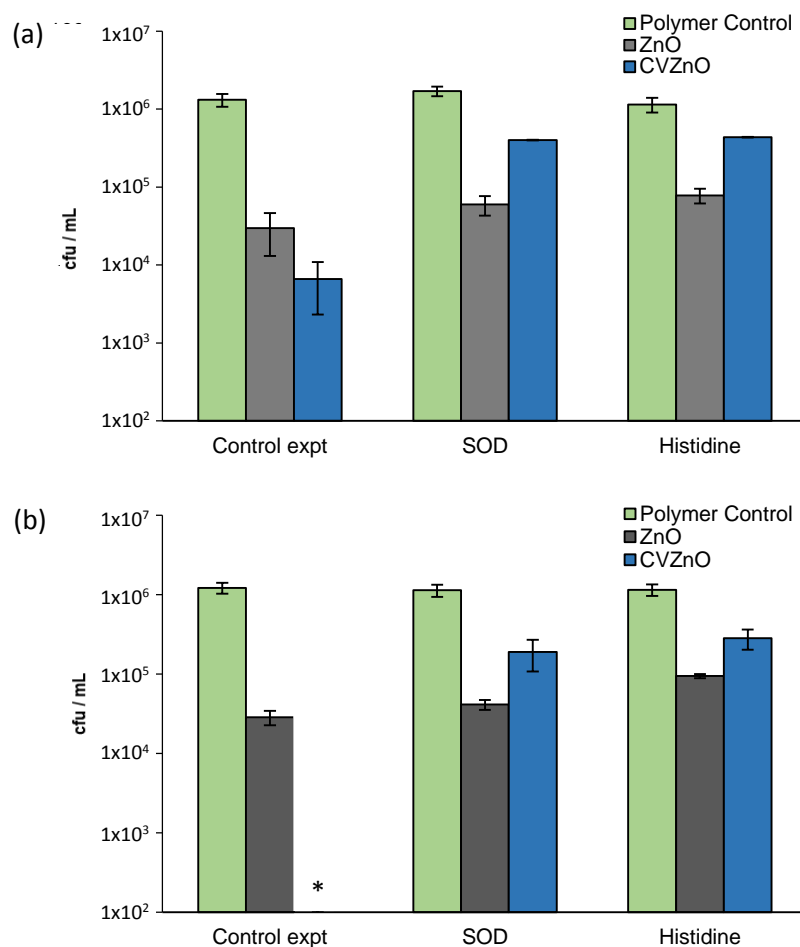


Fig. 6.18 Viable counts of *E. coli* ATCC 25922 after (a) 2 h in the dark and (b) 2 h of exposure to standard laboratory white light (500 ± 300 lux) on modified polyurethane samples for a control, superoxide dismutase (SOD) and L-histidine experiment. * indicates bacterial counts were reduced to below the detection limit of 100 colony forming units/mL (cfu/mL).

Further experiments were carried out to investigate the effect of adding bovine serum albumin (BSA; 0.03%) to the bacteria as an organic contaminant as well as a singlet oxygen quencher.^{18,23} After 2 h of white light exposure and in the dark, BSA was able to reduce the bactericidal efficacy of CZnO_oleate against both *E. coli* ATCC 25922 and *S. aureus* NCTC 13143. Conversely, BSA did not affect the antibacterial activity of ZnO_oleate, which suggests that singlet oxygen is not involved in killing the bacteria. This also implies that ZnO_oleate polyurethane samples would be unaffected by possible organic contamination that would be

present in hospitals, which is a great advantage compared to other photoactivated systems (i.e. 18 nm CVZnO).²³

Table 6.5 Bacterial reduction (in log form) of *E. coli* ATCC 25922 and *S. aureus* NCTC 13143 after 2 h exposure to ZnO_oleate and CVZnO_oleate-incorporated polyurethane with and without the addition of bovine serum albumin (BSA; 0.03%) (a) in the dark and (b) following white light incubation (500 ± 300 lux).

(a) <i>E. coli</i> ATCC 25922 (dark)			<i>S. aureus</i> NCTC 13143 (dark)		
Polymer	Bacterial Reduction without BSA	Bacterial Reduction with BSA	Polymer	Bacterial Reduction without BSA	Bacterial Reduction with BSA
<i>Control</i>	No kill	No kill	<i>Control</i>	No kill	No kill
<i>ZnO_oleate</i>	~2.5 log	~2.5 log	<i>ZnO_oleate</i>	No kill	No kill
<i>CVZnO_oleate</i>	~3 log	~2 log	<i>CVZnO_oleate</i>	~2.2 log	~3.5 log

(b) <i>E. coli</i> ATCC 25922 (~500 lux)			<i>S. aureus</i> NCTC 13143 (~500 lux)		
Polymer	Bacterial Reduction without BSA	Bacterial Reduction with BSA	Polymer	Bacterial Reduction without BSA	Bacterial Reduction with BSA
<i>Control</i>	No kill	No kill	<i>Control</i>	No kill	No kill
<i>ZnO_oleate</i>	~2 log	~2 log	<i>ZnO_oleate</i>	No kill	No kill
<i>CVZnO_oleate</i>	≥4 log	~3 log	<i>CVZnO_oleate</i>	≥4 log	~3 log

To confirm singlet oxygen production within CVZnO_oleate under white light activation, two widely used chemical traps of singlet oxygen, furfuryl alcohol (FFA)²⁷ and L-ascorbic acid,²⁸ were added separately to the antibacterial protocol. At 222 nm wavelength, FFA consumption was monitored after 3 h exposure to CVZnO_oleate. Table 6.6 shows a much greater decrease in FFA absorbance in the photoactivation of CVZnO_oleate compared to polyurethane containing CV alone (and none produced from ZnO_oleate or the control polymer). None of the modified polymers showed any quenching of FFA in the dark (data not shown) and it should be noted that FFA does not absorb in the visible spectrum and thus, was not deactivated during the 3 h experiment.

Using the same experimental set-up as described with SOD, L-histidine and BSA, L-ascorbic acid (1 mM) was added to the *E. coli* ATCC 25922 suspension. Following 4 h of white light exposure, CVZnO_oleate with L-ascorbic acid resulted in a ~2 log reduction of the bacteria, compared to ≥ 4 log reduction without the presence of the quencher (Fig. 6.19). L-ascorbic acid added to CV alone reduced *E. coli* ATCC 25922 by ~1 log, in comparison to CV alone which caused ~2 log reduction after white light illumination. The quencher did not affect the antibacterial activity of the modified polymers in the dark (data not shown). These results show that upon light activation, singlet oxygen is chemically quenched as it reacts readily with ascorbate, producing hydrogen peroxide.²⁸ In addition, CVZnO_oleate produces more singlet oxygen than CV alone, despite the fact that ZnO_oleate itself does not produce singlet oxygen. It should be noted that L-ascorbic acid is not active in the dark.

Table 6.6 UV-vis absorbance values at 222 nm of furfuryl alcohol after 3 h exposure to standard laboratory white light (500 ± 300 lux) on control, ZnO_oleate CV, and CVZnO_oleate-incorporated polymer samples.

Polymer	Absorbance (A)
Control	0.158
ZnO_oleate	0.153
CV	0.138
CVZnO_oleate	0.039

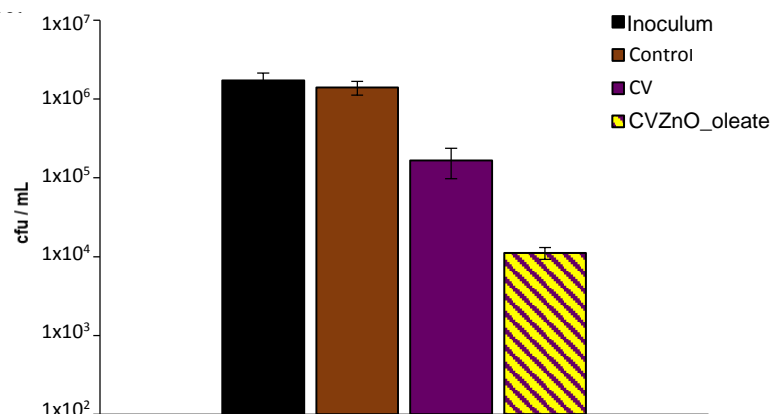


Fig. 6.19 Viable counts in colony forming units/mL (cfu/mL) of *E. coli* ATCC 25922 after 4 h exposure to standard laboratory white light (500 ± 300 lux) on modified polyurethane samples with the addition of L-ascorbic acid (1 mM).

6.4 Conclusion

In this chapter, 3 nm ZnO NPs have been synthesised with two different capping agents and incorporated into polyurethane with CV dye. They were tested against *E. coli* ATCC 25922 and a clinical strain of EMRSA-16 (*S. aureus* NCTC 13143) for up to 3 h and demonstrated highly significant bactericidal activity. For the first time, these NPs demonstrated considerable antibacterial activity without a photosensitiser when incorporated into the polymer. Oleate-capped ZnO NPs demonstrated greater bactericidal activity than DOPA-capped ZnO NPs, suggesting that the oleate ligand is partially responsible for the enhanced antibacterial activity exhibited from the NPs. CVZnO_oleate samples were then tested against more resistant bacteria found in hospitals, such as *P. aeruginosa* NTCC 10662 and a highly resistant form of *E. coli*. Additionally, a statistically significant reduction in the number of *C. difficile* spores was exhibited using CVZnO_oleate with 72 h of white light (~ 1.2 log reduction; $P = 0.001$). These polymer surfaces have obtained exceptional results against *C. difficile* endospores that can survive on surfaces for many

months and pose a major threat to hospitals as they are resistant to many forms of cleaning methods.^{43,44}

In this investigation, singlet oxygen and radical species inhibitors have been used to give mechanistic evidence for the photochemical pathways occurring from CVZnO_oleate when exposed to light and in the dark. The data has shown that both Type I and Type II mechanisms are occurring in the bactericidal activity of CVZnO_oleate. However, the antibacterial activity of ZnO_oleate polymer samples is barely affected by the presence of the inhibitors, indicating that it does not involve the production of superoxide or singlet oxygen. ICP-OES analysis indicated small amounts of Zn²⁺ leaching from ZnO_DOPA and a slightly greater extent of Zn²⁺ leaching was observed from ZnO_oleate within 2 h. This suggests that the ligand could be partially responsible for the leaching mechanism, as any Zn²⁺ ions released from the polymer could be taken up by the bacteria.

The results from this investigation have clearly demonstrated that the combination of the smaller ZnO NPs and the oleic acid capping agent results improves the antibacterial activity observed from these polymers, as the DOPA-capped ZnO NPs were not as effective. Furthermore, the antibacterial activity of 18 nm ZnO NPs combined with CV was also not as effective as these smaller 3 nm-sized particles. The addition of BSA to the bacterial suspension exposed to 18 nm CVZnO_oleate (Fig. 5.12; Chapter 5) and 3 nm CVZnO_oleate shows that the smaller NPs are less affected by the organic contaminant and singlet oxygen quencher. This suggests that the smaller NPs in CVZnO_oleate operate *via* a more equal contribution of Type I and Type II mechanisms, or it implies that the antibacterial activity of the 3 nm CVZnO_oleate system is more effective because of the NPs themselves rather than the dye, as the NPs are unaffected by BSA. The smaller NPs have the potential of electrostatically interacting with the bacterial cell wall due to a larger surface area, or penetrating through to the cell membrane at a higher concentration than the larger NPs.

These polymers have demonstrated exceptional antibacterial activity as potential surfaces in hospitals to minimise the risk and spread of HAIs. They have various prospective applications, including covers for laptops, keyboards mousepads and iPad covers. Highly significant bacterial kills have been achieved under low intensity lighting (~500 lux) and in the dark, proving more effective than other antibacterial polymer systems previously tested which used much higher white light intensities (3,000-10,000 lux).^{23,27,30,41,45-47} The antibacterial efficacy of these samples has been tested without the use of a coverslip to spread the bacteria evenly onto the entire polymer surface and without a humidity chamber to prevent evaporation. This has created an experimental set-up that represents a more realistic clinical environment and demonstrates how effective these polymers would be in a hospital setting. Furthermore, these polymers have exhibited bactericidal activity against a much higher bacterial load than what would be present in a hospital; $\sim 1 \times 10^5$ cfu/cm² of bacteria used in this investigation compared to an average of 1×10^2 cfu/cm² found in a clinical setting.^{31,46,47}

References

- 1 Simone CB, Friedberg JS, Glatstein E. Photodynamic therapy for the treatment of non-small cell lung cancer. *Journal of Thoracic Disease*. 2012;4(1):63-75.
- 2 Ormond AB, Freeman HS. Dye Sensitizers of Photodynamic Therapy, *Materials*. 2013;6(3):817-840.
- 3 Dougherty TJ. Photodynamic therapy (PDT) of malignant tumours. *Critical Reviews in Oncology/Hematology*. 1984;2(2):83-116.
- 4 Castano AP, Demidova TN, Hamblin MR. Mechanisms in photodynamic therapy: part one – photosensitisers, photochemistry and cellular localization. *Photodiagnoses Photodynamic Therapy*. 2004;1(4):279-293.
- 5 Rajesh S, Koshi E, Philip K, Mohan A. Antimicrobial photodynamic therapy: An overview. *Journal of Indian Society of Periodontology*. 2011;15(4):323-327.
- 6 Sydnor ERM, Perl TM. Hospital Epidemiology and Infection Control in Acute-Care Settings. *Clinical Microbiology Reviews*. 2011;24(1):141-173.
- 7 Ventola CL. The Antibiotic Resistance Crisis: Part 1: Causes and Threats. *Pharmacy and Therapeutics*. 2015;40(4):277-283.
- 8 Yoshikawa TT, Epidemiology and unique aspects of aging and infectious diseases. *Clinical Infectious Diseases*. 2000;30(6):1414-1422.
- 9 Hickson M, Probiotics in the prevention of antibiotic-associated diarrhoea and Clostridium difficile infection, *Therapeutic Advances in Gastroenterology*. 2011;4(3):185-197.
- 10 Khanna S, Pardi DS. Clostridium difficile Infection: New Insights Into Management. *Mayo Clinic Proceedings*. 2012;87(11):1106-1117.
- 11 Klevens RM, Edwards JR, Gaynes RP. The impact of Antimicrobial-Resistant, Health Care-Associated infections on Mortality in the United States. *Clinical Infectious Diseases*. 2008;47(7):927-930.

- 12 Fujitani S, Moffet KS, Yu VL. *Pseudomonas aeruginosa*, Antimicrobe, Infectious disease Antimicrobial agents. [cited 2016 03/06/2016]; Available from: <http://www.antimicrobe.org/new/b112.asp>
- 13 Rai AV, Bai JA. Nanoparticles and their potential application as antimicrobials. *Science against microbial pathogens: communicating current research and technological advances*, Mendez-Vilas, A. (Ed.). University of Mysore, India. 2011;197-209.
- 14 Reddy KM, Feris K, Bell J, Wingett DG, Hanley C, Punnoose A, Selective toxicity of zinc oxide nanoparticles to prokaryotic and eukaryotic systems. *Applied Physics Letters*. 2007, 90(213902):2139021-2139023.
- 15 Sirelkhatim A, Mahmud S, Seeni A, Kaus NHM, Ann LC, Bakhori SKM, Hasan H, Mohamad D. Review on Zinc Oxide Nanoparticles: Antibacterial Activity and Toxicity Mechanism. *Nano-Micro Letters*. 2015;7(3):219-242.
- 16 Wu W, He Q, Jiang C. Magnetic Iron Oxide Nanoparticles: Synthesis and Surface Functionalization Strategies. *Nanoscale Research Letters*. 2008;3(11):397-415.
- 17 Liu Y, Tan J, Thomas A, Ou-Yang D, Muzykantov VR. The shape of things to come: importance of design in nanotechnology for drug delivery. *Therapeutic delivery*. 2012;3(2):181-194.
- 18 Sehmi SK, Noimark S, Weiner J, Allan E, MacRobert AJ, Parkin IP. Potent Antibacterial Activity of Copper Embedded into Silicone and Polyurethane. *ACS Materials & Interfaces*. 2015;7(41):22807-22813.
- 19 Das S, Anderson CJ, Grayes A, Mendoza K, Harazin M, Schora DM, Peterson LR. Nasal Carriage of Epidemic Methicillin-Resistant *Staphylococcus aureus* 15 (EMRSA-15) Clone Observed in Three Chicago-Area Long-Term Care Facilities. *Antimicrobial Agents and Chemotherapy*. 2013;57:4551-4553.
- 20 Ali M, Winterer M. ZnO Nanocrystals: Surprisingly 'Alive'. *Chemistry of Materials*. 2010;22(1):85-91.

- 21** Orchard KL, Shaffer MSP, Williams CK, Organometallic Route to Surface-Modified ZnO Nanoparticles Suitable for In Situ Nanocomposite Synthesis: Bound Carboxylate Stoichiometry Controls Particle Size or Surface Coverage. *Chemistry of Materials*. 2012;24(13):2443-2448.
- 22** Burns DA, Heap JT, Minton NP, SleC is essential for germination of *Clostridium difficile* spores in nutrient-rich medium supplemented with the bile salt taurocholate. *Journal of Bacteriology*. 2010;192(3):657-664.
- 23** Sehmi SK, Noimark S, Bear JC, Peveler WJ, Bovis M, Allan E, MacRobert AJ, Parkin IP. Lethal photosensitisation of *Staphylococcus aureus* and *Escherichia coli* using crystal violet and zinc oxide-encapsulated polyurethane. *Journal of Materials Chemistry B*. 2015;3:6490-6500.
- 24** Huang L, Xuan Y, Koide Y, Zhiyentayev T, Tanaka M, Hamblin MR. Type I and Type II mechanisms of antimicrobial photodynamic therapy: An in vitro study on Gram-negative and Gram-positive bacteria. *Lasers in surgery and medicine*. 2012;44(6):490-499.
- 25** Ergaieg K, Chevanne M, Cillard J, Seux R. Involvement of both Type I and Type II mechanisms in Gram-positive and Gram-negative bacteria photosensitization by a meso-substituted cationic porphyrin. *Solar Energy*. 2008;82(12):1107-1117.
- 26** Allen JM, Gossett CJ, Allen SF, Photochemical formation of singlet molecular oxygen (1O_2) in illuminated aqueous solutions of p-aminobenzoic acid (PABA). *Journal of Photochemistry and Photobiology B*. 1996;32:3-37.
- 27** Hwang GB, Noimark S, Page K, Sehmi S, MacRobert AJ, Allan E, Parkin IP. White light-activated antimicrobial surfaces: effect of nanoparticles type on activity. *Journal of Materials Chemistry B*. 2016;4:2199-2207.
- 28** Kramarenko GG, Hummel SG, Martin SM, Buettner GR, Ascorbate reacts with singlet oxygen to produce hydrogen peroxide. *Photochemistry and Photobiology*. 2006;82(6):1634-1637.

- 29 Meulenkamp EA. Synthesis and Growth of ZnO Nanoparticles. *The Journal of Physical Chemistry B*. 1998;102(29):5566-5572.
- 30 Samuel SM, Bose L, George KC. Optical Properties of ZnO Nanoparticles. *1 & 2 SB Academic Review*. 2009;16(1):57-65.
- 31 Noimark S, Weiner J, Noor N, Allan E, Williams CK, Shaffer MSP, Parkin IP. Dual-Mechanism Antimicrobial Polymer-ZnO Nanoparticle and Crystal Violet-Encapsulated Silicone. *Advanced Functional Materials*. 2015;25(9):1367-1373.
- 32 Gerding DN, Muto CA, Owens RC. Measures to Control and Prevent *Clostridium Difficile* Infection. *Clinical Infectious Diseases*. 2008;46(supplement 1):S43-S49.
- 33 Jump RL. *Clostridium difficile* infection in older adults. *Aging health*. 2013;9(4):403-414.
- 34 Collins AS. Preventing Health Care–Associated Infections. In: Hughes RG, editor. *Patient Safety and Quality: An Evidence-Based Handbook for Nurses*. Rockville (MD): Agency for Healthcare Research and Quality (US); 2008 Apr. Chapter 41.
- 35 Zheng CJ, Yoo J, Lee T, Cho H, Kim Y, Kim W, Fatty acid synthesis is a target for antibacterial activity of unsaturated fatty acids. *FEBS Letters*. 2005;579(23):5157-5162.
- 36 Chandrasekaran M, Kannathasan K, Venkatesalu V, Z. Antimicrobial activity of fatty acid methyl esters of some members of Chenopodiaceae, *Z Naturforsch C*. 2008;63:331-336.
- 37 Choi J, Park N, Hwang S, Sohn JH, Kwak I, Cho KK, Choi IS. The antibacterial activity of various saturated and unsaturated fatty acids against several oral pathogens. *Journal of Environmental Biology*. 2013;34:673-676.
- 38 Raghupathi KR, Koodali RT, Manna AC. Size-dependent bacterial growth inhibition and mechanism of antibacterial activity of zinc oxide nanoparticles. *Langmuir*. 2011;27(7):4020-4028.

- 39 Xie Y, He Y, Irwin PL, Jin T, Shi X. Antibacterial activity and mechanism of action of zinc oxide nanoparticles against *Campylobacter jejuni*. *Applied Environmental Microbiology*. 2011;77:2325-2331.
- 40 Fong J, Kasimova K, Arenas Y, Kaspler P, Lazic S, Mandel A, Lilge L. A novel class of ruthenium-based photosensitisers effectively kills in vitro cancer cells and in vivo tumors. *Photochemical and Photobiological Sciences*. 2015;14:2014-2023.
- 41 Wan MT, Lin JT. Current evidence and applications of photodynamic therapy in dermatology. *Clinical, Cosmetic and Investigational Dermatology*. 2014;7:145-163.
- 42 Bovis MJ, Noimark S, Woodhams JH, Kay CWM, Weiner J, Peveler WJ, Correia A, Wilson M, Allan E, Parkin IP, MacRobert AJ. Photosensitisation studies of silicone polymer doped with methylene blue and nanogold for antimicrobial applications. *RSC Advances*. 2015;5:54830-54842.
- 43 Hargreaves KR, Clokie MRJ. *Clostridium difficile* phages: still difficult? *Frontiers in Microbiology*. 2014;5:184.
- 44 Guideline for Disinfection and Sterilization in Healthcare Facilities, Centers for Disease Control and Prevention, 2008.
- 45 Perni S, Piccirillo C, Pratten J, Prokovich P, Chrzanowski W, Parkin IP, Wilson M. The antimicrobial properties of light-activated polymers containing methylene blue and gold nanoparticles. *Biomaterials*. 2009;30(1):89-93.
- 46 Noimark S, Allan E, Parkin IP. Light-activated antimicrobial surfaces with enhanced efficacy induced by a dark-activated mechanism. *Chemical Science*. 2014;5(6):2216-2223.
- 47 Ozkan E, Ozkan FT, Allan E, Parkin IP. The use of zinc oxide nanoparticles to enhance the antibacterial properties of light-activated polydimethylsiloxane containing crystal violet. *RSC Advances*. 2015;5:8806-8813.

Chapter 7

Conclusion

As bacterial drug resistance rises, the need to decrease the spread of bacterial contamination in hospitals and reduce the risk of hospital-acquired infections becomes increasingly urgent. Antibacterial surfaces can significantly reduce the risk of these infections by minimising the spread of bacterial contamination between patients, staff and frequently touched surfaces. In this thesis, different antibacterial surfaces have been prepared with the potential to kill bacteria that come into contact with the surface within only a few hours.

In the first experimental chapter, Chapter 3, small copper nanoparticles were incorporated into two widely used polymers, medical grade silicone and polyurethane squares. These polyurethane-encapsulated Cu samples were able to reduce Gram-negative and Gram-positive bacteria without any white light activation or a photosensitiser. The bactericidal activity of polyurethane-encapsulated Cu was more effective than silicone-encapsulated Cu, since polyurethane was able to swell more and thus, incorporate more nanoparticles within the polymer matrix. Silicone-encapsulated Cu was able to completely reduce *E. coli* and MRSA within 6 hours, whereas polyurethane-encapsulated Cu completely reduced bacterial numbers within only 3 hours. Further experiments showed that these polymers were stable for more than 90 days after preparation and were unaffected by bovine serum albumin (BSA), which was added to the bacteria as an organic contaminant (and singlet oxygen quencher).

Secondly as described in Chapter 4, a well-known disinfectant used in hospitals, glutaraldehyde, was incorporated into polyurethane to determine its antibacterial activity. Glutaraldehyde is a commonly used biocide for sterilising medical devices and equipment, but its use in hospitals is somewhat questionable at high concentrations due to possible

toxicity towards mammalian cells. Therefore, a very low concentration of glutaraldehyde was incorporated into the polymer to test its bactericidal properties. Additionally, polyurethane samples were prepared with glutaraldehyde only coated onto the polymer, in order to investigate the efficacy of the 'swell-encapsulation-shrink' method that has been used to impregnate antibacterial agents effectively into the polymer substrate. As predicted, the bactericidal activity of polyurethane-encapsulated glutaraldehyde was far more effective than glutaraldehyde coated onto polyurethane. These modified polymers were highly effective within a few hours and did not require any light activation. However, after 14 days, the antibacterial activity of the samples dramatically reduced due to polymerisation of the aldehyde groups under basic conditions. Thus, these biocidal polymers would be more effective as disposable or short-term antibacterial covers or surfaces, unless their stability was improved at lower concentrations.

Next, this thesis focused on the use of photodynamic therapy to kill the bacteria by coating polyurethane with crystal violet (CV) dye, as described in Chapter 5 and 6. To enhance the bacterial reduction observed from CV-coated polyurethane, 18 nm zinc oxide nanoparticles (ZnO NPs) were also incorporated into the polymer. Polyurethane-encapsulated CV and ZnO samples (CVZnO) were highly effective at reducing both *E. coli* and *S. aureus* within 4 h of white light activation, and more significantly, in the dark. For the first time, the mechanism operating within the dye-nanoparticle combination was investigated by using radical species and singlet oxygen quenchers: bovine catalase, L-histidine and BSA. The results indicated that both radical species (Type I) and singlet oxygen (Type II) were involved in the bactericidal mechanism of CVZnO.

Following the efficacious results achieved from CVZnO, smaller 3 nm ZnO NPs were synthesised with two different capping agents and incorporated into polyurethane with CV dye. Previous studies carried out by Perni *et al* demonstrated that smaller Au NPs exhibited greater antibacterial activity

when combined with methylene blue. Therefore, this thesis investigated the bactericidal activity of a different nanoparticle-dye combination. In this study, 3 nm DOPA-capped ZnO and oleate-capped ZnO NPs were synthesised and incorporated into the polymer. Most strikingly, these smaller ZnO NPs demonstrated highly significant bactericidal activity without a photosensitiser within only 3 hours in the light and dark.

Furthermore, CV combined with these smaller ZnO NPs achieved even greater antibacterial activity in the light and in the dark. These results confirmed that smaller nanoparticles elicited better antibacterial activity, presumably because the smaller NPs can penetrate through the bacterial cell wall more efficiently. It is also possible that the smaller NPs can interact more effectively with the dye itself, causing a greater enhancement in bacterial kill than what was observed in Chapter 5. Noimark *et al* studied the antibacterial activity of CV combined with DOPA-capped ZnO NPs incorporated into silicone, which was not as effective as polyurethane. This has also been demonstrated in Chapter 3, where Cu NPs reduced bacterial numbers more effectively when incorporated into polyurethane compared to silicone. Moreover, Ozkan *et al* investigated the bactericidal activity of CV and commercially available <100 nm ZnO NPs incorporated into silicone, which also were not as effective as these smaller NPs.

The combination of CV and ZnO NPs capped with an oleate ligand (CVZnO_oleate) exhibited the most significant bactericidal activity and was then tested against more resistant bacteria, as well as *C. difficile* endospores. For the first time, CVZnO polymers were exposed to highly resistant bacteria and spores. These polymers were able to reduce bacteria such as *P. aeruginosa* and a wild strain of *E. coli* within 6 h in the light and dark. More significantly, CVZnO_oleate displayed significant photobactericidal activity against *C. difficile* spores within 72 h. CVZnO_oleate achieved outstanding results against highly resistant bacterial strains using a much lower light intensity than previously used in

the experiments (~500 lux compared to ~6600 lux). This suggested that the oleic acid capping agent is crucial for this bactericidal activity, even though the ligand displayed no significant antibacterial activity on its own. ZnO NPs were synthesised with linoleate and stearate capping agents and did not show the same bactericidal activity as oleate-capped ZnO NPs. Furthermore, DOPA-capped NPs did not demonstrate the same lethal activity exhibited from the oleate-capped NPs, even though they were similar in size.

Moreover, the experimental set-up was changed to replicate a more realistic clinical setting by removing the use of a coverslip and a humidity chamber. An extensive investigation was carried out to study the mechanism operating within the CVZnO_oleate polymer system. ZnO NPs were synthesised again with a varied metal:ligand ratio, as well as using different ligands (i.e. stearate and linoleate ligands). However, these newer ZnO NPs with alternative ligands did not reduce the bacteria as effectively as the original CVZnO_oleate, confirming that the oleate ligand plays a role in its bactericidal activity. In addition, mechanistic studies on the ROS-mediated processes involved in bacterial killing were carried out. ROS inhibitors were added to the bacteria to determine the involvement of each photochemical pathway in the antibacterial activity of CVZnO_oleate. The results indicated that both Type I (superoxide) and Type II (singlet oxygen) photochemical pathways were operating in the light and dark.

The antibacterial activity of 3 nm CVZnO_oleate was more effective than 18 nm CVZnO_oleate. This is most likely due to the differences in NP size, as both NPs were synthesised with an oleate-capping agent. BSA affected 18 nm CVZnO_oleate more than 3 nm CVZnO_oleate, which could be due to the fact that BSA affects the antibacterial activity of the photosensitiser more than the antibacterial activity of the NPs. The protocol used to determine the antibacterial activity of 18 nm CVZnO_oleate used a higher light intensity (~6600 lux) which showed significant bactericidal activity from the sample. However, CV was not as effective on its own using ~200

lux intensity as shown from the 3 nm CVZnO_oleate investigation. The NPs are more responsible for the bactericidal activity observed from 3 nm CVZnO_oleate than 18 nm CVZnO_oleate (as they did not kill on their own). This was also confirmed from ZnO_oleate and Cu-incorporated polymer samples, as their antibacterial activities were not affected by the addition of BSA to the bacterial suspension.

The overall results have shown that all polymer surfaces are capable of reducing bacteria within short incubation times against hospital pathogens. Two polymeric materials were tested for bactericidal activity, which demonstrated that polyurethane performed more effectively. Additionally, the 'swell-encapsulation-shrink" method was established to be a much better method for preparing these materials compared to dip-coating the polymers with the active agent. Smaller sized nanoparticles (2-3 nm Cu and ZnO NPs) exhibited considerable antibacterial activity without light-activation. The mechanism operating within these systems differ to the mechanism operating within light-activated antibacterial polymers. The mechanism by which the nanoparticles kill bacteria on their own needs to be further investigated in order to understand the longevity of their activities, i.e. if the ions are operating *via* a leaching mechanism. It is possible that the nanoparticles are killing the bacteria by an electrostatic interaction between the metal ions and the negatively charged bacterial cell wall. The smaller NPs may be able to diffuse through the bacterial membrane more effectively than larger NPs; hence they have demonstrated better antibacterial activity. The results also showed that nanoparticles incorporated into polyurethane alone are not affected by organic contamination. On the other hand, the mechanism of photo-activated polymers clearly operates *via* the combination of a Type I and Type II photochemical pathway, but are affected by organic contamination.

This thesis has described the preparation and antibacterial activity of novel materials that are highly effective at reducing resistant bacteria and has progressed our understanding on the mechanism that kills the bacteria.

The efficacy of these antibacterial surfaces has vastly improved, as this thesis presents work which demonstrates highly significant bacterial reduction under very low intensity white light and in the dark. Previous work has focused on laser light activation to cause bacterial kill, however, in a hospital environment it would be highly beneficial for the surface to be self-sterilising and efficient in low lighting conditions. Additionally, this thesis presents surfaces which are able to reduce bacteria without a photosensitiser, and thus, are not affected by radical and singlet oxygen inhibitors. To progress on the work presented in this thesis, clinical studies are underway to investigate the bactericidal activity of these surfaces against more resistant pathogens. For these polymers to be used as antibacterial surfaces for hospitals, such as iPad, keyboard and phone covers, there needs to be a greater understanding on their durability over a longer period of time and how they could be commercially manufactured at a larger scale.

7.1 Future Work

It is very important to understand the stability and longevity of these polymer samples to see how effective they are months/years after preparation. Even though these samples are able to reduce bacterial numbers within short exposure times, it is crucial to understand how effective they are after longer periods of time, with and without routine cleaning. It would also be interesting to directly compare the effect of using a coverslip vs. no coverslip in the same experiment, as well as using BSA and a lower light intensity in all future experiments. It is important to replicate a realistic clinical setting as much as possible when studying the antibacterial activity of these surfaces. This thesis has investigated the effects of organic contamination and humidity on the bactericidal activity of these antibacterial polymers. It would be interesting to see how factors

such as temperature and method/frequency of cleaning would alter the antibacterial efficacy of the samples.

Furthermore, a different method could be used to drop-cast the bacteria onto the polymer samples. For example, an aerosol-type spray method could be used to coat the polymer with bacteria, which would more accurately reflect the natural situation, i.e. sneezing or coughing or other aerosol generated from body fluids. Moreover, the antibacterial activity of these surfaces should be assessed against biofilms as well as planktonic bacteria, since biofilm formation would enhance the ability of the bacteria to survive harsh conditions and resist antibacterial treatment. To investigate the antibacterial efficacy of these polymer samples in an actual clinical setting, experiments are currently underway to see how they will behave in a naturally contaminated hospital environment.

Further investigation on the interaction between the bacterial cells and the polymer surface would give valuable information on how the nanoparticles kill the bacteria (without a photosensitiser), i.e. using electron microscopy to see the larger nanoparticles inside the bacterial cell. Live-dead could be used to determine the proportion of bacteria live-dead in a time course. Additionally, atomic-force microscopy (AFM) could be used to determine the strength of interaction between the bacteria and the modified polymer surface.